EPA/600/R-12/058A

Watershed Modeling to Assess the Sensitivity of Streamflow, Nutrient, and Sediment Loads to Potential Climate Change and Urban Development in 20 U.S. Watersheds

National Center for Environmental Assessment
Office of Research and Development
U.S. Environmental Protection Agency
Washington, DC 20460

DISCLAIMER

This document is distributed solely for the purpose of pre-dissemination peer review under applicable information quality guidelines. It has not been formally disseminated by EPA. It does not represent and should not be construed to represent any Agency determination or policy. Mention of trade names or commercial products does not constitute endorsement or recommendation for use.

Preferred Citation:

FOREWORD

AUTHORS AND REVIEWERS

The National Center for Environmental Assessment (NCEA), Office of Research and Development, was responsible for preparing this External Review Draft report. An earlier draft report was prepared by Tetra Tech Inc., under EPA Contract EP-C-05-061.

AUTHORS

Tetra Tech Inc.
Jonathan Butcher, Andrew Parker, Saumya Sarkar, Scott Job, Mustafa Faizullabhoy, Peter Cada, Jeremy Wyss

Texas A&M University
Raghavan Srinivasan, Pushpa Tuppad, Deb Debjani

Aqua Terra Consultants
Anthony Donigian, John Imhoff, Jack Kittle, Brian Bicknell, Paul Hummel, Paul Duda

U.S. Environmental Protection Agency, Office of Research and Development
Thomas Johnson, Chris Weaver, Meredith Warren (ORISE Fellow), Daniel Nover (AAAS Fellow)

REVIEWERS

Comments on a previous draft of this report were provided by EPA staff David Bylsma, Chris Clark, Steve Klein, and Chris Weaver.

ACKNOWLEDGEMENTS

The authors acknowledge and thank for their hard work the entire project team at Tetra Tech (Tt), Texas A&M University (TAMU), AQUA TERRA (AT), Stratus Consulting, and FTN Associates. We also thank Seth McGinnis of the National Center for Atmospheric Research (NCAR) for processing the NARCCAP output into change statistics for use in the watershed modeling. NCAR is supported by the National Science Foundation. We acknowledge the modeling groups, the Program for Climate Model Diagnosis and Intercomparison (PCMDI) and the WCRP's Working Group on Coupled Modeling (WGCM) for their roles in making available the WCRP CMIP3 multi-model dataset. Support of this dataset is provided by the Office of Science, U.S. Department of Energy.

TABLE OF CONTENTS

LIST OF APPENDICES

LIST OF TABLES

LIST OF FIGURES

LIST OF ABBREVIATIONS

AET	actual evapotranspiration
BASINS	Better Assessment Science Integrating Point and Non-point Sources
CAT	Climate Assessment Tool
cfs	cubic feet per second
CMIP3	Coupled Model Intercomparison Project Phase 3
cms	cubic meters per second
E	Nash-Sutcliffe model efficiency coefficient
ET	evapotranspiration
GCM	global climate model
GIS	geographic information system
HRU	hydrologic response unit
HSPF	Hydrologic Simulation Program-FORTRAN
HUC	hydrologic unit code
IPCC	Intergovernmental Panel on Climate Change
NARCCAP	North American Regional Climate Change Assessment Program
NCAR	National Center for Atmospheric Research
NCDC	National Climatic Data Center
NLCD	National Land Cover Data
NOAA	National Oceanic and Atmospheric Administration
NRCS	Natural Resource Conservation Service
PET	potential evapotranspiration
PRISM	Parameter-elevation Regressions on Independent Slopes Model
R^2	coefficient of determination
RCM	regional climate model
RMSE	root mean square error
STATSGO	State Soil Geographic Database
SWAT	Soil Water Assessment Tool
TN	total nitrogen
TP	total phosphorus
TSS	total suspended solids
U.S. EPA	U.S. Environmental Protection Agency
USDA	U.S. Department of Agriculture
USGS	U.S. Geologic Survey

1. EXECUTIVE SUMMARY

There is growing concern about the potential effects of climate change on water resources. The 2007 Fourth Assessment Report of the Intergovernmental Panel on Climate Change (IPCC) states that warming of the climate system is now unequivocal (IPCC, 2007). Regionally variable changes in the amount and intensity of precipitation have also been observed in much of the U.S. (Groisman et al., 2005). Climate modeling experiments suggest these trends will continue throughout the 21st century, with continued warming accompanied by a general intensification of the global hydrologic cycle (IPCC, 2007; Karl et al., 2009). Water and watershed systems are highly sensitive to climate. In many areas, climate change is expected to exacerbate current stresses on water resources from population growth and economic and land-use change, including urbanization (IPCC, 2007). Responding to this challenge requires an improved understanding of how we are vulnerable, and the development of strategies for managing climate risk.

This report describes watershed modeling in 20 large, U.S. drainage basins (6,000-27,000 mi^2) to characterize the sensitivity of U.S. streamflow, nutrient (N and P) loading, and sediment loading to a range of potential mid-21st century climate futures, to assess the potential interaction of climate change and urbanization in these basins, and to improve our understanding of methodological challenges associated with integrating existing tools (e.g., climate models, downscaling approaches, and watershed models) and datasets to address these scientific questions. Study areas were selected to represent a range of geographic, hydroclimatic, physiographic, and land use conditions together with practical considerations such as the availability of data to calibrate and validate watershed models. Climate change scenarios are based on mid-21^{st} century climate model projections downscaled with regional climate models (RCMs) from the North American Regional Climate Change Assessment Program (NARCCAP) and the bias-corrected and spatially downscaled (BCSD) data set described by Maurer et al. (2007). Urban and residential development scenarios are based on EPA's national-scale Integrated Climate and Land Use Scenarios (ICLUS) project (U.S. EPA, 2009d). Watershed modeling was conducted using the Hydrologic Simulation Program-FORTRAN (HSPF) and Soil and Water Assessment Tool (SWAT) watershed models.

Climate change scenarios based on global climate model (GCM) simulations in the NARCCAP and BCSD datasets show a continued general warming trend throughout the nation over the next century, although the magnitude of the warming varies from place to place. Wetter winters and earlier snowmelt are likely in many of the northern and higher elevation watersheds. Changes in other aspects of local climate such as the timing and intensity of precipitation show greater variability and uncertainty. ICLUS urban and residential development scenarios show continued growth in urban and developed land over the next century throughout the nation with most growth occurring in and around existing urban areas. Model simulations of watershed response to these changes provide a national scale perspective on the range of potential changes in streamflow and water quality in different regions of the nation. Simulations evaluating the variability in watershed response using different approaches for downscaling climate data and different watershed models provide guidance on the use of existing models and datasets for assessing climate change impacts. Key findings are summarized below.

There is a high degree regional variability in the model simulated responses of different streamflow and water quality endpoints to a range of potential mid-21st century climatic conditions throughout the nation. Comparison of watershed simulations in all 20 study areas for the 2041-2070 time horizon suggests the following hydrologic changes may occur:

- Potential flow volume decreases in the Rockies and interior southwest, and increases in the east and southeast coasts.
- Higher peak flows will increase erosion and sediment transport; loads of nitrogen and phosphorus are also likely to increase in many watersheds.
- Streamflow responses are determined by the interaction of changes in precipitation and evapotranspiration; nutrient and sediment loads are generally correlated with changes in hydrology.

The simulated responses of streamflow and water quality endpoints to climate change scenarios based on different climate models and downscaling methodologies in many cases span a wide range and sometimes do not agree in the direction of change. The ultimate significance of any given simulation of future change will depend on local context, including the historical range of variability, thresholds and management targets, management options, and interaction with other stressors. The simulation results in this study do, however, clearly illustrate that the potential streamflow and water quality response in many areas could be large. Given these uncertainties, successful climate change adaptation strategies will likely need to encompass practices and decisions to reduce vulnerabilities and risk across a range of potential future climatic conditions.

Simulated responses to urban development scenarios were small relative to those resulting from climate change in this study. This is likely due to the relatively small changes in developed lands as a percent of total watershed area at the large spatial scale of watersheds in this study. At the finest spatial scale evaluated in this study, that of an 8 digit HUC, urban and residential growth scenarios represented changes on the order of <1 to about 12 percent of total watershed area. As would be expected, such small changes in development did not have a large effect on streamflow or water quality. It is well documented, however, that urban and residential development at higher levels can have significant impacts on streamflow and water quality. At smaller spatial scales where changes in developed lands represent a larger percentage of watershed area the effects of urbanization are likely to be greater. The scale at which urbanization effects may become comparable to the effects of a changing climate is uncertain.

Simulation results are sensitive to methodological choices such as different approaches for downscaling global climate change simulations and use of different watershed models. Watershed simulations in this study suggest that the variability in watershed response resulting from a single GCM downscaled using different RCM models can be of the same order of magnitude as the ensemble variability between the different GCMs evaluated. Watershed simulations using different models with different structures and methods for representing watershed processes (HSPF and SWAT in this study) also resulted in increased variability of outcomes. SWAT simulations accounting for the influence of increased atmospheric CO_2 on evapotranspiration significantly affected results. One notable insight from these results is that, in many watersheds, increases in precipitation amount and/or intensity, urban development, and

atmospheric CO_2 can have similar or additive effects on streamflow and pollutant loading, e.g., a more flashy runoff response with higher high flows and lower low flows.

Next steps. This study is a significant contribution to our growing understanding of the complex and context dependent relationships between climate change, urban development, and water throughout the nation. It is only an incremental step, however, towards fully addressing these questions. Limitations of model simulations in this study include:

- Several of the study areas are complex, highly managed systems; all infrastructure and operational aspects of water management are not represented in full detail.
- Changes in agricultural practices, water demand, other human responses, and natural ecosystem changes such as the prevalence of forest fire or plant disease that will influence streamflow and water quality are not considered in this study.
- Watershed simulations are constrained by the specific climate change and urban development scenarios used as input to watershed models; scenarios represent a plausible range but are not comprehensive of all possible futures.
- The models used in this study each require calibration, and the calibration process inevitably introduces potential biases related to the approach taken and individual modeler choices.

Further study is required to fully address the implications of these and other questions.

2. INTRODUCTION

It is now generally accepted that human activities including the combustion of fossil fuels and land-use change have resulted, and will continue to result in long-term changes in climate (IPCC, 2007; Karl et al., 2009). The 2007 Fourth Assessment Report of the Intergovernmental Panel on Climate Change (IPCC) states that "warming of the climate system is unequivocal, as is now evident from observations of increases in global average air and ocean temperatures, widespread melting of snow and ice and rising global average sea level" (IPCC, 2007). Regionally variable changes in the amount and intensity of precipitation have also been observed in much of the U.S. (Groisman et al., 2005). Climate modeling experiments suggest these trends will continue throughout the 21st century, with continued warming accompanied by a general intensification of the global hydrologic cycle (IPCC, 2007; Karl et al., 2009). While significant uncertainty remains, particularly with respect to precipitation changes at local and regional spatial scales, the presence of long-term trends in the record suggests many parts of the U.S. could experience future climatic conditions unprecedented in recent history. Such changes challenge the assumption of climate stationarity that has provided the foundation for water management for decades (e.g., Milly et al., 2008).

Water and watershed systems are highly sensitive to changes in climate. Air temperatures are anticipated to increase throughout most of the nation. Warmer air temperatures can result in increased evaporation from soils and surface water; changes in the dynamics of snowfall and snowmelt affecting runoff; changes in land cover affecting pollutant loading and watershed biogeochemical cycling. Warming air temperatures are also likely to cause warming of rivers and lakes with cascading effects on individual species, community composition, and water quality. Such changes together with decreased precipitation could contribute to more regions experiencing drought. Precipitation changes are more regionally variable and not as well understood. Generally, runoff is projected increase at higher latitudes and in some wet tropical areas, and decrease over dry and semi-arid regions at mid-latitudes due to decreases in rainfall and higher rates of evapotranspiration (IPCC, 2007). Northern and mountainous areas that receive snow in the winter are likely to see increased precipitation occurring as rain versus snow. In addition, most regions of the U.S. are expected to experience increasing intensity of precipitation events, i.e., the fraction of total precipitation occurring in large magnitude events, due to a warming induced general intensification of the global hydrologic cycle. Precipitation changes can result in hydrologic effects including changes in amount and seasonal timing of streamflow, changes in soil moisture and groundwater recharge, changes in land cover watershed biogeochemical cycling, changes in non-point pollutant loading to water bodies, and increased demands on water infrastructure including urban stormwater and other engineered systems. Regions exposed to increased storm intensity could experience increased coastal and inland flooding.

Climate change is expected to exacerbate current stresses on water resources from population growth and economic and land-use change, including urbanization (IPCC, 2007). Some systems and regions are likely to be more affected by climate change than others. The effects of climate change in different regions of the country will vary due to differences in the type of climate change, watershed physiographic setting, and interaction with local scale land-use, pollutant sources, and human use and management of water. At the national scale, a relatively large

literature exists concerning the potential effects of climate change on water quantity. Less is known about the potential effects of climate change on water quality and aquatic ecosystems. Earlier studies illustrate the sensitivity of stream nutrients, sediments, and flow characteristics of relevance to aquatic species and ecosystems to potential changes in climate (e.g., see Poff et al., 1996; Williams et al., 1996; Wilby et al., 1997; Longfield and Macklin, 1999; Murdoch et al., 2000; Monteith et al., 2000; Chang et al., 2001; Bouraoui et al., 2002; and SWCS, 2003). A review (Whitehead et al., 2009) details progress on these questions but emphasizes that still relatively little is known about the link between climate change and water quality.

Water managers are faced with important questions concerning the implications of long-term climate change for water resources. U.S. EPA's *National Water Program Strategy: Response to Climate Change* outlines a series of key actions to ensure the continued success of core programs under a changing climate (U.S. EPA, 2008). Potential concerns include risk to water management goals including the provision of safe, sustainable water supplies, compliance with water quality standards, urban drainage and flood control, and the protection and restoration of aquatic ecosystems. Responding to this challenge requires an improved understanding of how we are vulnerable, and the development of strategies for managing climate risk. Central to this is an improved understanding of how future climate and land-use change could impact the hydrology and water quality of major U.S. watersheds.

Despite continuing advances in our understanding of climate science and modeling, we currently have a limited ability to predict long-term (multidecadal) future climate at the local and regional scales needed by decision makers (Sarewitz et al., 2000). It is therefore not possible to know with certainty the future climatic conditions to which a particular region or water system will be exposed. In addition, water resources in many areas are also vulnerable to existing, non-climatic stressors such as land-use change. For example, stormwater runoff from roads, rooftops, parking lots, and other impervious surfaces in urban and suburban environments is a well-known cause of stream degradation that is projected to continue throughout the next century. Climate change will interact with urban development in different settings in complex ways that are not well understood. An understanding of the extent to which changes in climate will exacerbate or ameliorate the impacts of other stressors such as urban development is particularly important because, in many situations the only viable management strategies for adapting to future climatic conditions involve increased implementation, or improved methods for addressing non-climatic stressors.

Scenario analysis using computer simulation models is a useful and common approach for assessing vulnerability to plausible but uncertain future conditions (Lempert et al., 2006; Sarewitz et al., 2000; Volkery and Ribeiro, 2009). Watershed models such as the Hydrologic Simulation Program-FORTRAN (HSPF) and Soil and Water Assessment Tool (SWAT) have been widely applied to simulate watershed response under a range of watershed and hydroclimatic settings. Current global and regional climate models (GCMs, RCMs) are excellent tools for understanding the complex interactions and feedbacks associated with future emissions scenarios and identifying a set of plausible, internally consistent scenarios of future climatic conditions. Multiple scenarios can be evaluated to capture the full range of underlying uncertainties associated with different drivers such as future climate and land use change on water resources. This information can be useful to developing an improved understanding of

system behavior and sensitivity to a wide range of plausible future climatic conditions and events, identifying how we are most vulnerable to these changes, and ultimately to guide the development of robust strategies for reducing risk (Sarewitz et al., 2000).

2.1. ABOUT THIS REPORT

This report describes a large scale, watershed modeling effort designed to address gaps in our knowledge of the sensitivity of U.S. streamflow, nutrient (nitrogen and phosphorus) and sediment loading to potential mid-21st century climate change. Modeling also considers the potential interaction of climate change with future urban and residential development in these watersheds, and provides insights concerning the effects of different methodological choices (e.g., method of downscaling climate change data, choice of watershed model) on simulation results. This report documents the overall structure of this effort – including sites, methods, models, and scenarios – and provides results for each of the study areas.

A unique feature of this study is the use of a consistent watershed modeling methodology and a common set of climate and land-use change scenarios in multiple locations across the nation. It should be noted that several of the study watersheds are complex, highly managed systems. Given the difficulty and level of effort involved with modeling at this scale it was necessary to standardize model development for efficiency. We do not attempt to represent these all operational aspects in full detail. Simulation results are thus not intended as forecasts. Rather, the intent of this study is to assess the general sensitivity of underlying watershed processes to changes in climate and urban development and not to develop detailed, place-based models that represent all management and operational activities in full detail. Potential future changes in management and operational activities are also not considered in this study.

3. STUDY AREAS

This project evaluates watershed response to climate change in 20 large drainage basins located throughout the contiguous U.S. and Alaska (Table 1 and Figure 1**)**. Study areas were selected to represent a range of geographic, physiographic, land use, and hydroclimatic settings (Table 2). A detailed summary of current land-use and land cover in the 20 study areas is shown Table 3. Land use summaries are based on 2001 data from the National Land Cover Dataset (NLCD). Site selection also considered the availability of necessary data for calibration and validation of watershed models, and opportunities for leveraging the availability of pre-existing watershed models. Data needs for model calibration and validation include a selection of United States Geological Survey (USGS) streamflow monitoring gages (at varying spatial scales) and an adequate set of water quality monitoring data (e.g., USGS National Water Quality Assessment NAWQA study areas).

The 20 study areas are of a similar scale to HUC4 basins, ranging in size from approximately 6,000 to 27,000 mi^2, but do not correspond exactly with established HUC 4 basins. In some cases study areas are composed of a single, contiguous watershed. In other cases, study areas include several adjacent but non-contiguous watersheds (e.g., separate rivers draining to the coast). Where possible, watersheds strongly influenced by upstream dams, diversions, or other human interventions were avoided.

Five of the 20 sites were selected as "pilot" sites. The pilot sites were assessed for a wider range of climate and land use change scenarios than other study areas, and watershed simulations were developed independently using both the HSPF and SWAT watershed models. The results of simulations in the five pilot study watersheds were used to select a single watershed model and a reduced set of climate change scenarios to be used in simulations of the non-pilot watersheds. In addition to the general criteria for selection of study sites, the five pilot watersheds were selected to leverage pre-existing model applications, and to span a geographic range across the country. The study areas selected as pilot sites are the Minnesota River watershed (Minn), the Apalachicola-Chattahoochee-Flint River watersheds (ACF), the Willamette River watershed (Willa), the Salt/Verde/San Pedro River watershed (Ariz), and the Susquehanna River watershed (Susq).

Table 1. Site names, ID codes, and state locations of the 20 study areas.

Site ID	Watershed / Region	Location
ACF (pilot site)	Apalachicola-Chattahoochee-Flint Basins	GA, AL, FL
Ariz (pilot site)	Salt, Verde, and San Pedro River Basins	AZ
CenNeb	Loup/Elkhorn River Basin	NE
Cook	Cook Inlet Basin	AK
Erie	Lake Erie Drainages	OH, IN, MI
GaFla	Georgia-Florida Coastal Plain	GA, FL

Site ID	Watershed / Region	Location
Illin	Illinois River Basin	IL, WI, IN
Minn (pilot site)	Minnesota River Basin	MN, SD
NewEng	New England Coastal Basins	MA, ME, NH
Pont	Lake Pontchartrain Drainage	LA, MS
RioGra	Rio Grande Valley	CO, NM
Sac	Sacramento River Basin	CA
SoCal	Coastal Southern California Basins	CA
SoPlat	South Platte River Basin	CO, WY
Susq (pilot site)	Susquehanna River Basin	PA, MD, NY
TarNeu	Tar and Neuse River Basins	NC
Trin	Trinity River Basin	TX
UppCol	Upper Colorado River Basin	CO, UT
Willa (pilot site)	Willamette River Basin	OR
Yellow	Powder/Tongue River Basins	MT, WY

1

Figure 1. Locations of the 20 study areas.

Table 2. Summary of the 20 study areas.

Model Area	Pilot Status	Location (States)	Total Area (mi^2)	Elevation Range (ft MSL)	Percent Urban	Percent Acric.	Percent Forest	Avg Precip (in/yr)	Avg Temp (°F)	Major Cities
ACF	Pilot	GA, AL, FL	19,258	0 – 4,347	9.3	21.6	48.0	54.26	63.43	Atlanta, GA
Coastal Southern CA	Non-pilot	CA	6,978	0 – 11,488	36.4	3.9	11.3	20.21	61.2	Greater Los Angeles, CA
Cook Inlet	Non-pilot	AK	22,223	0 – 18,882	0.8	0.2	24.1	28.50	34.16	Anchorage, AK
Georgia-Florida Coastal Plain	Non-pilot	GA, FL	15,665	0 -485	10.1	17.9	36.2	53.21	68.24	Tallahassee, FL; Tampa, FL; Spring Hill, FL
Illinois River	Non-pilot	IL, IN, WI	17,004	365 – 1,183	18.1	68.1	10.3	38.25	49.00	Chicago, IL; Milwaukee, WI; Peoria, IL
Lake Erie	Non-pilot	OH, IN, MI	11,419	339 – 1,383	14.7	67.0	13.0	38.15	49.10	Fort Wayne, IN; Cleveland, OH; Akron, OH
Lake Pontchartrain	Non-pilot	LA, MS	5,570	0 - 502	11.3	14.7	24.0	66.33	66.64	New Orleans, LA; Baton Rouge, LA
Loup/Elkhorn Rivers	Non-pilot	NE	21,730	1,069 – 4,292	2.7	27.8	1.1	26.10	48.35	No major cities
Minnesota River	Pilot	MN, IA, SD	16,898	683 – 2,134	6.6	78.0	2.9	28.26	43.90	Mankato, MN, Minneapolis, MN
New England Coastal	Non-pilot	MA, NH, ME	10,225	0 – 5,422	16.5	5.6	63.7	48.45	46.23	Portland, ME, Greater Boston, MA
Powder/ Tongue Rivers	Non-pilot	MT, WY	18,729	2,201 – 13,138	0.5	1.6	10.0	17.70	44.15	No major cities
Rio Grande Valley	Non-pilot	NM, CO	15,316	4,726 – 14,173	2.8	5.9	43.7	15.18	44.71	Santa Fe, NM; Albuquerque, NM
Sacramento River	Non-pilot	CA	8,315	17 – 10,424	4.3	50.2	22.4	37.47	57.45	Chico, CA; Reading, CA
Salt/Verde/ San Pedro Rivers	Pilot	AZ	14,895	1,918 – 11,407	1.2	0.2	41.8	19.67	56.81	Flagstaff, AZ; Sierra Vista, AZ
South Platte River	Non-pilot	CO, WY	14,598	4,291 – 14,261	7.1	18	23.7	16.82	43.46	Fort Collins, CO; Denver, CO
Susque-hanna River	Pilot	PA, NY, MD	27,491	0 – 3,141	7.4	27.0	61.1	41.30	48.26	Scranton, PA; Harrisburg, PA
Tar/Neuse Rivers	Non-pilot	NC	9,821	0 - 854	9.4	28.6	33.5	49.91	59.91	Raleigh, NC; Durham, NC; Greenville, NC
Trinity River	Non-pilot	TX	13,119	0 – 2,150	18.6	37.7	22.4	40.65	64.78	Dallas, TX
Upper Colorado River	Non-pilot	CO, UT	17,772	4,323 – 14,303	1.4	4.3	54.0	16.36	41.73	Grand Junction, CO; Edwards, CO
Willamette River	Pilot	OR	11,203	0 – 10,451	7.2	20.7	56.2	58.38	51.19	Portland, OR; Salem, OR; Eugene, OR

Note: Precipitation and temperature are averages over the weather stations used in simulation for the modeling period (approximately 1970 – 2000, depending on model area).

Table 3. Current (2001) land use and land cover in the 20 study areas.

Model Area	Total Area (mi^2)	Water %	Barren %	Wetland %	Forest %	Shrub %	Pasture/ Hay %	Cultivated %	Developed pervious* %	Impervious %	Snow/ Ice %
ACF	19,258	1.85	0.35	9.31	47.96	9.64	9.12	12.44	7.28	2.04	0.00
Coastal Southern CA	6,978	0.55	0.58	0.35	11.31	46.94	0.93	2.99	20.87	15.48	0.00
Cook Inlet	22,223	2.55	18.99	7.59	24.12	38.06	0.05	0.11	0.58	0.24	7.71
Georgia-Florida Coastal Plain	15,665	0.77	0.20	24.64	36.17	10.20	6.48	11.42	7.90	2.22	0.00
Illinois River	17,004	1.86	0.10	1.44	10.26	0.13	5.54	62.55	11.91	6.19	0.00
Lake Erie	11,419	1.03	0.10	2.70	12.97	1.50	5.69	61.35	11.19	3.46	0.00
Lake Pont-chartrain	5,570	3.06	0.37	31.74	24.01	14.83	10.44	4.25	8.36	2.95	0.00
Loup/ Elkhorn Rivers	21,730	0.82	0.06	3.14	1.07	64.42	1.15	26.60	2.37	0.37	0.00
Minnesota River	16,898	2.97	0.10	4.90	2.85	4.63	5.85	72.14	5.51	1.05	0.00
Neuse/Tar Rivers	9,821	4.56	0.21	13.73	33.53	9.99	7.32	21.26	7.69	1.70	0.00
New England Coastal	10,225	4.06	0.44	7.59	63.66	2.16	4.52	1.10	10.88	5.59	0.00
Powder/ Tongue Rivers	18,729	0.08	0.66	1.69	10.04	85.50	0.58	0.98	0.40	0.08	0.00
Rio Grande Valley	15,316	0.39	1.29	2.60	43.68	43.35	5.06	0.83	2.14	0.68	0.00
Sacramento River	8,315	0.53	0.48	1.99	22.39	20.13	30.51	19.66	3.59	0.73	0.00
Salt/Verde/San Pedro Rivers	14,895	0.16	0.30	0.27	41.84	56.05	0.07	0.12	1.01	0.19	0.00
South Platte River	14,598	0.87	1.03	2.28	23.74	46.31	1.50	16.53	5.03	2.07	0.63
Susque-hanna River	27,491	1.14	0.36	1.24	61.12	1.80	17.13	9.83	5.87	1.50	0.00
Trinity River	13,119	5.10	0.46	10.66	22.44	5.06	28.12	9.58	12.88	5.70	0.00
Upper Colorado River	17,772	0.48	3.69	1.65	53.96	33.88	3.17	1.11	1.03	0.38	0.65
Willamette River	11,203	0.86	0.96	1.78	56.18	12.32	12.55	8.16	4.70	2.50	0.00

*Developed pervious land includes the pervious portion of open space and low, medium, and high density land uses.

3.1. DESCRIPTION OF STUDY AREAS

3.1.1. Apalachicola-Chattahoochee-Flint (ACF) River Basin (Pilot Study Area)

The Apalachicola-Chattahoochee-Flint (ACF) River basin is located in Georgia, Alabama, and Florida (Figure 2). The Chattahoochee and Flint Rivers merge to form the Apalachicola River, which flows through the panhandle of Florida into the Apalachicola Bay and into the Gulf of Mexico. The study area consists of 12 of the 13 HUC8s that make up HUC 0313 (excluding one small, separate coastal drainage), with a total area of 19,869 mi^2.

Approximately 64 percent of the basin is forested. Approximately 25 percent of these forests are timberlands used for manufacturing wood products. Agricultural land represents a mix of cropland, pasture, orchards, and areas of confined feeding for poultry and livestock production. The dominant agricultural land use in the Piedmont Province is pasture and confined feeding for dairy or livestock production. Most of the poultry operations in the ACF River basin are concentrated in the upper part of the Chattahoochee River basin. Row-crop agriculture, orchards, and silviculture are most common in the Coastal Plain areas. Common crops in the watershed include peanuts, corn, soybeans, wheat, and cotton. The largest concentration of urban land in the basin is in the Atlanta area. Nearly 90 percent of the total population in the basin lives in Georgia, and nearly 75 percent live in the Atlanta metropolitan area.

The ACF River basin is characterized by a warm and humid, temperate climate. Precipitation is greatest in the mountains and near the Gulf of Mexico, lowest in the center of the basin. Average annual precipitation in the basin is about 55 inches, but ranges from a low of 45 inches in the east-central part of the basin to a high of 60 inches in the Florida panhandle. Throughout the ACF River basin, low flows usually occur from September to November and peak flows usually occur from January to April when rainfall is high and evapotranspiration is low.

The basin is underlain by five major aquifer systems. The aquifers include the Floridan aquifer system, which is one of the most productive aquifers in the world and underlies about 100,000 mi^2 in Florida, southern Alabama, southern Georgia, and southern South Carolina. Basin hydrology is influenced by 16 reservoirs, 13 of which are on the Chattahoochee River. These reservoirs play a major role in controlling flow and influencing the quality of water in the basin.

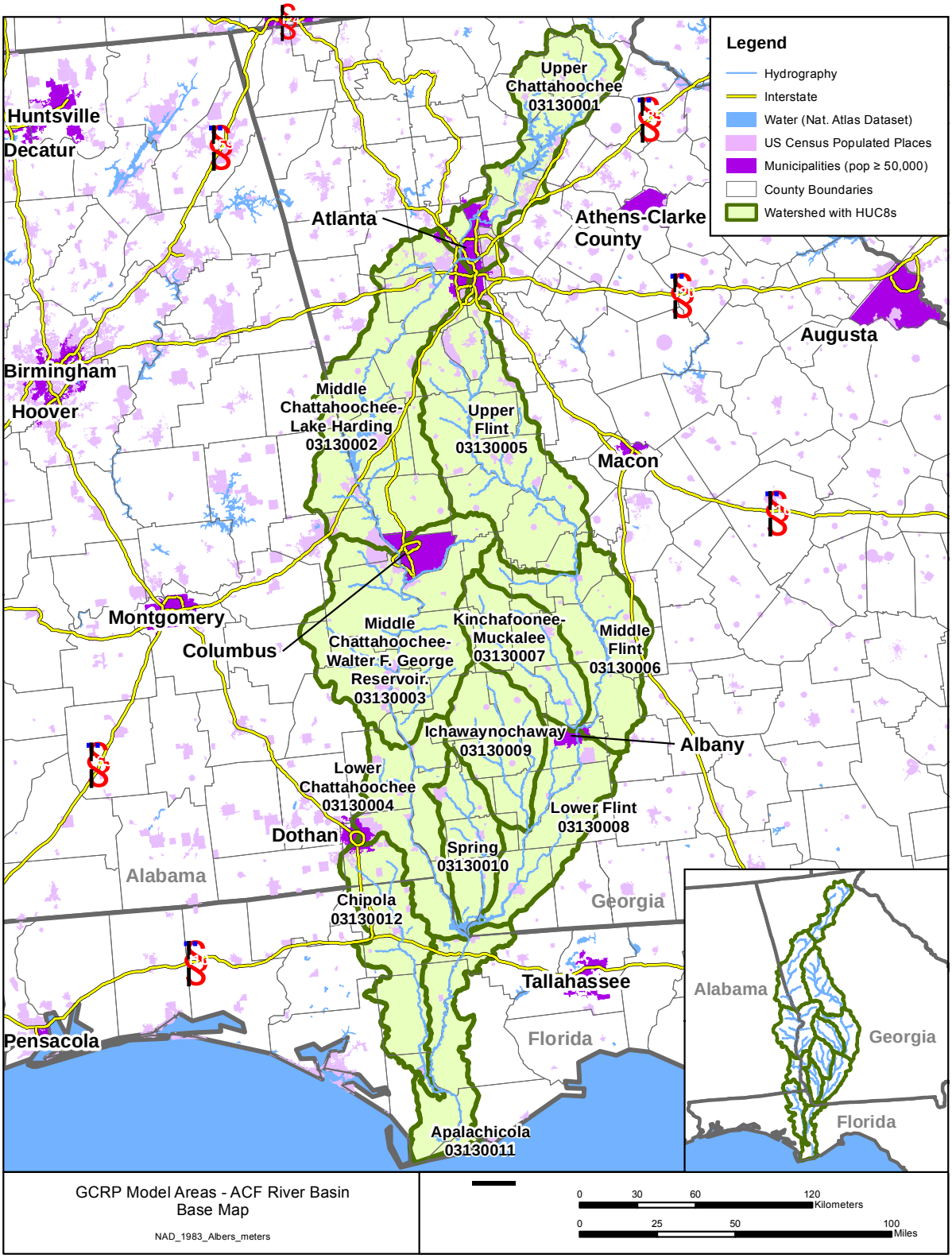

Figure 2. Apalachicola-Chattahoochee-Flint (ACF) River basin.

3.1.2. Minnesota River Basin (Pilot Study Area)

The Minnesota River (HUC 0702) constitutes 12 HUC8s, covering 16,901 mi^2, predominantly in the Western Corn Belt ecoregion (Figure 3). The Minnesota River Basin is located primarily in southern Minnesota with headwaters in South Dakota and is tributary to the Upper Mississippi River. Major cities include Mankato and Minneapolis, MN.

Precipitation, evapotranspiration, and air temperature exhibit a gradient from southwest to northeast, with a warmer, wetter climate to the southeast and a colder, drier climate to the northwest. Topography is flat to gently rolling, except in the area of the high bluffs adjoining the Minnesota River mainstem, created by glacial runoff. The dominant land use in the watershed is row crop agriculture (72 percent; mostly in corn / soybean rotation), with another 6 percent in pasture and hay. The surficial geology of the watershed consists of glacial till, moraines, and lake deposits and in its natural state was poorly drained with numerous lakes and wetlands. This topography was largely drained to establish agriculture and the use of tile drainage is now prevalent in the watershed.

The maximum streamflow occurs in spring and early summer as a result of rain and melting snow. Streamflow variation is greatest during late summer and fall, when precipitation ranges from drought conditions to locally heavy rains. Streamflow varies least during winter, when groundwater discharge to streams is dominant. Flow from the upper portions of the Minnesota River is influenced by Lac qui Parle, a U.S. Army Corps of Engineers impoundment of the Minnesota River near Montevideo, MN.

Water quality in the basin is affected by agricultural activities and point sources. The combination of extensive corn production and tile drainage results in a high risk of nitrogen export. Erosion, sedimentation, and turbidity problems are also frequent in the basin; however, analysis of radionuclide data suggests that only about a third of the sediment transported in stream channels is derived from upland sheet and rill erosion, with the remainder coming from gullies (often associated with tile drain outfalls), bank erosion, and bluff collapse.

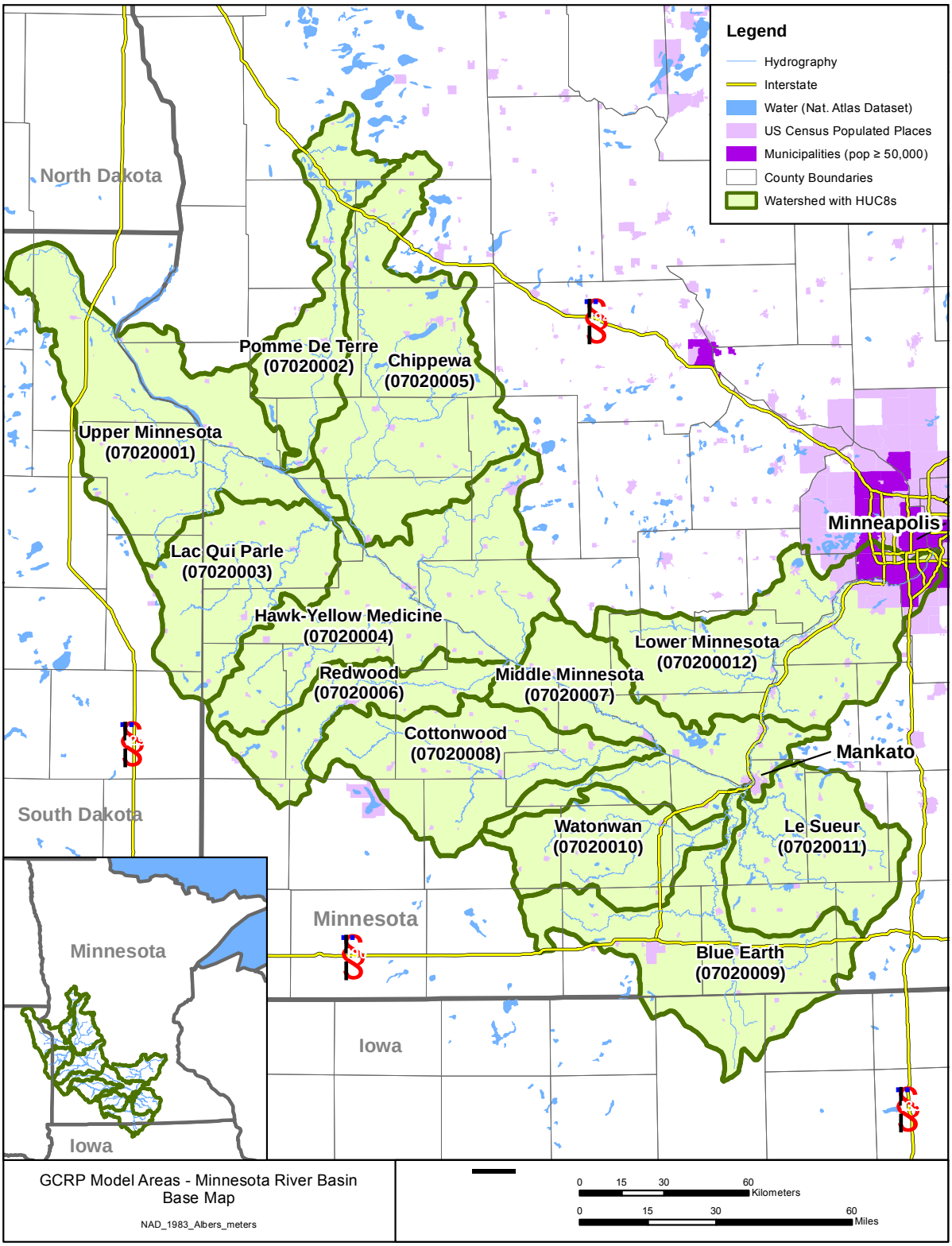

Figure 3. Minnesota River watershed.

3.1.3. Salt/Verde/San Pedro River Basin (Pilot Study Area)

The Central Arizona watersheds include areas dominated by ephemeral streams and significant impoundments. The selected model area includes perennial portions of the Salt and Verde River basins (in HUC 1506) that lie upstream of major impoundments, along with the San Pedro River (HUC 1505), for a total of 10 HUC8s with an area of 16,128 mi^2 (Figure 4 and Figure 5).

Land cover is primarily desert scrub and rangeland at low elevations with sparse forest at higher elevations (USGS, 2004; Cordy et al., 2000). The two major population centers of Arizona, Phoenix and Tucson, are located just downstream of the model area, while portions of Flagstaff, Prescott, and several smaller towns are within the Verde River watershed. Population growth is resulting in increasing demands on the limited water resources of the area. The climate is arid to semiarid and is characterized by variability from place to place as well as large differences in precipitation from one year to the next. Precipitation can be three times greater in wet years than in dry years.

The Verde and Salt River watersheds are in the Central Highlands hydrologic province, characterized by mountainous terrain with shallow, narrow intermountain basins. Forests and rangeland cover most of the area with limited areas of agriculture. Perennial streams derive their flow from mean annual precipitation of more than 25 inches in the mountains. The San Pedro watershed is in the Basin and Range Lowlands hydrologic province, characterized by deep, broad alluvial basins separated by mountain ranges of small areal extent characterize this hydrologic province. There is very little natural streamflow because of an average annual rainfall of less than 10 to 15 inches except at the highest elevations. With the exception of some small, higher elevation streams and sections of the San Pedro River supported by regional groundwater discharge, most perennial streams in the Basin and Range Lowlands are dependent on treated wastewater effluent for their year-round flow. Rangeland is the predominant land use in the Basin and Range Lowlands. Because of the general lack of surface water resources in the Basin and Range Lowlands, groundwater is relied upon heavily to meet agricultural and municipal demands. More than 50 percent of the water used in the CAZB is groundwater, which is often the sole source available.

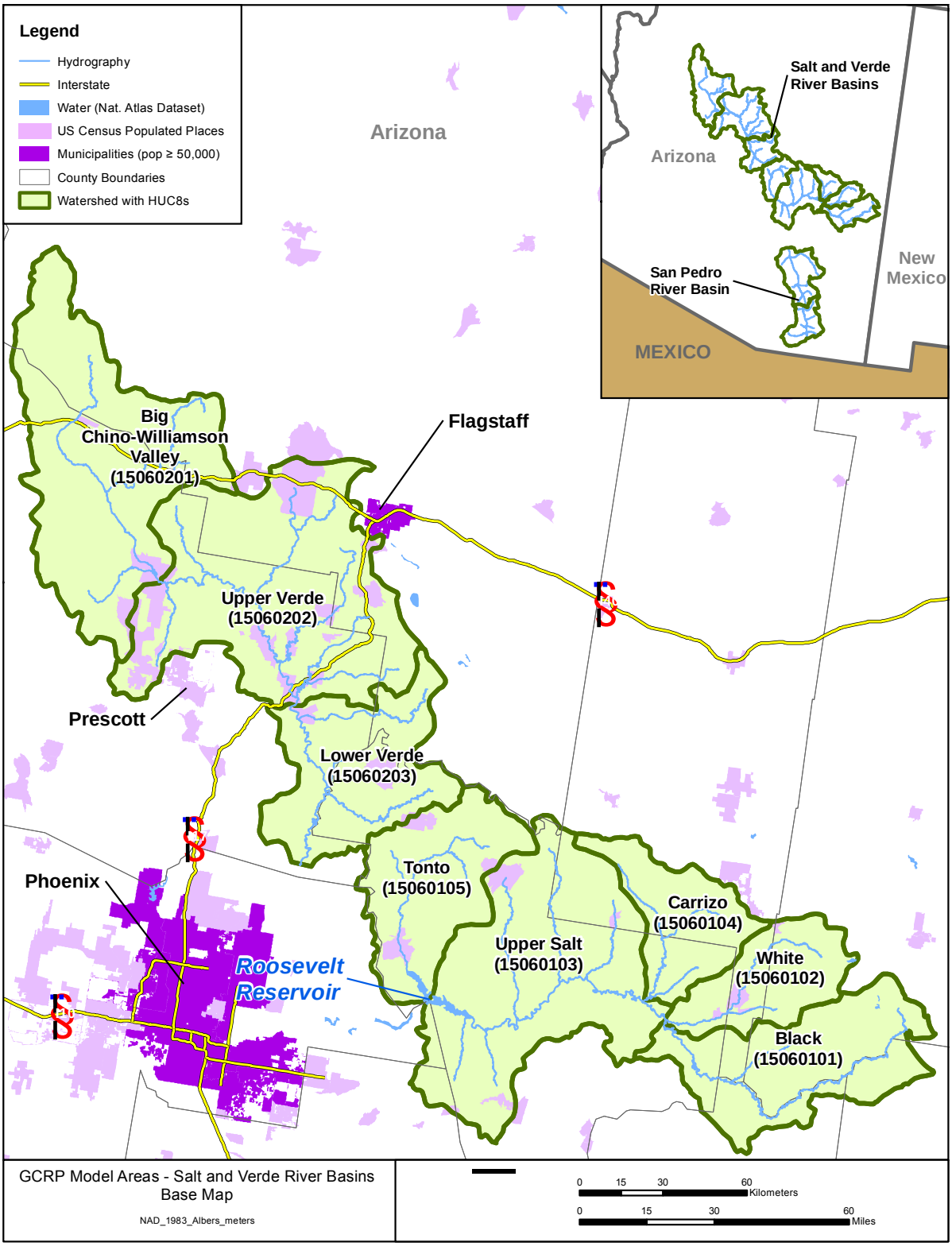

Figure 4. The Central Arizona basins – Verde and Salt River sections.

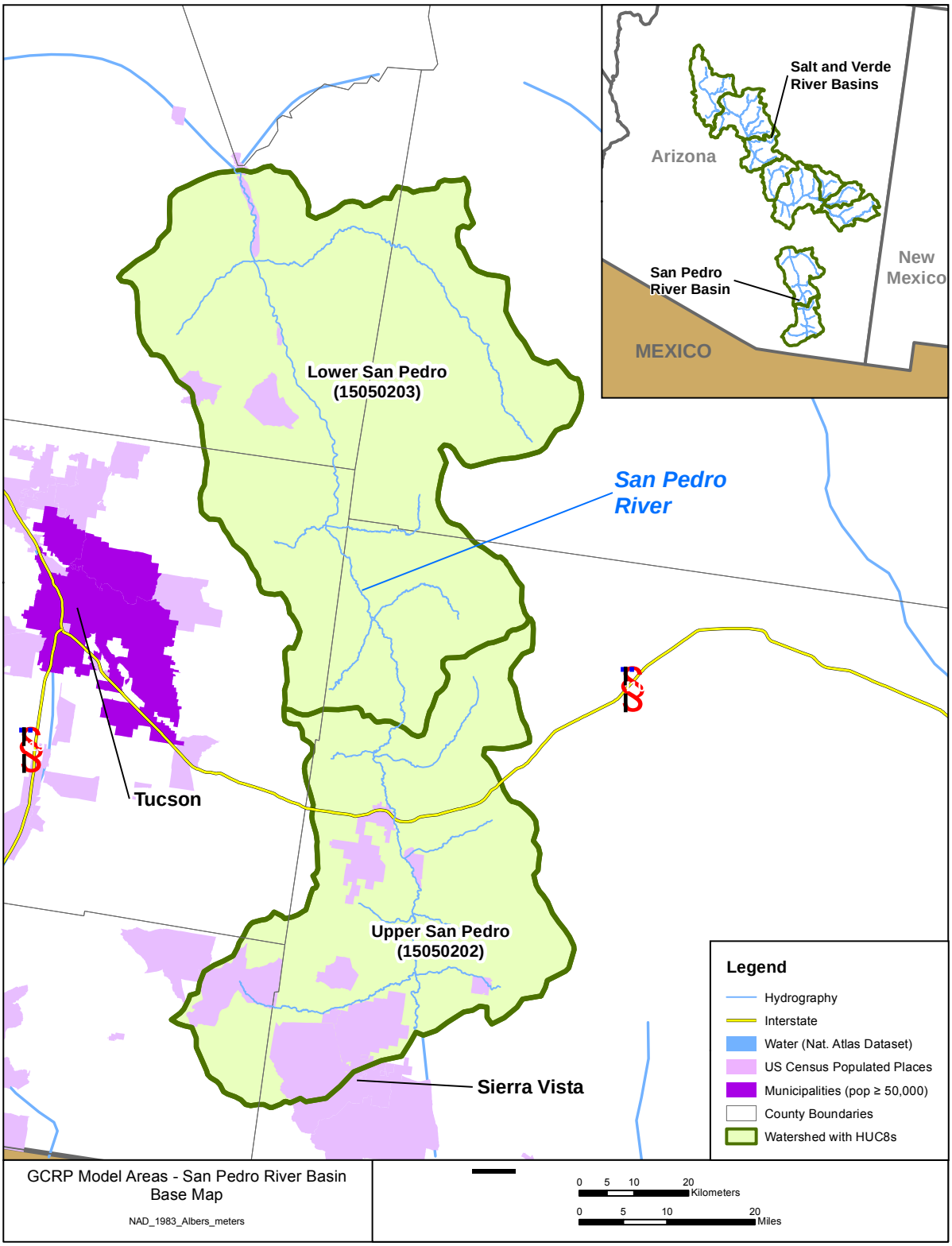

Figure 5. The Central Arizona basins – San Pedro River section.

3.1.4. Susquehanna River Basin (Pilot Study Area)

The entire Susquehanna River basin (upper and lower) was modeled for consistency with ongoing efforts by the Chesapeake Bay Program (Figure 6). The Susquehanna River drains about 27,500 mi^2 in the states of New York, Pennsylvania, and Maryland and includes a total of 19 HUC8s in HUC 2050. The watershed makes up 43 percent of the Chesapeake Bay's drainage area, providing 50 percent of its freshwater flows.

The Susquehanna River basin includes three physiographic provinces: the Appalachian Plateau, the Valley and Ridge, and the Piedmont Provinces (SRBC, 2008). The Appalachian Plateau Province is characterized by high, flat-topped hills and deep valleys cut by the Susquehanna River and its tributaries. The Valley and Ridge physiographic province contains steep mountains and ridges separated by valleys. The Piedmont physiographic province consists of uplands and lowlands. The Piedmont physiographic province generally has terrain that is gently rolling to hilly. Sixty-nine percent of the watershed is forested. However, the well-drained areas with rolling hills and valleys in the southern part of the basin contain most of the population and some of the most productive agricultural land in the U.S. The population centers are located in and around Binghamton, New York and Harrisburg, Lancaster, York, Lebanon, and Altoona, Pennsylvania.

The Susquehanna River basin has a continental type of climate. The average annual temperature in the basin ranges from about 44 degrees in the northern part of the basin to about 53 degrees in the southern part. Average annual precipitation is about 40 inches over the entire basin and ranges from 33 inches in the northern part of the basin to 46 inches in the southern part. Virtually all the major streams experience their highest flows in March, April, and May, when melting snows combine with spring rains. These three months account for about one-half of the yearly runoff. Flows are lowest in these streams during the summer and early fall months, with most streams falling to their lowest levels in September. The Susquehanna River basin is one of the country's most flood prone areas. Generally, floods occur each year somewhere in the basin, and major floods can occur in all seasons of the year, and a major flood occurs on average every 13 years.

Groundwater flow maintains the base flow of perennial streams during periods of little or no precipitation and constitutes an average of 50 percent of the flow of most streams at other times. The use of groundwater resources in the basin is extensive. Groundwater plays a critical role in supplying drinking water and maintaining economic viability. Outside of the major population centers, drinking water supplies are heavily dependent on groundwater wells. Approximately 20 percent of the basin population is served by public water suppliers that use groundwater as a source.

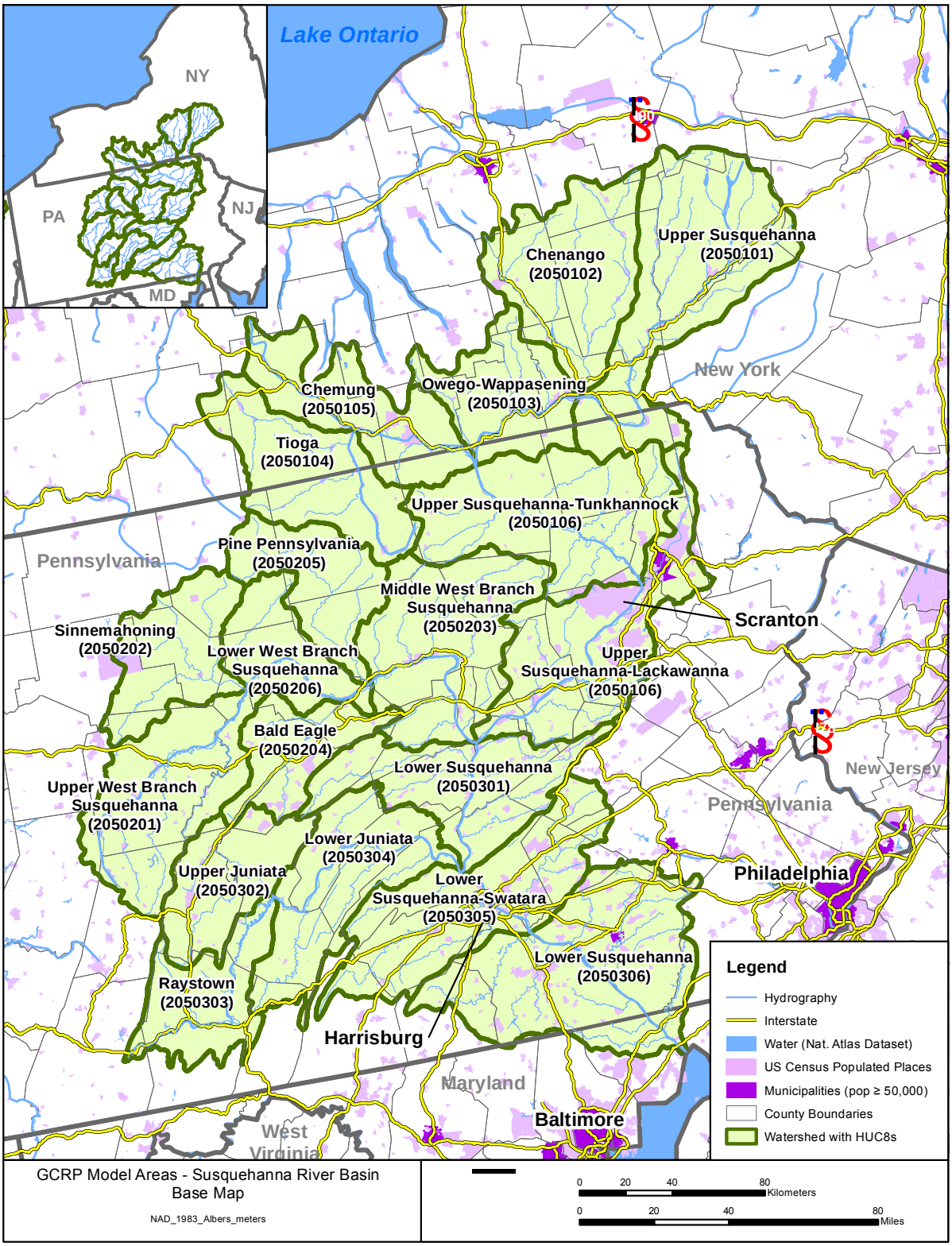

Figure 6. Susquehanna River watershed.

3.1.5. Willamette River Basin (Pilot Study Area)

The Willamette River basin is located in northwestern Oregon. The model study area is within HUC 1709, consisting of 11 HUC8s and covering 11,203 mi^2. The Willamette River is the 13^{th} largest river in the conterminous U.S. in terms of streamflow and produces more runoff per unit area than any of the larger rivers. It discharges to the Columbia River, which flows west to the Pacific Ocean along Oregon's northern border (Figure 7).

The basin is bordered on the west by the Coast Range, where elevations exceed 4,000 ft, and on the east by the Cascade Range, with several peaks higher than 10,000 ft. The Willamette Valley, with elevations near sea level, lies between the two ranges (USGS, 2001). Forested land covers approximately 70 percent of the watershed and dominates the foothills and mountains of the Coast and Cascade Ranges. Agricultural land, mostly cropland, comprises 22 percent of the basin and is located predominantly in the Willamette Valley. About one-third of the agricultural land is irrigated, and most of this is adjacent to the main stem Willamette River in the southern basin or scattered throughout the northern valley. Urban land comprises 6 percent of the watershed and is located primarily in the valley along the main stem Willamette River. The Willamette River flows through Portland, Oregon's largest metropolitan area, before entering the Columbia River. About 70 percent of Oregon's population lives in the Willamette basin.
The Willamette basin is characterized by cool, wet winters and warm, dry summers. About 70-80 percent of the annual precipitation falls from October through March. Most precipitation falls as snow above about the 5,000 ft level of the Cascades; however, the Coast Range and Willamette Valley receive relatively little snow. Mean monthly air temperatures in the valley range from about 3-5^{o} C during January to 17-20^{o} C during August. Although annual precipitation averages 62 inches in the Willamette basin, topography strongly influences its distribution. Yearly amounts range from 40-50 inches in the valley to as much as 200 inches near the crests of the Coast and Cascade Ranges.

Streamflow in the Willamette basin reflects the seasonal distribution of precipitation, with 60-85 percent of runoff occurring from October through March, but less than 10 percent occurring during July and August. Releases from 13 tributary reservoirs are managed for water quality enhancement by maintaining a flow of 6,000 cfs in the Willamette River at Salem during summer months. Flows in the lower Willamette River watershed are dominated by the effects of 13 reservoirs and their associated dams operated by the U.S. Army Corps of Engineers for water supply, flood control, and navigation. These reservoirs control much of the runoff from the southern and eastern mountainous portions of the watershed where precipitation and snow fall are highest. Incorporation of the reservoirs in the model was a significant part of the model development effort.

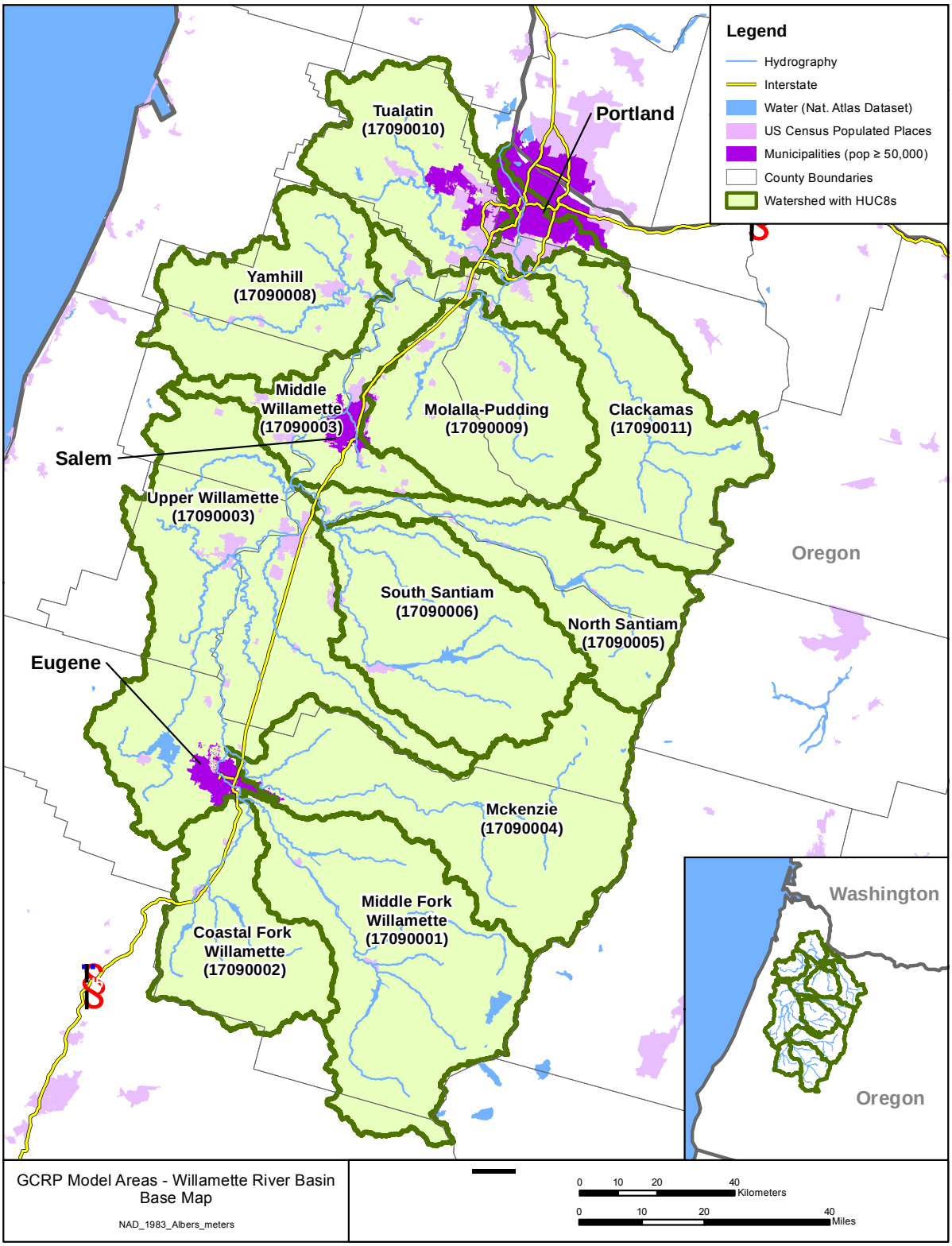

Figure 7. Willamette River watershed.

3.1.6. Coastal Southern California basins

The Coastal Southern California basins encompass a land area of over 11,000 mi^2 located along the southern coast of California. The modeled area includes 12 HUC8s within HUC 1807. Major subbasins included in this study are the Santa Clara River, Los Angeles River, San Gabriel River, Santa Ana River, San Juan River, and Santa Margarita River (Figure 8). The Coastal Southern California watersheds are characterized by a mild semi-arid climate with an average rainfall of 15 inches per year. The region is highly urbanized, with substantial amounts of residential, commercial, and industrial developed land (36 percent) on flatter terrain at lower elevations; the rugged mountains in the watershed are primarily in forest and rangeland, which together account for 58 percent of the area.

The Santa Clara River is the largest river system in southern California that remains in a relatively natural state. The watershed drains 1,634 mi^2 from its headwaters in the San Gabriel Mountains to its mouth at the Pacific Ocean. Ninety percent of the watershed consists of rugged mountains, ranging up to 8,800 feet high; the reminder consists of valley floor and coastal plain. The climate in the watershed varies from moist, Mediterranean in Ventura County near the Pacific coast to near desert at the extreme eastern boundary in Los Angeles County.

The Los Angeles and San Gabriel River watersheds are highly urbanized watersheds that encompass 835 mi^2 and 640 mi^2, respectively. The Los Angeles and San Gabriel Rivers both originate in mountainous areas including a large portion of the Angeles National Forest. They flow from the mountains into the San Fernando and San Gabriel Valleys. The rivers then continue on over the coastal plain of Los Angeles and eventually into the Pacific Ocean. Both rivers have been highly modified with dams (51 in the Los Angeles River watershed and 26 in San Gabriel River watershed). Virtually the entire Los Angeles River has been channelized and paved. The San Gabriel River is also channelized and developed for much of its length. These modifications have resulted in a loss of habitat and human access to the rivers. Diversion of water for use in groundwater recharge, significant discharges of sewage treatment plant reclaimed waters, and urban runoff have dramatically changed the natural hydrology of the rivers.

The Santa Ana River is the largest stream system in southern California and encompasses an area of about 2,700 mi^2 in parts of Orange, San Bernardino, Riverside, and Los Angeles Counties. The headwaters are in the San Bernardino Mountains, which reach altitudes over 10,000 feet. The river flows more than 100 miles to the Pacific Ocean. The population of over 4 million people relies on water resources that originate within the watershed as well as water imported from northern California and the Colorado River. The Santa Ana watershed is highly urbanized with about 32 percent of the land use residential, commercial, or industrial. Agricultural land use accounts for about 10 percent of the watershed. Under natural conditions, the Santa Ana River would be intermittent with little or no flow in the summer months. Groundwater is the main source of water supply in the watershed, providing about 66 percent of the consumptive water demand. Imported water from northern California and the Colorado River account for 27 percent of the consumptive demand. Other sources of supply include surface water derived from precipitation within the watershed (4 percent) and recycled water (3 percent).

The San Juan River watershed encompasses about 500 mi^2. Watershed concerns include channelization, poor surface water quality from discharge of nonpoint sources, loss of habitat in the floodplain, loss of riparian habitat, paving of the flood plain, decline of water supply and flows, biodiversity loss, invasive species, surface erosion, and over use of existing resources. The majority of the watershed is urbanized.

The Santa Margarita River watershed encompasses 750 mi^2. The headwaters are on Palomar Mountain and there are 27 miles of free-flowing river. It is the least disturbed river system south of the Santa Ynez River in Santa Barbara County. Unlike most of the rivers of the southern coast of California, the riparian habitat is of particularly high quality, and is essential for the protection of waterfowl and a number of endangered plants and animals.

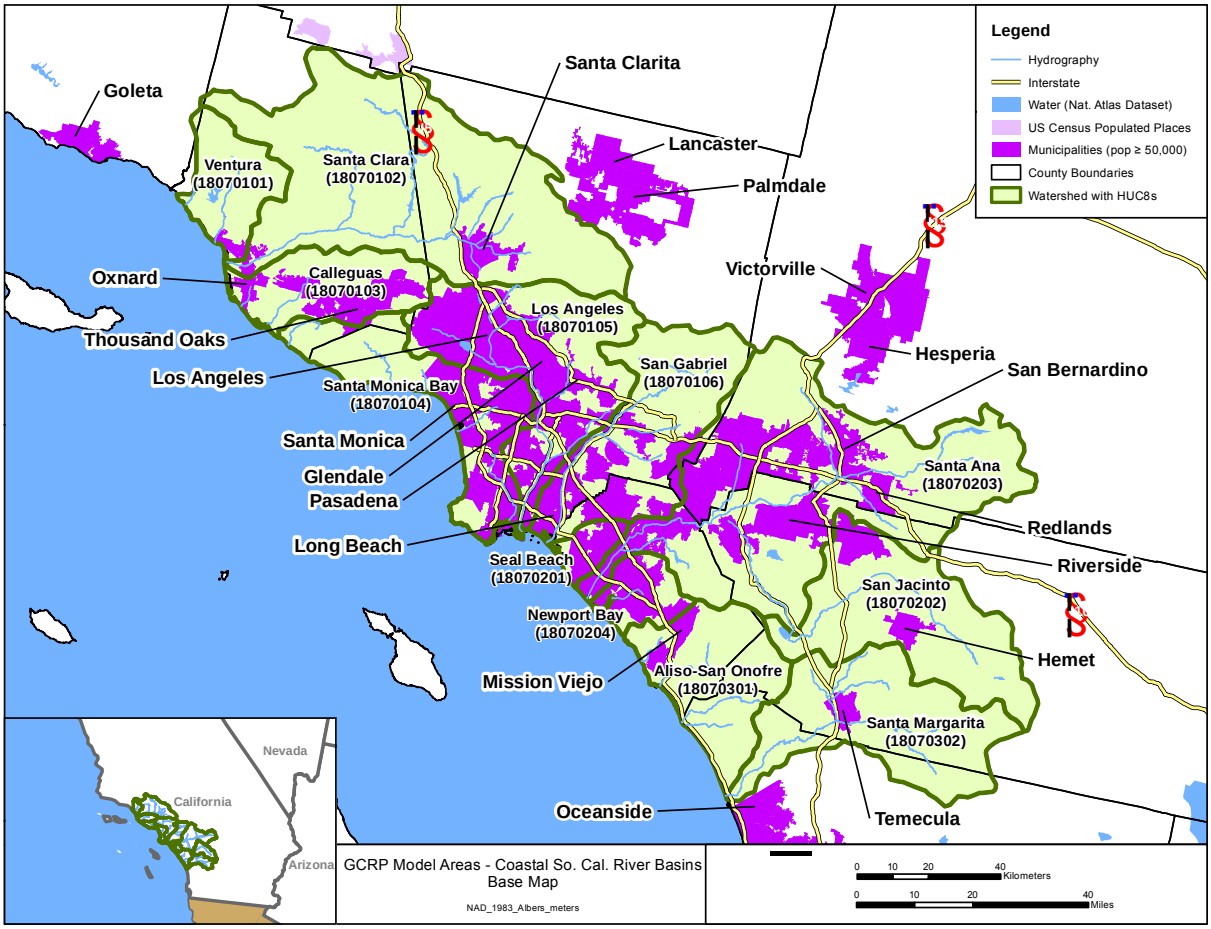

Figure 8. Coastal Southern California River basins model area.

3.1.7. Cook Inlet basin

The Cook Inlet stretches 180 miles (290 km) from the Gulf of Alaska to Anchorage in south-central Alaska. The watershed draining to Cook Inlet covers 47,000 square miles east of the Aleutian Range and south of the Alaska Range including the drainage area of Mount McKinley (Figure 9). The model area includes seven HUC8s within HUC 1902. The Cook Inlet watershed receives water from its tributaries the Kenai, the Susitna and Matanuska rivers from the melting snow and ice from Mount McKinley, the Chugach Mountains, and the Aleutian Range. Cook Inlet branches into the Knik Arm and Turnagain Arm at its northern end, almost surrounding Anchorage.

The watershed is dominated by igneous rocks in the mountains and by continental shelf and alluvial deposits in the lowlands. Glaciation has dramatically altered the landscape and glaciers are extensive on the southeastern and northwestern boundaries of the watershed. Five physiographic regions – grading from plains and lowlands to extremely high rugged mountains – are represented in the watershed. Altitude ranges from sea level to 20,320 ft at the highest point in North America, Mount McKinley. Rugged mountains surround Cook Inlet and include four active volcanoes on the western side of the inlet. Precipitation is closely associated with altitude and ranges from about 15 to more than 200 inches annually (USGS, 2008b).

Numerous river systems drain the watershed, including the Susitna, Matanuska, and Kenai Rivers. The largest river, the Susitna, drains about half of the watershed. Most rivers have relatively small drainages but yield large quantities of water because of substantial snowfall in the mountains. Many streams are fed by glaciers and have different physical characteristics than streams that do not have glacial contributions. Glacier-fed streams have periods of sustained high flow during summers and are more turbid than streams lacking glacial contributions. Numerous wetlands and lakes also influence the physical and chemical characteristics of streams by moderating peak flows and trapping sediment and nutrients.

Land cover is dominated by forests (30 percent). Glaciers cover 20 percent of the area, and lakes and wetlands cover another 12 percent. Less than 1 percent of the basin is used for agricultural purposes. The Municipality of Anchorage dominates the urban and residential features of the basin; however, the total urban and residential land cover is less than 1 percent of the basin. More than half of the state's population lives in the metropolitan Anchorage area. Expansion of suburban areas continues to the north of Anchorage and residential density is increasing throughout the municipality. The remainder of the basin is largely unpopulated; however, native villages exist at a number of locations.

Watersheds of the Cook Inlet basin are largely undeveloped and contain parts of four national parks totaling about 6,300 mi^2. Nearly 1,800 mi^2 of the Chugach National Forest and the 3,000 mi^2 Kenai National Wildlife Refuge also are within the boundaries of the watershed.

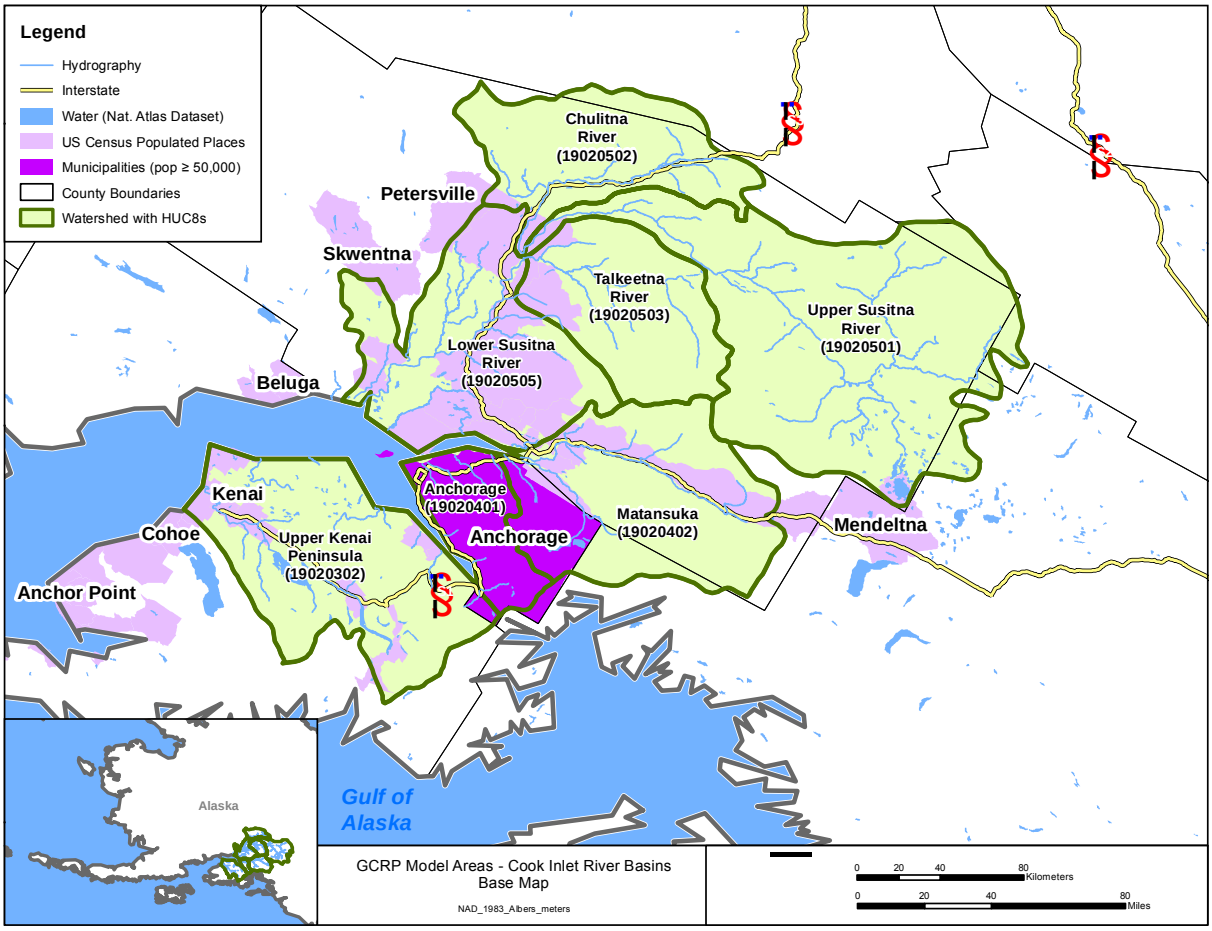

Figure 9. Cook Inlet basin model area.

3.1.8. Georgia-Florida Coastal basins

The Georgia-Florida Coastal Plain basins model covers an area about 15,665 mi^2 in portions of Georgia and Florida. The modeled area includes 15 HUC8s in two groups, one group draining to Tampa Bay (HUC 0310) and the remainder in southern Georgia and northwest Florida (in HUC 0311 and 0312; Figure 10). The watershed contains an EPA ORD Ecosystems Research Area (in the Tampa Bay drainage) and Tampa Bay is part of EPA's National Estuary Program.

Climate in the watershed is humid subtropical and influenced by air masses from the Gulf of Mexico. Average annual rainfall is around 45 to 53 inches per year, while the average annual temperatures is around 70 – 72 °F. The majority of precipitation is associated with summer convective storms, and tropical storms cross the area frequently.

The major land uses in the watershed include forest, agriculture (citrus and row crops), wetlands, urban, and rangeland. Forested areas cover approximately 36 percent of the watershed. Much of the forest lands are softwood pines used to manufacture paper products (facial tissue, toilet paper, hand towels, bags, and boxes). Wetlands occupy about 25 percent of the watershed. Cultivated land covers approximately 11 percent, while developed land occupies over 10 percent of the area.

The populations of cities in the watershed increased from 10 to 30 percent between 1990 and 1999. The largest city in the watershed is Tampa, FL. Most water used in the watershed is derived from groundwater, primarily from the highly productive Floridan aquifer system.

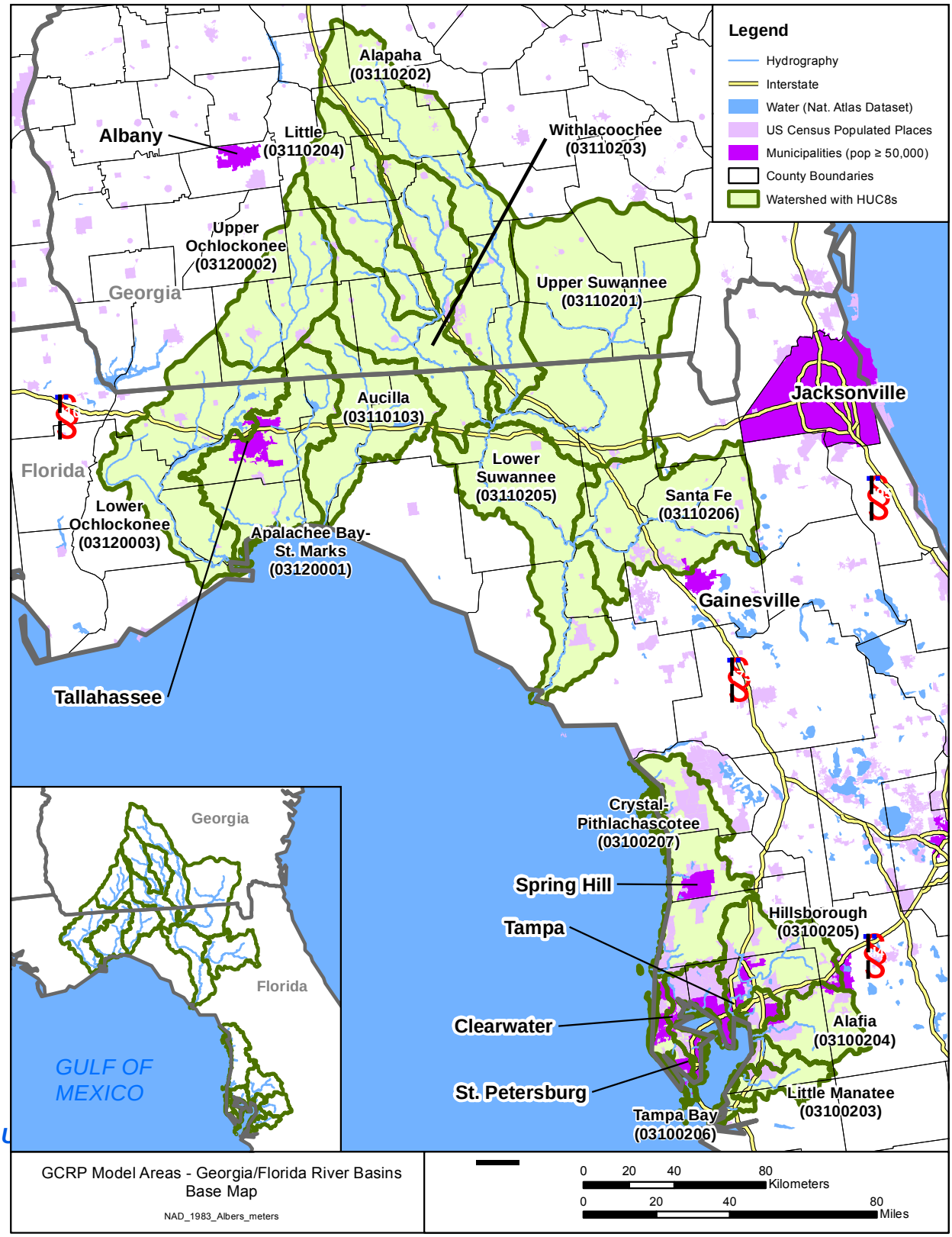

Figure 10. Georgia-Florida Coastal Plain basins model area.

3.1.9. Upper Illinois River basin

The Illinois River is approximately 273 miles in length and is one of the major tributaries to the Mississippi River. The Illinois River joins the Mississippi River near Grafton, IL, about 20 miles upstream from the confluence of the Missouri and the Mississippi rivers. This study addresses the upper portion of the basin (Figure 11), which has a drainage area of 17,004 mi^2 (44,040 km^2) and includes eleven HUC8s within HUC 0712 and HUC 0713 (Figure 11).

Within the upper portion of the basin (HUC 0712), over 80 percent of the land area is classified as part of the Central Corn Belt Plains ecoregion. With the exception of the Chicago metropolitan area, land use in the Central Corn Belt Plains is mostly corn and soybean cultivation for livestock feed crops and some livestock production. The flat topography of the lower portion of the basin (HUC 0713) is in the Till Plains Section of the Central Lowland physiographic province. The altitude of the land surface ranges from 600 to 800 ft above sea level. The area of greatest topographic relief is along the river valley, where topographic relief can range from 200 to 400 ft. The majority of the basin is extremely flat with less than 20 ft of relief.

Agriculture accounts for about 63 percent of the land use in the study area. Most of the recent urbanization is the result of development of new suburban and residential areas. Urban areas account for about 18 percent of the land use in the basin and are mainly concentrated in the metropolitan areas in and around Chicago. Forests cover about 10 percent of the study area and are concentrated along large-stream riparian areas.

Wetlands now make up a relatively small amount (1 percent) of land cover, but were once a major feature of the basin. The majority of wetlands in the basin were drained prior to the 1850's for the development of farmland. Remaining wetlands in the basin are mainly in riparian areas.

The climate of the Illinois River basin is classified as humid continental because of the cool, dry winters and warm, humid summers. The average annual temperature for the UIRB ranges from 46° F in the north of the basin to 55° F in the south of the study area. Lake Michigan has a moderating effect on temperature near the shoreline. Average annual precipitation, including snowfall, ranges from less than 32 inches in the northern Wisconsin part of the basin to more than 38 inches near the southern and eastern Lake Michigan shoreline in the Indiana part of the basin.

Streamflow in the study area consists of overland flow, groundwater discharge, agricultural drainage, and point-source return flow. Local flooding generally is caused by isolated thunderstorms, whereas widespread flooding is caused by more extensive thunderstorms that cover a wide area, by rapid snowmelt in the spring, or by a combination of these factors. Flooding is common in the basin, in some years resulting in significant loss of life and property.

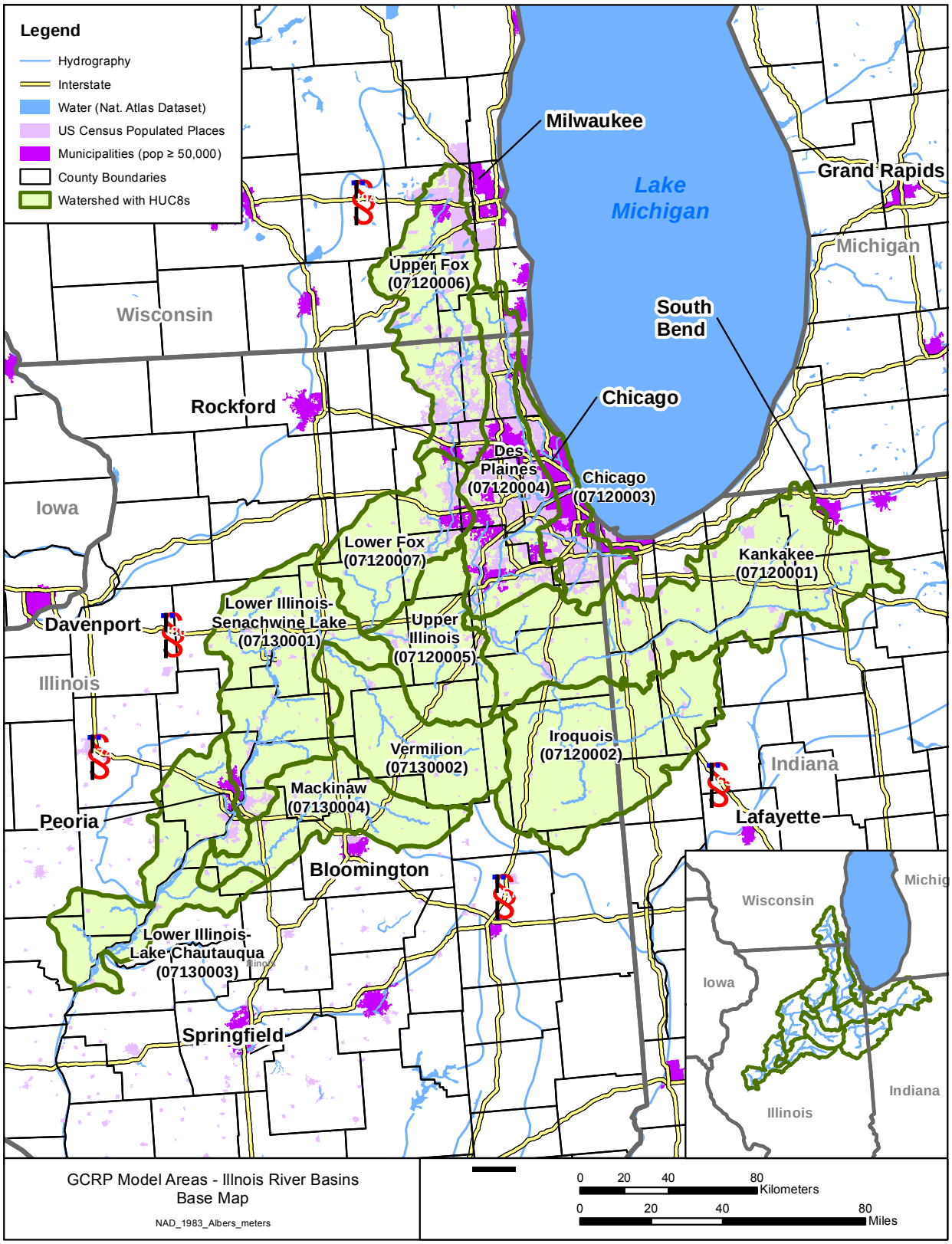

Figure 11. Illinois River basin model area.

3.1.10. Lake Erie Drainages

Lake Erie is the eleventh largest freshwater lake in the world. About two-thirds of the contributing watershed is in the United States, and includes portions of Michigan, Indiana, Ohio, Pennsylvania, and New York. The model study area focuses on drainages to the southwestern portion of Lake Erie and encompasses over 11,400 mi^2 in 11 HUC8s, all within HUC 0411 (Figure 12).

Situated in two major physiographic provinces, the Appalachian Plateaus and the Central Lowland, the watershed includes varied topographic and geomorphic features that affect the hydrology. The watershed consists of multiple independent drainages. The principal river in the study unit, the Maumee River, drains an area of 6,608 mi^2, or roughly one-third of the model study area. Other principal streams and their drainage areas in Ohio are the Sandusky River (1,420 mi^2, the Cuyahoga River (809 mi^2), and the Grand River (705 mi^2). The land surface is gently rolling to nearly flat (Myers et al., 2000).

The majority of the land use in the model area is agriculture (61 percent). The remaining land uses are urban land (18 percent), forest (10 percent), and open water or wetlands (3 percent). Corn, soybeans, and wheat are the typical parts in the western part of the basin. Other agricultural land uses include pasture and forage crops, grown predominantly in the eastern part of the basin. Forest and wetlands have been greatly reduced in the watershed since the mid-1800s. Major urban areas in the model area include Cleveland, Toledo, and Akron, Ohio, along with Fort Wayne, Indiana. These cities are important industrial and manufacturing centers. Major urban centers rely on abundant supplies of water for shipping, electric power generation, industry, domestic consumption, and waste assimilation.

Average annual precipitation across the model study area ranges from about 30 to 45 inches. Precipitation is highest to the northeast because of lake effect. The lowest amounts of precipitation are in the northwestern part of the basin near the Michigan border. The highest streamflows are typically in February, March, and April, as a result of increased precipitation, cold temperatures and little vegetative growth. The lowest streamflows are in August, September, and October. During low streamflow, groundwater typically contributes most of the flow.

Cooling during power generation accounts for 71 percent of the water use in the watershed. Public and domestic supply account for 17 percent, and industry and mining account for 10 percent of the total water use. Normal precipitation is generally adequate for agriculture, so irrigation accounts for less than 1 percent of water use. Most of the major cities are near Lake Erie and Lake Saint Clair and derive their water from the lakes or their connecting channels.

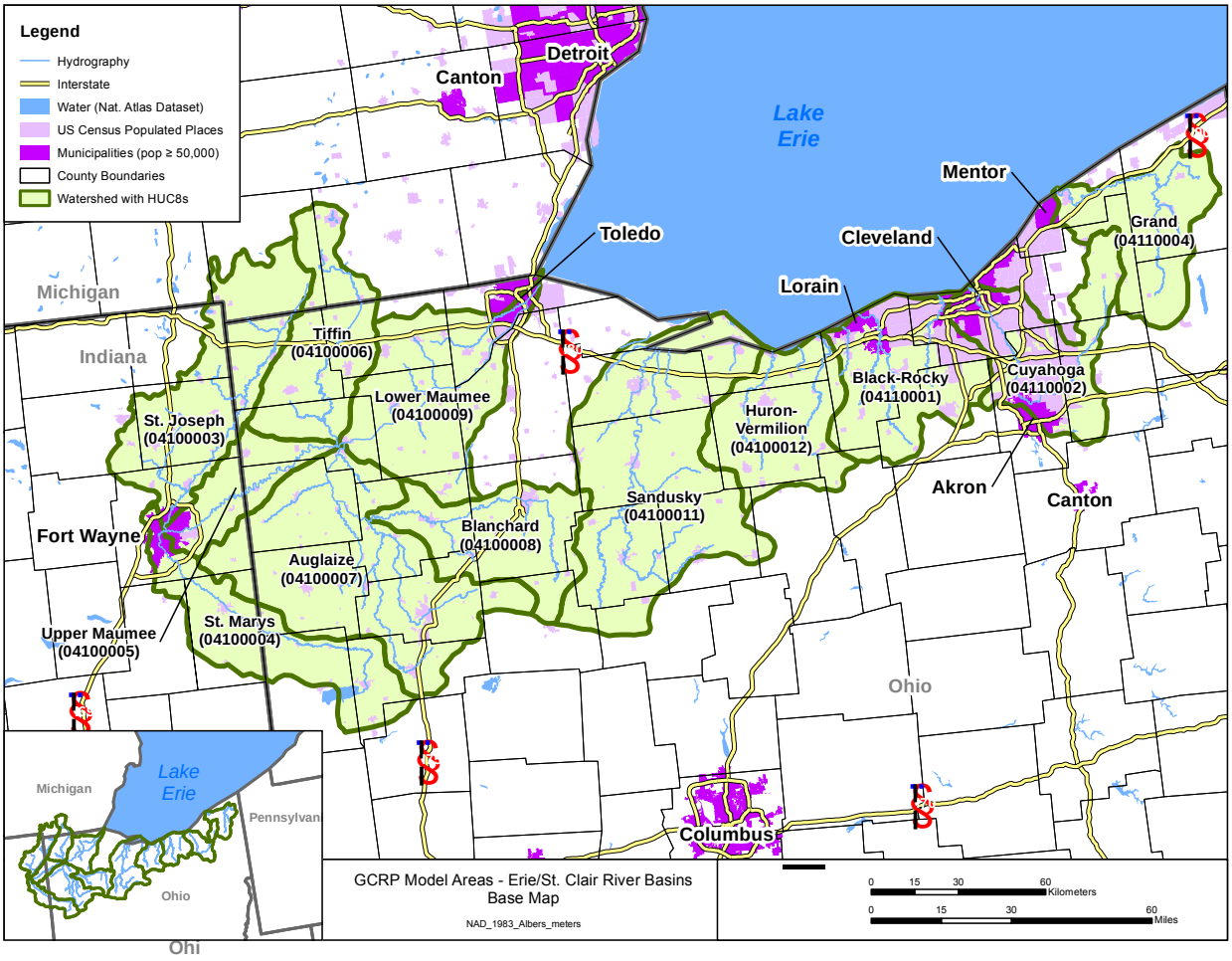

Figure 12. Lake Erie drainages model area.

3.1.11. Lake Pontchartrain basin

The Acadian-Pontchartrain NAWQA study area encompasses 26,408 mi^2 in the southern half of Louisiana and includes downstream portions of major rivers, such as the Mississippi with drainage areas far larger than the target size for this project. Therefore, the focus of modeling in this study was the Pontchartrain portion of the study area, including the rivers that drain to Lake Pontchartrain and the cities of New Orleans and Baton Rouge (Figure 13). The resulting model area encompasses over 5,500 mi^2 and seven HUC8s within HUCs 0807 and 0809.

The entire model area is near sea level and frequently impacted by tropical storms from the Gulf of Mexico. The climate is classified as humid subtropical, with an average annual temperature around 70 °F and average annual precipitation of 64 inches per year (USGS, 2002).

Ecosystems and communities in the watershed include cypress-tupelo swamp; freshwater marsh; saltwater marsh; wet prairie; oak cheniers; bottomland hardwood forest; Piney Hills; and longleaf pine savanna. The coastal zone of the watershed is affected by the ocean and its tides. Different wetland types are determined by the salinity of the water in them, which may infiltrate naturally through bayous or reach further inland through canals.

Land uses include a mixture of urban and rapidly urbanizing/industrial areas (11 percent), large areas of mixed forest and pasture (34 percent), wetlands (32 percent) and areas of rice and sugarcane crops (4 percent). Population is rapidly increasing on the north shore of Lake Pontchartrain and surrounding Baton Rouge, causing changes in rainfall-runoff characteristics and quality. Urban streams in the Baton Rouge area are usually channelized, and cleared of woody vegetation to speed drainage during high water.

Surface water in the watershed includes the lower Mississippi delta and wet prairie streams as well as upland streams. Lower Mississippi delta and wet prairie streams tend to have very slow flow, and water can also be pushed upstream by tides or wind causing generally stagnant, backwater conditions. Wetlands develop naturally in poorly drained areas. Streams in the uplands have a moderate flow gradient and sandy, shifting beds that are reshaped quickly in the fast water that is usual for flood conditions.

Modifications to flow include levees, and canals and drainage. Levees are created both naturally during the flooding process (sediment drops out of floodwater next to the waterbody) and by man along many bayous and rivers to reduce floods and to maintain a deeper channel for shipping.

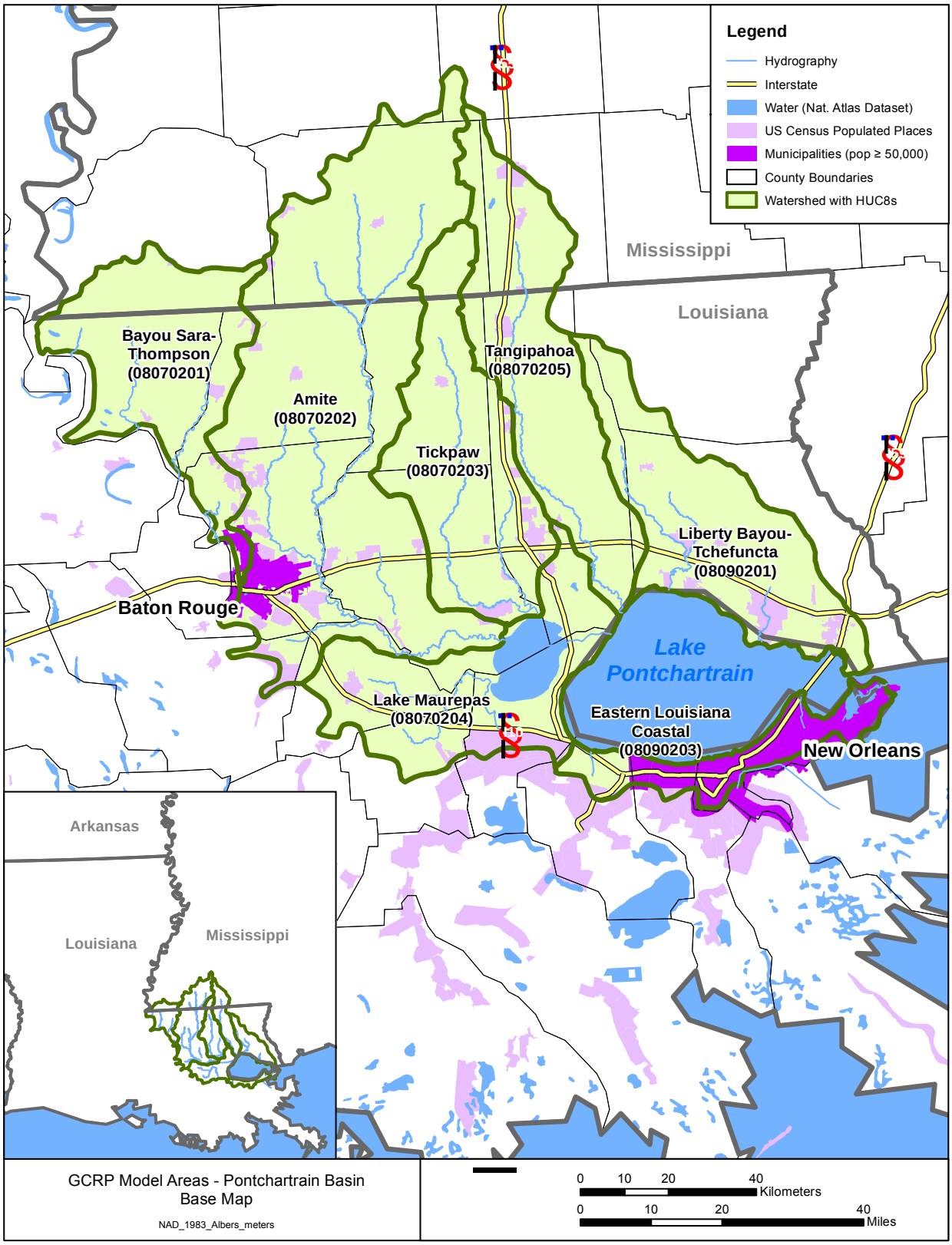

Figure 13. Lake Pontchartrain basin model area.

3.1.12. Loup/Elkhorn River basin

The Loup and Elkhorn River basins are tributary to the Platte River in the Central Nebraska NAWQA study area (Huntzinger and Ellis, 1993). Together they include 15 HUC8s within HUC 1021 and 1022 and cover approximately 21,500 mi^2 (Figure 14).

The watershed provides representation of rangeland and cropland in the Central Plains ecoregion (Huntzinger and Ellis, 1993). The city of Omaha lies just outside the watershed. The portion of the watershed along the eastern boundary is influenced by the Omaha suburban area and is located near the mouth of the Platte River. Most of the water in the watershed is consumed by irrigation or used for power generation and returned to the stream for reuse. The water used for irrigation is primarily from groundwater. The few urban areas within the watershed, such as Lincoln and Grand Island, use groundwater as a municipal water supply. The city of Omaha obtains part of its water supply from wells in the Elkhorn and Platte River Valleys.

The watershed is dominated by rural areas. The land use is predominantly pasture and rangeland (64 percent) and croplands of row-cropped feed grains (27 percent). Groundwater development for irrigation has increased the productivity of agriculture in the valleys and uplands. Large areas have soils well suited to cultivated crops whereas other large areas are not suited to crops but to productive grasslands. Counties that are primarily cropland agriculture without urban areas have population densities of 50 persons per square mile or less. Areas in the west that are primarily rangeland have population densities of less than five persons per square mile.

The Loup River and its major tributaries originate in the Nebraska Sandhills, a region of steep grass-covered dunes, and then flows through dissected plains with broad valleys. Permeable soils and subsurface materials in the Loup River basin provide flows sustained by shallow groundwater and little if any runoff. The Elkhorn River, in the eastern and northeastern part of the watershed, flows through rolling hills and well-defined valleys of stable glacial material in the Western Corn Belt Plains except where it originates in the Sandhills. Runoff in the Elkhorn basin is the largest in the watershed because of the steeper slopes and fine-grained soils.

The central Nebraska climate ranges from semiarid in the northwest to subhumid in the east. Hot summers, cold winters, and large daily and annual variations in temperature are typical. Precipitation is greatest in May and June. Mean annual precipitation varies from about 18 inches in the western part of the watershed to about 30 inches in the eastern part. Most of the study unit has at least 20 inches of annual precipitation, and more than one-half occurs during the growing season, April through September. Snowfall is a dominant climatic characteristic of central Nebraska. Mean annual snowfall ranges from about 25 inches in the southeast to about 35 inches in the northwest.

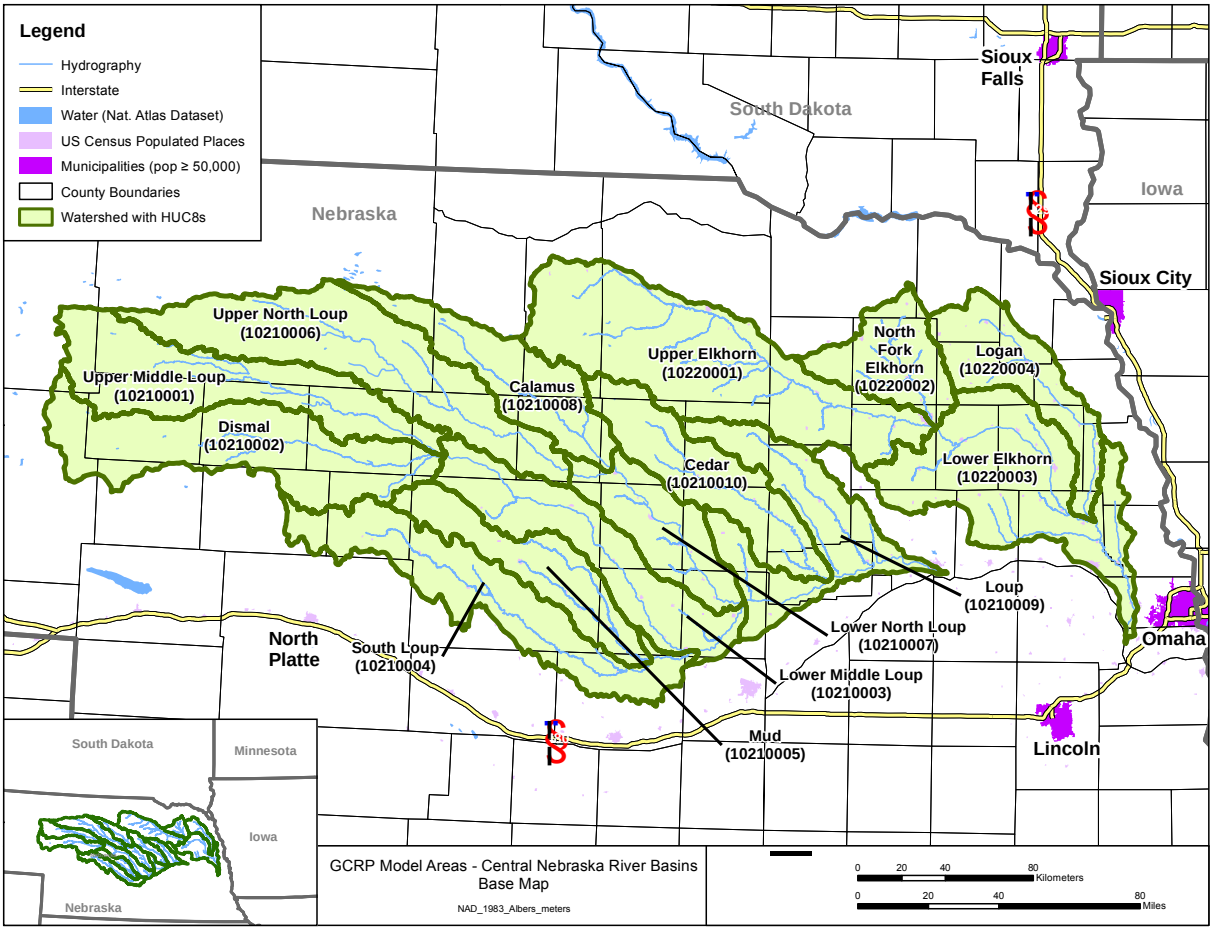

Figure 14. Loup and Elkhorn River basins model area.

3.1.13. Tar/Neuse River basins

The Tar and Neuse River drainages (Figure 15) are located entirely within North Carolina, and drain to two important estuaries (Pamlico and Neuse Estuaries) that have been impacted by excess nutrient loads. The watershed covers an area of 9,821 mi^2 in 8 HUC8s, all within HUC 0302. The watershed is divided between the Piedmont, and Coastal Plain physiographic provinces. Land-surface elevations range from about 885 feet above sea level in the Piedmont northwest of Durham to sea level in the eastern Coastal Plain (McMahon and Lloyd, 1995).

The watershed as a whole is dominated by forested (34 percent) and agricultural crop and pasture land (29 percent). Agricultural land in the study area is used primarily for growing crops (soybeans, corn, wheat, peanuts, tobacco, and cotton) and raising livestock (chickens, turkeys, hogs, and cattle.)

Less than 10 percent of the watershed consists of developed land, primarily in and around the cities of Raleigh, Durham, and Greenville, NC are prominent in the eastern third of the watershed and occupy 13 percent of the study area.

Average annual temperatures in the watershed range from about 58 °F in the western headwaters to slightly more than 62° F along Pamlico Sound in the eastern part of the Coastal Plain. Average annual precipitation ranges from about 44 to about 55 inches per year, but can be much greater in years

impacted by tropical storms. The highest average monthly streamflow typically occurs during the months that include the non-growing season when temperatures are low and evapotranspiration rates are low. The lowest average monthly streamflow occurs during the growing season when evapotranspiration rates are high. Groundwater is a significant component of the total water discharged to the Albemarle-Pamlico estuarine system.

The greatest uses of surface water in the Albemarle-Pamlico drainage basin are for public water supplies and thermoelectric power. Domestic groundwater use and agricultural surface water use are comparable in size, and both are slightly less than groundwater use for public water supplies. Surface water use is highest in areas with large urban populations served by surface water diversions for public water supplies (e.g., Neuse River basin) and in areas with large commercial, industrial, or mining water users (e.g., the Tar-Pamlico River basin). Groundwater use is generally highest in the Coastal Plain.

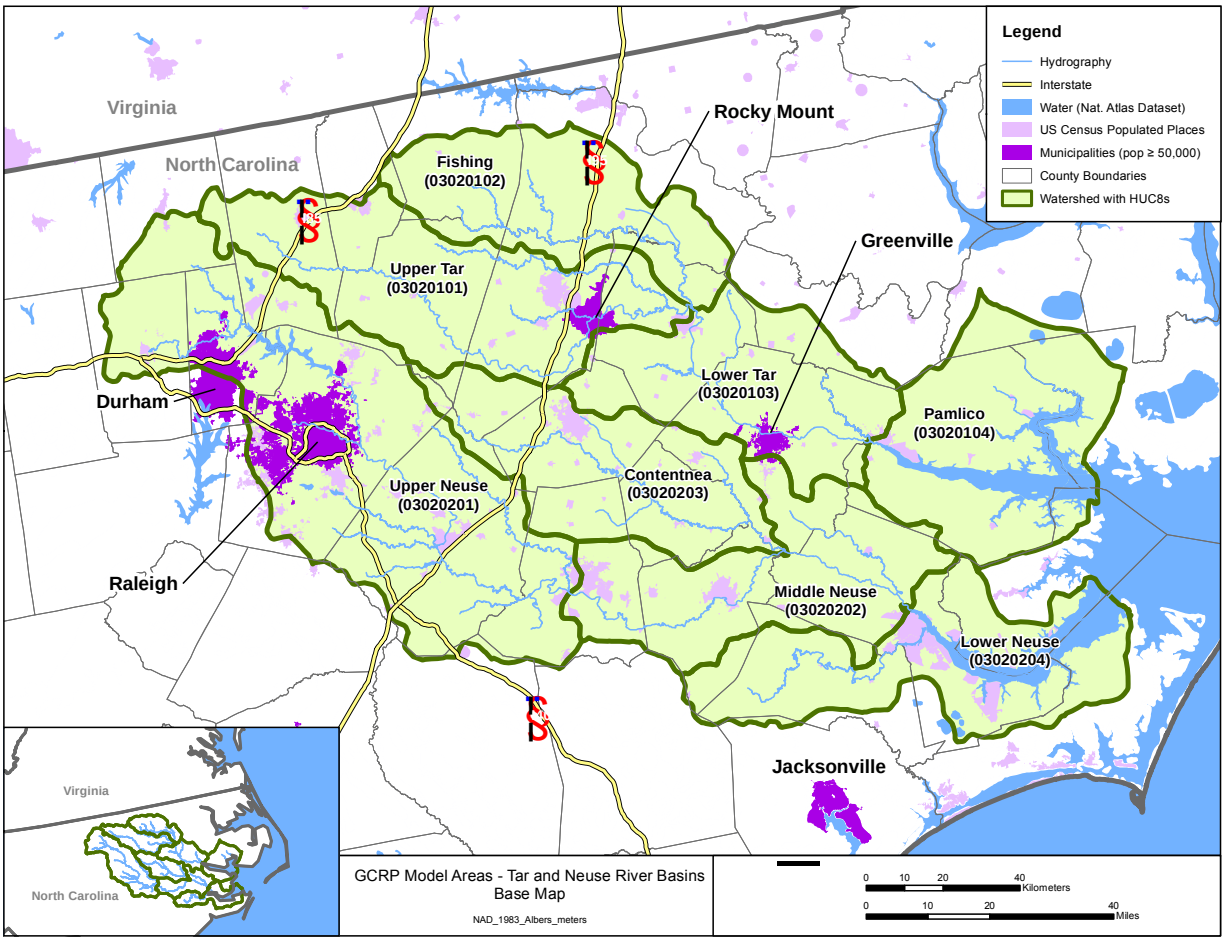

Figure 15. Tar/Neuse River basin model area.

3.1.14. New England Coastal basins

The New England Coastal basins study area encompasses 10 HUC8s and 10,225 mi^2 in Massachusetts, Maine, and New Hampshire (Figure 16).The watershed includes one of EPA's National Estuary Program sites (Massachusetts Bays), which is also one of EPA's Climate Ready Estuaries sites. The

entire model area is in the New England Physiographic Province. Elevations in the watershed range from sea level along the coast to greater than 6,000 ft in the White Mountains of New Hampshire.

Average annual precipitation in the watershed ranges from 40 to 50 inches, with higher amounts in the mountainous regions – up to 100 inches per year at the summit of Mount Washington. About one-half of this precipitation becomes surface runoff. Average annual air temperature varies from about 43^{o} F in the north to about 50^{o} F in the south.

Most of the rivers in this watershed originate in mountainous forested areas with headwaters defined by fast-flowing water with cobble and boulder-bottom streams. Flow in these rivers is generally regulated by upstream lakes, reservoirs, flood-control dams, and power plants. The watershed also contains a large number of natural lakes, many of which are enlarged and controlled by dams.

The land uses in the watershed are approximately 64 percent forested; 16 percent residential, commercial, and industrial; and 6 percent agricultural. Cities include Boston, MA, Portland, ME, Worcester, MA, and a variety of smaller cities near the Boston area. Major industries include light manufacturing, pulp and paper production, silviculture, hydroelectric-power generation, tourism, and seasonal recreation.

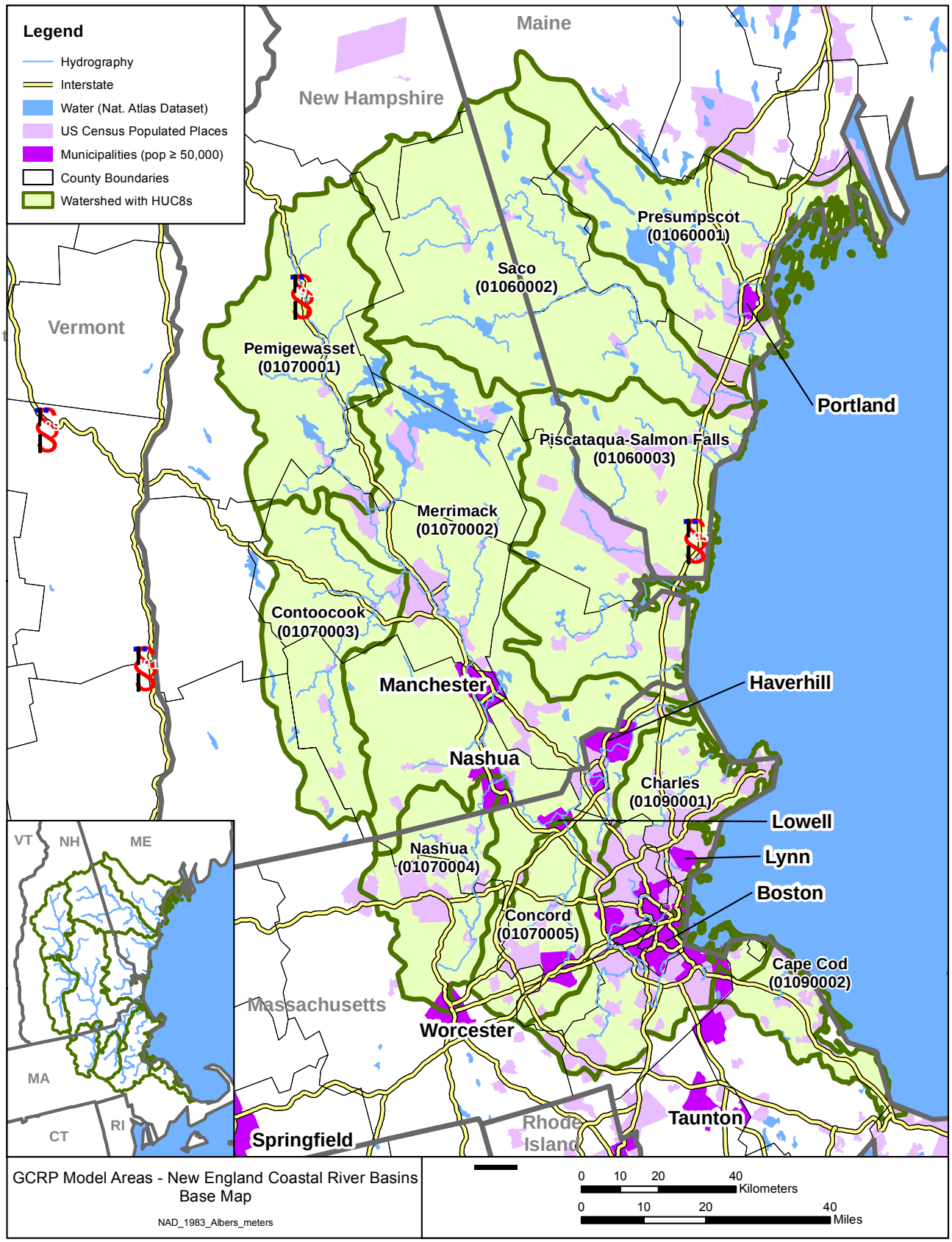

Figure 16. New England Coastal basins model area.

3.1.15. Powder/Tongue River basin

The Powder River and Tongue River are major tributaries to the Yellowstone River, which in turn is part of the Missouri River system on the east side of the Rocky Mountains. The model study area consists of almost 19,000 mi^2 in Montana and Wyoming and consists of 12 HUC8s in HUC 1009 (Figure 17).

The watershed lies in parts of the Great Plains, Middle Rocky Mountains, Wyoming Basin, and Northern Rocky Mountains physiographic provinces (Zelt et al., 1999). Elevation ranges from over 13,000 ft on the crest of the Big Horn Range to less than 3,000 ft at the confluence of the Powder and Yellowstone Rivers. This large elevation range has important impacts on climate in the watershed, which ranges from cold and moist in the mountainous areas to temperate and semiarid in the plains areas. Mean annual temperatures range from less than 32° F at the highest elevations to about 50° F along the river valleys in Montana. Annual temperature extremes range from about -40° F during the winter to hotter than 100° F during the summer. Mean annual precipitation ranges from about 12 inches in the plains to more than 35 inches at high elevations. Snowfall composes a substantial part of annual precipitation in most years.

Streams in the mountainous areas of the basin generally are perennial and derived primarily from snowmelt runoff. Most streams originating in the plains areas of the basin are ephemeral, flowing only as a result of local snowmelt or intense rainstorms. In some subbasins, where irrigated agriculture is a major land use, most of the streamflow results from agricultural return flow and sustained base flows.

Rangeland is the dominant land cover (85 percent of the watershed). Cropland and pasture compose less than 2 percent of the watershed. Silviculture is another important land use activity and forests cover about 10 percent of the model study area. The watershed is sparsely populated and developed land accounts for only 0.5 percent of the watershed.

In addition to agriculture, silviculture, and urban uses, other important land uses in the watershed include metals and coal mining and hydrocarbon production. One of the nation’s largest natural gas fields lies in the watershed and production from the low-sulfur coal beds in the Powder River basin is increasing rapidly in response to the demand for low-sulfur steam coal by electric utility consumers. All of the active coal mines in the watershed are surface (strip) mines.

There are no major storage reservoirs in the watershed, although the Tongue River is impounded near the state line. However, hundreds of small impoundments for water supply, recreation, power, and flood control have been constructed in the watershed.

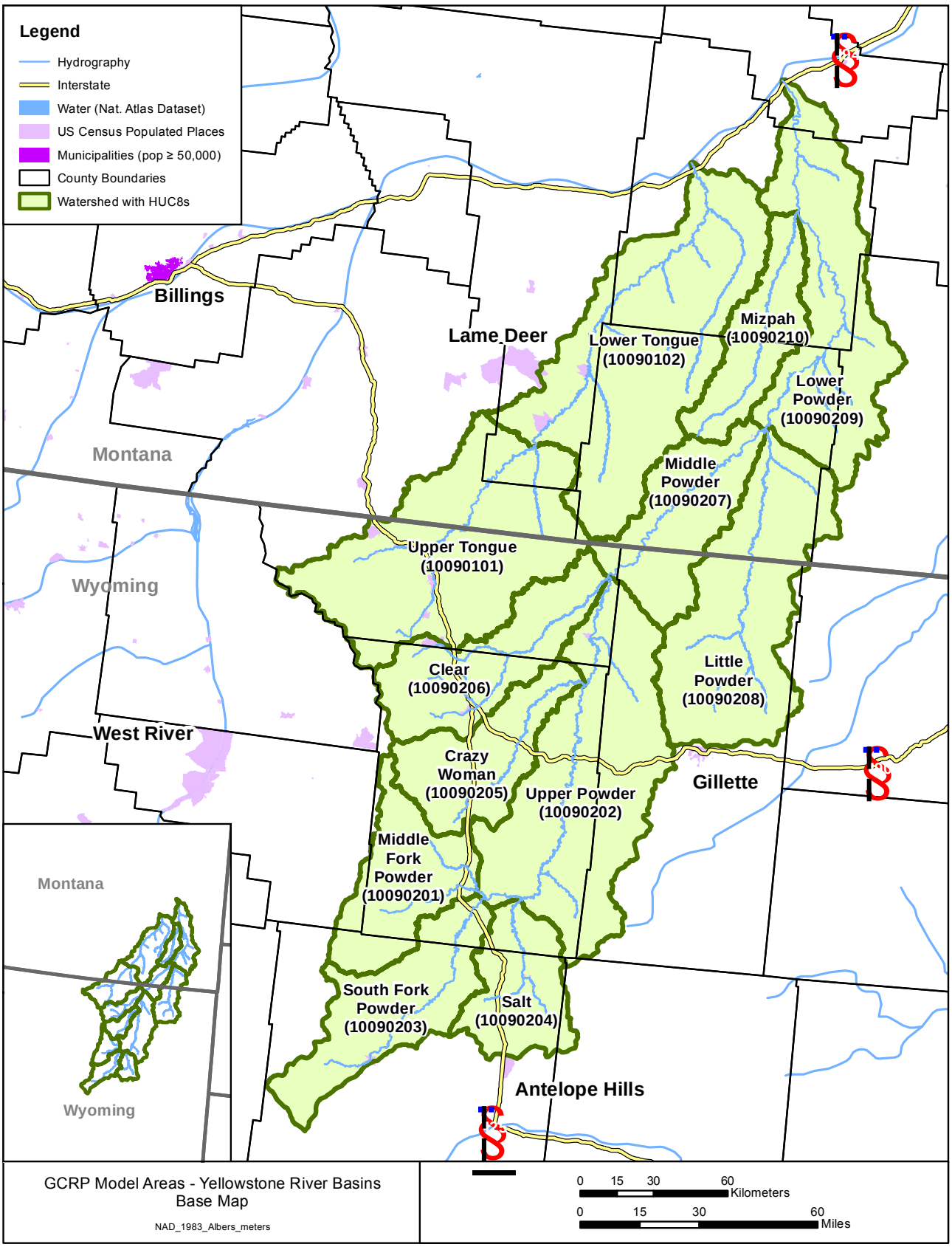

Figure 17. Tongue and Powder River basins model area.

3.1.16. Rio Grande Valley basin

The Rio Grande flows from southwestern Colorado to the Gulf of Mexico. The model study area is the upstream portion of the Rio Grande Valley, spanning parts of Colorado and New Mexico (Figure 18). This includes an area of more than 15,300 mi^2 in ten HUC8s within HUCs 1301 and 1302.

The watershed is located in three physiographic provinces: Southern Rocky Mountains; Basin and Range Provinces; and Colorado Plateaus Provinces. Extreme contrasts in precipitation, runoff, and temperature characteristics exist between the Southern Rocky Mountains and the Basin and Range Provinces. These characteristics strongly affect land and water use in the watershed (Levings et al., 1998; USGS, 2009a).

The headwaters of the Rio Grande originate in the mountains of southern Colorado at an altitude of over 13,000 ft. At the lower end of the watershed, just downstream of Albuquerque, NM, the altitude is approximately 3,700 ft. The climate in the high mountain headwater areas of the Rio Grande and its northern tributaries is alpine tundra where average annual precipitation can exceed 50 inches, most in the form of snow. In contrast, near the lower boundary of the model area, the Rio Grande flows through desert where average annual precipitation is less than 9 inches, most in the form of summer thunderstorms.

Rangeland is dominant in the Basin and Range Province, and forest is dominant in the Southern Rocky Mountains and Colorado Plateaus Provinces; each occupies 43 percent of the model study area. The cities of Taos, Santa Fe, Albuquerque, and Las Cruces, NM are located in the watershed but developed land constitutes less than 3 percent of the land area. Agricultural land use (6 percent) is limited primarily to areas where surface water or shallow groundwater is available for irrigation. Almost all public and domestic water supplies rely on groundwater, primarily from deeper aquifers. Surface water availability typically is necessary for agriculture with the exception of a few areas where groundwater is available in sufficient quantities.

Historically, streamflow in the Rio Grande was caused by spring snowmelt and summer monsoon thunderstorms. This natural streamflow pattern has been altered and regulated by the construction of reservoirs on the main stem and tributaries that impound and store water for later use, primarily irrigation. Complex interactions occur between groundwater and surface water in the Rio Grande flood plain. A system of canals distributes surface water for agricultural irrigation and a system of drains intercepts shallow groundwater and returns it to the Rio Grande. Surface water leaks from the Rio Grande and canals to recharge the shallow groundwater system. In places, deeper groundwater flows upward to recharge the shallow groundwater system and/or to contribute flow to the Rio Grande. In addition, excess applied irrigation water infiltrates and recharges the shallow groundwater system.

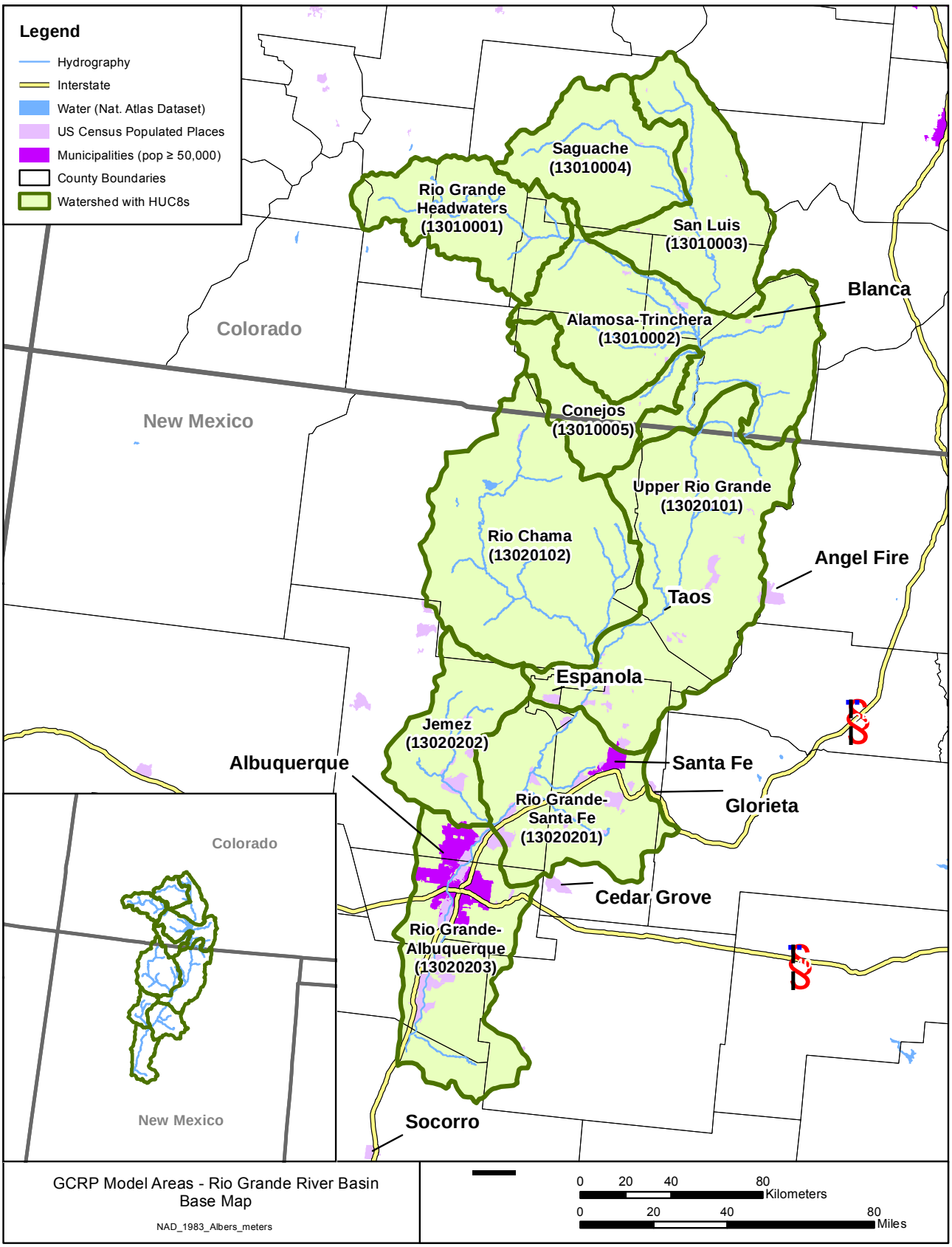

Figure 18. Rio Grande Valley basin model area.

3.1.17. Sacramento River basin

The Sacramento River in northern California is vital to the state's economy and for providing freshwater flow to the San Francisco Bay. Lake Shasta impounds the mainstem and is subject to complex operational rules. This study considers only the portion of the Sacramento River basin from Lake Shasta to just before the confluence with the Feather River (Figure 19). Information was not available for this study to represent changes in reservoir operations in response to climate change. Lake Shasta outflow time series were thus considered a fixed upstream boundary condition. The resulting model area contains over 8,300 mi^2 in 11 HUC8s, all within HUC 1802.

The average annual precipitation in the entire watershed ranges from 18 in/yr near Sacramento to about 75 in/yr at the highest elevations, mostly occurring from November through March. Snow melt is the major source of flow for the rivers of the watershed.

The Sacramento River is a major source of drinking water for residents of northern and southern California, and is a principal source of irrigation water for Sacramento and San Joaquin Valley farmers. The land uses in the valley portion of the Sacramento River basin model area are dominated by agriculture (31 percent pasture/hay, 21 percent cultivated). The Sacramento Valley supports a diverse agricultural economy, much of which depends on the availability of irrigation water. Dairy products and crops including rice, fruits and nuts, tomatoes, sugar beets, corn, alfalfa, and wheat are important agricultural commodities. The larger cities in the watershed, located in the Sacramento Valley, include Chico and Redding, with developed land occupying a little over 4 percent of the watershed. The remaining areas are primarily forest and range.

Agriculture is the largest consumer of water in the basin. Up to about 6 million acre-feet per year of water also is exported from the basin, principally to areas in southern California. Part of the runoff from winter rains and spring snowmelt is stored in reservoirs and released during the normally dry summer months. Most of the water supplies are derived from these reservoirs. The water is mainly used to provide irrigation water to the Sacramento and San Joaquin Valley agricultural communities, and to provide drinking water to Central Valley residents and residents of southern California, and to protect water quality of the delta of the Sacramento and San Joaquin Rivers.

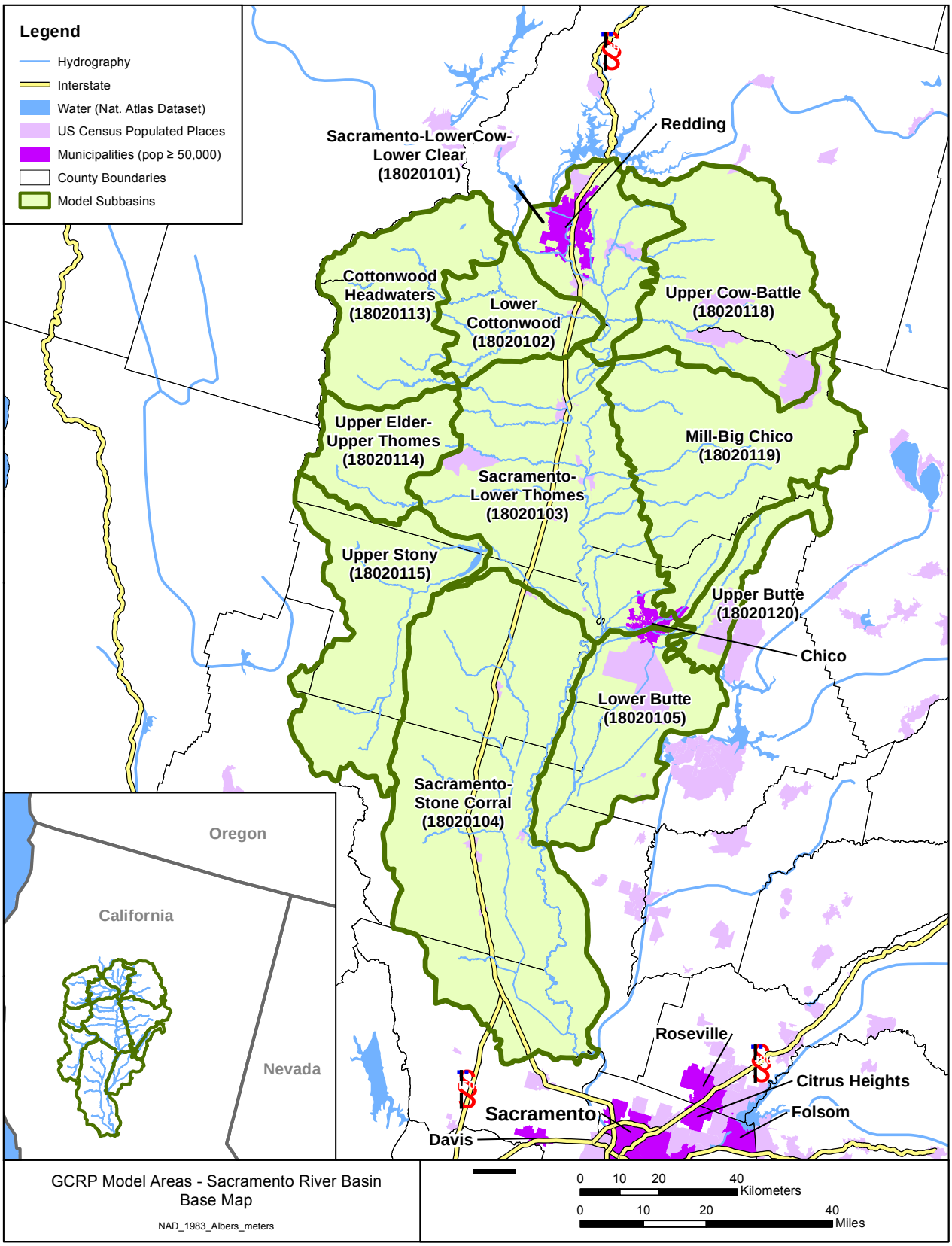

Figure 19. Sacramento River basin model area. Lake Shasta is located upstream of the modeled study area, north of Reading, CA.

3.1.18. South Platte River basin

The South Platte River originates in the mountains of central Colorado at the Continental Divide and flows about 450 miles northeast across the Great Plains to its confluence with the North Platte River at North Platte, Nebraska. The model study area is almost 15,000 mi^2 in size and extends from the headwaters to the plains of central Colorado, consisting of 11 HUC8s within HUC 1019 (Figure 20).

Elevation in the model study area ranges from 14,286 ft at Mt. Lincoln on the Continental Divide to about 4,400 ft at the downstream end of the model area. The basin includes two physiographic provinces, the Front Range Section of the Southern Rocky Mountain Province and the Colorado Piedmont Section of the Great Plains Province (Dennehy et al., 1998; USGS, 2008c).

The basin has a continental-type climate modified by topography, in which there are large temperature ranges and irregular seasonal and annual precipitation. Mean temperatures increase from west to east and on the plains from north to south. Areas along the Continental Divide average 30 inches or more of precipitation annually, which includes snowfall in excess of 300 inches. In contrast, the annual precipitation on the plains east of Denver, Colorado, and in the South Park area in the southwest part of the basin, ranges from 7 to 15 inches. Most of the precipitation on the plains occurs as rain, which typically falls between April and September, while most of the precipitation in the mountains occurs as snow, which typically falls between October and March.

Land use and land cover in the South Platte River basin is divided into rangeland (41 percent), agricultural land (37 percent), forest land (16 percent), urban land (3 percent), and other land (3 percent). Rangeland is present across all areas of the basin except over the high mountain forests. Agricultural land is somewhat more restricted to the plains and the South Park area near Fairplay, Colorado. Forest land occurs in a north-south band in the mountains. Urban land is present primarily in the Front Range urban corridor. Irrigated agriculture comprises only 8 percent of the basin but accounts for 71 percent of the water use. Urban lands comprise only 3 percent of the basin but account for 12 percent of the water use (or 27 percent if power generation is considered an urban water use).

To augment water supplies in the basin there are significant diversions of water into the South Platte tributaries from tunnels that connect to the wetter, western side of the Continental Divide, most notably the Colorado-Big Thompson Project (Adams Tunnel) which transports about 285,000 acre-feet per year of Colorado River water through a 13-mile tunnel under the Continental Divide into the Big Thompson River. Overall there are 15 inter-basin transfers into the basin and almost 1,000 reservoirs. Only the three largest mainstem reservoirs are explicitly represented in the model. The limited data available on reservoirs and inter-basin transfers creates significant challenges for hydrologic simulation in this watershed.

The population of the South Platte River basin is about 2.8 million people, over 95 percent of them in Colorado. The basin contains the most concentrated population density in the Rocky Mountain region, located in the Denver metropolitan area and along the Front Range urban corridor in Colorado where the mountains meet the plains. Population densities outside the urban corridor are small and centered in small towns located along the principal streams. The principal economy in the mountainous headwaters is based on tourism and recreation; the economy in the urbanized south-central region mostly is related to manufacturing, service and trade industries, and government services; and the economy of the basin downstream from Denver is based on agriculture and livestock production.

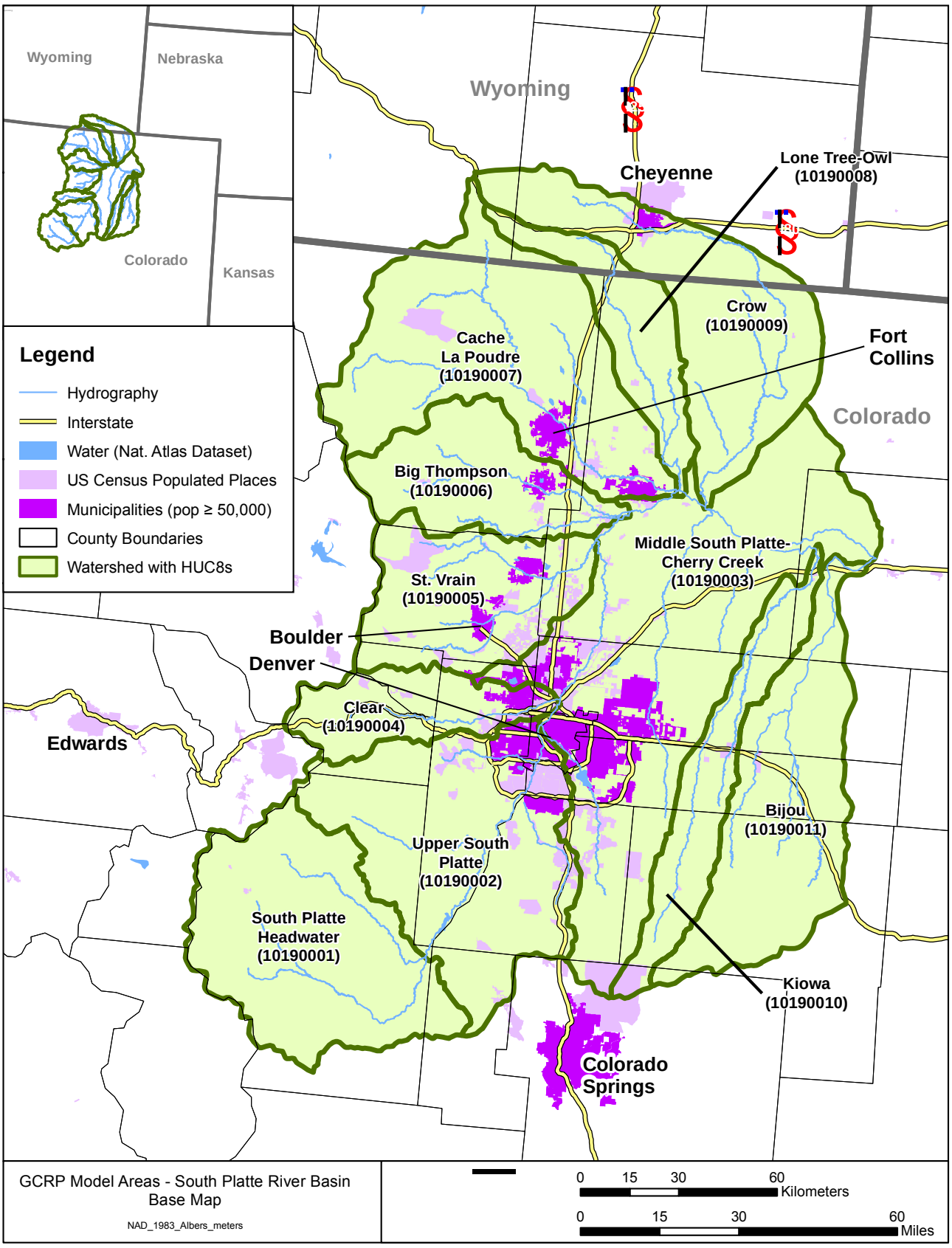

Figure 20. South Platte River basin model area.

3.1.19. Trinity River basin

The Trinity River basin is located in east central Texas. It extends on a southeast diagonal, from immediately south of the Oklahoma-Texas border to the Trinity Bay at the Gulf of Mexico. The model study area encompasses a little over 13,000 mi^2 in 12 HUC8s in HUC 1203 (Figure 21). The watershed is dissected by alternate bands of rolling, treeless prairies, smooth to slightly rolling prairies, rolling timbered hills, and a relatively flat coastal plain. The watershed slopes gradually from about 1,200 ft above sea level in the northwest, to about 600 ft mid-basin, and on to sea level in the southeastern section of the area, at Trinity Bay (Land et al., 1998; Ulery et al., 1993).

Past and current human activities, including construction of reservoirs, urbanization, farming, ranching, and oil and gas production, have greatly altered the natural environment in the Trinity River basin. Approximately 37 percent of the watershed is cropland or pasture. Major crops include corn, cotton, peanuts, sorghum, soybeans, rice, and wheat. Wheat and cotton are dry cropland crops, while rice is an irrigated crop. Forest and wetlands represent about 33 percent of the watershed and developed land makes up about 19 percent of the watershed. The population in the watershed is mainly clustered in the Dallas-Fort Worth metropolitan area, with a few secondary population clusters (Denton, McKinney, Corsicana, and Waxahachie).

The climate of the basin is described as modified-marine, subtropical-humid, having warm summers and a predominant onshore flow of tropical maritime air from the Gulf of Mexico. Precipitation varies considerably across the watershed. Average annual precipitation ranges from less than 27 inches in the northwest part of the watershed to greater than 52 inches in the southeast. On average, the watershed experiences a winter surplus and a summer deficiency of precipitation. Average annual temperature is fairly uniform throughout the basin, ranging from about 69° F in the southeastern area of the watershed to about 65° F in the northwest.

There are 22 large reservoirs in the Trinity River basin and hundreds of smaller reservoirs, mostly flood control structures. Reservoirs have been built to retain runoff on all major tributaries and the mainstem of the Trinity River. Diversions move water within the basin and to and from adjacent river basins. The largest interbasin diversion is out of the basin, from the Trinity River below Livingston Reservoir to the Houston metropolitan area. There are numerous other inter- and intrabasin diversions.

The largest consumptive use in the watershed is domestic with the majority being used in Dallas and Tarrant counties because of their large populations. Surface water, almost entirely from reservoirs, supplies more than 90 percent of the water used in the basin. Groundwater is used for municipal and domestic supply in some of the smaller towns and in rural areas. Transfers of water, from the adjoining basins and from reservoirs below Dallas and Fort Worth, are required to meet the needs of the Dallas-Fort Worth area. Relatively little water is used for irrigating crops.

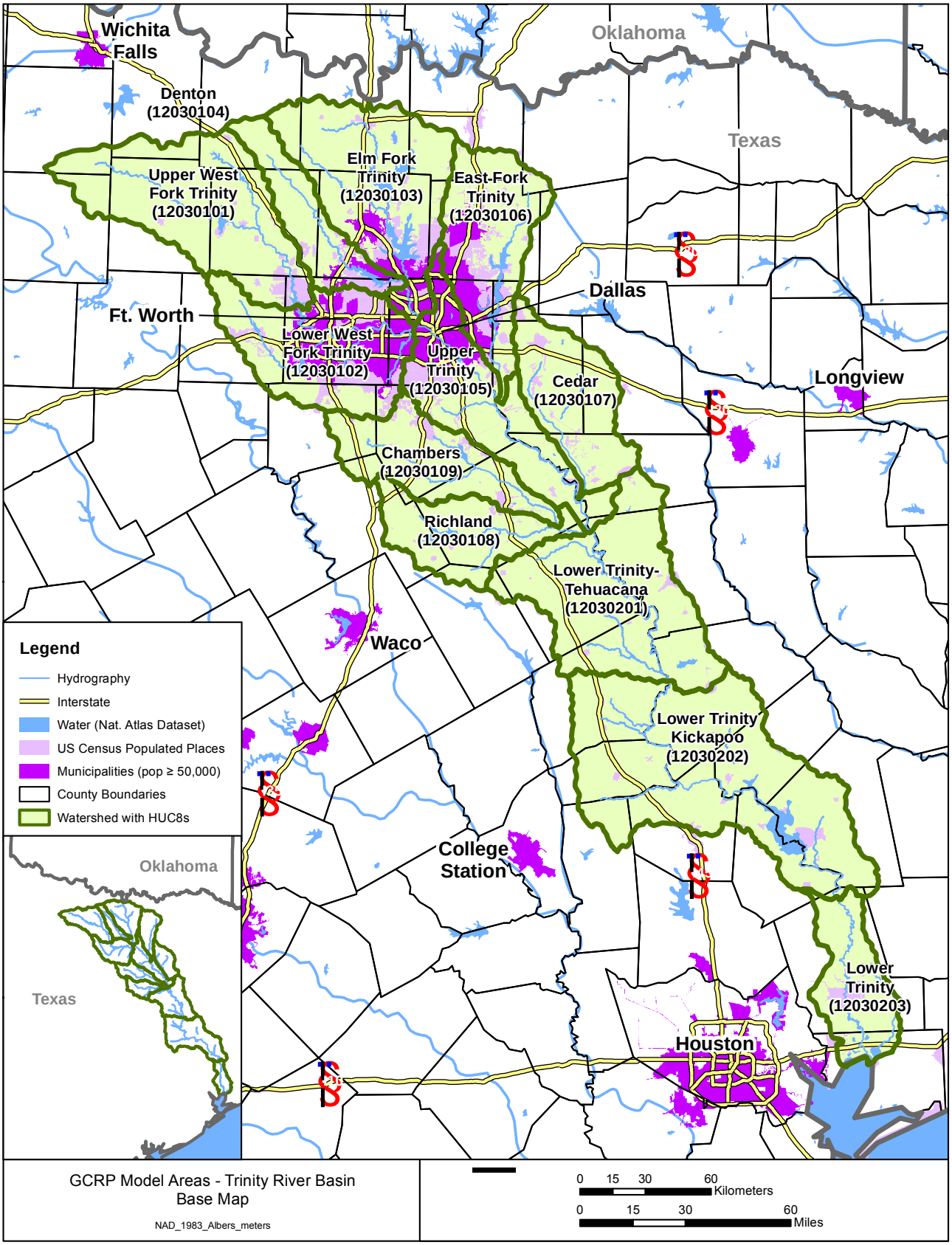

Figure 21. Trinity River basin model area.

3.1.20. Upper Colorado River basins

The Upper Colorado River basin model area has a drainage area of about 17,800 mi² and contains 12 HUC8s within HUC 1401 and 1402. All except 100 mi² of this area is in Colorado (Figure 22).

The Colorado River and its tributaries originate in the mountains of central Colorado and flow about southwest into Utah. The Continental Divide marks the eastern and southern boundary of the basin, with altitudes over 14,000 ft. Topography in the western part of the basin generally consists of high plateaus bordered by steep cliffs along the valleys, and the lowest altitude (4,300 ft) is near the Colorado-Utah border. The basin is divided almost equally into two physiographic provinces: the Southern Rocky Mountains in the east and the Colorado Plateau in the west (USGS, 2006; Apodaca et al., 1996).

Because of large changes in altitude, the climate in the basin varies from alpine conditions in the east to semiarid in the west. Mean annual temperatures range from as low as 32.8° F in Gunnison County near the Continental Divide to as high as 54.1° F near Grand Junction, Colorado. Precipitation in the basin ranges from more than 40 inches per year in the eastern mountainous regions to less than 10 inches per year in the lower altitude western regions. Mountain areas receive most of their precipitation during the winter months when accumulation of snow can exceed an annual average of 100 inches.

The Upper Colorado River basin is largely rural. Rangeland and forest occupy about 88 percent of the basin. Livestock (sheep and cattle) use large areas of rangeland for foraging. Forest land that includes most of the mountain and plateau areas is used for some commercial lumber production. Large parts of the watershed are set aside for recreational use, including all or parts of 4 National Park Service areas, 5 National Forests and numerous wilderness areas, 11 state parks, numerous State Wildlife Management areas, and 17 ski areas. Mining activities are also an important land use and have included the extraction of metals and energy fuels.

Less than 2 percent of the land area is developed. The largest population center is Grand Junction (population less than 60,000 in 2010), which is located at the confluence of the Colorado and Gunnison Rivers. The larger cities in the basin are located predominantly near agricultural lands or in mountain recreational communities. Agricultural activities (about 4 percent of the area) include production of crops such as alfalfa, fruits, grains, hay, and vegetables. Little crop production is possible without irrigation because of the semiarid climate. Irrigated lands are predominantly in river valleys or low-altitude regions where the water is supplied by an extensive system of canals and ditches.

The natural hydrology of the Upper Colorado River basin has been considerably altered by water development, which includes numerous reservoirs and diversions. In the watershed, there are 9 major interbasin water transfers, 7 major water diversions, 9 major reservoirs, and 10 major municipal discharges. The interbasin water transfers provide supplementary irrigation and municipal water supplies to the South Platte, Arkansas, and Rio Grande drainages. About 25 percent of the interbasin water transfers are to the South Platte watershed for the municipal water supply for the Denver metropolitan area. Most of the water used in the watershed comes from surface water sources. Groundwater sources account for less than 1 percent of the water used. Irrigation accounts for about 97 percent of off-stream water use. Besides off-stream water uses, there are in-stream water uses such as hydroelectric power generation.

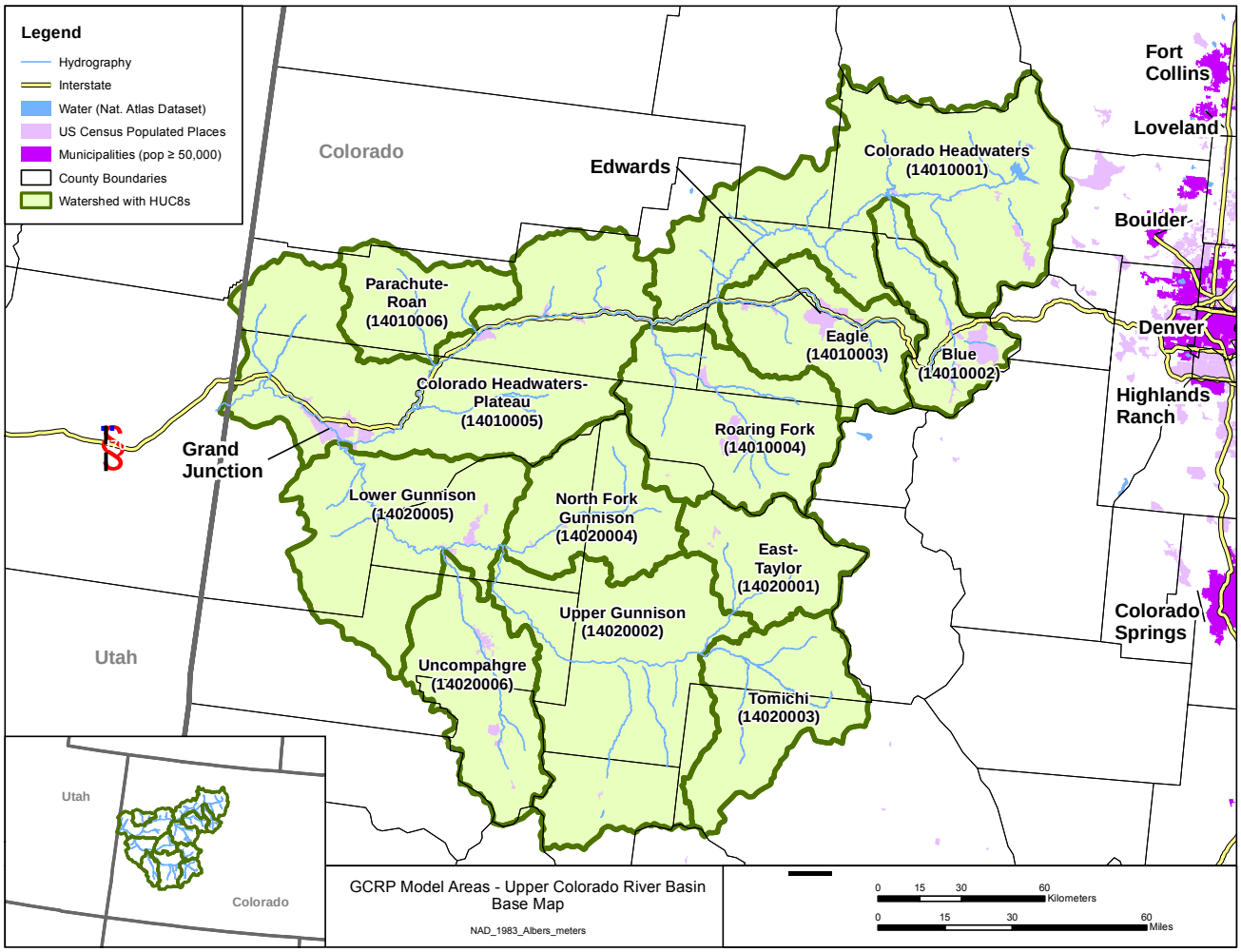

Figure 22. Upper Colorado River basin model area.

4. MODELING APPROACH

This study involves application of dynamic watershed models to simulate the watershed response to potential changes in climate, changes in urban development, and the combined effects of changes in climate change and urban development. Watershed modeling was conducted using two watershed models, Hydrologic Simulation Program – FORTRAN (HSPF; Bicknell et al. 2001) and Soil and Water Assessment Tool (SWAT; Neitsch et al., 2005). The SWAT model was applied in all 20 study areas. In a subset of five of the 20 sites (hereafter referred to as "Pilot Sites"), simulations were also conducted independently using HSPF. Simulations focus on changes in streamflow, nutrient (nitrogen and phosphorus) and sediment loads.

A watershed model is a useful tool for providing a quantitative linkage between external forcing and in-stream response. It is essentially a series of algorithms applied to watershed characteristics and meteorological data to simulate naturally occurring, land-based processes over an extended period, including hydrology and pollutant transport. Many watershed models are also capable of simulating in-stream processes. After a model has been set up and calibrated for a watershed, it can be used to quantify the existing loading of pollutants from subbasins or from land use categories and can also be used to assess the effects of a variety of management scenarios.

The results of watershed assessment are shaped by the characteristics of the watershed model that serves to translate climate forcing into hydrologic and water quality responses. Two watershed models were selected for initial application to the five pilot study sites: Hydrological Simulation Program – FORTRAN (HSPF) (Bicknell et al., 2001) and Soil Water Assessment Tool (SWAT) (Neitsch et al., 2005). These models were selected because they met the following criteria:

- Dynamic simulation with a sub-daily or daily time step to give an indication of changes in frequency of extreme events
- Process-based, but at a level that model parameters can be easily identified from available data
- Able to simulate water quality responses
- Widely used and accepted for hydrologic and water quality applications
- In the public domain to enable ready replication of results

Application of both HSPF and SWAT to the five pilot watersheds allowed assessment of the variability associated with use of different watershed models in simulating watershed response to climate change. The two watershed models are described below. The rationale for selecting the SWAT model for use in non-pilot watersheds is discussed in Section 6.1 (Comparison of Models).

4.1. MODEL BACKGROUND

4.1.1. HSPF

The Hydrological Simulation Program – FORTRAN (HSPF; Bicknell et al., 2001) is a comprehensive, dynamic watershed and receiving water quality modeling framework that was originally developed in the mid-1970s. During the past several decades, it has been used to develop hundreds of EPA-approved Total Maximum Daily Loads (TMDLs), and it is generally considered among the most advanced hydrologic and watershed loading models available. The hydrologic portion of HSPF is based on the Stanford Watershed Model (Crawford and Linsley, 1966), which was one of the pioneering watershed models developed in the 1960s. The HSPF framework is developed modularly with many different components that can be assembled in different ways, depending on the objectives of a project. The model includes three major modules:

- PERLND for simulating watershed processes on pervious land areas
- IMPLND for simulating processes on impervious land areas
- RCHRES for simulating processes in streams and vertically mixed lakes

All three of these modules include many subroutines that calculate the various hydrologic and water quality processes in the watershed. Many options are available for both simplified and complex process formulations.

HSPF models hydrology as a water balance in multiple surface and subsurface layers and is typically implemented in large watersheds at an hourly time step. The water balance is simulated based on Philip's infiltration (Bicknell et al., 2001, 2005) coupled with multiple surface and subsurface stores (interception storage, surface storage, upper zone soil storage, lower zone soil storage, active groundwater, inactive (deep) groundwater). Potential evapotranspiration (PET) is externally specified to the model.

Sediment erosion in HSPF uses a method that is formally similar to, but distinct from the USLE sediment-detachment approach coupled with transport capacity based on overland flow. Nutrients may be simulated at varying levels of complexity, but are most typically represented by either buildup/washoff or sediment potency approaches on the land surface coupled with user-specified monthly concentrations in interflow and groundwater.

Spatially, the watershed is divided into a series of subbasins representing the drainage areas that contribute to each of the stream reaches. The stream network (RCHRES) links the surface runoff and groundwater flow contributions from each of the land segments and sub-basins and routes them through waterbodies. The stream model includes precipitation and evaporation from the water surfaces as well as flow contributions from the watershed, tributaries, and upstream stream reaches. It also simulates a full range of stream sediment and nutrient processes, including detailed representations of scour, deposition, and algal growth.

The version of HSPF used in this study is WinHSPF as distributed with BASINS version 4.0. WinHSPF is a Windows interface to HSPF and is a component of the EPA's Better Assessment Science Integrating point and Nonpoint Sources (BASINS) Version 4.0 (U.S. EPA, 2009b, 2009c). WinHSPF itself is a user interface to HSPF that assists the user in building User Control

Input (UCI) files (containing model input parameters) from GIS data (Duda et al., 2001). After the UCI file is built, WinHSPF is used to view, understand, and modify the model representation of a watershed. HSPF can be run from within WinHSPF. The actual model executable engine distributed with BASINS is called WinHSPFLt, which can be run in batch mode independent of the BASINS/WinHSPF interface. The model code for HSPF is stable and well-documented. Detailed descriptions of the model theory and user control input are provided in Bicknell et al., (2001, 2005).

WinHSPF also provides access to the Climate Assessment Tool (CAT), which is a component of BASINS 4.0. BASINS CAT facilitates watershed-based assessments of the potential effects of climate variability and change on water and watershed systems (namely streamflow and pollutant loads) using the HSPF model (U.S. EPA, 2009b, 2009c). BASINS CAT is capable of creating climate change scenarios that allow users to assess a wide range of *what if* questions related to climate change.

4.1.2. SWAT

The Soil Water Assessment Tool (SWAT, version 2005) model (Neitsch et al., 2005) was also applied to the watersheds to simulate flow and nitrogen, phosphorus and sediment loads. SWAT was developed by the U.S. Department of Agriculture to simulate the effect of land management practices on water, sediment, and agricultural chemical yields in large, complex watersheds with varying soils, land use, and management conditions over long periods of time (Neitsch et al., 2005). SWAT requires data inputs for weather, soils, topography, vegetation, and land use to model water and sediment movement, nutrient cycling, and numerous other watershed processes. SWAT is a continuous model appropriate to long-term simulations.

SWAT, as implemented here, employs a curve number approach to estimate surface runoff and then completes the water balance through simulation of subsurface flows, evapotranspiration, soil storages, and deep seepage losses. The curve number approach requires a daily time step. PET is typically calculated internally by SWAT based on other weather inputs.

Sediment yield and erosion are calculated by SWAT using the Modified Universal Soil Loss Equation (MUSLE) (Williams, 1975). The MUSLE is based on several factors including surface runoff volume, peak runoff rate, area of hydrologic response unit (HRU), soil erodibility, land cover and management, support practice, topography, and a coarse fragment factor and implicitly combines the processes of sediment detachment and delivery. Nutrient load generation and movement is simulated using overland runoff and subsurface flow.

A key feature of SWAT is the incorporation of an explicit plant growth model, including plant interactions with water and nutrient stores. The transformation of various nitrogen and phosphorus species is simulated in detail in the soil; however, concentrations of nutrients in groundwater discharges are user-specified, as in HSPF.

Instream simulation of sediment in SWAT 2005 includes a highly simplified representation of scour and deposition processes. Nutrient kinetics in receiving waters are based on the numeric representation used in the QUAL2E model but implemented only at a daily time step.

An important component of the SWAT model is the weather generator (WXGEN). SWAT requires daily values of precipitation, maximum and minimum temperature, solar radiation, relative humidity, and wind speed. The user may read these inputs from a file or generate the values using SWAT's weather generator model based on monthly average data summarized over a number of years (Neitsch et al., 2005). The weather generator model (Sharpley and Williams, 1990) can be used to generate climatic data or to fill in gaps in weather data. The weather generator first independently generates precipitation for the day. Maximum temperature, minimum temperature, solar radiation, and relative humidity are then generated based on the presence or absence of rain for the day. Finally, wind speed is generated independently.

The version SWAT used in this study is SWAT2005 as distributed with ArcSWAT 2.1, which was the most recent stable version of SWAT available at the start of this study. ArcSWAT 2.1 is an ArcGIS-ArcView extension and a graphical user input interface for the SWAT watershed model (TAMU, 2010). As with HSPF, the underlying executable code can be run in batch mode independent of the user interface. Unlike HSPF, the SWAT code is continuously evolving, with frequent enhancements and bug fixes. For a detailed description of the version of SWAT used here, see Neitsch et al. (2005).

4.2. MODEL SETUP

The watershed models were configured to simulate the study areas as a series of hydrologically connected subbasins. Configuration of the models involved subdivision of the watersheds into modeling units, followed by continuous simulation of flow and water quality for these units using meteorological, land use, soil, and stream data. The specific pollutants modeled were nitrogen, phosphorus, and sediment.

Many study areas are highly managed systems influenced by humans including dams, water transfers and withdrawals, point source discharges and other factors. Given the difficulty modeling at the large spatial scale in this study, detailed representation of all management was not possible. The following assumptions were made to simplify modeling among all 20 study areas:

- External boundary conditions (where needed), such as upstream inflows and pollutant loads, are assumed constant.
- Interactions with deep groundwater systems are assumed constant.
- Large-scale shifts in natural cover type in response to climate change are not simulated.
- Point source discharges and water withdrawals are assumed constant at current levels.
- Only large dams that have a significant impact on hydrology at the HUC8 scale are included in the models. Where these dams are simulated an approximation of current operating rules (using a target storage approach) is assumed to apply in all future scenarios.
- Human adaptation response to climate change, such as shifts in water use or cropping practices, are not simulated.

Results therefore represent the behavior and potential responses of watersheds to different change scenarios but should not be considered quantitative forecasts of future conditions.

The modeling effort in this study was extensive and involved multiple modelers. To ensure consistency of results, a common set of procedures and assumptions was established as follows (e.g., see appendix A). Both HSPF and SWAT were implemented using a hydrologic response unit (HRU) approach to upland simulation. An HRU consists of a unique combination of land use/land cover, soil, and land management practice characteristics, and thus represents areas of similar hydrologic response. This is the default for SWAT, but is also good practice with HSPF. Consistent with the broad spatial scale of the models, the land cover component is interpreted to a relatively small number of categories (e.g., forest, wetland, range, grass/pastureland, crop, developed pervious, low-density impervious, and high-density impervious).

Initial processing took place primarily in ArcGIS for the entire study area. Processed GIS inputs were then used in ArcSWAT (which runs as an extension in ArcGIS), and imported into BASINS4 (which uses MapWindow GIS). Spatial data sources are discussed in more detail in Section 4.2.3. Additional initial setup tasks included:

1. Identification of BASINS4 weather stations in proximity of model watersheds
2. Identification of locations and characteristics of any major reservoirs or needed calibration points
3. Identification of locations and characteristics of any major features in the watershed affecting water balance (e.g., diversions, upstream areas not modeled, reaches that lose flow to groundwater). Irrigation was considered only where needed (e.g., Rio Grande)
4. Identification of locations of major point sources
5. Identification of flow gaging station and water quality monitoring station locations
6. Modification of subbasin boundaries as needed to accommodate the previous four items
7. Identification of nearest precipitation weather station to each subbasin, and identification of subbasin assignment for elevation bands and other characteristics (e.g., soil and geology) that needed to be represented on a regional basis in the models
8. Atmospheric deposition of nitrogen – each model was set up appropriately to model a constant concentration for wet deposition and a constant load for dry deposition

4.2.1. SWAT Setup Process

SWAT model setup followed directly from the initial setup, using the ArcSWAT extension in ArcGIS. The following steps were implemented first for the calibration HUC8 subbasins then repeated for the entire modeled watershed. A detailed description of the SWAT model setup for the 15 non-pilot watersheds is included in Appendix A.

The first step was watershed delineation. In general, subbasin boundaries and reach hydrography were defined from NHDPlus catchments (U.S. EPA, 2010), aggregated to approximately the HUC10 scale. The subbasin and reach shapefiles were imported into the SWAT interface and subbasin parameters were calculated automatically. The next step was to add major reservoirs in the watershed. Study sites were selected to minimize the presence of reservoirs to reduce the difficulty of representing operational rules, and model included only major reservoirs that have a significant effect on flows at the scale of HUC8s or greater. Inclusion of reservoirs was left to the

discretion of individual modelers; however, reservoirs included are generally those that drain an area greater than a single HUC8 and provide a retention time of half a year or greater. If a reservoir was located at the terminus of the model area it was generally ignored so that the model represented input to, rather than output from, the terminal reservoir.

Only those permitted point sources identified as major facilities (greater than 1 MGD discharge) were included in the model. It was also necessary to define an upstream boundary condition "point source" for some watersheds.

Land use for the model comes from the 2001 NLCD (Homer et al., 2004; Homer et al., 2007), while soils use the STATSGO state soils coverage (USDA, 1991) distributed with ArcSWAT. Topography was represented by digital elevation models (DEMs) with a resolution of 30 meters. The next step was development of HRUs from an intersection of land use, slope, and major soils. Individual land parcels included within an HRU are expected to possess similar hydrologic and load generating characteristics and can thus be simulated as a unit. These soil/land use combinations are then assigned appropriate curve numbers and other physical and chemical parameter values.

In the HRU analysis, SWAT was used to classify the slopes into two categories: above and below 10 percent. A single breakpoint was chosen to represent major differences in runoff and erosive energy without creating an unmanageable number of individual HRUs. The STATSGO soils coverage was assigned using the dominant component method in which each soil polygon is represented by the properties of the dominant constituent soil. The NLCD 2001 land use coverage was loaded directly into ArcSWAT without modification. The default NLCD class to SWAT class mapping was appropriate for most areas. Impervious percentage was assigned to developed land use classes in the SWAT urban database using values calculated from the NLCD impervious coverage. The same assumptions were applied for the future developed land use classes (i.e., the future classes have the same total and connected impervious fractions as the corresponding existing urban land uses). HRUs were created by overlaying land use, soil, and slope at appropriate cutoff tolerance levels to prevent the creation of large numbers of insignificant HRUs. Land use classes were retained if they occupied at least 5 percent of the area of a subbasin (with the exception of developed land uses, which were retained regardless of area). Soils were retained if they occupied at least 10 percent of the area within a given land use in a subbasin. Slope classes were retained if they occupied at least 5 percent of the area within a given soil polygon. Land uses, soils, and slope classes that fall below the cutoff value are reapportioned to the dominant classes so that 100 percent of the watershed area is modeled (Winchell et al., 2008).

The SWAT models were linked to the BASINS4 meteorological station locations (U.S. EPA, 2008). The models used observed time series for precipitation and temperature; other weather data were simulated with the SWAT weather generator. Potential evapotranspiration (PET) option was specified as Penman/Monteith in General Watershed Parameters. Elevation bands were turned on if necessary to account for orographic effects in areas with a sparse precipitation network and significant elevation changes. This was generally appropriate where elevations within subbasins spanned a range of 250 m or more. Daily Curve Number hydrology with

observed precipitation and air temperature were used. Atmospheric nitrogen wet deposition concentrations were specified.

Next, land management operations were assigned, primarily to account for agricultural practices. For urban lands, the USGS regression method for pollutant load estimation was specified. In-stream water quality options started with program defaults.

The target time period for simulation was 31 water years, with the first year dropped from analysis to account for model spinup (initialization). Some weather stations may have been absent for the spinup year, but SWAT fills in the missing records using the weather generator. The remaining 30 years span a period for which the supplied weather data were complete and included the year 2000 (with the exception of the Loup/Elkhorn basins in Nebraska, for which the simulation period ended in 1999 due to the termination of a number of precipitation gauges prior to the end of 2000).

4.2.2. HSPF Setup Process

The HSPF models were developed from the same spatial coverages used to set up the SWAT models. The model segmentation is identical for the two models. The HRUs for HSPF were calculated from the SWAT HRUs, but differ in that soils were aggregated to hydrologic soil group, while pervious (PERLND) and impervious (IMPLND) land fractions were specified separately.

Setup of the HSPF model used the WinHSPF interface to create the user control input (UCI) and water data management (WDM) files. A starter UCI file was prepared that defined default values for HRUs. Initial parameter values were based on previous modeling where available. For areas without previous modeling, hydrologic parameters were based on recommended ranges in BASINS Technical Note 6 (U.S. EPA, 2000) and related to soil and meteorological characteristics where appropriate. Snowmelt simulation used the simplified degree-day method.

The stage-storage-discharge hydraulic functional tables (FTables) for stream reaches were generated automatically during model creation. The WinHSPF FTable tool calculates the tables using relationships to drainage area. FTables were adjusted in WinHSPF if specific information was available to the modeler. Hydraulic characteristics for major reservoirs and flow/load characteristics for major point sources were defined manually based on available information.

Nutrients on the land surface were modeled as inorganic nitrogen, inorganic phosphorus, and total organic matter. The latter was transformed to appropriate fractions of organic nitrogen and organic phosphorus in the linkage to the stream. The in-stream simulation represented total nitrogen and total phosphorus as general quality constituents (GQUALs) subject to removal approximated as an exponential decay process. Initial values for decay rates were taken from USGS SPARROW studies (e.g., Alexander et al., 2008).

4.2.3. Watershed Data Sources

4.2.3.1. *Watershed Boundaries and Reach Hydrography*

Subbasin boundaries and reach hydrography (with connectivity) for both SWAT and HSPF were defined using NHDPlus data (U.S. EPA, 2010), a comprehensive set of digital spatial data

representing the surface water of the U.S. including lakes, ponds, streams, rivers, canals, and oceans. NHDPlus provided catchment/reach flow connectivity, allowing for creation of large model subbasins with automation. NHDPlus incorporates the National Hydrography Dataset (NHD), the National Elevation Dataset (NED), the National Land Cover Dataset (NLCD), and the Watershed Boundary Dataset (WBD). A MapWindow script was developed to automate (with supervision) the aggregation of NHDPlus catchments/reaches into model subbasins and reaches. The general approach was to first run the aggregation script with a smaller target subbasin size (i.e., create several hundred to a thousand subbasins), then run the script again to create watersheds of the target model size (comparable to the HUC10 scale). The two tiered approach has several benefits; it was found to be more time efficient, it allowed for greater control over the final basin size, and it provided a midpoint that could be used to redefine subbasin boundaries to match specified locations, such as gaging stations and dams/diversions.

Each delineated subbasin was conceptually represented with a single stream assumed to be a completely mixed, one-dimensional segment with a constant cross-section. For the HSPF model, reach slopes were calculated based on Digital Elevation Model (DEM) data and stream lengths were measured from the original NHD stream coverage. Assuming representative trapezoidal geometry for all streams, mean stream depth and channel width were estimated using regression curves that relate upstream drainage area to stream dimensions developed for three regions in the Eastern United States. Existing and more detailed models provided additional site-specific information on channel characteristics for some watersheds (e.g., Minnesota River; Tetra Tech, 2008b).

The SWAT model also automatically calculates the initial stream geometric values based on subbasin drainage areas, standard channel forms, and elevation, using relationships developed for numerous areas of the United States. Channel slope is automatically calculated from the DEM.

4.2.3.2. *Elevation*

Topography was represented by digital elevation models (DEMs) with a resolution of 30 meters obtained from USGS' National Elevation Dataset (Gesch et al., 2002). Multiple DEM coverages were grouped and clipped to the extent of the model watershed area (with a 10-mile buffer to allow for unforeseen changes to watershed boundaries).

4.2.3.3. *Land Use and Land Cover*

The SWAT and HSPF models use a common land use platform representing current (calibration) conditions and derived from the 2001 National Land Cover Database or NLCD (Homer et al., 2004; Homer et al., 2007). The 2001 NLCD land cover was used to ensure consistency between all models for the project. The 2001 land use was chosen rather than the 2006 coverage because it is closer in time to the calibration period of the models, which typically runs through 2002/3. The 2001 land use is assumed to apply throughout the baseline model application period.

Some additional processing of the NLCD data was necessary. Several of the land use classes were aggregated into more general categories to provide a more manageable set of HRUs. The developed land classes were kept separate for SWAT but aggregated for HSPF. This is because SWAT assigns percent imperviousness to total developed area, whereas HSPF explicitly

separates developed pervious and impervious areas. The regrouping of the NLCD classes for SWAT and HSPF is shown in Table 4.

Table 4. Regrouping of the NLCD 2001 land-use classes for the HSPF and SWAT models.

NLCD Class	SWAT class	HSPF class
11 Water[a]	WATR (water)	WATER
12 Perennial ice/snow	WATR (water)	BARREN
21 Developed open space	URLD (Urban Residential-Low Density)	DEVPERV (Developed Pervious) IMPERV (Impervious)
22 Dev. Low Intensity	URMD (Urban Residential-Medium Density)	
23 Dev. Med. Intensity	URHD (Urban Residential – High Density)	
24 Dev. High Intensity	UIDU (Urban Industrial and High Intensity)	
31 Barren Land	SWRN (Range-Southwestern U.S.)	BARREN
41 Forest - Deciduous	FRSD (Forest-Deciduous)	FOREST
42 Forest - Evergreen	FRSE (Forest-Evergreen)	
43 Forest - Mixed	FRST (Forest-Mixed)	
51-52 Shrubland	RNGB (Range-Brush)	SHRUB
71-74 Herbaceous Upland	RNGE (Range grasses)	GRASS BARREN
81 Pasture/Hay	HAY	GRASS
82 Cultivated	AGRR (Agricultural Land-Row Crops)	AGRI (Agriculture)
91-97 Wetland (emergent)	WETF (Wetlands-Forested), WETL (Wetlands), WETN (Wetlands–Non-forested)	WETL (Wetlands)
98-99 Wetland (non-emergent)	WATR (water)	WATER

[a] Water surface area is usually accounted for as reach area

The percent impervious area was specified for each developed land class from the NLCD Urban Impervious data coverage.

The NLCD 2001 Urban Imperviousness coverage was mosaic-ed and clipped to the extent of the model watershed area (with 10-mile buffer) to calculate the impervious area. The percent impervious area was then specified by combining data from the 2001 NLCD Land Cover and Urban Impervious data products. Specifically, average percent impervious area was calculated over the whole basin for each of the four developed land use classes. These percentages were then used to separate out impervious land. The analysis was performed separately for each of the 20 study areas, since regional differences occur. Table 5 presents the calculated impervious areas for each study area.

Table 5. Calculated fraction impervious cover by developed land class for each study area.

Site ID	Open Space	Low Intensity	Medium Intensity	High Intensity
ACF	8.04%	30.16%	60.71%	89.90%
Ariz	7.37%	29.66%	53.71%	73.85%
CenNeb	8.34%	29.68%	60.14%	86.59%
Cook	10.11%	29.79%	61.48%	87.17%
Erie	7.30%	32.53%	60.72%	86.75%
GaFla	7.20%	31.87%	60.14%	87.47%
Illin	8.83%	32.36%	61.24%	88.70%
Minn	6.59%	29.20%	55.01%	83.31%
NewEng	8.22%	32.81%	60.90%	87.25%
Pont	7.53%	32.91%	60.11%	88.08%
RioGra	8.76%	32.36%	60.49%	84.32%
Sac	5.95%	30.02%	55.41%	81.20%
SoCal	7.75%	35.39%	61.31%	88.83%
SoPlat	6.41%	33.46%	60.79%	86.76%
Susq	6.90%	31.26%	60.90%	85.41%
TarNeu	7.17%	30.90%	61.05%	87.31%
Trin	7.74%	31.65%	60.78%	89.15%
UppCol	9.78%	31.89%	60.48%	87.41%
Willa	9.56%	32.31%	61.49%	88.94%
Yellow	7.42%	31.64%	59.16%	85.99%

4.2.3.4. *Soils*

Soils data were implemented using SWAT's built-in STATSGO (USDA, 1991) national soils database. The SWAT model uses the full set of characteristics of dominant soil groups directly, including information on infiltration, water holding capacity, erodibility, and soil chemistry. A key input is infiltration capacity, which is used, among other things, to estimate the runoff curve number. Curve numbers are a function of hydrologic soil group, vegetation, land use, cultivation practice, and antecedent moisture conditions. The NRCS (SCS, 1972) has classified more than 4,000 soils into four hydrologic soil groups (HSGs) according to their minimum infiltration rate for bare soil after prolonged wetting. The characteristics associated with each HSG are provided in Table 6.

Table 6. Characteristics of soil hydrologic groups.

Soil Group	Characteristics	Minimum Infiltration Capacity (in/hr)
A	Sandy, deep, well drained soils; deep loess; aggregated silty soils	0.30-0.45
B	Sandy loams, shallow loess, moderately deep and moderately well drained soils	0.15-0.30
C	Clay loam soils, shallow sandy loams with a low permeability horizon impeding drainage (soils with a high clay content), soils low in organic content	0.05-0.15
D	Heavy clay soils with swelling potential (heavy plastic clays), water-logged soils, certain saline soils, or shallow soils over an impermeable layer	0.00-0.05

In the HSPF setup the HRUs are not based directly on dominant soils; instead, these were aggregated to represent HSGs. The HSGs include special agricultural classes (A/D, B/D, and

C/D) in which the first letter represents conditions with artificial drainage and the second letter represents conditions without drainage. The first designator was assumed to apply to all crop land, while the second designator was assumed for all other land uses.

4.2.3.5. *Point Source Discharges*

The primary objective of this study is to examine relative changes that are potentially associated with changes in climate and land use. From that perspective, point source discharges can be characterized as a nuisance parameter. However, point sources that are large enough relative to native flows to affect the observed flows and nutrient loads in river systems need to be included to calibrate the models. This is done in a simplified way, and the point sources were then held constant for future conditions, allowing analysis of relative change. Only the major dischargers, typically those with a discharge rate greater than 1 million gallons per day (MGD) were included in the models. The major dischargers account for the majority of the total flow from all permitted discharges in most watersheds, so the effect on the calibration of omitting smaller sources is relatively small, except perhaps during extreme low flow conditions. Data were sought from the EPA's Permit Compliance System (PCS) database for the major dischargers in the watersheds. Facilities that were missing TN, TP, or TSS concentrations were filled with a typical pollutant concentration value from literature based on Standard Industrial Classification (SIC) code. The major dischargers were represented at long-term average flows, without accounting for changes over time or seasonal variations.

4.2.3.6. *Atmospheric Deposition*

Atmospheric deposition can be a significant source of inorganic nitrogen to watersheds and waterbodies. SWAT2005 allows the user to specify wet atmospheric deposition of nitrate nitrogen. This is specified as a constant concentration across the entire watershed. Wet deposition of ammonia and dry deposition of nitrogen is not addressed in the SWAT2005 model.

HSPF allows the specification of both wet and dry deposition of both nitrate nitrogen and ammonia nitrogen and both were included in the model. Dry deposition is specified as a loading series, rather than concentration series. Because wet deposition is specified as a concentration it will vary in accordance with precipitation changes in future climate scenarios, whereas the dry deposition series (HSPF only) is assumed constant for future scenarios.

Total oxidized nitrogen (NOx) emissions in the U.S. remained relatively constant to a first approximation across the model period considered in this study from the early 1970s up through 2002 (U.S. EPA, 2002). There is strong geographic variability in atmospheric deposition, but much smaller year to year variability at the national scale over this period (Suddick and Davidson, 2012). The National Acid Deposition Program (NADP; http://nadp.sws.uiuc.edu/) monitors wet deposition across the country and produces yearly gridded maps of NO_3 and NH_4 wet deposition concentrations. Dry deposition rates are monitored (and interpreted with models) by the EPA Clean Air Status and Trends Network (CASTNET; http://epa.gov/castnet/javaweb/index.html). Results for year 2000 were selected as generally representative and each study watershed was characterized by a spatial average wet deposition concentration (and dry deposition loading rate for HSPF). Atmospheric deposition of phosphorus and sediment was not considered a significant potential source and is not addressed in the models.

4.2.3.7. *Impoundments, Diversions, and Withdrawals*

The hydrology of many large watersheds in the United States is strongly impacted by anthropogenic modifications, including large impoundments and withdrawals for consumptive use. It is necessary to take these factors into account to develop a calibrated model. At the same time, these anthropogenic factors constitute a problem for evaluating response to future changes, as there is no clear basis for evaluating future changes in reservoir operations or water withdrawals. In addition, information on impoundments, withdrawals, and trans-basin water imports is often difficult to obtain. The approach taken in this project is to minimize the importance of impoundments and withdrawals by focusing on relative changes between present and future conditions with these factors held constant. In this way, the results that are presented are estimates of the change that may be anticipated based on changes to meteorological and land use forcing within the subject study area, with other factors held constant. The results provided here are not complete estimates of future hydrology and pollutant conditions because the adaptive response of human society to water resources management is not included.

The general approach adopted for this project was to select study areas avoiding major human interventions (e.g., reservoirs) in the flow system where possible, to ignore relatively minor interventions, and where necessary to represent significant interventions in a simplified manner. In the first instance, study watersheds were delineated to avoid major reservoirs where possible. For example, the model of the Verde River watershed in the Central Arizona basins is terminated at the inflow to Horseshoe Reservoir. In some cases, as in the Sacramento River watershed, an upstream reservoir is treated as a constant boundary condition because information on future reservoir management responses to climate change was not available.

Impoundments, withdrawals, and water imports that do not have a major impact on downstream flows were generally omitted from the large scale models. Inclusion or omission of such features was a subjective choice of individual modelers; however, it was generally necessary to include such features if they resulted in a modification of flow at downstream gages on the order of 10 percent or more. Where these features were included they were represented in a simplified manner: (1) impoundments were represented by simplified (two-season) stage-discharge operating rules, developed either from documented operational procedures or from analysis of monitored discharge; (2) large withdrawals were represented as either annual or monthly constant average rates; and (3) major trans-basin water imports were also represented as either annual or monthly constant average rates depending on availability of data. Use of surface water for irrigation was simulated only in those basins where it was determined during calibration that it was a significant factor in the overall water balance. These simplifying assumptions decrease the quality of model fit during calibration and validation, but provide a stable basis for the analysis of relative response to climate and land use change within the basin.

The impoundments and other anthropogenic influences on hydrology included in each watershed model are presented in the Assumptions sections of each of the individual calibration reports for the 20 study watersheds (see Appendices D through W).

4.2.4. Weather Representation

Meteorological data (for SWAT and HSPF) were obtained from the 2006 BASINS4 Meteorological Database (U.S. EPA, 2008). The database contains records for 16,000 stations from 1970-2006, set up on an hourly basis, and has the advantage of providing a consistent set of parameters with missing records filled and daily records disaggregated to an hourly time step. A typical site-specific watershed project would assemble additional weather data sources to address under-represented areas, but this requires significant amounts of QA and data processing. It was assumed that the use of the BASINS 2006 data was sufficient to produce reasonable results at the broad spatial scale that is the focus of this project, particularly for evaluating the relative magnitude of change. Significant orographic variability was accounted for through use of lapse rates as the available stations typically under-represent high mountain areas.

The required meteorological data series for both SWAT and HSPF (as implemented for this project) included precipitation, air temperature, and potential evapotranspiration. SWAT uses daily meteorological data, while HSPF requires hourly data. Scenario application required simulation over 30+ years, so the available stations were those with a common 30-year or more period of record (or one that could be filled from an approximately co-located station).

Table 7 presents a summary of annual precipitation and temperature data for each of the modeled watersheds from 1971-2000. Figure 23 and Figure 24 present average monthly precipitation and temperature, respectively, for each of the 20 watersheds. For more specific details on the meteorological data used for each of the modeled watersheds, see the individual calibration memos in Appendices D through W.

Table 7. Weather station statistics for the 20 study areas (1971-2000).

Model Area	Number of precipitation stations	Average annual precipitation total (inches)	Number of temperature stations	Average annual temperature (°F)
Lake Pontchartrain	26	66.33	15	66.64
Neuse/Tar Rivers	40	49.91	28	59.91
ACF	37	54.26	22	63.43
Verde/Salt/San Pedro	29	19.67	25	56.81
Loup/Elkhorn Rivers	81	26.10	31	48.35
Cook Inlet	14	28.50	14	34.16
Georgia-Florida Coastal Plain	51	53.21	37	68.24
Illinois River	72	38.25	47	49.00
Lake Erie-Lake St. Clair	57	38.15	41	49.10
New England Coastal	52	48.45	36	46.23
Rio Grande Valley	53	15.18	41	44.71
Sacramento River	28	37.47	18	57.45
Coastal Southern California	85	20.21	33	61.20
South Platte River	50	16.82	23	43.46
Susquehanna River	60	41.30	27	48.26
Trinity River	64	40.65	32	64.78
Upper Colorado River	47	16.36	39	41.73
Minnesota River	39	28.26	32	43.90
Willamette River	37	58.38	29	51.19
Tongue/Powder R.	37	17.70	30	44.15

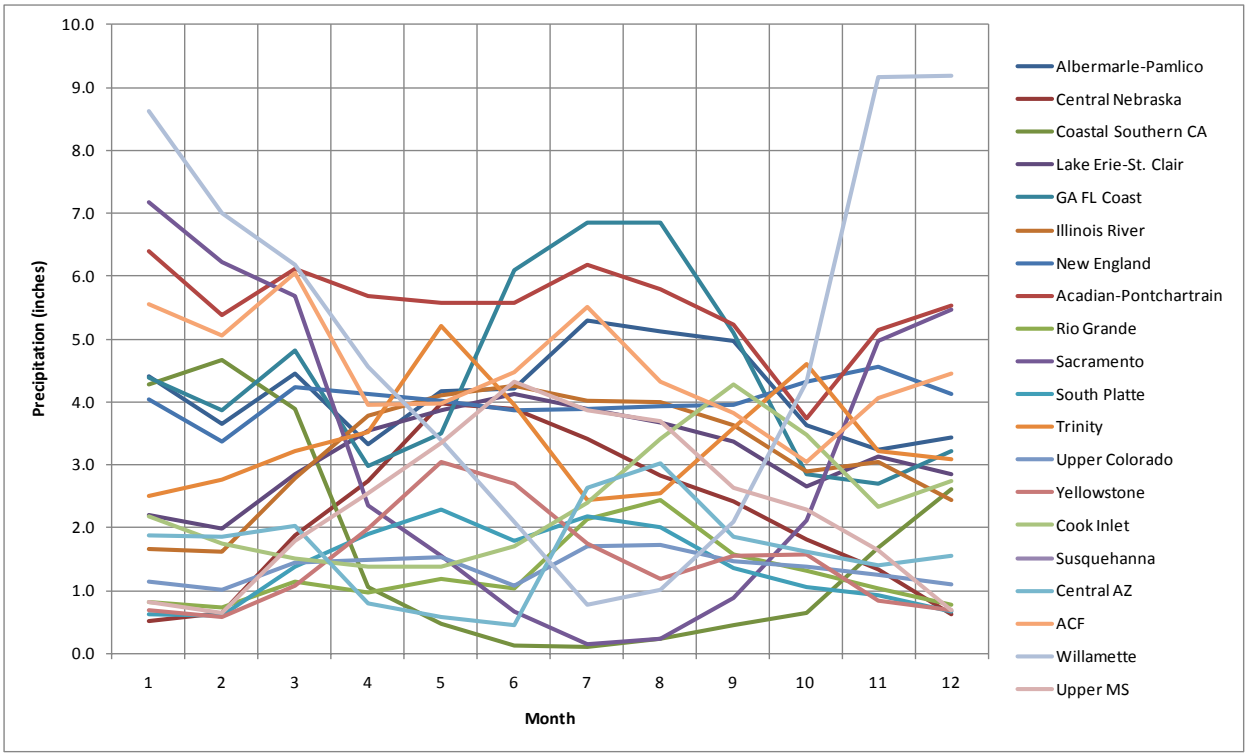

Figure 23. Average monthly precipitation in the 20 study areas (1971-2000).

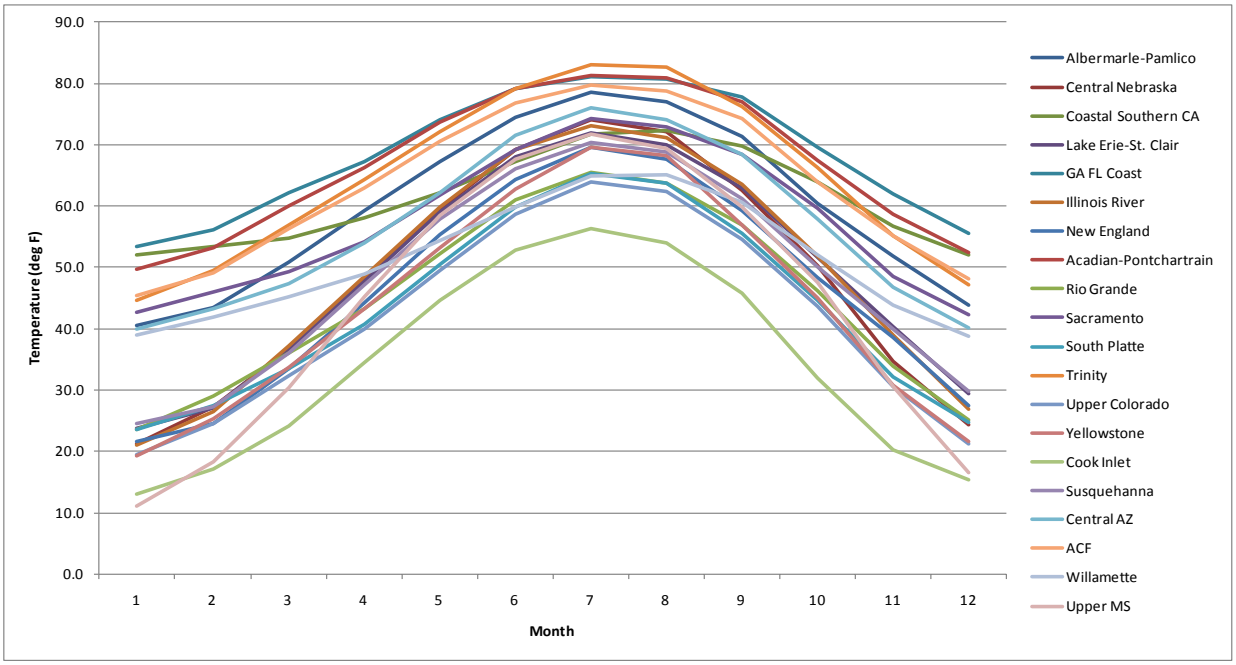

Figure 24. Average monthly temperature in the 20 study areas (1971-2000).

Watershed models are very sensitive to the specification of PET, particularly for simulating low streamflow conditions and events. Many watershed modeling efforts perform well with simplified approaches to estimating PET, such as the Hamon method (included as an option in

the BASINS dataset), which depend primarily on air temperature. However, the robustness of watershed model calibrations conducted with simplified PET is suspect under conditions of climate change, since a variety of other factors that influence PET, such as wind speed and cloud cover, are also likely to change. Therefore, we implemented the Penman-Monteith PET, which employs a full energy balance (Monteith, 1965; Jensen et al., 1990). The implementation varies slightly between SWAT and HSPF: In SWAT the full Penman-Monteith method (Allen et al., 2005) is implemented as an internal option in the model, and includes feedback from crop height. For HSPF, Penman-Monteith reference evapotranspiration at each weather station was calculated externally using observed precipitation and temperature coupled with SWAT weather generator estimates of solar radiation, wind movement, cloud cover, and relative humidity. An evaluation of the parameters used to calculate potential evapotranspiration indicated gaps (especially for solar radiation and cloud cover); hence the SWAT weather generator was used to estimate these parameters. HSPF does not simulate crop growth, so monthly coefficients are incorporated in the model to convert reference crop PET to values appropriate to different crop stages using the Food and Agriculture Organization (FAO) method (Allen et al., 1998).

4.3. MODEL SIMULATION ENDPOINTS

Climate and land use change both have the potential to introduce significant changes in the hydrologic cycle. At the larger scale, flow volumes and the seasonal timing of flow are of immediate and obvious concern. Flows are analyzed in a variety of ways over the 30-year analysis period, including the minimum, median, mean, and maximum change relative to existing conditions among the different scenarios. Because of biases inherent in modeling at this scale, estimates of relative change between historical and future simulations are most relevant. In addition to basic flow statistics, comparisons are made for 100-year flood peak (fit with Log Pearson type III distribution; USGS, 1982), average annual 7-day low flow, Richards-Baker flashiness index (a measure of the frequency and rapidity of short term changes in streamflow; Baker et al., 2004), and days to the centroid of mass for the annual flow on a water-year basis (i.e., days from previous October 1 at which half of the flow for the water year is achieved, an important indicator of changes in the snow accumulation and melt cycle). For the Log Pearson III estimator, use of a regionalized skew coefficient is not appropriate to climate change scenario applications as the regional map represents existing climate. Therefore, the K factor is estimated using the skew coefficient from the model output only, without any weighting with the regional estimate.

Each of the flow metrics discussed in the preceding section has been evaluated for each scenario at the output of each HUC8 contained within a study area. Several other summary measures of the water balance, largely drawn from the work of Hurd et al. (1999), are summarized as averages at the whole-watershed scale. These are:

- Dryness Ratio, defined here as the fraction of precipitation that is lost to evapotranspiration (ET) as reported by the SWAT model. Hurd et al. calculated a dryness ratio by computing ET as the difference between precipitation and basin outflow. Results are generally similar, but the latter approach does not account for additional factors such as channel loss and is affected by reservoir management and boundary conditions.
- Low Flow Sensitivity, expressed as the rate of baseflow generation by shallow groundwater, tile drainage, and lateral subsurface flow pathways in units of cfs/mi^2.

- Surface Runoff Fraction - the fraction of total flow from the uplands that is predicted to proceed through overland flow pathways.
- Snowmelt Fraction – the fraction of total flow from the uplands that is generated by melting snow.
- Deep Recharge Rate – the annual average depth of water simulated as recharging deep aquifers.

Table 8 provides a summary of streamflow and water quality endpoints evaluated in this study.

The mobilization and transport of pollutants will also be affected by climate and land use change, both as a direct result of hydrologic changes and through changes in land cover and plant growth. Monthly and annual loads of sediment, phosphorus, and nitrogen are likely the most useful and reliable measures of water quality produced by the analysis. Accordingly, the focus of comparison among scenarios is on monthly and average annual loads for TSS, total nitrogen, and total phosphorus. As with the flow simulation, it is most appropriate to examine relative rather than absolute changes in simulated pollutant loads when comparing scenarios to current conditions. All models are calibrated and validated, but in many cases current loads are imprecisely known due to limited monitoring data.

Because the sediment load in rivers/streams is often dominated by channel adjustment processes, which are highly site-specific and occur at a fine spatial scale, it is anticipated that precision in the prediction of sediment and sediment-associated pollutant loads will be relatively low. Nutrient balances can also be strongly affected by biological processes in the channels, which can only be roughly approximated at the scale of modeling proposed.

Note that the modeling protocol assumes that several external and anthropogenic factors remain constant in the change simulations:

- External boundary conditions (if needed), such as upstream inflows and pollutant loads, are assumed constant.
- Interactions with deep groundwater systems are assumed constant
- Point source discharges and water withdrawals are assumed constant
- No provision is made for human adaptation in rural land management, such as shifts in crop type in response to climate change
- Plant growth responses to climate change are simulated to the extent they are represented in the SWAT plant growth model; however, large-scale shifts in natural cover type in response to climate change are not simulated.

These assumptions, along with the known large uncertainties associated with modeling regional climate and land use changes several decades into the future, mean that the results that are presented reflect the effects of simulated climate and land use changes on simulated direct hydrologic and pollutant loading impacts that arise within a study area. They represent the range of responses consistent with the current state-of-the-art of modeling future climate and land use

conditions, given the assumptions above, as well as additional assumptions such as reliance on the Intergovernmental Panel on Climate Change (IPCC) A2 emissions scenario, but in no way should be construed to represent forecasts of future conditions.

Table 8. Summary of streamflow and water quality endpoints.

Endpoint	Dimension	Description	Calculation
Future Flow Volume	L^3/t	Average of simulated flow volume	Sum of annual flow volume simulated by the watershed model
Average Seven Day Low Flow	L^3/t	Average annual 7-day low flow event	Lowest 7-day-average flow simulated for each year
100 Year Peak Flow	L^3/t	Estimated peak flow based on annual flow maxima series, Log Pearson III method	Log Pearson III extreme value estimate following USGS (1982), based on simulated annual maxima series
Days to Flow Centroid	t (days)	Number of days from the previous October 1 (start of water year) at which half of the flow volume for that water year is achieved	Count of days to 50% of simulated total annual flow volume for each water year.
Richards-Baker Flashiness Index	dimension-less	Indicator of the frequency and rapidity of short term changes in daily flow rates	Analyzed by method given in Baker et al., 2004, applied to daily flow series for each year
Dryness Ratio	dimension-less	Fraction of input precipitation lost to evapotranspiration (ET)	Calculated as (precipitation – outflow)/precipitation for consistency with Hurd et al. (1999)
Low Flow Sensitivity	L/t	Rate of baseflow contributions from shallow groundwater, tile drainage, and lateral subsurface flow pathways	Sum of simulated flow from shallow groundwater, tile drainage, and lateral subsurface flow pathways divided by area.
Surface Runoff Fraction	dimension-less	Fraction of streamflow contributed by overland flow pathways	Surface runoff divided by total outflow.
Snowmelt Fraction	dimension-less	Fraction of streamflow contributed by snowmelt	Estimated as water equivalent of simulated snowfall divided by total precipitation
Deep Recharge	L/t	Depth of water recharging deep aquifers per unit time	Total water volume simulated as lost to deep recharge divided by area
AET	L/t	Actual depth of evapotranspiration lost to the atmosphere per unit time	Evapotranspiration simulated by the watershed model
PET	L/t	Theoretical potential evapotranspiration assuming moisture not limiting	Potential evapotranspiration simulated by the Penman-Monteith method (Jensen et al., 1990)
Total Suspended Sediment (TSS)	mass/t	Mass load of suspended sediment exiting stream reach per unit time	Sum of simulated mass exiting a stream reach

Total Phosphorus (TP)	mass/t	Mass load of total phosphorus exiting stream reach per unit time	Sum of simulated mass exiting a stream reach
Total Nitrogen (TN)	mass/t	Mass load of total nitrogen exiting stream reach per unit time	Sum of simulated mass exiting a stream reach

4.4. MODEL CALIBRATION AND VALIDATION

Hydrology and water quality calibration and validation were conducted for HSPF and SWAT in each of the five pilot study areas, and for SWAT in 15 non-pilot study areas. The following section provides a brief summary of calibration and validation methods and results. Detailed description of calibration and validation methods and results are included in Appendices D through W.

Calibration refers to the adjustment or fine-tuning of modeling parameters to reproduce observations based on field monitoring data. Calibration is required for parameters that cannot be deterministically and uniquely evaluated from topographic, climatic, physical, and chemical characteristics of the watershed and compounds of interest. Validation is performed by application of the calibrated model to different time periods without further parameter adjustments to test the robustness of the calibrated parameter set. If the model exhibited a significant degradation in performance in the validation period, the calibration process was revisited.

The calibration and validation approach for the very large watersheds addressed in this study was to first focus on a single HUC8 within the larger study area (preferably one for which some modeling was already available along with a good record of flow gaging and water quality monitoring data), then extend the calibration to adjacent areas with modifications as needed to achieve a reasonable fit at multiple spatial scales. Each HUC8 watershed was generally subdivided into approximately 8 subbasins, approximating the HUC10 scale.

The base period for model application was approximately 1970 to 2000, with some variation depending on availability of meteorological data, while the base land use was from 2001 NLCD. In watersheds with significant land use change, moving back too far from 2001 may not provide a firm basis for calibration. Therefore, calibration generally focused on approximately the 1991-2001 time period, although the full 1971-2000 period was used for comparison to future changes. Validation was typically performed on the period before 1991 and/or data from post-1991 at different locations.

4.4.1. Hydrology

The calibration for both HSPF and SWAT endeavored to achieve the range of error statistics for total volume, seasonal flows, and high and low flows recommended by Lumb et al. (1994) and Donigian (2000) for HSPF applications while also maximizing the Nash-Sutcliffe coefficient of model fit efficiency. Standardized spreadsheet tools were developed to help ensure consistency in the calibration and validation process across watersheds as well as to speed processing through use of automation and to provide a standardized set of statistics and graphical comparisons to

data. These statistics were used to adjust appropriate model parameters until a good statistical match was shown between the model output and observed flow.

Lumb et al. (1994) and Donigian (2000) recommend performance targets based on relative mean errors calculated from simulated and observed daily average flows. Donigian classified these into qualitative ranges, which were modified slightly for application to both HSPF and SWAT in this project (Table 9). In general, hydrologic calibration endeavored to achieve a "good" level of model fit where possible. It is important to clarify that the tolerance ranges are intended to be applied to mean values, and that individual events or observations may show larger differences and still be acceptable (Donigian, 2000).

Table 9. Performance targets for hydrologic simulation (magnitude of annual and seasonal relative mean error). From Donigian (2000).

Model Component	Very Good	Good	Fair	Poor
1. Error in total volume	≤ 5%	5 - 10%	10 - 15%	> 15%
2. Error in 50% lowest flow volumes	≤ 5%	5 - 10%	10 - 25%	> 25%
3. Error in 10% highest flow volumes	≤ 10%	10 - 15%	15 - 25%	> 25%
4. Error in storm volume	≤ 10%	10 - 20%	20 - 30%	> 30%
5. Winter volume error	≤ 15%	15 - 30%	30 - 50%	> 50%
6. Spring volume error	≤ 15%	15 - 30%	30 - 50%	> 50%
7. Summer volume error	≤ 15%	15 - 30%	30 - 50%	> 50%
8. Fall volume error	≤ 15%	15 - 30%	30 - 50%	> 50%
9. Error in summer storm volumes	≤ 25%	25 – 50%	50 – 75%	> 75%

The Nash-Sutcliffe coefficient of model fit efficiency (E) is also widely used to evaluate the performance of models that predict time series. Nash and Sutcliffe (1970) define E as:

$$E = 1 - \frac{\sum_{i=1}^{n}\left(O_i - P_i\right)^2}{\sum_{i=1}^{n}\left(O_i - \overline{O}\right)^2},$$

where O_i and P_i represent members of a set of n paired time series observations and predictions, respectively, and $\overline{O}$ is the mean of the observed values. E ranges from minus infinity to 1.0, with higher values indicating better agreement. The coefficient represents the ratio of the mean square error to the variance in the observed data, subtracted from unity (Wilcox et al., 1990). A value of zero for E indicates that the observed mean is as good a predictor of time series values as the model, while negative values indicate that the observed mean is a better predictor than the model. A value of E greater than 0.7 is often taken as an indicator of a good model fit (Donigian, 2000). Note, however, that the value depends on the time basis on which the coefficient is evaluated. That is, values of E for monthly average flows are typically noticeably greater than

values of *E* for daily flows, as watershed models, in the face of uncertainty in the representativeness of precipitation records, are often better predictors of inter-seasonal trends than of intra-seasonal variability. Moriasi et al., (2007) recommend a Nash Sutcliffe *E* of 0.50 or better (applied to monthly sums) as an indicator of adequate hydrologic calibration when accompanied by a relative error of 25 percent or less.

A potential problem with the use of *E* is that it depends on squared differences, making it overly sensitive to extreme values (Legates and McCabe, 1999). This is particularly problematic for sparse time series, such as water quality observations, in which poor estimation of one or a few high outliers may strongly influence the resulting statistic. It is an even greater problem for the comparison of model output to load estimates based on sparse concentration data, as these estimates are themselves highly uncertain (using point-in-time grab samples to represent daily averages and interpolating to unobserved days), further increasing the leverage associated with high outliers.

To address these issues and lessen the effect of outliers, Garrick et al. (1978) proposed use of a baseline adjusted coefficient of model fit efficiency, E_1', which depends on absolute differences rather than squared differences:

$$E_1' = 1 - \frac{\sum_{i=1}^{n} |O_i - P|}{\sum_{i=1}^{n} |O_i - \overline{O}'|}$$

Garrick's proposed statistic is actually more general, allowing $\overline{O}$' to be a baseline value that may be a function of time or of other variables, rather than simply the mean. E_1' may be similar to or greater or less than *E* for a given set of predictions and measurements depending on the type of outliers that are present.

For most watershed models, *E* is an appropriate measure for the fit of flow time series in which complete series of observations are known with reasonable precision. E_1' is a more appropriate and stable measure for the comparison of simulated pollutant loads to estimates based on sparse observed data.

4.4.1.1. *Calibration Adjustments*

HSPF and SWAT hydrology calibration adjustments were made for a range of sensitive parameters selected to represent key watershed processes affecting runoff (U.S. EPA, 2000; Neitsch et al., 2005; see Table 10 and Table 11, respectively, for selected key parameters most frequently adjusted). The adjustment of other parameters and the degree of adjustment to each parameter vary by watershed. Details are provided in the individual calibration reports for each of the watersheds in Appendices D through W.

Table 10. Key hydrology calibration parameters for HSPF.

Parameter name	Definition
INFILT	Nominal infiltration rate parameter
AGWRC	Groundwater recession rate
LZSN	Lower zone nominal soil moisture storage
BASETP	ET by riparian vegetation
KMELT	Degree-day melt factor
PET factor	Potential evapotranspiration
DEEPFR	Fraction of groundwater inflow that will enter deep groundwater
LZETP	Lower zone E-T parameter

Table 11. Key hydrology calibration parameters for SWAT.

Parameter name	Definition
CN	Curve numbers – varied systematically by land use
ESCO	Soil evaporation compensation factor
SURLAG	Surface runoff lag coefficient
ALPHA_BF	Baseflow alpha factor
GW_DELAY	Groundwater delay time
CANMAX	Maximum canopy storage
OV_N, CH_N2, CH_N1	Manning's "n" values for overland flow, main channels, and tributary channels
Sol_AWC	Available water capacity of the soil layer, mm water/mm of soil
Bank storage and recession rates	Bank storage and recession rates
Snow parameters SFTMP, SMTMP, SMFMX and SMFMN	Snowfall temperature, snowmelt base temperature, maximum melt rate for snow during year, and minimum melt rate for snow during year
TIMP	Snow pack temperature lag factor
CH_K1	Effective hydraulic conductivity in tributary channel alluvium

4.4.2. Water Quality

The models in this study are designed to simulate total suspended solids (TSS), total nitrogen, and total phosphorus. The first objective of calibration was to reduce the relative absolute deviation between simulated and estimated loads to below 25 percent if possible. The water quality calibration focuses on the replication of monthly loads, as specified in the project QAPP (Appendix B). While a close match to individual, instantaneous concentration observations cannot be expected given the approach taken in the model simulations of water quality, the calibration also examined the general relationship of observed and predicted concentrations with the intent of minimizing bias relative to flow regime or time of year. Comparison to monthly loads presents challenges, as monthly loads are not observed. Instead, monthly loads must be estimated from scattered concentration grab samples and continuous flow records. As a result, the monthly load calibration is inevitably based on the comparison of two uncertain numbers. Nonetheless, calibration is able to achieve a reasonable agreement. Further, the load comparisons were supported by detailed examinations of the relationships of flows to loads and concentrations and the distribution of concentration prediction errors versus flow, time, and season, as well as standard time series plots.

For application on a nationwide basis, the modeling protocols in this study assume that TSS and total phosphorus loads will likely exhibit a strong positive correlation to flow (and associated erosive processes), while total nitrogen loads, which often have a dominant subsurface loading component, will not (Allan, 1986; Burwell et al., 1975; Follett, 1995). Accordingly, TSS and total phosphorus loads were estimated from observations using a flow-stratified log-log regression approach, while total nitrogen loads were estimated using a flow-stratified averaging estimator, consistent with the findings of Preston et al. (1989).

4.4.2.1. *Calibration Adjustments*

Water quality calibration began with sediment processes. Observed suspended sediment concentrations are the result of multiple processes, including sediment detachment, sediment transport in overland flow, and channel scour and deposition processes. The sediment detachment routines for both SWAT and HSPF were related to USLE parameters available in the soils database. Calibration focuses, for most basins, on sediment transport in overland flow, using the peak rate or transport rate factors available in both models. Channel scour and deposition processes were modified where needed to achieve a fit to observations or where detailed work with prior models provided a basis for modifying default parameters.

In HSPF, nitrogen loading from the land surface was simulated as a buildup/washoff process, while phosphorus was simulated as sediment-associated. Both N and P also were simulated with dissolved-phase loads from interflow and groundwater discharge. Calibration for nutrients in HSPF primarily addressed adjustments of the buildup/washoff coefficients or sediment potency (concentration relative to sediment load) factors and monthly subsurface discharge concentrations. In SWAT, the nutrient simulation is intimately linked to the plant growth model, but is sensitive to initial nutrient concentrations and the ability of plants to withdraw nutrients from various soil layers. In watersheds where significant channel scour was simulated, the nutrient content of scoured sediment was also an important calibration parameter.

4.4.3. Accuracy of the Watershed Models

Significant effort was required to bring the models to an acceptable degree of accuracy in representing existing conditions. Ability to project future conditions under different change scenarios will only be revealed over time.

In general, the full suite of SWAT models for the 20 watersheds – after calibration – provide a good to excellent representation of the water balance at the monthly scale and a fair to good representation of hydrology at the daily scale (see Table 12 for the initial calibration site results). The quality of model fit to hydrology as measured at multiple stations (HUC8 scale and larger) throughout the watershed was, not surprisingly, better when a spatial calibration approach was used. Full results for all calibration sites are provided in the appendices.

Calibration and validation for water quality is more problematic, due to limited amounts of monitoring data and a simplified representation of the multiple complex processes that determine instream pollutant concentrations. The primary objective of water quality simulation in this project is to assess relative changes in pollutant loads, but loads are not directly observed. Inferring loads from point-in-time concentration data and flows introduces another layer of

uncertainty into the calibration process. Calibration also examined observed versus predicted concentrations; however, SWAT, as a daily curve number model, does not have a high level of skill in simulating instantaneous concentrations, particularly during high flow events, and is better suited to the prediction of loads at the weekly to monthly scale.

As with the hydrology calibration, the reliability of the models for simulating changes in water quality appears to increase with calibration at multiple locations. In general, it is more difficult to obtain a high level of precision for simulated water quality than for hydrology in a watershed model, as the processes are complex, the data typically sparse, and any errors in hydrology tend to be amplified in the water quality simulation. The water quality calibration is based on loads, but loads are not directly observed. Instead, loads are inferred from sparse concentration monitoring data and flow gaging. Thus, both the simulated and "observed" loads are subject to considerable uncertainty. Comparison based on concentrations can also be problematic, as most water quality samples are grab samples that represent points in time and space, whereas model output is integrated over a stream segment and may produce large apparent errors due to small shifts in timing. Finally, most stations at the HUC8 scale include upstream point sources, which often have a strong influence on low-flow concentrations and load estimates. Limited knowledge about point source loads thus also creates a challenge for the water quality calibration. In most cases, the pollutant load simulations from the SWAT model appear to be in the fair to good range (Table 12) – except in a few cases where parameters were extended from one station to another watershed without adjustment giving poor results. This suggests limits to the reliability of simulation results in the portions of watersheds for which calibration was not pursued. Nonetheless, predictions of relative response to climate and land use change scenarios are likely to be more reliable than quantitative predictions of observed concentrations – as long as the significant processes that determine pollutant load and transport within a watershed are represented.

For the pilot sites, HSPF model calibration provided a somewhat stronger fit to daily flows in four of the five watersheds (Table 13), presumably at least in part due to HSPF's use of sub-daily precipitation. In two models, the fit to sediment load was notably worse for HSPF, apparently due to the difficulties in adjusting the more complex channel scour and deposition routines of this model with limited data and on a compressed schedule.

Table 12. Summary of SWAT model fit for initial calibration site (20 Watersheds).

Study Area	Initial Calibration/ Validation Watershed	Initial Calibration/ Validation USGS Gage	Hydrology Cal. /Val. Years	Total Volume Cal./Val. (Daily *E*)	Total Volume Cal./Val. (% Error)	Water Quality Cal./Val Years	TSS Load Cal./Val. (% Error)	TP Load Cal./Val. (% Error)	TN Load Cal./Val. (% Error)
Apalachicola-Chattahoochee-Flint	Upper Flint River	02349605	1993-2002/ 1983-1992	0.62/0.56	7.28/3.33	1999-2002/ 1991-1998	-9/17	-50/-30	-18/9
Coastal Southern California Basins	Santa Ana River	11066460	1991-2001/ 1981-1991	0.63/0.59	3.71/1.61	1998-2000/ ND	19/NA	-14.7/NA	-5.5/NA
Cook Inlet Basin	Kenai River	15266300	1992-2001/ 1982-1991	0.68/0.55	-18.96/19.49	1985-2001/ 1972-1984	66.4/64.1	83.2/82.18	57.3/50.4
Georgia-Florida Coastal Plain	Ochlockonee River	02329000	1992-2002/ 1982-1992	0.71/0.8	4.25/-5.54	1992-2002/ 1982-1992	9.5/-6.6	-7.4/-5.8	-8/-5
Illinois River Basin	Iroquois River	05526000	1992-2001/ 1982-1992	0.7/0.67	-16.99/-2.98	1985-2001/ 1978-1984	38/39	5/-1	56/60
Lake Erie-Lake St. Clair Drainages	Lake Erie-St. Clair Basin	04208000	1990-2000/ 1980-1990	0.61/0.62	-3.32/-13.38	1990-2000/ 1980-1990	67.9/69.8	23.9/-12.5	35.8/13.7
Lake Pontchartrain Drainage	Amite River	07378500	1995-2004/ 1985-1994	0.79/0.69	-1.61/-0.93	1984 – 1994/ ND	9.2/NA	2.4/NA	-8.9/NA
Loup/Elkhorn River Basin	Elkhorn River	06800500	1989-1999/ 1978-1988	0.42/0.52	-2.59/-8.81	1990-1995/ 1979-1989	59.6/66.8	24.2/34.9	28.1/18.1
Minnesota River Basin	Cottonwood River	05317000	1992-2002/ 1982-1992	0.79/0.74	-5.41/-0.84	1993-200 /1986-1992	9.2/9	9.3/-21.6	-8.9/-1.3
Neuse/Tar River Basins	Contentnea Creek	02091500	1993-2003/ 1983-1993	0.68/0.64	-3.98/-1.18	1993-2003/ 1983-1993	-19.9/9.9	15.9/5.3	-5.6/5.3
New England Coastal Basins	Saco River	01066000	1993-2003/ 1983-1993	0.61/0.76	1.08/0.67	1993-2003/ 1983-1993	-9/3.2	9.6/-11.5	27.5/26.3
Powder/Tongue River Basin	Tongue River	06306300	1993-2003/ 1983-1993	0.72/0.7	9.26/-9.95	1993-2003/ 1982-2002	-21.8/-3.4	8.8/35.1	3.9/31.5
Rio Grande Valley	Saguache Creek	08227000	1993-2003/ 1983-1993	0.47/0.07	-4.92/32.99	1985-2003/ 1973-1984	57.3/41	-46.9/-653.98	-28.3/-909.1
Sacramento River Basin	Sacramento River	11377100	1992-2001/ 1983-1992	0.75/0.57	10.23/10.06	1997-2001 /1973-1996	-2/-55	-8/-33	-135/-156

Study Area	Initial Calibration/ Validation Watershed	Initial Calibration/ Validation USGS Gage	Hydrology Cal. /Val. Years	Total Volume Cal./Val. (Daily *E*)	Total Volume Cal./Val. (% Error)	Water Quality Cal./Val Years	TSS Load Cal./Val. (% Error)	TP Load Cal./Val. (% Error)	TN Load Cal./Val. (% Error)
Salt, Verde, and San Pedro River Basins	Verde River	09504000	1992-2002/ 1982-1992	0.03/-1	-2.46/5.68	1993-2002/ 1986-1992	16.9/-42.6	83.5/31.4	-14.4/-15.9
South Platte River Basin	South Platte River	06714000	1991-2000/ 1981-1990	0.74/0.52	9.82/-16.28	1993-2000/ ND	86.6/	-14/NA	6.1/NA
Susquehanna River Basin	Raystown Branch of the Juniata River	02050303	1995-2005/ 1985-1995	0.29/0.42	-5.41/16.3	1991-2000/ 1990	-10.1/-33.6	-0.5/-9.2	28.6/43.9
Trinity River Basin	Trinity River	05330000	1992-2001/ 1982-1991	0.62/0.47	-6.88/0.7	1985-2001/ 1972-1984	9.2/-17.4	3/-21.58	-3.8/-31.9
Upper Colorado River Basin	Colorado River	09070500	1992-2002/ 1982-1992	0.83/0.78	8.18/0.93	1992-2002/ 1992-1992	0.4/NA	47.4/NA	15.1/NA
Willamette River Basin	Tualatin River	14207500	1995-2005/ 1985-1995	0.49/0.39	-4.76/-12.1	1991-1995/ 1986-1990	-12/-7	-114/-105	-72/-66

Table 13. Summary of HSPF model fit for initial calibration sites (5 Pilot Watersheds)

Study Area	Initial Calibration/ Validation Watershed	Initial calibration/ Validation USGS Gage	Hydrology Cal. /Val. Years	Total Volume Cal./Val. (Daily *E*)	Total Volume Cal./Val. (% Error)	Water Quality Cal./Val Years	TSS Load Cal./Val. (% Error)	TP Load Cal./Val. (% Error)	TN Load Cal./Val. (% Error)
Apalachicola-Chattahoochee-Flint Basins	Upper Flint River	02349605	1993-2002/ 1983-1992	0.707/0.651	5.50/5.79	1999-2002/ 1991-1998	-117/-78	-59/-23	-30/-22
Minnesota River Basin	Cottonwood River	05317000	1992-2002/ 1982-1992	0.754/0.779	1.61/14.78	1993-2002 / 1986-1992	7.5/13.1	23/15.8	15.4/16.2
Salt/Verde/San Pedro River Basins	Verde River	09504000	1992-2002/ 1982-1992	0.481/0.451	2.43/6.31	1993-2002 / 1986-1992	31/-41	87/66	1.6/-2.7
Susquehanna River Basin	Raystown Branch of the Juniata River	02050303	1995-2005/ 1985-1995	0.698/0.553	-0.16/-8.0	1991-2000 / 1990	-78.2/-89.7	26.0/21.5	7.0/17.2
Willamette River Basin	Tualatin River	14207500	1995-2005/ 1985-1995	0.731/0.811	-3.92/-9.80	1991-1995/ 1986-1990	3.0/4.8	-1.2/-9.3	2.2/-6.3

5. CLIMATE CHANGE AND URBAN DEVELOPMENT SCENARIOS

The SWAT and HSPF models were applied to simulate historical baseline conditions, and watershed response to future urban development, climate change, and the combined response to climate change and urban development.

Historical conditions were simulated for each of the 20 watersheds to define baseline, or existing, climate and land use conditions. The base period for model application was 30 years within the range of 1969-2005, depending on data availability, while the base land use was from the 2001 NLCD, which is also the basis for ICLUS projections. The individual calibration reports in Appendices D through W present the baseline conditions in greater detail.

Climate change scenarios are based on mid-21st century climate model projections downscaled with regional climate models (RCMs) from the North American Regional Climate Change Assessment Program (NARCCAP) and the bias-corrected and spatially downscaled (BCSD) data set described by Maurer et al. (2007). Fourteen different climate scenarios were applied to the five pilot watersheds, and a subset of 6 climate scenarios from the NARCCAP archive were applied to the non-pilot watersheds. Urban and residential development scenarios are based on EPA's national-scale Integrated Climate and Land Use Scenarios (ICLUS) project (U.S. EPA, 2009d). The following sections discuss in more detail climate change and urban development scenarios.

5.1. CLIMATE CHANGE SCENARIOS

The scientific uncertainties related to our understanding of the physical climate system are large, and they will continue to be large for the foreseeable future. It is beyond our current capabilities to predict with accuracy decadal (and longer) climate changes at the regional spatial scales of relevance for watershed processes (e.g., see Cox and Stephenson, 2007; Stainforth et al., 2007; Raisanen, 2007; Hawkins and Sutton, 2009; among many others). The uncertainties associated with socioeconomic trajectories, technological advances, and regulatory changes that will drive greenhouse gas emissions changes (and land use changes) are even larger and less potentially tractable.

Faced with this uncertainty, an appropriate strategy is to take a scenario-based approach to the problem of understanding climate change impacts on water quality. A scenario is a plausible description of how the future may develop, based on a coherent and internally consistent set of assumptions about driving forces and key relationships (IPCC, 2007). Scenarios are used in assessments to provide alternative views of future conditions considered likely to influence a given system or activity. By systematically exploring the implications of a wide range of plausible alternative futures, or scenarios, we can reveal where the greatest vulnerabilities lie. This information can be used by decision makers to help understand and guide the development of response strategies for managing climate risk. A critical step in this approach is to create a number of plausible future states that span the key uncertainties in the problem. The goal is not to estimate a single, "most likely" future trajectory for each study watershed, but instead to understand, to the extent feasible, how big an envelope of potential future impacts we are unable to discount and must therefore incorporate into future planning.

Note that, for climate change studies, the word "scenario" is often used in the context of the Intergovernmental Panel on Climate Change (IPCC) greenhouse gas storylines. The IPCC emissions scenarios describe alternative development pathways, covering a range of demographic, economic, and technological driving forces that affect GHG emissions. This can produce some confusion when phrases like "climate change scenarios" are used to refer to the future climates simulated using these greenhouse gas storylines. For the purposes of this study, "scenario" is a generic term that can be applied to any defined future, including a climate future or a land-use future, among others.

Initial simulation of watershed response to climate change scenarios focused on the five pilot study basins using both the HSPF and SWAT watershed models. Meteorological datasets representing a suite of potential climate change scenarios for the period 2041-2070 were developed from the North American Regional Climate Change Assessment Program (NARCCAP) archive of dynamically downscaled climate products and the BCSD statistically downscaled output, along with raw (un-downscaled) Global Climate Model (GCM) output (Table 14). We also explored use of GCMs without downscaling and use of bias-corrected statistically downscaled (BCSD) scenarios, for a total of 14 climate scenarios. These datasets were combined with scenarios of future land-use change (residential and urban) acquired from EPA's ICLUS project. For the five pilot basins a full range of 14 climate scenarios were implemented with both the HSPF and SWAT models with and without future land-use change. For the remaining 15 non-pilot basins, the 6 available NARCCAP dynamically downscaled climate products were simulated, with and without land-use change, using the SWAT model only.

The general strategy for developing meteorological change scenarios appropriate for input to the watershed models from the climate change scenarios is to take an approximately 30-year time series of observed local climate observations (to which the watershed models have been calibrated) and adjust these observed data to reflect the change in climate as simulated by the global and regional climate models (and downscaling approaches). This approach is implemented for a number of reasons. First, the GCM and RCM output, including the 50-km NARCCAP scale is still too coarse for watershed modeling. In addition, climate models do not necessarily archive all the meteorological forcing variables that watershed models expect. Finally, many GCMs display well-documented biases with regard to precipitation frequency and intensity. Specifically, there is a tendency for GCMs to generate too many low-intensity events and to under-simulate the intensity of heavy events (Sun et al., 2006; Dai, 2006). The frequency and duration of large events can have significant effects on hydrology, pollutant loading, and other watershed processes. Applying the model-derived change statistics to the observed precipitation time series mitigates this problem.

In practice, when relying on models to develop climate scenarios, this means sampling across multiple Global Climate Models (GCMs), multiple methodologies for regionalizing or "downscaling" the model output to finer scales, and, depending on the time horizon considered, multiple greenhouse gas pathways. Use of a single model run is not considered scientifically rigorous for climate impacts studies. This is because, while the leading GCMs often produce very different results for future climate change in a given region, there is no consensus in the

climate sciences communities that any of these are across-the-board better or more accurate than the others (e.g., see Gleckler et al., 2008). In this study, six different regionally downscaled climate scenarios for the 2041 – 2070 period are applied to all watersheds; a total of 14 scenarios (including statistically downscaled products and un-downscaled GCM output) were applied to the five pilot study areas. Descriptions of the climate models used to develop the scenarios are provided in sections 5.1.1. to 5.1.3.

Table 14 shows climate models and source of model data used to develop climate change scenarios evaluated in this study. The table also contains a numbering key for shorthand reference to climate scenarios. For example, climate scenario 2 refers to the HadCM3 GCM, downscaled with the HRM3 RCM. All 14 scenarios are applied in the 5 pilot sites. Only scenarios 1 through 6 are applied for the non-pilot sites.

Table 14. Climate models and source of model data used to develop climate change scenarios. Model abbreviations are as follows: CGCM3=Third Generation Coupled GCM; HADCM3=Hadley Centre Coupled Model v3; GFDL=Geophysical Fluid Dynamics Lab GCM; CCSM=Community Climate System Model; CRCM= Canadian Regional Climate Model; RCM3= Regional Climate Model v3; HRM3= Hadley Region Model 3; WRFP= Weather Research and Forecasting Model; GFDL hi res= Geophysical Fluid Dynamics Laboratory 50-km global atmospheric time slice.

Scenario #	Climate Model(s) (GCM / RCM)
NARCCAP (dynamically downscaled)	
1	CGCM3 / CRCM
2	HadCM3 / HRM3
3	GFDL / RCM3
4	GFDL / GFDL high res
5	CGCM3 / RCM3
6	CCSM / WRFP
GCM (without downscaling)	
7	CGCM3
8	HadCM3
9	GFDL
10	CCSM
BCSD (statistically downscaled)	
11	CGCM3
12	HadCM3
13	GFDL
14	CCSM

5.1.1. North American Regional Climate Change Assessment Program (NARCCAP) Scenarios

Six regionally downscaled climate change scenarios (based on four underlying GCMs) were acquired from the National Center for Atmospheric Research (NCAR) North American Regional Climate Change Assessment Program (NARCCAP) project (representative of the future period 2041-2070) (Mearns, 2009; http://www.narccap.ucar.edu). The NARCCAP program uses a variety of different Regional Climate Models (RCMs) to downscale the output from a few of the IPCC Global Climate Models (GCMs) to higher resolution over the conterminous United States and most of the rest of North America. NARCCAP's purpose is to provide detailed scenarios of regional climate change over the continent, while, by employing the RCMs and GCMs in different combinations, systematically investigating the effect of modeling uncertainties on the scenario results (i.e., uncertainties associated with using different GCMs, RCMs, model physical parameterizations and configurations). The downscaled output is archived for the periods 1971-2000 and 2041-2070 at a temporal resolution of three hours.

NARCCAP uses the IPCC's A2 greenhouse gas storyline. The A2 scenario is a relatively pessimistic scenario that assumes a very heterogeneous world with high population growth, slow economic development, and slow technological change. While no likelihood is attached to any of the SRES scenarios, emissions are currently rising at rates comparable to those assumed under the IPCC A2 scenario. Use of a single greenhouse gas storyline is reasonable in this case where the focus is on a mid-century future period, as the different IPCC greenhouse gas storylines have not yet diverged much by this point, and model uncertainty is therefore correspondingly more important.

5.1.2. Bias-Corrected and Spatially Downscaled (BCSD) Scenarios

At the time modeling was initiated (mid 2010), only six out of a total of 14 planned downscaled scenarios (GCM-RCM combinations) were available from NARCCAP. The dynamically downscaled atmospheric models available from NARCCAP are the core climate scenarios for evaluation of watershed response. However, implementation of RCMs for dynamical downscaling is a time-consuming and expensive process. A subsidiary research objective for the five pilot sites was to compare results obtained without full dynamical downscaling. These included output from the bias-corrected and spatially downscaled (BCSD) methodology (Wood et al., 2004; Maurer et al., 2007) provided by the World Climate Research Programme's (WCRP's) Coupled Model Intercomparison Project phase 3 (CMIP3) multi-model dataset (Bureau of Reclamation/Santa Clara University/Lawrence Livermore archive of downscaled IPCC model runs).

The BCSD climate projections derived from CMIP3 data are served at http://go-dcp.ucllnl.org/downscaled_cmip3_projections/. These data use statistical bias correction to interpret GCMs over a large spatial domain based on current observations. The principal potential weakness of this approach is an assumption of stationarity. That is, the assumption is made that the relationship between large-scale precipitation and temperature and local precipitation and temperature in the future will be the same as in the past. Thus, the method can successfully account for orographic effects that are observed in current data, but not for impacts

that might result from the interaction of changed wind direction and orographic effects. A second assumption included in the bias-correction step of the BCSD method is that any biases exhibited by a GCM for the historical period will also be exhibited in simulations of future periods.

The BCSD scenarios, while all derived from the A2 climate storyline, do not in all cases use the output of the exact same GCM run that was used to construct the NARCCAP archive. Specifically, the BCSD results for the GFDL and CGCM3 GCMs use exactly the same GCM output as NARCCAP, but BCSD results for HadCM3 and CCSM use different runs of the A2 scenario than used by NARCCAP. The HadCM3 run used in NARCCAP was a custom run generated specifically for NARCCAP and has not been downscaled for the CMIP3 archive. The CCSM run used in NARCCAP is run number 5, but this is not available in the CMIP3 archive. Instead, the BCSD results use the HadCM3 run 1 and CCSM run 4 from the CMIP3 archive for the A2 scenario. As a result, the most direct comparisons between NARCCAP dynamic downscaling and BCSD output are for these two models, HadCM3 and CCSM. However, we still expect comparisons between NARCCAP and BCSD downscaling for the GFDL and CGCM3 GCMs to provide useful insights when considered along with the HadCM3 and CCSM comparisons.

5.1.3. Global Climate Models (GCMs) without Downscaling

Scenarios for the five pilot sites also examined use of the direct output from the GCM runs used to drive the NARCCAP downscaling (i.e., no downscaling). Comparison of results from these scenarios to full dynamical downscaling is expected to inform the accuracy with which simpler methods can be used to address watershed response.

5.1.4. Translation of Climate Model Projections to Meteorological Model Inputs

Meteorological time series for input to the watershed models were created using a “change factor” or “delta change” method. Approximately 30-year time series of observed local climate observations (to which the watershed models have been calibrated) were adjusted to reflect the changes in climate as simulated by the climate models. The benefits of this approach include its simplicity, elimination of the need for bias correction, and ability to create spatially variable climate change scenarios that maintain the observed historical spatial correlation structure among different watershed locations. Limitations include the inability to adjust the number and timing of precipitation events (e.g., to add precipitation events on dry days), and potential bias introduced through the selection of an arbitrary historical base period that is adjusted.

Change factors for temperature and precipitation were calculated for each month of the year as the differences between simulated average monthly values for the 2041-2070 and 1971-2000 periods. These change statistics were then used to perturb existing records of hourly observed precipitation and temperature contained in the BASINS Meteorological Database using the Climate Assessment Tool (CAT) (U.S. EPA, 2009c). CAT permits the sequential modification of weather records to introduce a number of alterations, each reflecting various assumptions concerning the regional manifestations of climate change. Precipitation records can be modified by (1) multiplying all records by an empirical constant reflecting projected climate change to simulate a shift in total precipitation, applied uniformly to all periods and intensity classes, (2) selective application of such a multiplier to specific seasons or months, (3) selective application of the multiplier to a range of months or years within the record, and (4) selective application of

the multiplier to storm events of a specific size or intensity class (U.S. EPA, 2009c). Modification can be iteratively applied to more than one event size class, allowing changes in frequency and intensity as well as changes in overall volume of precipitation to be represented. Temperature records can be modified by adding or subtracting a constant to all values in the record, or selective application to certain months or years within the record.

The base weather data for simulation relies on the 2006 Meteorological Database in EPA's BASINS system, which contains records for 16,000 stations for 1970-2006, set up on an hourly basis. Use of this system has the advantage of providing a consistent set of parameters with missing records filled and daily records disaggregated to an hourly time step. Whereas, a site-specific watershed project would typically assemble additional weather data sources to address under-represented areas, use of the BASINS 2006 data is sufficient to produce reasonable results of the relative magnitudes of potential future change at the broad spatial scales and wide geographic coverage of this project.

The parameters requested from NARCCAP for the dynamically downscaled model runs were:

- Total precipitation change (mm/day and percent)
- Total accumulated precipitation data for five different percentile bins - 0-25, 25-50, 50-75, 75-90, and greater than 90 percent.
- Surface air temperature, average, daily maximum, and daily minimum (°K and percent)
- Dew point temperature change (°K and percent)
- Relative humidity change
- Surface downwelling shortwave radiation change (W m^{-2} and percent)
- 10-meter wind speed change (m s^{-1} and percent)
-

The cited statistics were provided for locations corresponding to each of the BASINS meteorological stations and SWAT weather generator stations used in the watershed models. The full suite of statistics is not available for the statistically downscaled model runs or the raw GCM archives. Data availability is summarized in Table 15.

Table 15. Climate change data available from each source used to develop scenarios.

Scenario #	RCM	GCM	Temp.	Prec.	Dew Point Temp	Solar Radiation	Wind Speed	Min Temp.	Max Temp.	Prec. Bin Data
NARCCAP RCM-downscaled scenarios										
1	CRCM	CGCM3	X	X	X	X	X	X	X	X
2	HRM3	HadCM3	X	X	X	X	X	X	X	X
3	RCM3	GFDL	X	X	X	X	X	X	X	X
4	GFDL high res	GFDL	X	X	X	X	X	X	X	X
5	RCM3	CGCM3	X	X	X	n/a	X	X	X	X

Scenario #	RCM	GCM	Temp.	Prec.	Dew Point Temp	Solar Radiation	Wind Speed	Min Temp.	Max Temp.	Prec. Bin Data
6	WRFP	CCSM	X	X	X	X	X	X	X	X
Driving GCMs of the NARCCAP scenarios (i.e., no downscaling)										
7		CGCM3	X	X	X	X	X	n/a	n/a	n/a
8		HadCM3	X	X	n/a	n/a	n/a	n/a	n/a	n/a
9		GFDL	X	X	n/a	X	X	n/a	n/a	n/a
10		CCSM	X	X	X	X	n/a	n/a	n/a	n/a
CMIP3 statistically downscaled scenarios										
11		CGCM3	X	X	n/a	n/a	n/a	n/a	n/a	n/a
12		HadCM3	X	X	n/a	n/a	n/a	n/a	n/a	n/a
13		GFDL	X	X	n/a	n/a	n/a	n/a	n/a	n/a
14		CCSM	X	X	n/a	n/a	n/a	n/a	n/a	n/a

5.1.4.1. *Temperature Changes*

Implementation of model simulated temperature time series is straightforward. Monthly variations (deltas) to the temperature time-series throughout the entire time-period were applied using the CAT tool. Monthly adjustments based on each scenario were used and a modified HSPF binary data (WDM) file was created. The temperature time series were adjusted based on an additive change using the monthly deltas (°K) calculated from the 2041-2070 to 1971-2000 climate simulation comparison. Beginning with the HSPF WDM, an automated script then creates the SWAT observed temperature files (daily maximum and daily minimum).

5.1.4.2. *Precipitation Changes*

Relative changes in the *frequency* and *intensity* of precipitation events associated with climate change may prove to be more influential in determining future patterns of discharge than changes in overall (annual, seasonal) precipitation. Appendix C presents a summary review of recent literature to address the following questions: (1) How should precipitation change as a consequence of lower atmosphere warming? (2) What is the historical evidence for increases in precipitation intensity over the United States? (3) What do climate models simulate with respect to precipitation frequency and intensity? (4) What are the important limitations in these simulations, and (5) What are the implications for the development of meteorological time series used in the modeling study? In particular, the partitioning of precipitation into re-evaporation, runoff, and percolation to groundwater is understood to be sensitive to the intensity and timing of precipitation events.

As a general pattern, warming of the lower atmosphere is projected to lead to a more vigorous hydrologic cycle, characterized by increases in global precipitation, and proportionally larger

increases in high-intensity precipitation events (Trenberth et al., 2007). Much of the U.S. is anticipated to experience an increasing proportion of annual precipitation as larger, more intense events (Kundzewicz et al., 2007; Groisman et al., 2005). Increasing intensity of precipitation could increase direct runoff during events, and increase non-point source loading of sediment, nutrients, and other pollutants to streams (Gutowski et al., 2008). To ensure that model simulations embody the most important dimensions of climate change affecting watershed response, it is important that climate change scenarios represent potential changes in precipitation intensity-frequency-duration (IFD) relationships.

In the delta method, future climate time series are constructed by applying changes to observed precipitation time series that represent the relative differences between historical simulations and future climate scenarios from the climate models. No modifications were made to the number of rainfall events in the observed record. The most rigorous approach to applying the downscaled climate scenario results to modification of the existing precipitation series would be to undertake a detailed analysis (by month) of the distribution of precipitation *event* volumes and intensities. Working on an event basis is important because many of the existing precipitation time series in the BASINS meteorological dataset are disaggregated from daily totals. However, analyzing volume-event data for each of the climate scenarios for all the precipitation stations was not feasible and the ability of the climate models to correctly simulate event durations is suspect. Therefore, a different approach was developed to apply changes in intensity in the precipitation time series.

Total accumulated precipitation data for different percentile bins (for each station location by month) were provided by NARCCAP for the dynamically downscaled climate products. The data consisted of total simulated precipitation volume (over 30 years) and the 0-25, 25-50, 50-70, and 70-90, and >90 percentile bins of the 3-hr intensity distribution (relative to the existing intensity distribution). These intensity percentiles yield information on where precipitation intensification occurs, but represent fixed 3-hr windows, not discrete event volumes, as required for the CAT tool. Most of the climate scenarios showed increases in precipitation volume in the larger events, while the smaller ones remained constant or decreased. The net effect of this was an increase in the proportion of annual precipitation occurring in larger events. Analysis of the comprehensive (percentile, total volume) climate scenario data showed that, for most weather stations, the change in the lower percentiles of the intensity distribution appeared to be relatively small compared to the changes above the 70^{th} percentile. However, in some cases (e.g., in Arizona, there is greater change in the $25\text{-}50^{th}$ percentile bin).

To account for changes in intensity, climate change scenarios were created using the delta method by applying climate change adjustments separately to precipitation events ≥ 70th percentile and events < 70th percentile, while maintaining the appropriate mass balance as described below.

Percentile bin-intensity data were available only for climate scenarios 1 through 6 (RCM-downscaled scenarios). Bin data were not available for climate scenarios 7 through 14 (GCM and statistically downscaled scenarios). Two approaches were developed to account for intensification of precipitation, depending on whether precipitation bin data were available. Each approach is discussed in detail below.

Approach 1: Precipitation Bin Data are Available

This approach is applicable to scenarios 1 through 6 for which the total accumulated precipitation data for different percentile bins were provided by NARCCAP. For these data the change in the volume about the 70th percentile intensity can be taken as an *index* of the change in the top 30 percent of events. The change in the top 30 percent was selected based on the information on the percentile values of the 3-hr events. At the same time, it is necessary to honor the data on the relative change in total volume. This can be accomplished as follows:

Let the ratio of total volume in a climate scenario (V_2) relative to the baseline scenario volume (V_1) be given by $r = (V_2/V_1)$. Further assume that the total event volume (V) can be decomposed into the top 30 percent (V_H) and bottom 70 percent (V_L). These may be related by a ratio $s = V_H/V_L$. To conserve the total volume we must have

$$V_2 = rV_1.$$

This equation can be rewritten to account for intensification of the top 30 percent of events (V_H) by introducing an intensification parameter, q:

$$V_2 = rV_{L,1} + rV_{H,1} + \left(rqV_{H,1} - rqV_{H,1}\right) = \left[rV_{L,1} - rqV_{H,1}\right] + \left[r(1+q)V_{H,1}\right],$$

Substituting for the first instance of $V_{H,1} = s\,V_{L,1}$ yields:

$$V_2 = (r - rqs)V_{L,1} + (r + qr)V_{H.1}.$$

Here the first term represents the change in the volume of the lower 70 percent of events and the second term the change in the top 30 percent. This provides multiplicative factors that can be applied to event ranges using CAT's built-in capabilities on a month-by-month basis.

The intensification parameter, q, can be calculated by defining it relative to the lower 70 percentile values (i.e., from 0 to 70th percentile). Specifically (r-rqs) which represents the events below the 70th percentile can be written as the ratio of the sum of the volumes below the 70th percentile in a climate scenario relative to the sum of the volumes below the 70th percentile for the current condition:

$$(r - rqs) = \frac{(V_{70})_2}{(V_{70})_1} \approx \frac{(Q_{70})_2}{(Q_{70})_1}$$

where $(Q_{70})_1$ and $(Q_{70})_2$ are the sum of the volumes reported up to the 70th percentile for a month for the current condition and future condition respectively.

Solving this equation for q yields:

$$q = (1 - A/r)/s$$

where A is defined as $A = \frac{(Q_{70})_2}{(Q_{70})_1}$

In sum, for each month at each station the following were calculated:

$r = V_2 / V_1$ from the summary of the climate scenario output,

$s = V_H / (V - V_H)$ from the existing observed precipitation data for the station, sorted into events and post-processed to evaluate the top 30 percent (V_H) and bottom 70 percent (V_L) event volumes. The numerator is calculated as the difference between total volume and the top 30 percent volume, rather than directly from V_L to correct for analyses in which some scattered precipitation is not included within defined "events." The *s* value was calculated by month and percentile (for every station, every month) using the observed precipitation time-series data that forms the template for the delta method representation of future climate time series.

$q = (1 - A/r)/s$ from the summary of the percentile bin climate scenario output summary

The multiplicative adjustment factors for use in the CAT tool can then be assembled as:

$r\,(1 - qs)$, for the events below the 70th percentile, and
$r\,(1 + q)$, for the events above the 70th percentile.

In addition to the typical pattern of intensification of large events, this approach is also sufficient for the cases where there is a relative increase in the low-percentile intensities. In those cases the change in the 70th percentile intensity is relatively small and tends to be less than current conditions under the future scenario, resulting in q being a small negative number. Then, application of the method results in a decrease in the fraction of the total volume belonging to the larger events, with a shift to the smaller events – thus approximating observed increases in intensity for smaller events.

In general, it is necessary to have $-1 < q < 1/s$ to prevent negative solutions to the multipliers. The condition that $q < 1/s$ is guaranteed to be met by the definition of q (because A/r is always positive); however, the lower bound condition is not guaranteed to be met. Further, the calculation of q from the percentile bin data is at best an approximation of the actual intensification pattern. To address this problem a further constraint is placed on q requiring that some precipitation must remain in both the high and low ranges after adjustment by requiring $-0.8 < q < 0.8/s$. It should be noted that the cases in which negative solutions arose were rare and mainly occurred for stations located in Arizona in the summer months.

Approach 2: Precipitation Bin Data not Available

This approach is applicable for climate scenarios 7 through 14, for which precipitation bin-intensity data were not available. For all these climate scenarios the distribution of volume

changes to events of different sizes is not known. However, as the majority of stations in the NARCCAP dynamically downscaled scenarios that had precipitation volume increases also showed strong intensification it was assumed that any increases in precipitation occur in the top 30 percent of events. In the cases where there was a decline in precipitation for a given month, the decreases were applied across all events.

For the case when $r = V_2/V_1 > 1$ (increasing precipitation), the future volume representing the climate scenario (V_2) can be defined as:

$$V_2 = V_{1L} + r^* \cdot V_{1H},$$

where r^* is the change applied to the upper range (>30%), V_H is the volume in the top 30 percent, and V_L is the volume in the bottom 70 percent of events.

Expressing $r^* = r + \cdot(r-1) \cdot {}^{V_{1L}}\!/_{V_{1H}}$, the overall change is satisfied, as:

$$V_2 = V_{1L} + r^* \cdot V_{1H} = V_{1L} + r \cdot V_{1H} - V_{1L} + r \cdot V_{1L} = r\,(V_{1H} + V_{1L}) = r \cdot V_1.$$

Further, as $r > 1$, r^* is always positive.

For the case of $r <= 1$ (decreasing precipitation), an across-the-board decrease in precipitation was applied as follows:

$$V_2 = r \cdot V_{1L} + r \cdot V_{1H}$$

The adjustment factors can then be assembled as follows:

For the events above the 70th percentile, if
- $r > 1$, then use r^*
- $r <= 1$, then use r.

For the events below the 70th percentile, if
- $r > 1$, then use 1 (no change)
- $r <= 1$, then use r.

5.1.4.3. *Potential Evapotranspiration Changes*

Potential evapotranspiration (PET) is simulated with the Penman-Monteith energy balance method. In addition to temperature and precipitation, the Penman-Monteith method requires as input dew point (or relative humidity), solar radiation, and wind as inputs. Because only a few stations have time series for all four additional variables that are complete over the entire 1971-2000 period, these variables are derived from the SWAT 2005 statistical weather generator (Neitsch et al., 2005). This is done automatically by SWAT. For HSPF implementation a standalone version of the weather generator code was created and used to create time series for each of the needed variables at each BASINS meteorological station based on the nearest SWAT weather generator station after applying an elevation correction.

The SWAT weather generator database (.wgn) contains the statistical data needed to generate representative daily climate data for the different stations. Adjustments to the wgn file parameters were made using monthly change for the NARCCAP dynamically downscaled

scenarios. Specifically solar radiation, dew point temperature and wind speed were adjusted for each scenario (Table 16).

Table 16. SWAT weather generator parameters and adjustments applied for scenarios.

SWAT wgn file Parameter	Description	Adjustment applied
SOLARAV1	Average daily solar radiation for month (MJ/m2/day)	Adjusted based on Surface Down welling Shortwave Radiation change (%)
DEWPT1	Average daily dew point temperature in month (ºC)	Additive Delta value provided for climate scenario for each month
WNDAV1	Average daily wind speed in month (m/s)	Adjusted based on 10-meter Wind Speed change (%)

The probability of a wet day following a dry day in the month (PR_W1) and probability of a wet day following a wet day in the month (PR_W2) were kept the same as in the original SWAT climate generator file for the station. Climate models showed a systematic bias, likely introduced by the scale mismatch (between a 50-km grid and a station observation) for weather generator parameters like wet day/dry day timing, resulting in too many trace precipitation events relative to observed. Thus it was not possible to use climate models to determine changes in these parameters. Also, an analysis of the dynamically downscaled raw 3-hourly time-series for the CRCM downscaling of the CGCM3 GCM demonstrated that the probability that a rainy day is followed by a rainy day (transition probability) did not change significantly at any of the five separate locations that were evaluated.

For the BCSD climate scenarios in the CMIP3 archive, information on these additional meteorological variables is not available. Many of these outputs are also unavailable from the archived raw GCM output. For these scenarios it was assumed that the statistical parameters remained unchanged at current conditions. While the lack of change is not physically realistic (e.g., changes in rainfall will cause changes in cloud cover and thus solar radiation reaching the land surface), this reflects the way in which output from these models is typically used.

One of the NARCCAP scenario archives (Scenario 5: CGCM3 downscaled with RCM3) does not include solar radiation, which may be affected by changes in cloud cover. Current condition statistics for solar radiation contained in the weather generator were used for this scenario. This does not appear to introduce a significant bias as the resulting changes in PET fall within the range of those derived from the other NARCCAP scenarios.

Appendix Z compares the reference crop estimates of Penman-Monteith PET for the five pilot watersheds. This is the PET used directly by the HSPF model, while the SWAT model performs an identical calculation internally, and then adjusts actual evapotranspiration (AET) for crop height and leaf area development. Because PET is most strongly a function of temperature, a fairly consistent increase in PET is simulated for most basins. It can be seen from the figures in the appendix, however, that the statistically downscaled and raw GCM scenarios (scenarios 7 – 14) that do not include solar radiation, dew point, and wind time series that are consistent with

the simulated precipitation and temperature, generally provide noticeably higher estimates of PET than do the dynamically downscaled models.

A comparison of the effects of data availability on PET calculations can be done through comparison of scenarios that are based on identical underlying GCM runs for CGCM3 and GFDL (as discussed in Section 5.1.2. For each of these GCMs there is a pair of dynamically downscaled climate scenarios. Annual average PET estimates from these pairs are generally close to one another, but may differ by up to 4.5 percent from their mean (Table 17). For the CGCM3 model, PET generated from the raw GCM is similar to that from the dynamically downscaled scenarios, but PET calculated from the statistically downscaled scenario is from 2 to 19 percent higher. This appears to be due to the fact that dew point temperature, which has an important impact on PET, is provided with the CGCM3 GCM but is not available from the statistically downscaled CMIP3 product (see Table 15 above). The difference is smallest for the Salt/Verde/San Pedro River basins, where dew point temperature is very low and not expected to change much under future climates. In contrast, the GFDL model does not provide dew point temperature from the raw GCM. For that model, both the non-downscaled and statistically downscaled products produce higher PET estimates than the dynamically downscaled products. As with CGCM3, the smallest effect is seen in the Salt/Verde/San Pedro River basins in Arizona, and the largest effect in the Susquehanna basin, where a greater change in dew point temperature and relative humidity is predicted. The observed sensitivity of PET estimates to climate variables other than air temperature and precipitation suggests that simulation of future climates that does not account for changes in the full suite of variables that influence PET could thus introduce significant biases into the simulated water balance.

Table 17. Comparison of PET estimation between different downscaling approaches

Scenario Type		NARCCAP dynamically downscaled		Non-downscaled GCM	CMIP3 statistically downscaled	NARCCAP dynamically downscaled		Non-downscaled GCM	CMIP3 statistically downscaled
Climate Scenario		1. CRCM-CGCM3	5.RCM3-CGCM3	7. CGCM3	11. CGCM3	3. RCM3-GFDL	4. GFDL (high res)	9. GFDL	13. GFDL
ACF (GA, AL, FL)	annual average PET (in)	60.32	58.59	59.85	64.75	60.46	57.16	67.88	65.97
	difference from NARCCAP mean	1.46%	-1.46%	0.67%	8.90%	2.81%	-2.81%	15.42%	12.17%
Minnesota River (MN, SD)	annual average PET (in)	58.57	55.24	56.22	63.90	54.92	60.02	64.99	63.65
	difference from NARCCAP mean	2.92%	-2.92%	-1.21%	12.29%	-4.44%	4.44%	13.08%	10.75%
Salt/Verde/ San Pedro (AZ)	annual average PET (in)	83.67	82.89	84.19	85.01	81.32	82.93	86.73	84.74
	difference from NARCCAP mean	0.47%	-0.47%	1.09%	2.07%	-0.98%	0.98%	5.60%	3.18%
Susquehanna (PA, NY, MD)	annual average PET (in)	43.78	42.24	42.91	51.15	43.06	42.69	50.18	50.17
	difference from NARCCAP mean	1.79%	-1.79%	-0.23%	18.94%	0.43%	-0.43%	17.05%	17.02%
Willamette (OR)	annual average PET (in)	44.18	44.51	45.24	50.73	45.44	43.91	49.16	49.17
	difference from NARCCAP mean	-0.37%	0.37%	2.01%	14.41%	1.70%	-1.70%	10.04%	10.06%

5.2. URBAN DEVELOPMENT SCENARIOS

The impacts of urban and residential development on watersheds are pervasive and widespread at the national scale. The relative effects of future climate change and urban and residential development on watersheds has important management implications. Moreover, because climate and urban development can result in similar types of impacts, e.g. higher peaks and lower low flow conditions, the management of land use impacts is a potentially important adaptive strategy for increasing resilience to climate change (Pyke et al., 2011).

5.2.1. Land Use Scenarios

In this study two land use scenarios were evaluated in each study area: a baseline scenario representing current (2001) conditions and a future scenario representing mid-21st century changes in urban and residential land. Projected changes in urban and residential development were acquired from EPA's Integrated Climate and Land Use Scenarios (ICLUS) project (U.S. EPA, 2009d). ICLUS has produced seamless, national-scale change scenarios for developed land that are compatible with the assumptions about population growth and migration that underlie the IPCC greenhouse gas emissions storylines. These scenarios were developed using a demographic model, consisting of a cohort-component model and gravity model, to estimate future population through 2100 for each county in the conterminous U.S. The resulting population is allocated to 1-hectare pixels, by county, using the spatial allocation model SERGoM (Spatially Explicit Regional Growth Model). The final spatial dataset provides decadal projections of housing density and impervious surface cover for the period 2000 through 2100.

Data from the ICLUS project are composed of grid-based housing density estimates with 100-m cells, whose values are set equal to *units/ha x 1,000*. Existing housing densities were estimated using a variety of sources and models, and future housing densities developed under various scenarios for each decade through 2100. For the existing housing density grid, two types of "undevelopable" area where residential developed was precluded were masked out during the production – a comprehensive spatial dataset of protected lands (including land placed in conservation easements), and land assumed to be commercial/industrial under current conditions. Undevelopable commercial/industrial land use was masked out according to the SERGoM method (U.S. EPA, 2009d) that eliminated commercial, industrial, and transportation areas that preclude residential development, identified as "locations (1 ha cells) that had >25% urban/built-up land cover but that also had lower than suburban levels of housing density."

The ICLUS projections used in this study thus do not account for potential growth in commercial/industrial land use. It is also important to note that the ICLUS projections do not explicitly account for changes in rural or agricultural land uses. These categories change only to the extent that they are predicted to convert to developed land.

5.2.2. Translating ICLUS Land Use Projections to Watershed Model Inputs

The ICLUS projections used in this study are for changes in housing density and impervious cover. This data cannot be used directly with the SWAT and HSPF watershed models which require land use data consistent with the NLCD. It was therefore necessary to translate between ICLUS projections and NLCD land use classes.

The baseline (2001) and future (2050) land use scenarios are referred to as "L0" and "L1", respectively. Baseline land use, derived from the 2001 NLCD, contains four developed land classifications (NLCD classes 21 through 24), nominally representing "developed, open space" (less than 20 percent impervious), developed, low intensity (20 – 49 percent impervious), developed, medium intensity (50 – 79 percent impervious), and developed, high density (greater than 80 percent impervious). Impervious fractions within each developed NLCD land use class were estimated separately for each study area, using the 2001 NLCD Land Cover and Urban Impervious data products. ICLUS land use change projections were implemented by modifying the existing land use distribution in the watershed models.

ICLUS estimates housing density on a continuous scale. To process the data more efficiently, the data were reclassified into ten housing density ranges.

In each study area, the ICLUS housing density ranges were cross-tabulated with NLCD 2001 classes based on percent imperviousness. It was assumed that the number of housing units changes, but that the characteristic percent impervious values for each NLCD developed class remains constant. The change in land area needed to account for the change in impervious area was then back calculated.

ICLUS housing density class estimates and the NLCD developed classes do not have a one-to-one spatial relationship because they are constructed on different underlying scales. ICLUS represents housing density based largely on the scale of census block groups. As a result, it represents the overall density within a relatively large geographic area when compared to the 30x30 meter resolution of NLCD 2001 land cover and can represent a mix of different NLCD classes. Therefore, land use changes must be evaluated on a spatially aggregated basis at the scale of model subbasins.

The gains (and losses) in NLCD class interpreted from ICLUS were tabulated separately for each subbasin. In almost every case, the gains far exceeded the losses and a net increase was predicted in all four NLCD developed classes. However, there were a few cases where there was an overall loss of the lowest density NLCD class. This tended to occur when a subbasin was already built out, and ICLUS predicted redevelopment at a higher density.

To represent the net change in future land cover, the developed land use was added (or subtracted) from the existing totals in each subbasin. Land area was then removed from each undeveloped NLCD class (excluding water and wetlands) according to their relative ratios in each subbasin to account for increases in developed area. If the undeveloped land area was not sufficient to accommodate the projected growth, development on wetlands was allowed. The reductions in undeveloped land were distributed proportionately among modeled soils (in SWAT) or hydrologic soil groups (in HSPF). The new developed lands were then assumed to have the parameters of the most dominant soil and lowest HRU slope in the sub-basin. For HSPF, the changed area was implemented directly in the SCHEMATIC block of the user control input (.uci) file. For SWAT, the land use change was implemented by custom VBA code that directly modified the SWAT geodatabase that creates the model input files.

The projected overall changes in developed land for 2050 as interpreted to the NLCD land cover classes and used for modeling are presented in Table 18. Note that even in areas of expected high growth (e.g., the area around Atlanta in the ACF basin), new development by 2050 is expected to constitute only a small fraction of the total watershed area at the large scale of the study areas in this project. The highest rate of land use change in the studied watersheds is Coastal Southern California, at 11.72 percent. Therefore, effects of land use change are likely to be relatively small at the scale of the studied basins, although greater impacts are likely at smaller spatial scales. The ICLUS project does not cover the Cook Inlet watershed in Alaska.

Table 18. ICLUS projected changes in developed land within different imperviousness classes by 2050.

	Change in Impervious Cover					
Model Area	**< 20% impervious (km^2)**	**20 – 49 % impervious (km^2)**	**50 – 79% impervious (km^2)**	**> 80 % impervious (km^2)**	**Total (km^2)**	**Percent of watershed**
ACF	665.2	809.7	212.3	90.8	1,778.0	3.56%
Verde/Salt/San Pedro	92.1	87.0	16.0	1.3	196.4	0.51%
Susquehanna	211.1	196.2	69.6	25.6	502.5	0.71%
Minnesota River	71.3	142.9	60.9	18.5	293.5	0.67%
Willamette	75.8	193.4	95.0	33.3	397.6	1.37%
Cook Inlet	ND	ND	ND	ND	ND	ND
Lake Erie	152.1	204.8	51.0	15.6	423.4	1.40%
Georgia-Florida Coastal Plain	873.9	776.1	361.5	102.2	2113.8	4.65%
Illinois River	353.5	1506.6	447.5	116.2	2424.0	5.50%
New England Coastal	238.6	327.2	215.5	59.2	840.4	3.13%
Sacramento River	103.6	58.1	29.5	8.2	199.3	0.93%
Coastal Southern California	162.0	1001.0	1089.1	114.1	2466.2	11.72%
Powder/Tongue River	1.3	0.5	0.1	0.0	1.9	0.00%
Lake Pontchartrain	307.2	308.3	91.4	23.4	730.1	4.82%
Rio Grande Valley	139.0	228.8	57.1	7.4	432.4	0.88%
South Platte River	329.4	1364.6	473.5	83.6	2251.1	5.93%
Neuse/Tar River	492.4	306.6	107.4	29.2	935.6	3.66%
Trinity River	978.9	1896.7	891.1	304.3	4071.0	8.76%

Loup/Elkhorn River	8.9	18.7	4.1	1.6	33.2	0.06%
Upper Colorado River	56.9	168.1	66.3	8.3	299.6	0.65%

1
2
3
4

6. RESULTS IN PILOT WATERSHEDS: SENSITIVITY TO DIFFERENT METHODOLOGICAL CHOICES

One goal of this study was to assess the implications of different methodological choices for conducting climate change impacts assessments on the variability of simulation results. This assessment was based on simulations in 5 Pilot study areas. The five pilot study basins are the Minnesota River, Apalachicola-Chattahoochee-Flint (ACF), Susquehanna, Willamette, and Verde/ Salt/ San Pedro Rivers). In each of the 5 pilot sites, independent simulations were conducted using the SWAT and HSPF watershed models, and in addition to the 6 dynamically downscaled NARCCAP scenarios, an additional set of climate change scenarios was evaluated, four based on the statistically downscaled BCSD dataset, and four based directly on GCMs with no downscaling. These simulations in Pilot sites allow assessment of the variability resulting from use of different watershed models, and variability resulting from use climate change scenarios developed using different downscaling methods. This level of effort was not feasible at all 20 sites due to resource limitations. A reduced modeling effort was conducted at the remaining 15 non-pilot sites. The more detailed analysis at Pilot sites was completed before initiating work at the other 15 sites, and results of this assessment were used to inform development of the reduced effort modeling conducted non-pilot sites. This section is a summary of results in the pilot study areas.

6.1. COMPARISON OF WATERSHED MODELS

Two different watershed models, SWAT and HSPF, were calibrated and applied to the five pilot study areas (the Willamette, Central Arizona, Minnesota (Upper Mississippi), Apalachicola-Chattahoochee-Flint (ACF), and Susquehanna basins). Evaluation of different watershed models can be considered an extension of the scenario-based, ensemble approach commonly used in climate change studies. The magnitude of the additional variability introduced by choice of a hydrologic model is of interest when simulating hydrologic responses to climate change and urban development.

This section provides a summary of the relative performance of the two models, along with theoretical and practical considerations, concluding with the rationale for selecting the SWAT model to implement in the remaining 15 non-pilot watersheds. Detailed examination of the calibration of each model in the five pilot study areas and the results of change scenarios conducted with each model are presented in separate sections.

Both HSPF and SWAT are public domain, government-supported models with a long history of application. Yet, they also take a rather different approach to watershed simulation and have different structures and algorithms, resulting in different strengths and weaknesses. Most notably, the two models differ in the way that they represent infiltration and plant-climate interactions. SWAT (in standard application mode) simulates rainfall-runoff processes using a Curve Number approach, operating at a daily time step. The Curve Number approach first partitions incoming moisture in to direct runoff and a remainder that is available for infiltration. In contrast, HSPF simulates rainfall-runoff processes using Green-Ampt infiltration, in which infiltration into the soil is simulated first, with the remainder available for direct runoff or surface storage.

HSPF is typically run at a sub-daily time step, usually hourly for large watersheds, and has a more sophisticated representation of runoff, infiltration, and channel transport processes than does SWAT. SWAT's advantage is that it incorporates a plant growth model (including representation of CO_2 fertilization) and can therefore simulate some of the important feedbacks between plant growth and hydrologic response. Both models simulate evapotranspiration of soil water stores, but HSPF does this using empirical monthly coefficients relative to potential evapotranspiration, while SWAT incorporates a plant growth model that can, in theory, dynamically represent plant transpiration of soil moisture.

6.1.1. Influence of Calibration Strategies

Model implementation, calibration, and validation was conducted in accordance with the modeling Quality Assurance Project Plan (QAPP) (see Appendix B; Tetra Tech, 2008) for each of the five pilot study areas. Development and setup of the two watershed models proceeded from a common basis, with both models using the same sub-basin delineations, land use coverage (2001 NLCD), soils coverage (STATSGO), hydrography, digital elevation model, impervious area fractions for developed land classes, and point source and dam representations. Other aspects of model setup were designed to be similar, although not identical. For instance, hydrologic response units (the fundamental building blocks of the upland simulation) were created as an overlay of land use and hydrologic soil group (HSG) for HSPF, while SWAT uses an overlay of land use and STATSGO dominant soil, associating various other properties in addition to HSG with the model hydrologic response units.

Both models also used the same calibration/validation locations and observed data series, and both initiated calibration at the same location. Further, the calibration of both models was guided by pre-specified statistical analyses that were performed using identical spreadsheet setups obtained from a common template. Despite these commonalities, the different models were developed by different research teams, with inevitable differences in results. Model calibration assignments were intentionally structured so that the same team did not apply both HSPF and SWAT to a single study area, and each watershed model was implemented by at least three different modeling teams for the pilot studies.

One key reason for differences in results is the extent to which spatial calibration of the model was pursued, which was left to modeler judgment. In all study areas, initial calibration and validation was pursued at an "initial calibration" gage and monitoring station at an HUC8 spatial scale. The calibration results were then carried to the larger study area. At this point, individual modeler preferences introduced some variability into results. Some modelers undertook detailed spatial adjustments to parameters; others extended the initial parameter set with only minor modifications. With more spatial adjustments a higher degree of fit is generally to be expected for model calibration – although this does not necessarily result in better performance in model validation. In general, limited spatial calibration adjustments beyond the parameter set obtained at the initial location was carried out for the Minnesota River, Susquehanna, and Willamette SWAT models and also for the Susquehanna HSPF model.

Another cause of different performance is the existence of prior modeling efforts in the basin. There were existing detailed HSPF models for the Susquehanna, ACF, and Minnesota River

basins, while SWAT models existed for the Minnesota River and Central Arizona basins. Where prior models existed they influenced calibration of the models used in this study – even though the spatial basis and representation of evapotranspiration typically differed from the earlier models.

The net effect of these factors is that the results should not be interpreted as a true head-to-head comparison of the two models, as the results for any given watershed may be skewed by exogenous factors such as modeler calibration strategy. Instead, it is most relevant to examine relative performance and potential inconsistencies between simulations using the two models.

6.1.2. Comparison of Model Calibration and Validation Performance

Models were calibrated and validated using multiple measures as summarized previously in this report and described in full detail in Appendices D - W. Model performance was evaluated based on ability to represent a variety of flow statistics and monthly loads of nitrogen, phosphorus, and suspended sediment. This section examines hydrologic simulations as compared to observed flow records based on total volume error and the daily Nash-Sutcliffe coefficient of model fit efficiency. Model performance is first examined in terms of the quality of fit for the initial calibration watershed followed by similar analyses for the largest-scale downstream watershed. Inter-comparisons then provide some insight into model performance relative to temporal change (calibration versus validation period) and relative to spatial change within each study area (calibration watershed versus downstream watershed).

6.1.2.1. *Streamflow Results*

Summary results for percent error in total volume and the Nash-Sutcliffe *E* coefficient for daily flows are shown in Table 19 and Table 20, respectively, for the initial calibration site along with the calibration fit for the most downstream gage in the watershed. In general, the quality of model fit is good for both models. In most, but not all cases, the quality of model fit is slightly better (smaller magnitude of percent error, larger *E* coefficient) for the HSPF simulations (e.g., Figure 25 for the calibration period). This is likely due in large part to the use of daily precipitation in SWAT versus hourly precipitation in HSPF, although the advantage accruing to HSPF is muted by the fact that many of the “hourly” precipitation input series used are actually disaggregated from daily totals. Monthly values of Nash-Sutcliffe *E* are higher for both models, but attention is called to the daily scale as this better reflects the models’ ability to separate surface and subsurface flow pathways. Note that *E* is low for the Arizona initial site on the Verde River because flow is dominated by relatively constant deep groundwater discharges.

Table 19. Percent error in simulated total flow volume for 10-year calibration and validation periods.

Study area	Model	Initial site calibration	Initial site validation	Downstream calibration
ACF	HSPF	5.50	5.79	16.79
	SWAT	7.28	3.33	16.53
Salt/Verde/San Pedro (Ariz)	HSPF	2.43	6.31	4.48
	SWAT	-2.46	5.68	9.43
Minnesota River (Minn)	HSPF	1.61	14.78	-4.25
	SWAT	-5.41	-0.84	7.89
Susquehanna (Susq)	HSPF	-0.16	-8.00	1.79
	SWAT	-5.41	-16.30	-9.74
Willamette (Willa)	HSPF	-3.92	-9.80	2.58
	SWAT	-4.76	12.10	-4.96

Table 20. Nash-Sutcliffe coefficient of model fit efficiency (*E*) for daily flow predictions, 10-year calibration and validation periods.

Study Area	Model	Initial Site Calibration	Initial Site Validation	Downstream Calibration
ACF	HSPF	0.71	0.65	0.72
	SWAT	0.62	0.56	0.64
Salt/Verde/San Pedro (Ariz)	HSPF	0.48	0.45	0.53
	SWAT	0.03	-1.00	0.22
Minnesota River (Minn)	HSPF	0.75	0.78	0.92
	SWAT	0.79	0.74	0.63
Susquehanna (Susq)	HSPF	0.70	0.55	0.77
	SWAT	0.29	0.42	0.45
Willamette (Willa)	HSPF	0.80	0.81	0.88
	SWAT	0.49	0.39	0.67

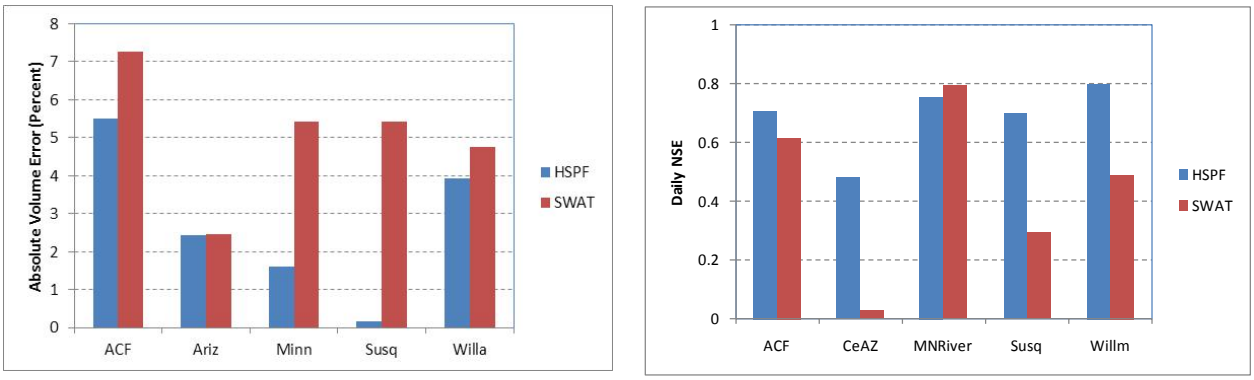

Figure 25. Comparison of model calibration fit to flow for the calibration initial site.

Note: Figures compare calibration results for HSPF and SWAT. Total volume error is converted to its absolute value.

The ability of the model to assess relative changes in response to altered climate forcing is of paramount importance in this project. Some insight on this topic can be gained by looking at the sensitivity of model fit to temporal and spatial changes in application. Figure 26 summarizes the sensitivity to temporal changes by looking at the change in the absolute magnitude of percent error and the change in *E* in going from the calibration period to the validation test. A smaller value in change in total volume error (left panel) or a larger value for the change in *E* represents better performance. It is interesting to note that for both the ACF and the Minnesota River, the SWAT model achieved an improvement in total volume error during the validation period. These are the two study areas with the greatest amount of row crop agriculture and the results may reflect SWAT's ability to reflect changing responses of crops to changes in climate over the last 20 years. The large decline in Nash-Sutcliffe *E* for the Central Arizona SWAT model seems to be due to the fact that flows at this gage are largely determined by deep groundwater discharges, resulting in reduced variability in flow.

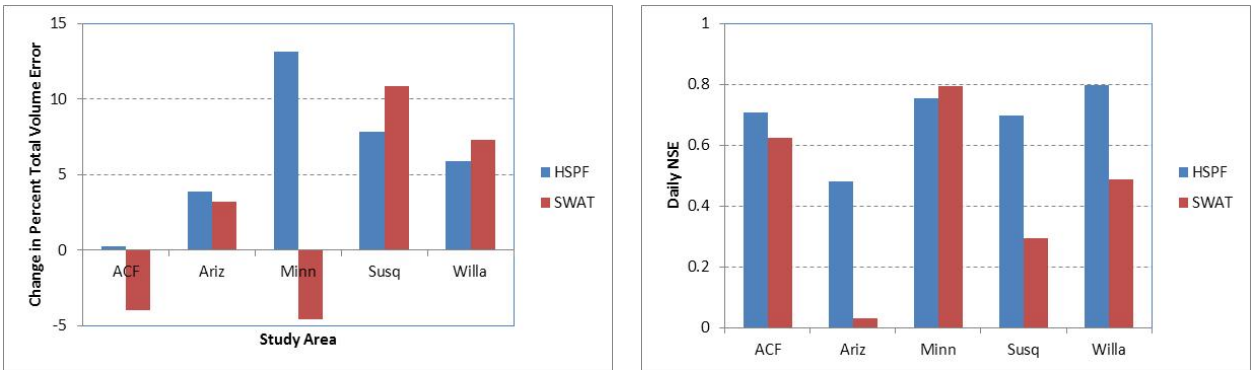

Figure 26. Sensitivity of model fit for total flow volume to temporal change.

Note: Change in percent total volume error represents the difference in the absolute value of percent error in going from the calibration to the validation period at the initial calibration site. Change in *E* represents the difference in the Nash-Sutcliffe *E* coefficient in going from the calibration to the validation period.

Figure 27 shows similar results for spatial changes, comparing performance during the calibration period for the calibration target gage and the most downstream gage in the model. The changes in total volume errors are generally small, regardless of whether or not detailed

spatial calibration was pursued. In most cases the models achieved an improvement in *E* (positive difference) in going from the smaller to the larger scale.

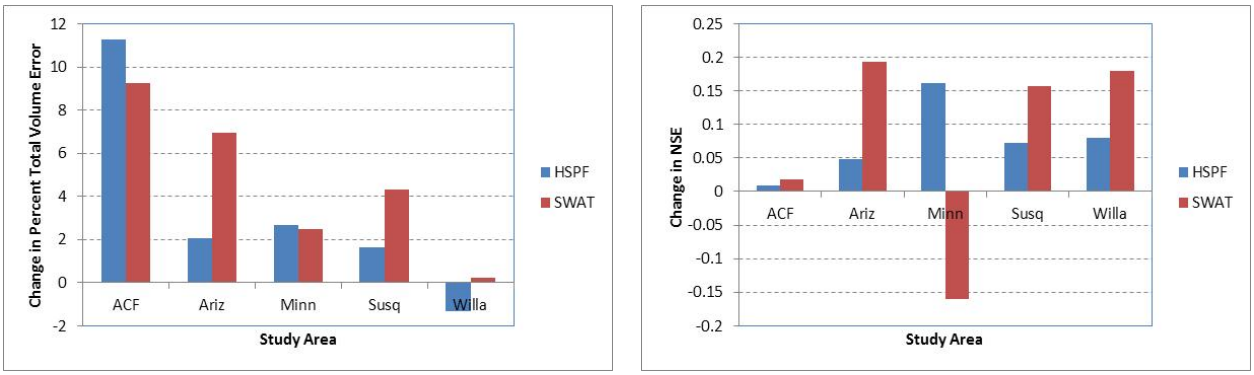

Figure 27. Sensitivity of model fit for flow to spatial change.

Note: Change in percent total volume error represents the difference in the absolute value of percent error in going from the initial calibration site to a larger-scale, typically downstream site. Change in *E* represents the difference in the Nash-Sutcliffe *E* coefficient in going from the calibration site to the larger-scale site.

6.1.2.2. *Water Quality Results*

The water quality calibration compared simulated monthly loads to monthly load estimates obtained from a stratified regression on (typically sparse) observed data. To compare these results between models the baseline adjusted E_1' coefficient of model fit efficiency is most appropriate. Results are summarized graphically for the calibration period at the calibration initial site and downstream site in Figure 28 through Figure 30. For suspended solids and total phosphorus the performances of the two models are similar, while HSPF appears to provide a somewhat better fit for total nitrogen.

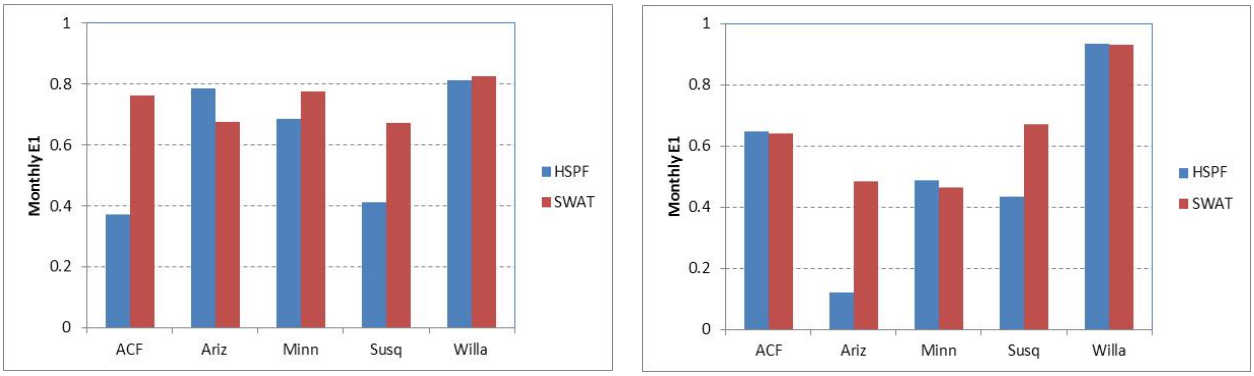

Figure 28. Comparison of baseline adjusted model fit efficiency for total suspended solids monthly loads for calibration site (left) and downstream site (right).

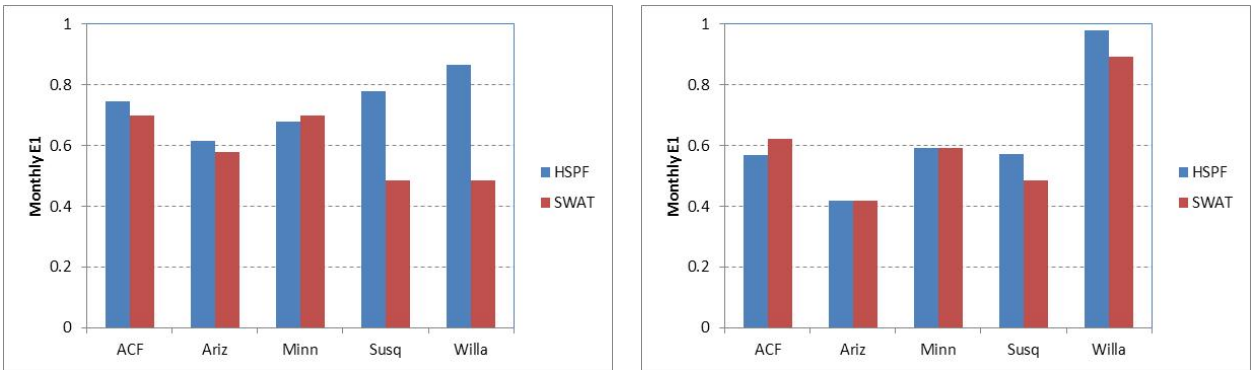

Figure 29. Comparison of baseline adjusted model fit efficiency for total phosphorus monthly loads for calibration site (left) and downstream site (right).

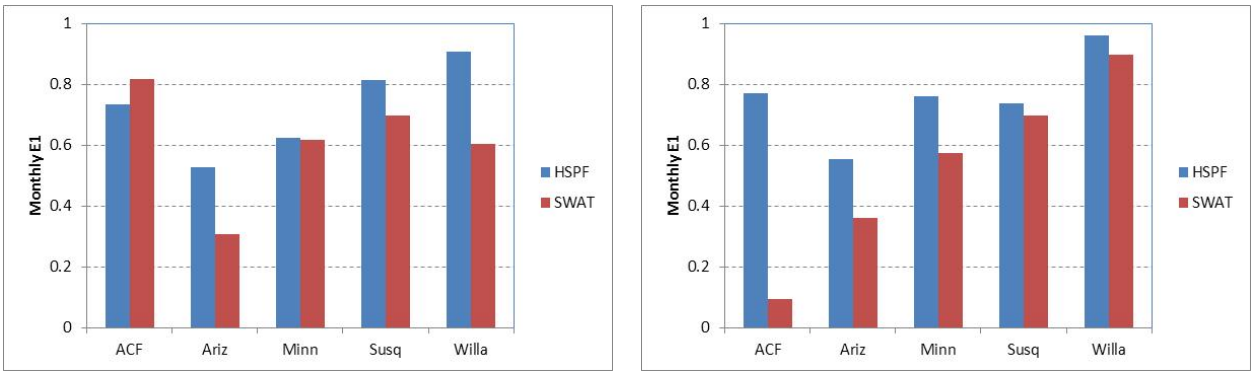

Figure 30. Comparison of baseline adjusted model fit efficiency for total nitrogen monthly loads for calibration site (left) and downstream site (right).

6.1.2.3. *Summary of Relative Model Performance*

In general, the HSPF model provides a somewhat better fit to observed flow and water quality data for the calibration periods. The effect is most noticeable in the coefficient of model fit efficiency (*E*) for daily flows, where the HSPF approach of applying Philip infiltration using hourly precipitation appears to yield an advantage over the SWAT daily curve number method. However, relative performance of the two models is more similar as the analysis moves to the validation period or to other sites for which detailed calibration has not been undertaken. Most importantly, both models appear to be capable of performing adequately, such that either could be chosen for analysis of the non-pilot sites.

6.1.3. Consistency of Simulated Changes Using SWAT and HSPF

Figure 31 compares HSPF and SWAT simulated changes in mean annual flow at the downstream station of each of the five pilot watersheds for all 28 combinations of climate and land use change scenarios (expressed as a percent of the baseline conditions, representing approximately 1970 - 2000). In general, the mean annual flow results provided by the two models are similar, as is shown quantitatively below. One notable difference is the for the Minnesota River where SWAT projects higher flows relative to HSPF under projected wet conditions. Subsequent testing showed that this was primarily due to reduced evapotranspiration in SWAT simulations caused by increased atmospheric CO_2 (see Section 6.1.4.). Note that points plotting close to or

on top of each other for a given study site in Figure 31 are scenarios representing the same climate change scenario with and without changes in urban development.

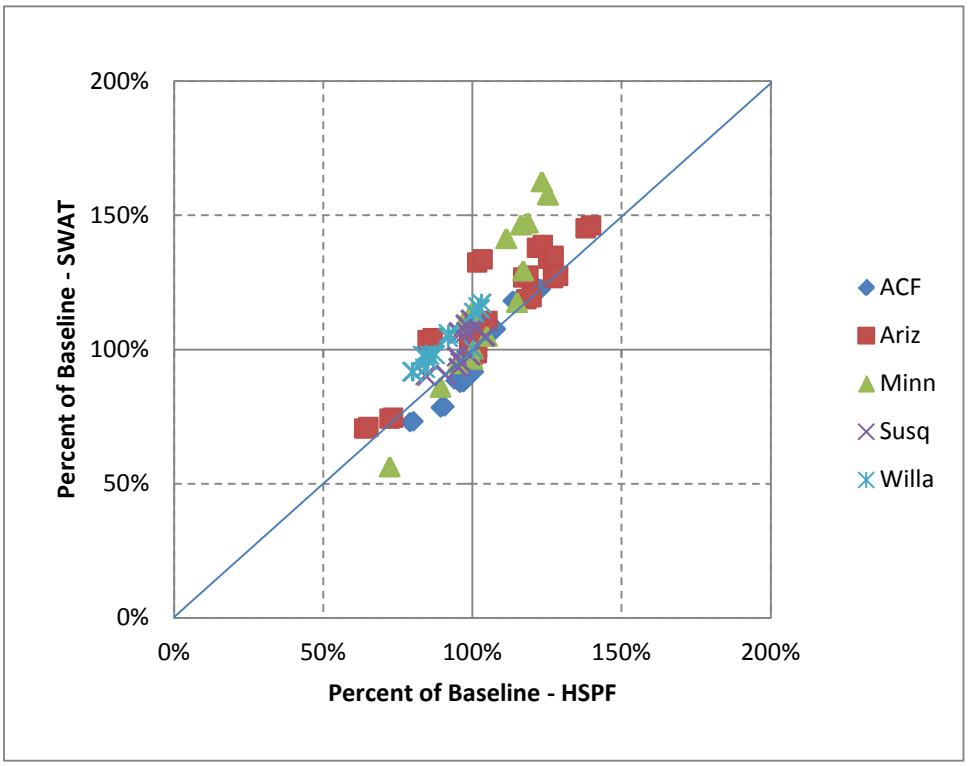

Figure 31. SWAT and HSPF simulated changes in total flow in pilot watersheds (expressed relative to current conditions).

Table 21 provides a statistical comparison of the HSPF and SWAT results at the downstream station. Three types of tests are summarized. The first is a t-test on the series of paired means (HSPF and SWAT for each climate and land use scenario), which has a null hypothesis that the mean of the differences between the series is not significantly different from zero. The second test is a two-way ANOVA that looks at choice of watershed model (HSPF or SWAT) as blocks and climate scenario as treatment. The null hypotheses for this test are that the difference between series for a given source of variance is zero. The third test is a linear regression on SWAT results as a function of HSPF results. Where the models are in full agreement, the intercept of such a regression should not be significantly different from zero and the slope should not be significantly different from unity.

For mean annual flow, both models produce similar results with a high Pearson correlation coefficient. The null hypothesis from the t-test that the mean difference is zero cannot be rejected. However, the two-way ANOVA shows that both the choice of watershed model and the climate scenario are significant sources of variability in flow, with probability values (p-value) well less than 0.1 percent. Together these results suggest that the SWAT and HSPF results are similar in the aggregate, but may contain an underlying systematic shift. This is shown in the regression analysis, where the slope coefficient of SWAT and HSPF is 0.933 and the 95% confidence interval does not overlap 1.0 and the intercept of 1,262 does not overlap zero. Thus, SWAT predicts a somewhat smaller response to increased rainfall, but results in

higher baseflow estimates (due, apparently, to the effects of increased CO_2 on evapotranspiration, as explained further below).

Table 21. Statistical comparison of HSPF and SWAT outputs at downstream station for the five pilot sites across all climate scenarios

Measure	Mean Annual Flow (cfs)	TSS Load (t/yr)	TP Load (t/yr)	TN Load (t/yr)
Paired t-test on sample means				
HSPF Mean	20,546	2,398,714	2,748	35,346
SWAT Mean	20.435	2,865,178	3,344	43,275
Pearson Correlation	0.989	0.733	0.644	0.948
t-statistic	0.616	-3.123	-4.783	-7.385
P (two-tail)	0.539	0.002	<0.001	<0.001
Two-way ANOVA on watershed model and climate scenario				
P value - Model	<0.001	0.071	0.006	0.044
P value - Climate	<0.001	0.960	0.999	1.000
Linear regression; SWAT result as a function of HSPF result				
Intercept	1261.7	141,717	954.0	-1173.1
Intercept, 95 % confidence	695 – 1828	-363,064 – 646,498	431 – 1,477	-4,194 – 1,848
Coefficient	0.933	1.136	0.870	1.257
Coefficient 95% confidence	0.911 – 0.956	0.964 – 1.307	0.702 – 1.038	1.189 – 1.326

The comparison for total suspended solids is obscured by the extremely large projected increases under certain scenarios for the Central Arizona basin (Verde River, in this case) (Figure 32). Those increases are mostly due to channel erosion, for which both models are likely to be highly uncertain outside the range of calibration data. The right panel in Figure 32 shows the same simulated TSS results but with the x-axis truncated to exclude these outlier scenarios. Results for the other four pilot sites appear generally consistent between models, although simulated increases from SWAT are generally less than those from HSPF for the ACF, Susquehanna, and Willamette. In part this is due to differences in the baseline simulation. For example, HSPF simulations show less channel transport and much smaller solids loads at the mouth of the Susquehanna than does SWAT for the baseline scenario, resulting in a larger relative change with increased future flows. The difference between results for SWAT and HSPF may also reflect the effects of CO_2 fertilization and longer growing periods simulated by SWAT leading to more litter and better soil erosion cover.

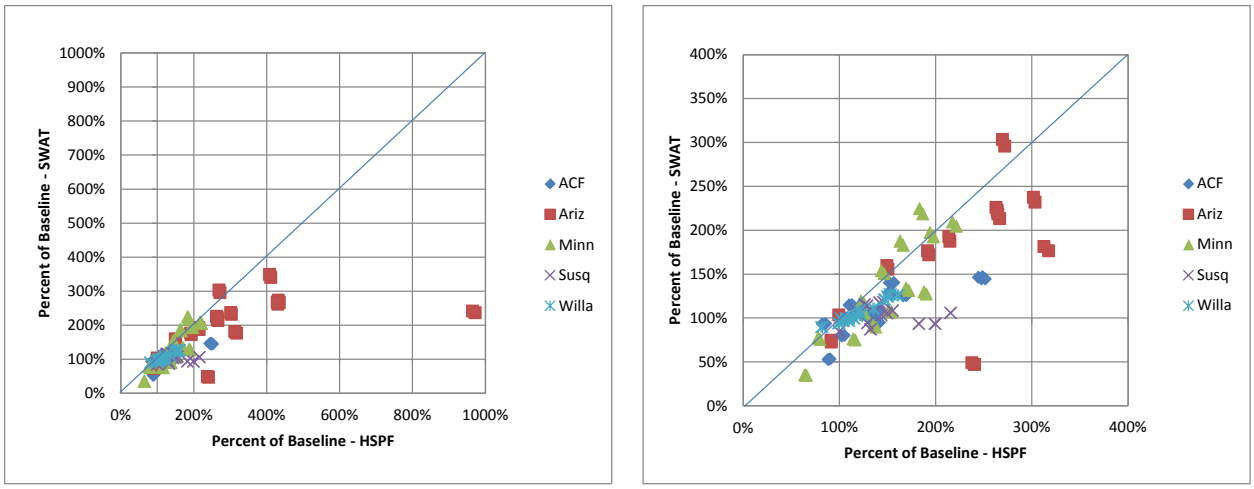

Figure 32. SWAT and HSPF simulated changes in TSS in pilot watersheds (expressed relative to current conditions).

Note: Panels on the right and left show the same data. The x-axis in the right panel is truncated.

For TSS, the baseline load is higher in SWAT than in HSPF for three of the five watersheds; thus the statistical comparison (Table 21) shows a higher mean load from SWAT, even though the percentage increases are often smaller. The t test on means shows that this difference is highly significant. However, the ANOVA show that neither the model choice nor the climate scenario is a significant explanatory variable for the variance at the 95% confidence level. The regression analysis shows that the intercept is large, but not significantly different from zero, while the slope is not significantly different from 1. Together these statistics indicate that the TSS simulation is subject to considerable uncertainty and that differences between sites are more important than other factors.

Results for total phosphorus are generally similar to those seen for total suspended solids, with much more extreme increases projected by both models for the Central Arizona basins. SWAT tends to simulate higher rates of increases for total nitrogen (Figure 33) than does HSPF (likely due to more rapid cycling of organic matter), with the notable exception of the ACF study area. However, it appears that projections of total nitrogen at the downstream end of the ACF may be significantly underestimated in the calibrated SWAT model. For both TN and TP the choice of model is a significant factor in the ANOVA and higher mean loads are produced by SWAT. The slope of a regression of SWAT on HSPF is not significantly different from 1 for TP, consistent with the solids simulation, but the intercept is significantly different from zero, indicating differences in the baseflow simulation of TP. For TN, the intercept is not significantly different from zero, but the slope is significantly greater than 1, suggesting that SWAT predicts a greater increase in TN loads under future climate conditions.

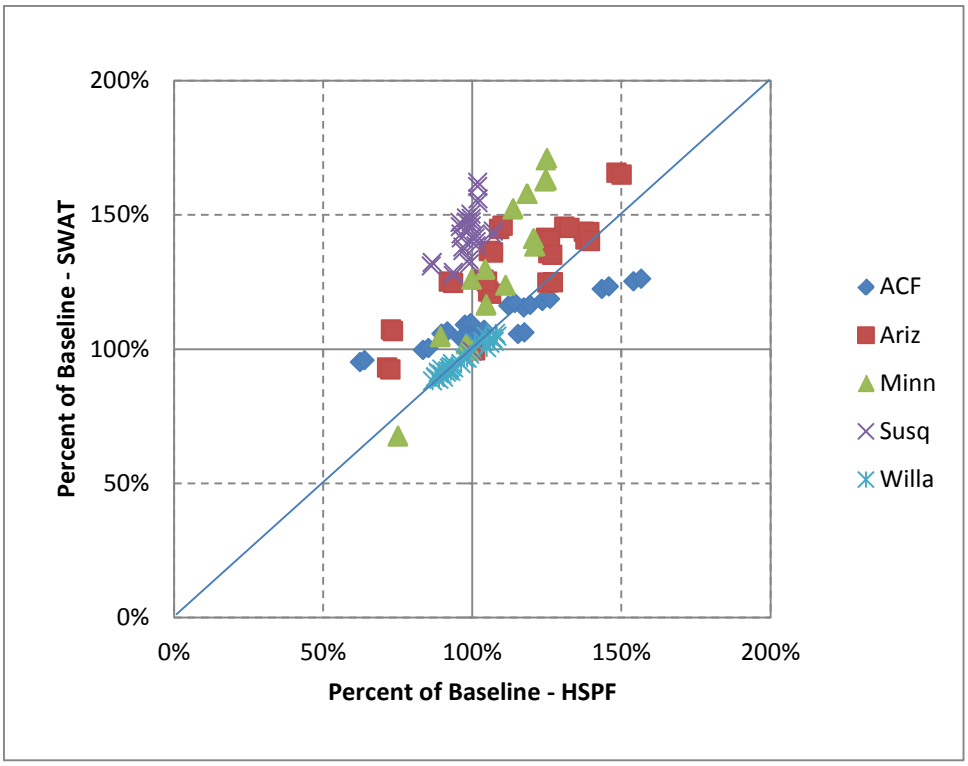

Figure 33. SWAT and HSPF simulated changes in total nitrogen load in pilot watersheds (expressed relative to current conditions).

In sum, the comparison of relative response to change scenarios indicates that the two models provide generally consistent results, with differences that may be in part due to the inclusion of explicit representation of several processes in SWAT (CO_2 fertilization, changes in planting time, changes in crop growth and litter production, and changes in nutrient recycling rates) that are not automatically included in HSPF.

6.1.4. Watershed Model Response to Increased Atmospheric CO_2

The two models have different structures and algorithms, resulting in different strengths and weaknesses. HSPF operates at a sub-daily time step and has a more sophisticated representation of runoff, infiltration, and channel transport processes than does SWAT. SWAT's advantage is that it incorporates a plant growth model (including representation of CO_2 fertilization) and can therefore simulate some of the important feedbacks between plant growth and hydrologic response.

IPCC estimates of future atmospheric CO_2 concentrations under the assumptions of the A2 emissions scenario (the basis of climate and land use change scenarios in this study) call for an increase from 369 ppmv CO_2 in 2000 to about 532 ppmv (using the ISAM model reference run) or 522 ppmv (using the Bern-CC model reference run) in 2050 (Appendix II in IPCC, 2001). Plants require CO_2 from the atmosphere for photosynthesis. An important effect of CO_2 fertilization is increased stomatal closure, as plants do not need to transpire as much water to obtain the CO_2 they need for growth (Leakey et al., 2009; Cao et al., 2010). This effect can potentially counterbalance projected increases in temperature and potential evapotranspiration. It

may also reduce water stress on plants, resulting in greater biomass and litter production, which in turn will influence pollutant loads.

In the past it has been argued that these effects, long documented at the leaf and organism level, might not translate to true ecosystem effects. However, recent research, particularly the FACE experiments summary (Leakey et al., 2009) seems to confirm that significant reductions in evapotranspiration do occur at the ecosystem level under CO_2 fertilization. Although there are differences in responses among plant species, with lesser effects with C_4 photosynthesis, the magnitude of the response to CO_2 levels projected by the mid-21st century appears to be on the order of a 10 percent reduction in evapotranspiration response (e.g., Bernacchi et al., 2007). Further, a recent study by Cao et al. (2010) suggests that up to 25 percent of the temperature increase projected for North America could result directly from decreased plant evapotranspiration under increased CO_2 concentrations.

To assess the sensitivity of streamflow and water quality endpoints to the effects of increased atmospheric CO_2 concentrations, we performed sets of SWAT simulations with and without CO_2 fertilization for all five pilot sites. SWAT simulates plant growth and models the effect of CO_2 fertilization on stomatal conductance using the equation developed by Easterling et al. (1992), in which increased CO_2 leads to decreased leaf conductance, which in turn results in an increase in the canopy resistance term in the PET calculation. The model also simulates the change in radiation use efficiency of plants as a function of CO_2 concentration using the method developed by Stockle et al. (1992). Figure 34 shows selected flow and water quality endpoints simulated with and without effects of CO_2 concentration changes for the six NARCCAP climate scenarios incorporating the ICLUS future land-use for each watershed. Simulations in the pilot sites suggest increases in mean annual flow from 3 to 38 percent due to increased CO_2, with a median of 11 percent, in the same range as the results summarized by Leakey et al. (2009). Simulations also suggest CO_2 fertilization results in increased pollutant loads. Loads of TSS show increases from 3 to 57 percent, with a median of 15 percent. TP loads increase from zero to 29 percent, with a median of 6 percent. TN loads increase from zero to 34 percent, with a median of 6 percent. The large increases in TSS load indicate that the effects of higher runoff under CO_2 fertilization (largely due to greater soil moisture prior to rainfall events) may outweigh benefits associated with greater ground cover. For the nutrients, the load increases are less than both the flow and TSS increases. This presumably is due to the fact that CO_2 fertilization allows greater plant growth per unit of water, resulting in greater uptake and sequestration of nutrients, and thus smaller increases in nutrient loads relative to flow and TSS.

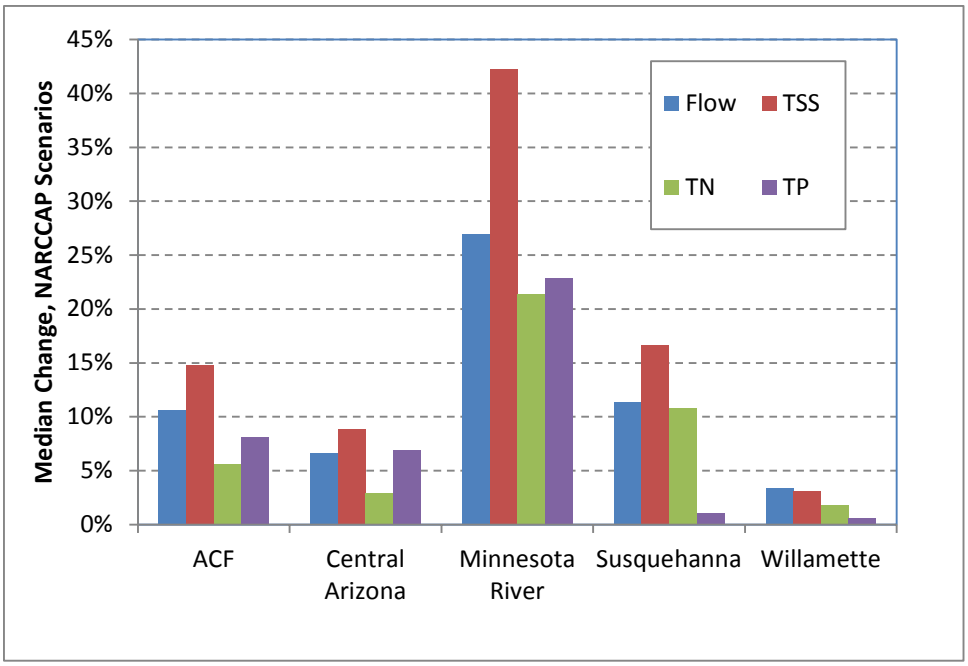

Figure 34. Simulated effect of changes in atmospheric CO_2 concentration on selected streamflow and water quality endpoints using SWAT.

The response to CO_2 fertilization varies greatly by study area, with the greatest effect simulated by SWAT for the Minnesota River basin and the smallest effect for the Willamette basin. The large effect in the Minnesota River basin apparently occurs because the land in this basin is predominantly in high-biomass corn-soybean rotation agricultural cropland with precipitation and evapotranspiration in approximate balance. In contrast the Willamette basin is dominated by evergreen forest and has a moisture surplus for much of the year.

Several important feedback loops other than the CO_2 effect are also included in the SWAT plant growth model:

- Planting, tillage, fertilization, and harvest timing for crops (and start and end of growth for native plants) can be represented by heat unit scheduling, allowing automatic adjustment to a changed temperature regime.
- Evapotranspiration is simulated with the full Penman-Monteith method, allowing dynamic consideration of leaf area development and crop height, instead of via a reference crop approach.
- Plant growth rates vary as a function of temperature, light, water, and nutrient availability.
- Organic matter residue accumulation and degradation on the land surface are dynamically simulated.
- Variations in land surface erosion as a function of leaf and litter cover are dynamically simulated.

All these factors are of potential importance in examining response to climate change. In contrast to SWAT, HSPF does not automatically compute these adjustments. Instead, the user would need to estimate changes in monthly parameters such as the lower zone evapotranspiration coefficient

(LZETP) and erosion cover (MON-COVER) externally and bring them into the model. While not well understood, use of calibrated parameters in HSPF without these modifications could introduce error to simulations under climatic conditions different from those during the calibration period.

6.1.5. Selection of Watershed Model for Use in All Study Areas

Resource limitations for this study precluded the application of SWAT and HSPF in all 20 study areas. Analyses at Pilot sites were used to select a single model for application in all 20 study areas. Analyses in the Pilot sites show HSPF and SWAT are each capable of providing a good fit to flow and pollutant loads for existing conditions. The quality of fit depends in part on the strategy and skill of the individual modeler. In this study, the quality of fit was also influenced by the availability in certain areas of pre-existing, calibrated models which were adapted for use as compared to locations where new models were developed and calibration subject to resource limitations.

For the purposes of this study, the SWAT model was considered to have a technical advantage because it can account for the important influences of CO_2 fertilization and other feedback responses of plant growth to climate change. HSPF does not automatically account for these effects. While it uncertain how well SWAT is able to represent the complex processes affecting plant growth, nutrient dynamics, and water budgets under changing climate, it was considered important to include some representation of these processes to better understand potential watershed sensitivity to a wide range of conditions. In addition, there are also some practical advantages to the choice of SWAT, as the model is somewhat easier to set up and calibrate than is HSPF.

On the other hand, the HSPF model proved generally better able to replicate observations during calibration, as shown in Section 6.1.2 , although the difference between HSPF and SWAT model performance was small for the selected response variables. HSPF is often able to provide a better fit to flow due to the use of hourly precipitation and a more sophisticated algorithm compared to SWAT's daily curve number approach – although this advantage is blunted by the need to use disaggregated daily total rainfall to drive the models in many areas. Increased accuracy in hydrology – especially the accurate partitioning between surface and subsurface runoff – should also provide increased accuracy in the simulation of sediment yield and the transport of sediment-associated nutrients. However, at the larger watershed scales studied here (HUC8 and greater), such advantages will tend to diminish as observations reflect the integration of flows and loads from multiple subwatersheds driven by multiple weather stations.

The file structure of the HSPF model is also considerably more efficient for implementing and running multiple scenarios. SWAT's use of the curve number approach to hydrology and a daily time step can also cause difficulties in representing the full hydrograph and introduces uncertainties into the simulation of erosion and pollutant loading as a function of surface flow (Garen and Moore, 2005).

Given that both models perform adequately, the SWAT model was selected for use in the remaining 15 non-pilot watersheds due to its integrated plant growth model and practical advantages of ease of calibration.

It should be recognized that there are other feedback cycles that are not incorporated in either model, such as the potential for any increased rate of catastrophic forest fires (Westerling et al., 2006), changes to vegetative communities as a result of pests and disease (Berg et al., 2006), and human adaptations such as shifts to different crops and agricultural management strategies (Polsky and Easterling, 2001).

6.2. EFFECTS OF DIFFERENT METHODS OF DOWNSCALING OF CLIMATE CHANGE PROJECTIONS

In general, the different climate scenarios provide a consistent picture of temperature increases by mid-century (on the order of 2 to 3 °C), although there do appear to be systematic differences between the scenarios (for example, the NARCCAP scenario using the GFDL model downscaled with RCM3 typically is the coolest scenario for the watersheds studied here). In contrast, changes in precipitation between the historical and future simulations differ widely across models, with some producing increases and some suggesting decreases in total precipitation.

In addition, as is evident from the detailed results presented in Section Appendix X, not only the selection of the underlying GCM, but also the choice of downscaling method, have a significant influence on the flow and water quality simulations. Indeed, in some basins (e.g., Minnesota River, ACF) the difference among watershed model simulations as driven by the six NARCCAP dynamically downscaled scenarios appears to be noticeably greater than the range of model predictions driven by BCSD statistically downscaled or raw GCM meteorology. This leads to the somewhat counter-intuitive observation that incorporating additional information, either from dynamic RCMs or via statistical methods, can actually increase the perceived level of uncertainty regarding climate change impacts – or, perhaps more accurately, provides a more realistic picture of the uncertainty in future climate impacts.

6.2.1. "Degraded" NARCCAP Climate Scenarios

To provide a consistent basis for comparison that focuses on the differences between climate model outputs rather than differences in post-processing, all scenarios were adjusted to a common minimum basis. Specifically, the raw GCM and BCSD climate products used in this study provide only precipitation volume and air temperature and do not include explicit information on potential changes in the intensity of precipitation events. The following steps were taken to develop a consistent set of climate scenario input series that differ only in the underlying climate model and downscaling technique:

- Representation of intensification in each of the NARCCAP dynamically downscaled scenarios was based on Approach 2 in Section 5.1.4.2, which assumes that all increases in precipitation occur in the top 30 percent of events, rather than using the direct analysis of intensity changes provided by NARCCAP.
- Complete information on changes in weather generator statistics for dew point temperature, solar radiation, and wind speed was removed for the NARCCAP dynamically downscaled scenarios, consistent with the information available for the

BCSD scenarios. Incomplete information on these variables provided by the non-downscaled GCMs was also removed. (For the raw GCMs this affects weather scenarios 7, 9, and 10 – see Table 15 above).

- Penman-Monteith PET was recalculated with the revised set of climate variables.
- Simulations use current land use to remove land use change effects.

Note that these simplified or "degraded" scenarios are used only for the comparisons presented in this section. Results presented in subsequent sections use the scenarios that contain all available meteorological information.

Comparison of the PET series generated with full climatological data to the degraded series in which only precipitation and temperature are updated shows the importance of including these additional variables. Further, the effect of individual meteorological time series is discernible because the original set lacked solar radiation for Scenario 5, dewpoint temperature for Scenario 9, and wind speed for Scenario 10 (see Table 14). Dewpoint temperature (which tends to increase in future, warmer climates) has the biggest impact. Including climate model-simulated dewpoint that is consistent with the scenario temperature and precipitation regime results in a reduction in estimated annual PET of about 11 percent across all the meteorological stations used for the five pilot watersheds. The effect appears to be greater at higher latitudes. The reduction in PET from including simulated dewpoint is around 10 - 20 percent for the Minnesota, New York, Oregon, and Pennsylvania stations, but only 3 – 10 percent for the Alabama, Arizona, Florida, and Georgia stations. In contrast, for Scenario 9 (for which dewpoint temperature was not available), the original PET series were on average 1.9 percent higher than the degraded series. Omission of solar radiation or wind speed results from the climate scenario appears to have at most a minor impact on the estimated PET.

Table 22. Effects of omitting simulated auxiliary meteorological time series on Penman-Monteith reference crop PET estimates for "degraded" climate scenarios

Location	Scen1	Scen2	Scen3	Scen4	Scen5	Scen6	Scen7	Scen9	Scen10
AL	-4.87%	-4.44%	-5.21%	-10.90%	-5.76%	-4.47%	-4.89%	2.66%	-7.11%
AZ	-2.38%	-3.01%	-4.12%	-3.59%	-2.97%	-3.08%	-0.99%	2.69%	-3.02%
FL	-7.14%	-8.48%	-7.45%	-16.69%	-9.04%	-9.02%	-7.35%	2.92%	-10.91%
GA	-9.30%	-7.21%	-7.79%	-18.01%	-10.15%	-7.27%	-8.71%	1.79%	-14.04%
MN	-14.68%	-10.30%	-13.73%	-10.30%	-16.46%	-21.16%	-13.83%	1.68%	-16.46%
NY	-23.27%	-16.99%	-17.68%	-20.62%	-22.95%	-18.30%	-23.01%	-1.29%	-20.48%
OR	-15.82%	-14.28%	-7.75%	-12.90%	-13.67%	-13.29%	-12.73%	0.11%	-10.17%

PA	-17.62%	-12.54%	-14.77%	-18.93%	-18.59%	-13.40%	-17.96%	0.28%	-17.28%
All	-12.53%	-9.93%	-9.97%	-12.62%	-12.86%	-12.48%	-11.37%	1.19%	-12.39%
All (in/yr)	-6.36	-5.27	-5.16	-6.48	-6.42	-6.31	-5.63	0.90	-6.55

Note: Auxiliary time series are solar radiation, dewpoint temperature, and wind. The full version of Scenario 5 did not have a solar radiation time series; Scenario 9 did not have a dewpoint temperature time series; Scenario 10 did not have a wind time series.

These results suggest that downscaling approaches that omit dewpoint temperature can introduce significant biases. Specifically, simulation without adjusting for future changes in dewpoint temperature is likely to over-estimate PET, leading to an under-estimation of soil moisture and flow.

6.2.2. Comparison of Downscaling Approaches

The effect of downscaling approach on uncertainty can be investigated quantitatively by comparing the results from simulations based on degraded NARCCAP, GCM, and BCSD scenarios. Table 23 presents results obtained with current land use and the SWAT watershed model (with CO_2 fertilization) at the most downstream gage in each study area. Table 24 presents detailed results for multiple flow and water quality parameters in the Minnesota River study area. In both cases, results are qualitatively similar for HSPF output and for simulations with land use change.

Table 23. Summary of SWAT-simulated total streamflow in the five pilot study areas for scenarios representing different methods of downscaling.

Study Area	Downscaling Method	Number of Scenarios	Median (cms)	Maximum (cms)	Minimum (cms)	Coefficient of Variation (CV)
ACF	NARCCAP	6	710.4	818.8	478.6	0.208
	BCSD	4	675.5	722.0	655.3	0.042
	GCM	4	655.0	750.7	581.3	0.105
Salt/Verde/San Pedro (Ariz)	NARCCAP	6	19.4	24.5	12.9	0.233
	BCSD	4	24.0	28.4	21.3	0.122
	GCM	4	26.0	27.0	19.9	0.131
Minnesota River (Minn)	NARCCAP	6	229.5	274.3	149.4	0.230
	BCSD	4	236.8	286.3	209.7	0.153
	GCM	4	238.3	277.0	124.4	0.301
Susquehanna	NARCCAP	6	834.8	855.5	705.6	0.068

(Susq)	BCSD	4	935.7	948.4	879.2	0.035
	GCM	4	868.7	1,017.1	807.0	0.106
Willamette (Willa)	NARCCAP	6	878.8	951.8	763.6	0.086
	BCSD	4	833.0	1,003.7	800.3	0.108
	GCM	4	843.3	970.7	810.6	0.082

Notes: Results shown are for most downstream station in each study area; CV (coefficient of variation) = standard deviation divided by the mean. Climate scenarios are degraded to a common basis of scenario precipitation and air temperature information only.

Table 24. Summary of SWAT-simulated streamflow and water quality in the Minnesota River study area for scenarios representing different methods of downscaling.

Endpoint	Downscaling Method	Number of Scenarios	Median	Maximum	Minimum	Coefficient of Variation (CV)
Total Streamflow (cms)	NARCCAP	6	229.5	274.3	149.4	0.230
	BCSD	4	236.8	286.3	209.7	0.153
	GCM	4	238.3	277.0	124.4	0.301
100-Year High Flow (cms)	NARCCAP	6	3,415.4	3,700.2	3,155.7	0.058
	BCSD	4	3,960.2	5,055.0	3,617.6	0.153
	GCM	4	3,565.7	4,432.3	2,508.7	0.227
7 Day Average Low Flow (cms)	NARCCAP	6	27.7	38.5	14.3	0.353
	BCSD	4	25.8	37.9	22.3	0.247
	GCM	4	28.2	37.0	12.9	0.395
Total Suspended Sediment (MT/yr)	NARCCAP	6	1,926,166	2,520,444	896,806	0.385
	BCSD	4	2,002,421	2,428,565	1,376,608	0.265
	GCM	4	1,914,800	2,557,634	633,793	0.460
Total Phosphorus (MT/yr)	NARCCAP	6	36,304	42,119	25,843	0.191
	BCSD	4	40,579	44,936	32,451	0.150
	GCM	4	38,747	42,087	21,538	0.264

Total Nitrogen (MT/yr)	NARCCAP	6	2,700	3,283	2,007	0.194
	BCSD	4	3,073	3,453	2,356	0.183
	GCM	4	2,889	3,162	1,489	0.292

Notes: Results shown are for most downstream station in each study area; CV (coefficient of variation) = standard deviation divided by the mean. Climate scenarios are degraded to a common basis of scenario precipitation and air temperature information only.

Results show considerable variability among climate models and downscaling techniques in different basins and for different streamflow and water quality endpoints. No consistent pattern attributable to downscaling method is evident for the case where all climate model outputs are degraded to a common basis of precipitation and air temperature only, As was discussed in Section 6.1.4. the additional information on other meteorological variables can have a profound effect on PET and watershed responses.

It is noteworthy that the dynamically downscaled results may differ significantly from the statistically downscaled results from the same GCM, and that the results may also be quite different when the same GCM is downscaled with a different RCM (e.g., compare scenarios W1 and W5 for CGCM3, also W3 and W4 for the GFDL). As noted in Section 5.1.2. , direct comparison between NARCCAP and BCSD downscaling of a single GCM can only be reliably undertaken for the GFDL and CGCM3 models, as slightly different GCM runs were used to produce NARCCAP and BCSD results for other GCMs.

Both the GFDL and CGCM3 A2 scenario runs for 2041-2070 were downscaled with two different NARCCAP RCMs - with one RCM (RCM3) in common between the two. A comparison in terms of the ratio of simulated future mean annual flow to simulated current mean annual flow, using SWAT, is made in Figure 35 for the GFDL and in Figure 36 for the CGCM3 model. For both GCMs, the NARCCAP downscaling, BCSD downscaling, and raw GCM output produce relatively consistent results for the Willamette and Susquehanna basins, but diverge for the Minnesota River. For the Arizona basin, the two different downscaling approaches diverge for the GFDL but not the CGCM3 GCM. Elevated CVs on mean annual flow in both the Minnesota River and Arizona basins appear to be largely due to the difference in downscaling results obtained with the GFDL high-resolution regional model, which suggests lower flow than other dynamically downscaled interpretations of the GFDL GCM.

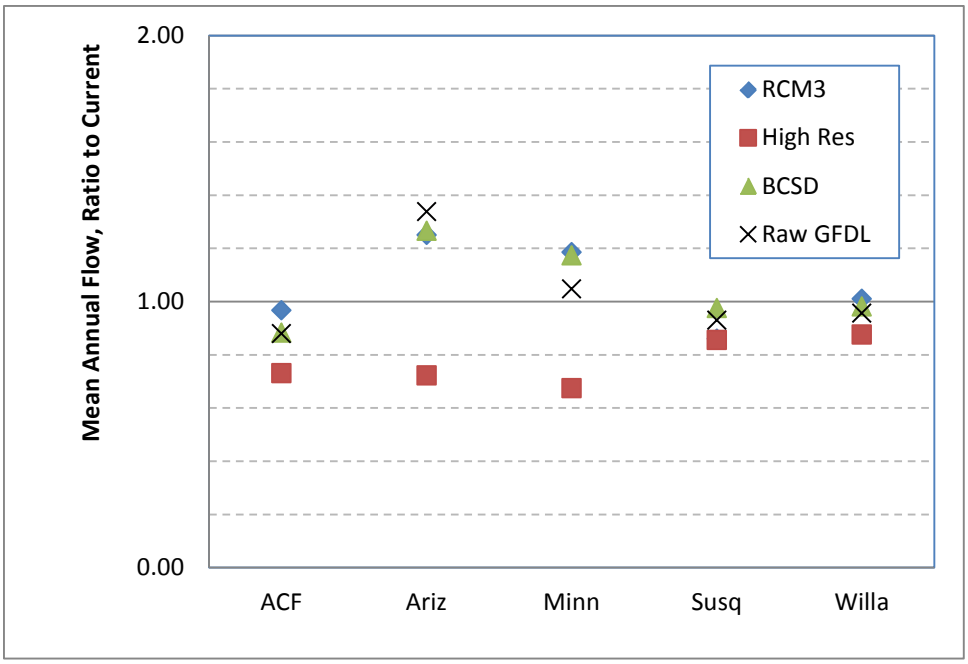

Figure 35. Consistency in SWAT model predictions of mean annual flow with downscaled (NARCCAP, BCSD) and GCM projections of the GFDL GCM

Note: The climate change scenarios used in this analysis are simplified to include changes only in air temperature and precipitation (variables common to the NARCCAP, BCSD, and GCM datasets) to provide a common basis for comparison.

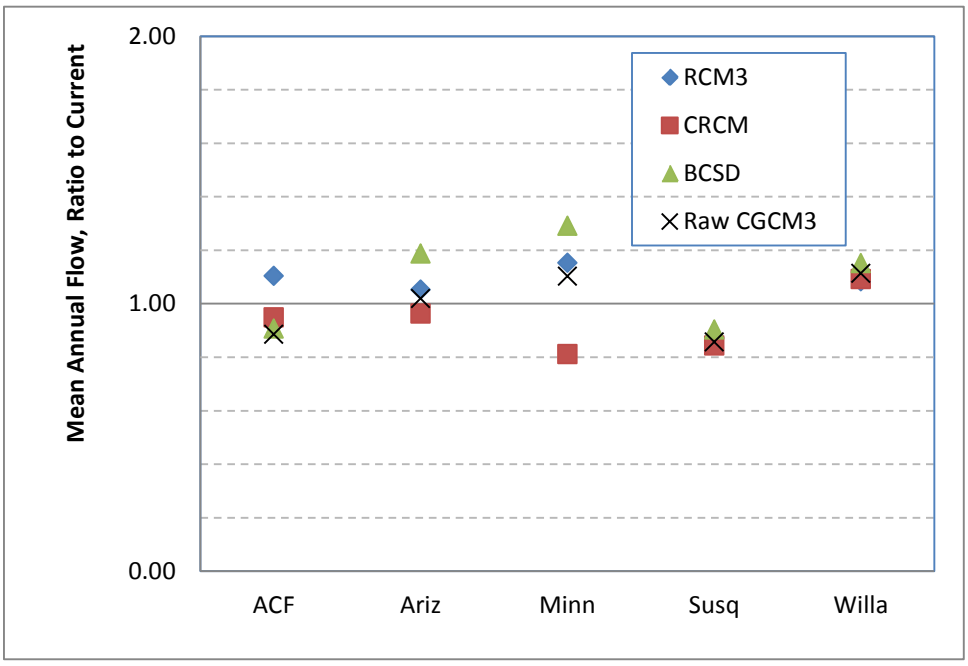

Figure 36. Consistency in SWAT model predictions of mean annual flow with downscaled (NARCCAP, BCSD) and GCM projections of the CGCM3 GCM

Note: The climate change scenarios used in this analysis are simplified to include changes only in air temperature and precipitation (variables common to the NARCCAP, BCSD, and GCM datasets) to provide a common basis for comparison.

To date, relatively few comparisons of RCM model performance in the NARCCAP datasets have been undertaken. An exception is the study of Wang et al. (2009) for the Intermountain Region of the Western U.S. Significant orographic effects in this area lead to a complex combination of precipitation annual and semiannual cycles that form four major climate regimes in this area. Wang et al. compared results from six RCMs over this region to the North American Regional Reanalysis (NARR) precipitation study (Mesinger et al., 2006) and found that each model produces its own systematic bias in the central Intermountain Region where the four different climate regimes meet. All six of the RCMs appeared to produce simulated annual cycles that are too strong and winter precipitation that is too high under current conditions. The BCSD statistical approach can correct this for current conditions; however, the statistical approach would not account for any future large-scale changes in the interaction of the major climate regimes.

Wang et al. (2009) also demonstrate that the different RCMs are largely consistent in the Cascade Range (OR, WA), where the dominant upper level flow first encounters land – which fits with the reduced level of variability between downscaling methods noted for the Willamette study area. The differences among RCMs reported by Wang et al., and their difference from NARR, are greatest on the windward side of the Rocky Mountains in Colorado and remain large into Arizona. Interestingly, the apparent wet bias of the CRCM and dry bias of most other RCMs relative to NARR in Arizona reported by Wang et al. does not appear to carry through into the future scenarios reported here – suggesting that the RCMs may be providing different simulated solutions to the future interaction of large-scale climate regimes in this area.

The ranges shown in Table 25 suggest that for 2041-2070 conditions it is not possible in most cases to even state the sign of change in watershed response with a high degree of assurance unless one is willing to assert that one of the RCMs is more reliable than another. Rather, the results tell us that the range of potential responses is large.

In addition to uncertainties in representing climate forcing at the watershed level, as discussed in this section, previous sections have shown that the results are sensitive to the selection of a watershed model, and to modeler skill in calibrating the model. Furthermore, the results are undoubtedly also sensitive to feedback loops that are not incorporated into the models. Results produced in this study thus likely do not span the full range of potential future impacts (even conditional on the A2 storyline) for the reasons given above, among others. Nonetheless, the range of uncertainty is considerable, and generally covers the zero point, as is summarized at selected downstream analysis points shown in Table 25. Based on the analysis presented here, however, we can state that the differences in simulation results in our study are largely a result of combined differences in the underlying GCM and the downscaling approach used, and more specifically, largely a result of heterogeneity in simulated precipitation amounts and patterns. For the 2041-2070 timeframe, these warming-induced increases in simulated PET are generally insufficient to overcome this range of variability in precipitation forecasts. This may not be the case, however, for more distant future simulation periods – given continually increasing temperature and PET, evapotranspiration increases are likely to ultimately exceed the range of variability in simulated precipitation in many basins, resulting in more uniform decreases in runoff.

Table 25. Range of simulated percent changes for NARCCAP climate scenarios; SWAT simulation with ICLUS land use for 2041 – 2070 (percent change in annual flow and load).

Location	Flow	Total solids	Total nitrogen	Total phosphorus
ACF – Apalachicola River Outlet	-26.7 to +23.9	-46.9 to +47.0	-4.1 to +26.2	+6.6 to +53.3
Ariz – Verde River below Tangle Creek	-28.9 to +27.6	-51.0 to +125.8	-7.6 to +45.9	-31.8 to +66.0
Susq – Susquehanna River Outlet	-9.8 to +11.3	-15.3 to +18.1	+31.0 to +60.6	+5.9 to +7.7
Minn – Minnesota River Outlet	-14.2 to +62.4	-24.4 to +118.5	+4.4 to +70.8	-3.2 to +59.6
Willa – Willamette River	-8.5 to +15.7	-10.6 to +24.1	-8.7 to +5.9	-6.3 to -0.2

7. RESULTS IN ALL 20 WATERSHEDS: REGIONAL SENSITIVITY TO CLIMATE CHANGE AND URBAN DEVELOPMENT

This section provides a summary of SWAT simulation results for all 20 watersheds. Tabular results are presented for a single representative analysis point in each study area (Table 26). For study areas composed of a single watershed, this is the outlet (pour point) of the entire study area. For study areas composed of multiple, adjacent watersheds draining to the coast, the analysis point reported here is at or near the outlet of the largest river within the study area. Graphical results for key indicators are shown for all HUC8s contained within the 20 watersheds in Section 7. More detailed scenario results including results at multiple stations within each study area are reported in Appendix X for the 5 pilot sites and Appendix Y for all other sites.

The comparison uses baseline climate and land use with the six mid-21st century NARCCAP climate change scenarios, and the 2050 ICLUS urban and residential development scenario. Scenarios also assumed future increases in atmospheric CO_2.

Table 26. Downstream stations where simulation results are presented.

Study Area	Location Reporting Results
Apalachicola-Chattahoochee-Flint (ACF) Basins	Apalachicola R at outlet
Coastal Southern California	Los Angeles R at outlet
Cook Inlet Basin	Kenai R at Soldotna
Georgia-Florida Coastal Plain	Suwanee R at outlet
Illinois River Basin	Illinois R at Marseilles, IL
Lake Erie-Lake St. Clair Drainages	Maumee R at outlet
Lake Pontchartrain Drainage	Amite R at outlet
Loup/Elkhorn River Basin	Elkhorn R at outlet
Minnesota River Basin	Minnesota R at outlet
Neuse/Tar River Basins	Neuse R at outlet
New England Coastal Basins	Merrimack R at outlet
Powder/Tongue River Basin	Tongue R at outlet
Rio Grande Valley	Rio Grande R below Albuquerque
Sacramento River Basin	Sacramento R at outlet
Salt, Verde, and San Pedro River Basins	Salt River nr Roosevelt
South Platte River Basin	S. Platte R at outlet
Susquehanna River Basin	Susquehanna R at outlet
Trinity River Basin	Trinity R at outlet
Upper Colorado River Basin	Colorado R nr State Line
Willamette River Basin	Willamette R at outlet

7.1. SENSITIVITY TO CLIMATE CHANGE SCENARIOS

Results across all watersheds for scenarios involving only climate change (that is, with land use held constant at existing conditions) are shown in this section. For endpoints other than days to flow centroid the results are shown as a percentage relative to the current baseline (generally, 1972-2003), allowing comparison across multiple basins with different magnitudes of flows and pollutant loads. The six NARCCAP dynamically downscaled climate scenarios are shown in columns, while the last column gives the median of the six NARCCAP scenarios at the selected analysis point. For Cook Inlet (Alaska) results are shown only for the three NARCCAP scenarios that provide climate projections for this portion of Alaska.

Table 27 summarizes results for total average annual flow volume, with results ranging from 63% to 240% of current average flows. Results for 7-day low flows and 100-year peak flows (estimated with log-Pearson III fit) are shown in Table 28 and Table 29, respectively. The Kenai River has by far the greatest increase in 7-day low flows because warmer temperatures alter the snow/ice melt regime, while the largest increases in 100-year peak flows are for the Neuse River on the east coast.

Table 30 summarizes the estimated change in days to flow centroid relative to the start of the water year. Many stations show negative shifts, indicating earlier snowmelt resulting in an earlier center of flow mass. In contrast, several stations show positive shifts due to increased summer precipitation.

Results for the Richards-Baker flashiness index (Table 31) show generally small percentage changes, with a few exceptions. Baker et al. (2004) suggest that changes on the order of 10 percent or more may be statistically significant. It is likely, however, that the focus on larger watersheds reduces the observed flashiness response.

Simulated changes in pollutant loads (TSS, TP, TN) are summarized in Table 34. The patterns are generally similar to changes in flow. Increases in pollutant loads are suggested for many watersheds, but there are also basins where loads decline, mostly due to reduced flows.

For most measures in most watersheds, there is a substantial amount of variability between predictions based on different downscaled climate products. This reflects our uncertainty in predicting future climate, especially the future joint distribution of precipitation and potential evapotranspiration that is fundamental to watershed response, and reinforces the need for an ensemble approach for evaluating the range of potential responses.

Table 27. Simulated total flow volume (climate scenarios only; percent relative to current conditions) for selected downstream stations.

Station	Study Area	CRCM_ cgcm3	HRM3_ hadcm3	RCM3_ gfdl	GFDL_ slice	RCM3_ cgcm3	WRFP_ ccsm	Median
Minnesota R at outlet	Minnesota River	109%	113%	147%	86%	146%	162%	130%
Susquehanna R at outlet	Susquehanna River	109%	106%	106%	108%	111%	90%	107%
Salt River nr Roosevelt	Salt, Verde, and San Pedro	80%	80%	149%	75%	94%	73%	80%
Willamette R at outlet	Willamette River	116%	106%	105%	92%	114%	98%	105%
Apalachicola R at outlet	ACF	107%	122%	108%	88%	124%	73%	107%
Kenai R at Soldotna	Cook Inlet	ND	154%	ND	132%	ND	167%	154%
Maumee R at outlet	Lake Erie Drainages	116%	150%	120%	136%	122%	88%	121%
Suwanee R at outlet	Georgia-Florida Coastal	114%	153%	128%	92%	156%	75%	121%
Illinois R at Marseilles, IL	Illinois River	94%	125%	101%	102%	105%	78%	101%
Merrimack R at outlet	New England Coastal	108%	115%	111%	111%	106%	94%	109%
Sacramento R at outlet	Sacramento River	104%	89%	98%	98%	100%	99%	99%
Los Angeles R at outlet	Coastal Southern California	92%	138%	102%	103%	106%	84%	103%
Tongue R at outlet	Powder/Tongue Rivers	101%	85%	140%	70%	130%	240%	115%
Amite R at outlet	Lake Pontchartrain Drainages	96%	110%	115%	84%	106%	77%	101%
Rio Grande R below Albuquerque	Rio Grande	72%	69%	112%	66%	69%	84%	71%
S. Platte R at outlet	South Platte	88%	80%	100%	74%	97%	101%	92%
Neuse R at outlet	Neuse/Tar Rivers	103%	158%	137%	110%	125%	86%	118%
Trinity R at outlet	Trinity River	98%	146%	106%	62%	118%	134%	112%
Elkhorn R at outlet	Loup/Elkhorn Rivers	118%	125%	138%	67%	140%	144%	131%
Colorado R nr State Line	Upper Colorado	86%	95%	116%	89%	92%	91%	91%

Table 28. Simulated 7-day low flow (climate scenarios only; percent relative to current conditions) for selected downstream stations.

Station	Study Area	CRCM_ cgcm3	HRM3_ hadcm3	RCM3_ gfdl	GFDL_ slice	RCM3_ cgcm3	WRFP_ ccsm	Median
Minnesota R at outlet	Minnesota River	115%	136%	201%	81%	182%	228%	159%
Susquehanna R at outlet	Susquehanna River	91%	120%	104%	89%	107%	86%	98%
Salt River nr Roosevelt	Salt, Verde, and San Pedro	58%	77%	131%	87%	79%	90%	83%
Willamette R at outlet	Willamette River	131%	113%	108%	83%	127%	102%	111%
Apalachicola R at outlet	ACF	97%	120%	105%	85%	113%	64%	101%
Kenai R at Soldotna	Cook Inlet	ND	267%	ND	280%	ND	401%	280%
Maumee R at outlet	Lake Erie Drainages	104%	184%	126%	132%	128%	58%	127%
Suwanee R at outlet	Georgia-Florida Coastal	104%	141%	121%	95%	136%	78%	113%
Illinois R at Marseilles, IL	Illinois River	85%	123%	97%	91%	100%	70%	94%
Merrimack R at outlet	New England Coastal	110%	140%	130%	118%	124%	120%	122%
Sacramento R at outlet	Sacramento River	101%	91%	95%	96%	99%	93%	95%
Los Angeles R at outlet	Coastal Southern California	96%	114%	98%	98%	100%	92%	98%
Tongue R at outlet	Powder/Tongue Rivers	102%	92%	145%	67%	127%	235%	115%
Amite R at outlet	Lake Pontchartrain Drainages	73%	106%	88%	74%	89%	62%	81%
Rio Grande R below Albuquerque	Rio Grande	81%	64%	120%	62%	74%	86%	77%
S. Platte R at outlet	South Platte	103%	99%	105%	99%	103%	104%	103%
Neuse R at outlet	Neuse/Tar Rivers	94%	170%	135%	113%	125%	70%	119%
Trinity R at outlet	Trinity River	26%	167%	64%	23%	70%	85%	67%
Elkhorn R at outlet	Loup/Elkhorn Rivers	117%	134%	154%	47%	148%	155%	141%
Colorado R nr State Line	Upper Colorado	85%	94%	121%	85%	91%	90%	91%

Table 29. Simulated 100-year peak flow (log-Pearson III; climate scenarios only; percent relative to current conditions) for selected downstream stations.

Station	Study Area	CRCM_ cgcm3	HRM3_ hadcm3	RCM3_ gfdl	GFDL_ slice	RCM3_ cgcm3	WRFP_ ccsm	Median
Minnesota R at outlet	Minnesota River	84%	83%	96%	88%	90%	96%	89%
Susquehanna R at outlet	Susquehanna River	107%	130%	106%	128%	172%	100%	118%
Salt River nr Roosevelt	Salt, Verde, and San Pedro	119%	101%	104%	68%	120%	66%	102%
Willamette R at outlet	Willamette River	116%	130%	114%	79%	116%	95%	115%
Apalachicola R at outlet	ACF	119%	144%	110%	90%	128%	94%	114%
Kenai R at Soldotna	Cook Inlet	ND	132%	ND	125%	ND	132%	132%
Maumee R at outlet	Lake Erie Drainages	96%	106%	87%	93%	93%	92%	93%
Suwanee R at outlet	Georgia-Florida Coastal	130%	145%	129%	94%	157%	107%	130%
Illinois R at Marseilles, IL	Illinois River	120%	153%	107%	99%	128%	97%	114%
Merrimack R at outlet	New England Coastal	114%	130%	111%	138%	89%	80%	112%
Sacramento R at outlet	Sacramento River	105%	98%	125%	117%	102%	131%	111%
Los Angeles R at outlet	Coastal Southern California	83%	89%	161%	95%	127%	77%	92%
Tongue R at outlet	Powder/Tongue Rivers	118%	113%	133%	82%	121%	146%	119%
Amite R at outlet	Lake Pontchartrain Drainages	105%	150%	108%	99%	105%	65%	105%
Rio Grande R below Albuquerque	Rio Grande	90%	77%	108%	66%	72%	92%	83%
S. Platte R at outlet	South Platte	124%	85%	97%	79%	152%	138%	110%
Neuse R at outlet	Neuse/Tar Rivers	71%	292%	161%	111%	224%	63%	136%
Trinity R at outlet	Trinity River	97%	106%	107%	60%	86%	106%	102%
Elkhorn R at outlet	Loup/Elkhorn Rivers	119%	108%	110%	83%	141%	110%	110%
Colorado R nr State Line	Upper Colorado	78%	84%	97%	91%	94%	84%	87%

Table 30. Simulated changes in the number of days to flow centroid (climate scenarios only; relative to current conditions) for selected downstream stations.

Station	Study Area	CRCM_ cgcm3	HRM3_ hadcm3	RCM3_ gfdl	GFDL_ slice	RCM3_ cgcm3	WRFP_ ccsm	Median
Minnesota R at outlet	Minnesota River	-13	-19	-6	-15	-3	2	-10
Susquehanna R at outlet	Susquehanna River	-18	16	-6	-12	-6	0	-6
Salt River nr Roosevelt	Salt, Verde, and San Pedro	-18	41	28	17	-6	53	22
Willamette R at outlet	Willamette River	3	-8	-1	3	1	8	2
Apalachicola R at outlet	ACF	-2	-2	1	8	-6	1	-1
Kenai R at Soldotna	Cook Inlet	ND	-3	ND	-5	ND	-1	-3
Maumee R at outlet	Lake Erie Drainages	-2	-4	1	0	10	-8	-1
Suwanee R at outlet	Georgia-Florida Coastal	-3	17	25	-8	-5	11	4
Illinois R at Marseilles, IL	Illinois River	-12	6	-3	-12	-2	-15	-7
Merrimack R at outlet	New England Coastal	-17	-14	-19	-13	-9	-18	-16
Sacramento R at outlet	Sacramento River	-4	-7	-4	-1	-3	-8	-4
Los Angeles R at outlet	Coastal Southern California	5	48	-3	10	-3	1	3
Tongue R at outlet	Powder/Tongue Rivers	-6	-3	1	-16	-4	7	-3
Amite R at outlet	Lake Pontchartrain Drainages	-14	13	-24	-7	-6	-11	-9
Rio Grande R below Albuquerque	Rio Grande	25	6	3	11	14	17	13
S. Platte R at outlet	South Platte	-11	-15	2	-16	-7	-14	-13
Neuse R at outlet	Neuse/Tar Rivers	-14	23	30	-12	10	-5	2
Trinity R at outlet	Trinity River	16	21	30	3	6	37	18
Elkhorn R at outlet	Loup/Elkhorn Rivers	-11	6	2	-23	-5	-7	-6
Colorado R nr State Line	Upper Colorado	-11	-14	-7	-10	-8	-10	-10

Table 31. Simulated Richards-Baker flashiness index (climate scenarios only; percent relative to current conditions) for selected downstream stations.

Station	Study Area	CRCM_ cgcm3	HRM3_ hadcm3	RCM3_ gfdl	GFDL_ slice	RCM3_ cgcm3	WRFP_ ccsm	Median
Minnesota R at outlet	Minnesota River	104%	112%	107%	100%	109%	108%	108%
Susquehanna R at outlet	Susquehanna River	107%	111%	107%	110%	112%	103%	109%
Salt River nr Roosevelt	Salt, Verde, and San Pedro	81%	102%	121%	98%	103%	119%	102%
Willamette R at outlet	Willamette River	101%	105%	100%	97%	101%	102%	101%
Apalachicola R at outlet	ACF	106%	125%	109%	94%	125%	90%	108%
Kenai R at Soldotna	Cook Inlet	ND	94%	ND	102%	ND	96%	96%
Maumee R at outlet	Lake Erie Drainages	99%	101%	99%	100%	100%	96%	100%
Suwanee R at outlet	Georgia-Florida Coastal	93%	62%	76%	117%	59%	187%	84%
Illinois R at Marseilles, IL	Illinois River	106%	104%	103%	106%	105%	104%	105%
Merrimack R at outlet	New England Coastal	101%	103%	99%	101%	98%	93%	100%
Sacramento R at outlet	Sacramento River	124%	103%	112%	109%	116%	123%	114%
Los Angeles R at outlet	Coastal Southern California	103%	119%	100%	105%	105%	99%	104%
Tongue R at outlet	Powder/Tongue Rivers	102%	108%	104%	100%	103%	109%	104%
Amite R at outlet	Lake Pontchartrain Drainages	105%	105%	106%	104%	104%	102%	104%
Rio Grande R below Albuquerque	Rio Grande	109%	117%	95%	119%	103%	106%	108%
S. Platte R at outlet	South Platte	99%	95%	106%	90%	104%	102%	100%
Neuse R at outlet	Neuse/Tar Rivers	96%	113%	115%	98%	103%	91%	101%
Trinity R at outlet	Trinity River	71%	68%	72%	73%	69%	68%	70%
Elkhorn R at outlet	Loup/Elkhorn Rivers	95%	96%	93%	93%	96%	93%	94%
Colorado R nr State Line	Upper Colorado	101%	107%	111%	105%	104%	101%	105%

Table 32. Simulated total suspended solids load (climate scenarios only; percent relative to current conditions) for selected downstream stations.

Station	Study Area	CRCM_ cgcm3	HRM3_ hadcm3	RCM3_ gfdl	GFDL_ slice	RCM3_ cgcm3	WRFP_ ccsm	Median
Minnesota R at outlet	Minnesota River	107%	119%	187%	77%	197%	225%	153%
Susquehanna R at outlet	Susquehanna River	117%	108%	108%	115%	118%	84%	112%
Salt River nr Roosevelt	Salt, Verde, and San Pedro	89%	79%	184%	66%	106%	74%	84%
Willamette R at outlet	Willamette River	124%	111%	109%	90%	121%	97%	110%
Apalachicola R at outlet	ACF	125%	146%	129%	93%	144%	53%	127%
Kenai R at Soldotna	Cook Inlet	ND	234%	ND	196%	ND	244%	234%
Maumee R at outlet	Lake Erie Drainages	123%	169%	126%	153%	129%	86%	128%
Suwanee R at outlet	Georgia-Florida Coastal	121%	176%	138%	90%	181%	74%	130%
Illinois R at Marseilles, IL	Illinois River	116%	142%	115%	128%	120%	90%	118%
Merrimack R at outlet	New England Coastal	118%	128%	117%	122%	111%	85%	118%
Sacramento R at outlet	Sacramento River	139%	94%	122%	118%	99%	108%	113%
Los Angeles R at outlet	Coastal Southern California	71%	111%	81%	81%	84%	65%	81%
Tongue R at outlet	Powder/Tongue Rivers	108%	84%	169%	66%	153%	351%	131%
Amite R at outlet	Lake Pontchartrain Drainages	100%	115%	128%	83%	111%	71%	106%
Rio Grande R below Albuquerque	Rio Grande	60%	53%	114%	49%	59%	71%	59%
S. Platte R at outlet	South Platte	68%	69%	77%	54%	77%	80%	73%
Neuse R at outlet	Neuse/Tar Rivers	106%	199%	162%	115%	143%	82%	129%
Trinity R at outlet	Trinity River	63%	124%	62%	27%	83%	113%	73%
Elkhorn R at outlet	Loup/Elkhorn Rivers	125%	129%	147%	59%	166%	163%	138%
Colorado R nr State Line	Upper Colorado	80%	90%	124%	82%	89%	85%	87%

Table 33. Simulated total phosphorus load (climate scenarios only; percent relative to current conditions) for selected downstream stations.

Station	Study Area	CRCM_ cgcm3	HRM3_ hadcm3	RCM3_ gfdl	GFDL_ slice	RCM3_ cgcm3	WRFP_ ccsm	Median
Minnesota R at outlet	Minnesota River	97%	115%	151%	97%	138%	160%	126%
Susquehanna R at outlet	Susquehanna River	128%	106%	111%	127%	115%	109%	113%
Salt River nr Roosevelt	Salt, Verde, and San Pedro	82%	83%	155%	70%	106%	88%	86%
Willamette R at outlet	Willamette River	100%	98%	96%	94%	100%	96%	97%
Apalachicola R at outlet	ACF	138%	152%	134%	118%	148%	106%	136%
Kenai R at Soldotna	Cook Inlet	ND	89%	ND	90%	ND	113%	90%
Maumee R at outlet	Lake Erie Drainages	118%	150%	132%	148%	117%	88%	125%
Suwanee R at outlet	Georgia-Florida Coastal	115%	171%	135%	89%	173%	76%	125%
Illinois R at Marseilles, IL	Illinois River	107%	112%	107%	113%	108%	99%	108%
Merrimack R at outlet	New England Coastal	111%	118%	111%	115%	106%	94%	111%
Sacramento R at outlet	Sacramento River	100%	86%	104%	115%	95%	108%	102%
Los Angeles R at outlet	Coastal Southern California	53%	88%	71%	60%	62%	54%	61%
Tongue R at outlet	Powder/Tongue Rivers	107%	86%	163%	67%	148%	324%	127%
Amite R at outlet	Lake Pontchartrain Drainages	113%	131%	135%	94%	115%	83%	114%
Rio Grande R below Albuquerque	Rio Grande	54%	43%	127%	51%	41%	67%	53%
S. Platte R at outlet	South Platte	91%	88%	103%	84%	97%	100%	94%
Neuse R at outlet	Neuse/Tar Rivers	112%	230%	169%	120%	166%	94%	143%
Trinity R at outlet	Trinity River	124%	163%	130%	83%	135%	160%	132%
Elkhorn R at outlet	Loup/Elkhorn Rivers	120%	123%	138%	66%	147%	148%	130%
Colorado R nr State Line	Upper Colorado	79%	88%	119%	81%	84%	83%	84%

Table 34. Simulated total nitrogen load (climate scenarios only; percent relative to current conditions) for selected downstream stations.

Station	Study Area	CRCM_ cgcm3	HRM3_ hadcm3	RCM3_ gfdl	GFDL_ slice	RCM3_ cgcm3	WRFP_ ccsm	Median
Minnesota R at outlet	Minnesota River	126%	130%	163%	105%	158%	171%	144%
Susquehanna R at outlet	Susquehanna River	162%	147%	147%	156%	150%	132%	149%
Salt River nr Roosevelt	Salt, Verde, and San Pedro	90%	91%	142%	86%	105%	84%	90%
Willamette R at outlet	Willamette River	104%	97%	95%	89%	103%	93%	96%
Apalachicola R at outlet	ACF	116%	125%	115%	106%	122%	95%	116%
Kenai R at Soldotna	Cook Inlet	ND	200%	ND	175%	ND	223%	200%
Maumee R at outlet	Lake Erie Drainages	128%	158%	162%	191%	125%	94%	143%
Suwanee R at outlet	Georgia-Florida Coastal	127%	160%	135%	112%	166%	85%	131%
Illinois R at Marseilles, IL	Illinois River	103%	118%	106%	110%	108%	93%	107%
Merrimack R at outlet	New England Coastal	119%	128%	117%	121%	114%	101%	118%
Sacramento R at outlet	Sacramento River	99%	89%	100%	110%	98%	107%	100%
Los Angeles R at outlet	Coastal Southern California	93%	140%	131%	98%	90%	101%	100%
Tongue R at outlet	Powder/Tongue Rivers	109%	91%	165%	71%	148%	320%	128%
Amite R at outlet	Lake Pontchartrain Drainages	123%	141%	143%	106%	120%	91%	121%
Rio Grande R below Albuquerque	Rio Grande	49%	38%	125%	47%	37%	64%	48%
S. Platte R at outlet	South Platte	87%	83%	102%	79%	95%	99%	91%
Neuse R at outlet	Neuse/Tar Rivers	111%	189%	154%	118%	144%	99%	131%
Trinity R at outlet	Trinity River	121%	165%	125%	80%	136%	164%	130%
Elkhorn R at outlet	Loup/Elkhorn Rivers	90%	94%	149%	92%	103%	105%	99%
Colorado R nr State Line	Upper Colorado	73%	82%	110%	76%	80%	79%	80%

7.2. SENSITIVITY TO URBAN AND RESIDENTIAL DEVELOPMENT SCENARIOS

Results for the pilot sites (Section 6) suggested that effects of urban and residential development by 2050 on flow and pollutant loads is likely to be comparatively small relative to the potential range of impacts associated with climate change. This is largely a reflection of the scale of the analysis: at the scale of large (HUC4 to HUC8) watersheds, developed land is rarely a large portion of the total land area. Significant effects may occur in smaller watersheds where extensive new development occurs.

Results across all 20 watersheds for land use change only generally confirm the relatively small magnitude of response to land use change alone at the large-scale summary stations in simulations with current meteorology (Table 35). Note that there are no results available for the Kenai River (Cook Inlet, AK study area) as the ICLUS product does not cover Alaska.

At the scale of the whole study areas, projected changes (increases) in developed land area range from 0 percent to 11.72 percent of the total area (see Table 18 above). At this scale it is not surprising that projected changes in urban and residential development have only a relatively small impact compared to climate change, which affects all portions of a watershed. The largest response of total flow volume to land use change at the full-basin scale is simulated for the Trinity River in Texas, where total flow increased by 6 percent, while the estimated 100-year peak flow decreased and days to flow centroid increased (i.e., later runoff). This reflects increases in development upstream in the Dallas-Fort Worth metropolitan area. A stronger response to land development is seen at smaller spatial scales where development can account for a larger fraction of watershed area. Development effects are also more likely be reflected in high or low flow statistics. For example, in the Los Angeles River projected changes in urban and residential development result in little change in model-simulated total flow volume, but the 100-year peak flow increases by nearly one quarter.

Table 35. Simulated response to projected 2050 changes in urban and residential development (percent or days relative to current conditions) for selected downstream stations.

Station	Study Area	Total Flow (%)	7-day low flow (%)	100-yr peak flow (%)	Days to flow centroid (days)	Richards-Baker flashiness (%)	TSS load (%)	TP load (%)	TN load (%)
Minnesota R at outlet	Minnesota River	100.2%	100.3%	99.9%	0.3	100.1%	98.0%	99.3%	99.5%
Susquehanna R at outlet	Susquehanna River	100.2%	100.7%	99.7%	0.1	100.1%	100.3%	99.7%	99.2%
Salt River nr Roosevelt	Salt, Verde, and San Pedro	100.1%	100.0%	100.2%	0.1	100.3%	100.2%	100.4%	100.2%
Willamette R at outlet	Willamette River	99.9%	100.1%	100.1%	0.0	100.7%	99.7%	99.9%	102.5%
Apalachicola R at outlet	ACF	100.3%	100.4%	100.3%	-0.1	100.0%	100.6%	101.1%	100.5%
Kenai R at Soldotna	Cook Inlet	ND	ND	ND	ND	ND	ND	ND	ND
Maumee R at outlet	Lake Erie Drainages	100.5%	100.8%	101.4%	0.2	100.9%	100.6%	101.3%	99.6%
Suwanee R at outlet	Georgia-Florida Coastal	100.3%	99.9%	100.6%	0.3	99.5%	100.4%	108.9%	102.5%
Illinois R at Marseilles, IL	Illinois River	102.4%	104.0%	102.1%	1.0	98.4%	100.5%	100.2%	99.2%
Merrimack R at outlet	New England Coastal	100.4%	100.5%	101.4%	0.0	101.3%	101.2%	103.8%	102.0%
Sacramento R at outlet	Sacramento River	100.1%	100.1%	99.9%	-0.1	100.4%	99.7%	102.1%	104.7%
Los Angeles R at outlet	Coastal Southern California	103.8%	103.2%	123.2%	0.5	103.1%	109.4%	133.4%	116.3%
Tongue R at outlet	Powder/Tongue Rivers	100.0%	100.0%	100.0%	0.0	100.0%	100.0%	100.0%	100.0%
Amite R at outlet	Lake Pontchartrain Drainages	100.8%	102.6%	101.6%	0.2	100.4%	98.7%	106.8%	103.9%
Rio Grande R below Albuquerque	Rio Grande	100.1%	100.1%	100.4%	0.0	100.2%	101.1%	95.4%	99.6%
S. Platte R at outlet	South Platte	104.0%	101.6%	100.0%	1.1	97.1%	106.0%	102.1%	102.6%
Neuse R at outlet	Neuse/Tar Rivers	101.7%	105.2%	102.1%	0.7	99.1%	102.3%	106.7%	103.3%
Trinity R at outlet	Trinity River	106.4%	188.1%	74.2%	3.7	68.8%	61.9%	110.0%	106.2%
Elkhorn R at outlet	Loup/Elkhorn Rivers	100.3%	100.4%	101.4%	0.0	102.8%	100.1%	100.1%	99.8%
Colorado R nr State Line	Upper Colorado	100.1%	100.6%	100.3%	-0.1	99.8%	100.0%	100.8%	100.2%

7.3. RELATIVE EFFECTS OF CLIMATE CHANGE AND URBAN DEVELOPMENT SCENARIOS

The effects of urban and residential development alone were evaluated by comparing the scenario with current climate and existing land use to the scenario for current climate and future land use. As shown above (Table 18), ICLUS projected changes in urban and residential development for 2050 may be important locally but are small relative to the area of large basins in the study areas. Increased development has long been recognized as a source of hydrologic changes and water quality degradation at local scales in urbanizing areas (e.g., U.S. EPA, 1984). The cumulative impacts of development, however, tend to be relatively small at the larger basin scale evaluated in this study simply because only a small fraction of most HUC4-scale watersheds is developed or predicted to be developed by 2050.

The relative magnitude of effects from urban development vs. climate change in our simulations is seen by examining changes in mean annual flow. Figure 37 compares the results of land use change to the range of climate change effects simulated under the six NARCCAP RCM-downscaled climate projections for the pilot study areas where the HSPF model was applied. The results summarize the range of responses across selected HUC8 outlets and additional calibration stations contained within a study area.

Table 36 shows the range of simulated responses of mean annual flow to projected mid-21st century climate and land use change at the HUC8 and larger scale based on SWAT simulations for the six NARCCAP climate change scenarios and ICLUS 2050 projected changes in developed land. Both models show a smaller range of response to projected future changes in urban development than to projected climate change. At the spatial scale of these simulations projected future changes in impervious cover were relatively small as a percent basis. Thus, the range of simulated hydrologic response to climate change scenarios was significantly greater than the response to urban development scenarios. At smaller spatial scales, however, the effects of urban and residential development could be greater. Results for pollutant loads are similar to those for streamflow.

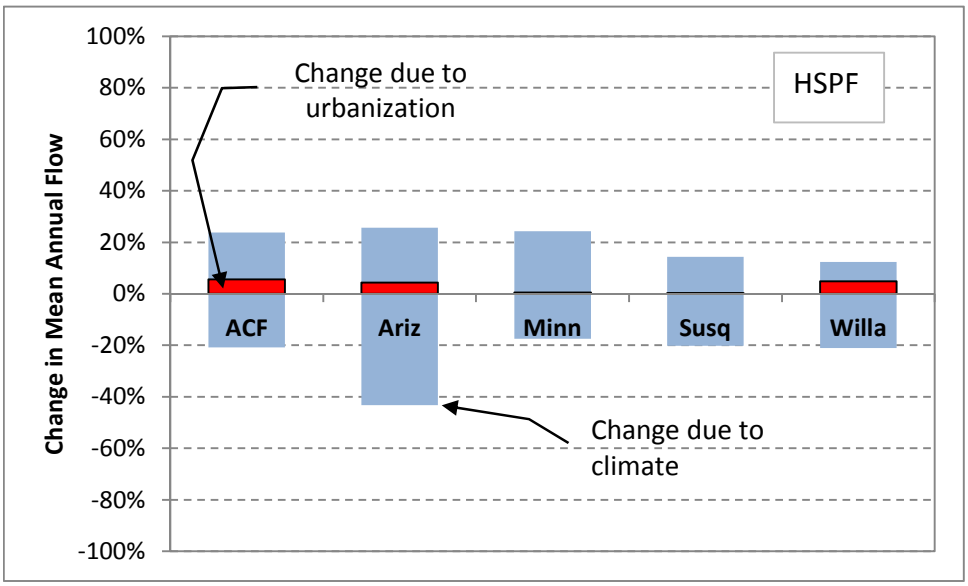

Figure 37. Comparison of simulated responses of mean annual flow to urban development and climate change scenarios – HSPF model.

Note: The blue area represents the range of responses to the six NARCCAP RCM-downscaled 2050 climate scenarios across the different HUC8-scale reporting sites (with no change in land use). The red bars represent the maximum response to land use change among the reporting sites (with no change in climate).

Table 36. Simulated range of responses of mean annual flow to mid-21st century climate and land use change at the HUC8 and larger scale.

	Climate Change Response		Land Use Change Response	
	Minimum	**Maximum**	**Minimum**	**Maximum**
Apalachicola-Chattahoochee-Flint Basins	-45.73%	24.84%	0.00%	0.68%
Coastal Southern California Basins	-26.91%	62.19%	1.66%	9.11%
Georgia-Florida Coastal Plain	-39.73%	69.85%	0.01%	7.36%
Illinois River Basin	-22.20%	34.00%	0.00%	11.90%
Lake Erie Drainages	-22.89%	72.13%	0.00%	1.84%
Lake Pontchartrain Drainage	-24.75%	21.82%	0.00%	1.24%
Loup/Elkhorn River Basin	-77.45%	974.20%	0.00%	0.27%
Minnesota River Basin	-23.39%	85.38%	0.00%	0.19%
New England Coastal Basins	-12.55%	19.80%	0.02%	0.76%
Powder/Tongue River Basins	-42.49%	206.01%	0.00%	0.00%
Rio Grande Valley	-45.38%	19.86%	-0.07%	0.13%
Sacramento River Basin	-20.79%	10.29%	-0.03%	0.47%
Salt, Verde, and San Pedro River Basins	-35.29%	152.52%	0.00%	1.48%
South Platte River Basin	-53.04%	59.23%	-1.00%	2.82%
Susquehanna River Basin	-23.80%	25.79%	0.00%	0.23%
Tar and Neuse River Basins	-13.65%	61.60%	0.28%	4.31%
Trinity River Basin	-60.57%	125.65%	7.09%	34.91%
Upper Colorado River Basin	-20.21%	22.93%	-0.38%	0.47%
Willamette River Basin	-17.51%	23.21%	-1.18%	0.00%

Note: Cook Inlet basin is not shown because ICLUS land use change information is not available. Results based on SWAT simulations for the six NARCCAP climate change scenarios and ICLUS 2050 projected changes in developed land.

The simulated response to land use change is sensitive to model choice – or, more precisely, an interaction between the model and the way in which the ICLUS is interpreted. In the SWAT setup, there are representations of both directly connected (effective) and disconnected impervious area. New developed land use implied by ICLUS is identified to the model as a total area in a given development density class, then subdivided by the model into pervious and impervious fractions using basin-specific estimates of total and effective impervious area. The effective impervious fraction for a given development category is calculated from the 2000 NLCD and assumed invariant. The model then assumes that the effective impervious area has a curve number of 98, while the remaining disconnected impervious area provides a small modification to the curve number assigned to the pervious fraction of the HRU.

In contrast, HSPF has pervious (PERLND) and impervious (IMPLND) land uses, but does not distinguish a separate disconnected impervious class. For HSPF, the new developed area in ICLUS is assigned to the relevant pervious and impervious land use fractions based on the basin-specific percent imperviousness for the land use class. In essence, this means that somewhat greater future connected imperviousness is being specified to the HSPF model than is specified to the SWAT model. While the two approaches are rather different, they are consistent with typical modeling practice for the two models.

Several other details of the SWAT modeling process adopted in this study affect results. The approach to implementing changes in urban development in SWAT was to remove land from existing undeveloped and non-exempt land uses and reassign it to new developed classes that have the parameters of the most dominant soil and lowest HRU slope in the sub-basin. In some cases (particularly when a sub-basin is already largely developed) the dominant soil in the watershed may have characteristics different from the soils and slopes of the remaining undeveloped land. For HSPF, the urban land uses are not associated with a specific soil or HSG.

In addition, a special circumstance occurs in the Willamette SWAT model. In that model, new developed land primarily comes from dense forest cover. The model tends to predict greater evapotranspiration for urban grass than for intact evergreen forest, which appears to offset increases in total flow volume due to increased impervious area.

The effects of land use change on simulated flow extremes can be more dramatic in basins where strong growth is expected, but also tend to be smaller than the range of simulated climate responses. For example, in the ACF basin, land use change alone can increase the simulated 100-yr flood peak by up to 27 percent, but the range of responses to the six NARCCAP climate scenarios is from 17 to 66 percent.

7.4. SENSITIVITY TO COMBINED CLIMATE CHANGE AND URBAN DEVELOPMENT SCENARIOS

Given the relatively small response to projected urban and residential development by 2050, results of the model scenarios that combine climate change and land use change are generally consistent with those for the climate scenarios. These results are given for the selected analysis stations in Table 37 through Table 44. Each table is followed by a scatterplot that presents the same information for the selected downstream station graphically. A map is then presented that shows change results for each HUC8 pour point in the study area (Figure 38 through Figure 58. Note the results shown are for the simulations combining climate change with urban development scenarios, with the exception of the Kenai River in the Cook Inlet basin. Development projections are not available for Kenai study area, but are anticipated to be small. Results for study sites comprised of a single watershed are shown for a downstream outlet. Results for study sites comprised of multiple adjacent basins are shown for a single representative basin, typically the largest.

Many study areas also show variability in response among subbasins within the larger watershed. One figure in each set shows the median values of selected endpoints for the six NARCCAP scenarios for the individual HUC-8 subbasins within each larger study site. It should be noted,

however, that use of the median values alone without taking into account the full range of simulated responses to all scenarios is potentially misleading. Median values are presented here only as an indicator of variability within and among study areas and should not alone be considered indicative of broad regional trends.

Figure 39 shows annual flow volume responses (median over all six NARCCAP scenarios) for each modeled HUC8. On this map, a neutral gray tone represents no change from current conditions (100 percent of current conditions). Reds indicate flow volumes less than current, with greater intensity reflecting lower flows; greens represent flow volumes greater than current, with greater intensity reflecting higher flows.
Results highlight a number of important regional trends simulated for the 2041-2070 time period under the A2 emissions scenario. Most notable is the reduction in flow volume in the central Rockies, accompanied by increases in flow in the northern plains. Only moderate changes are seen for the west coast and Mississippi Valley, while increases generally result for the east coast.

Several things stand out for model-simulated total flow volume changes in Figure 38. The first is that increases in flow volume for the Kenai River (Cook Inlet basin) are on average larger than for other basins. Perhaps more importantly, for a majority of the basins the different downscaled models do not provide a consistent sign for changes in flow for the 2041-2070 period, with some simulating increases and some decreases. The models are in complete agreement as to the sign of change only for Kenai River (increase). It is also worth noting that the WRFP downscaling of the CCSM GCM often seems to be an outlier relative to the other models.

Total average annual flow volume tells only part of the story; the timing and intensity of flows are also important. The detailed results contained in the appendices show seasonal shifts in flow timing in most of the study areas. At a national scale the number of days (since October 1, start of the water year) to the flow centroid – the point at which half the flow of an average year is achieved - is a useful summary measure of changes in seasonality. Figure 45 shows that the centroid of flow comes earlier in the year in model-simulated response to warmer temperatures for many of the snow-melt dominated basins, particularly Cook Inlet in Alaska and higher elevations in the Rockies, but also for many basins in the southeast. The latter result reflects changes in precipitation timing, with increased winter precipitation and decreased summer precipitation. Several of the western basins have later dates for the flow centroid due to a substantial increase in model-simulated spring or summer precipitation relative to winter snowpack that counteracts the effects of earlier snowmelt.

The geographic distribution of 100-year peak flows (Log-Pearson III) fit is displayed in Figure 43 and shows considerably more heterogeneity. Simulated peak flows increase in many basins, but show less of a clear pattern (Figure 42). Peak flows tend to decline in the area of the Southwest where total flows decline, while the greatest increases are seen in Alaska and the populated areas of the east and west coast.

Results also suggest a large (factor of 5) increase in low flows for the Kenai River (Figure 40). This reflects greater dry season melt rates of ice under a warmer climate in Alaska. The models also consistently show severe declines in low flows for the Rio Grande.

Table 37. Simulated total flow volume (climate and land use change scenarios; percent relative to current conditions) for selected downstream stations.

Station	Study Area	CRCM_ cgcm3	HRM3_ hadcm3	RCM3_ gfdl	GFDL_ slice	RCM3_ cgcm3	WRFP_ ccsm	Median
Minnesota R at outlet	Minnesota River	110%	113%	147%	86%	146%	162%	130%
Susquehanna R at outlet	Susquehanna River	109%	107%	106%	108%	111%	90%	108%
Salt River nr Roosevelt	Salt, Verde, and San Pedro	80%	80%	149%	75%	94%	73%	80%
Willamette R at outlet	Willamette River	116%	106%	104%	92%	114%	98%	105%
Apalachicola R at outlet	ACF	107%	122%	108%	89%	124%	73%	108%
Kenai R at Soldotna	Cook Inlet	ND	154%	ND	132%	ND	167%	154%
Maumee R at outlet	Lake Erie Drainages	117%	151%	120%	136%	123%	89%	122%
Suwanee R at outlet	Georgia-Florida Coastal	115%	154%	128%	93%	157%	75%	122%
Illinois R at Marseilles, IL	Illinois River	96%	126%	103%	104%	106%	79%	103%
Merrimack R at outlet	New England Coastal	108%	116%	111%	112%	106%	94%	110%
Sacramento R at outlet	Sacramento River	104%	89%	98%	98%	100%	99%	99%
Los Angeles R at outlet	Coastal Southern California	92%	140%	104%	103%	107%	85%	103%
Tongue R at outlet	Powder/Tongue Rivers	101%	85%	140%	70%	130%	240%	115%
Amite R at outlet	Lake Pontchartrain Drainages	96%	111%	116%	85%	107%	78%	102%
Rio Grande R below Albuquerque	Rio Grande	73%	69%	112%	66%	69%	84%	71%
S. Platte R at outlet	South Platte	91%	83%	103%	77%	100%	105%	95%
Neuse R at outlet	Neuse/Tar Rivers	104%	160%	138%	111%	127%	88%	119%
Trinity R at outlet	Trinity River	102%	150%	110%	66%	122%	138%	116%
Elkhorn R at outlet	Loup/Elkhorn Rivers	119%	125%	138%	67%	140%	145%	132%
Colorado R nr State Line	Upper Colorado	86%	95%	116%	89%	92%	91%	91%

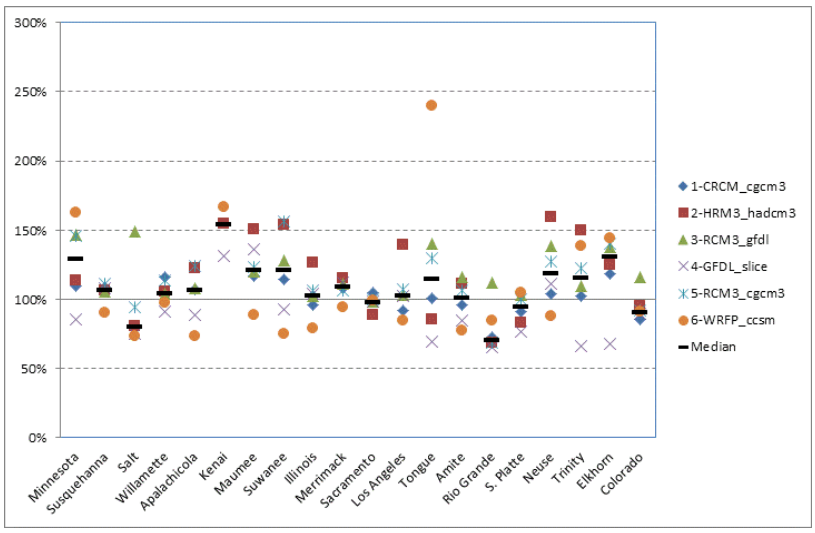

Figure 38. Simulated total future flow volume relative to current conditions (NARCCAP climate scenarios with urban development) for selected stations.

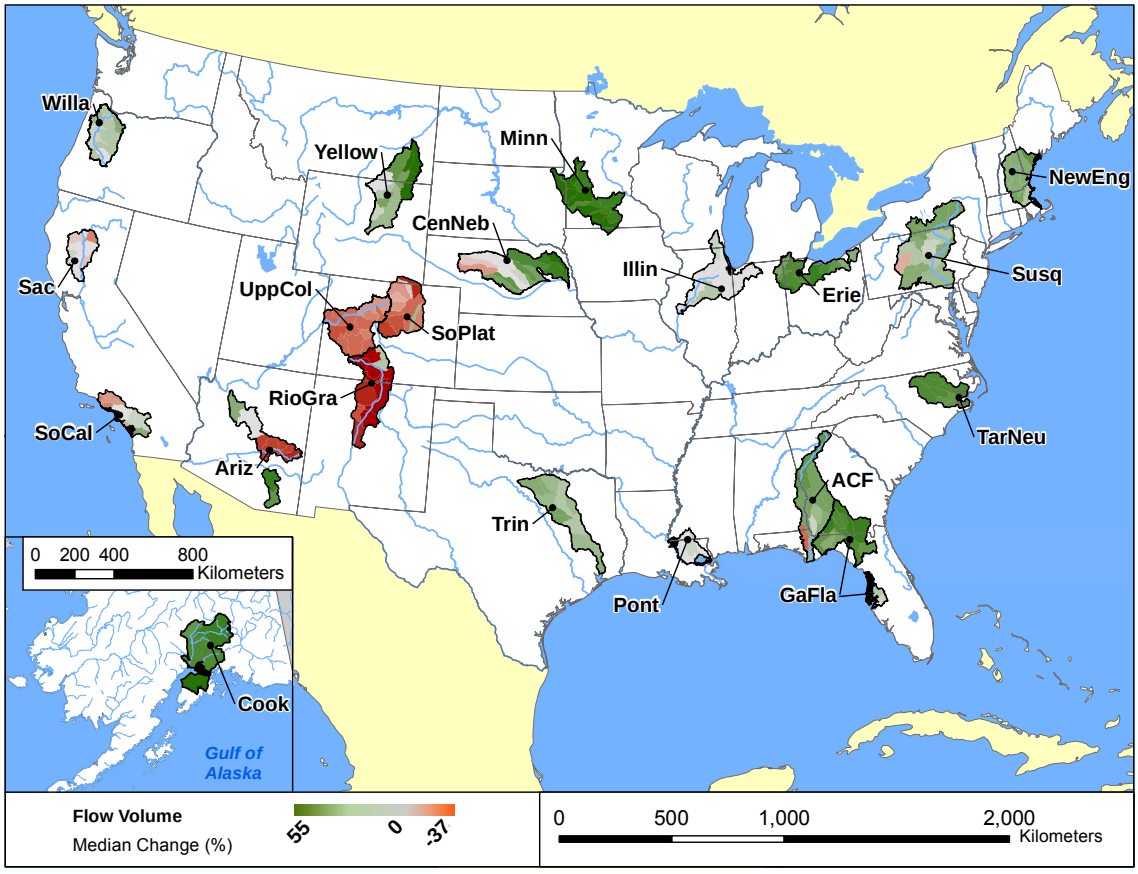

Figure 39. Median simulated percent changes in total future flow volume for 6 NARCCAP scenarios relative to current conditions by HUC8 (median of NARCCAP climate scenarios with urban development). Note: Cook Inlet results do not include land use change.

Table 38. Simulated 7-day low flow (climate and land use change scenarios; percent relative to current conditions) for selected downstream stations.

Station	Study Area	CRCM_ cgcm3	HRM3_ hadcm3	RCM3_ gfdl	GFDL_ slice	RCM3_ cgcm3	WRFP_ ccsm	Median
Minnesota R at outlet	Minnesota River	115%	137%	202%	82%	182%	228%	159%
Susquehanna R at outlet	Susquehanna River	92%	121%	105%	90%	108%	87%	98%
Salt River nr Roosevelt	Salt, Verde, and San Pedro	58%	77%	131%	87%	79%	90%	83%
Willamette R at outlet	Willamette River	131%	113%	108%	82%	127%	102%	111%
Apalachicola R at outlet	ACF	98%	120%	105%	86%	113%	64%	101%
Kenai R at Soldotna	Cook Inlet	ND	267%	ND	280%	ND	401%	280%
Maumee R at outlet	Lake Erie Drainages	105%	184%	127%	133%	129%	59%	128%
Suwanee R at outlet	Georgia-Florida Coastal	105%	141%	121%	95%	136%	78%	113%
Illinois R at Marseilles, IL	Illinois River	88%	126%	100%	94%	103%	73%	97%
Merrimack R at outlet	New England Coastal	112%	141%	131%	119%	125%	121%	123%
Sacramento R at outlet	Sacramento River	101%	91%	95%	96%	99%	93%	95%
Los Angeles R at outlet	Coastal Southern California	98%	115%	99%	100%	101%	93%	99%
Tongue R at outlet	Powder/Tongue Rivers	102%	92%	145%	67%	127%	235%	115%
Amite R at outlet	Lake Pontchartrain Drainages	76%	108%	91%	77%	92%	64%	84%
Rio Grande R below Albuquerque	Rio Grande	81%	64%	120%	62%	74%	86%	77%
S. Platte R at outlet	South Platte	105%	100%	107%	100%	104%	105%	104%
Neuse R at outlet	Neuse/Tar Rivers	100%	175%	139%	118%	129%	74%	123%
Trinity R at outlet	Trinity River	33%	199%	87%	36%	93%	102%	90%
Elkhorn R at outlet	Loup/Elkhorn Rivers	118%	134%	154%	46%	148%	156%	141%
Colorado R nr State Line	Upper Colorado	85%	94%	122%	86%	92%	91%	91%

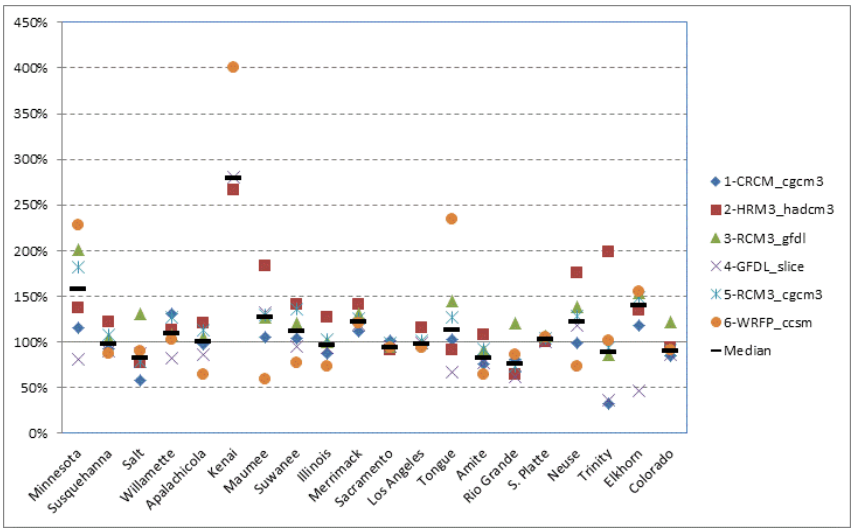

Figure 40. Simulated 7-day low flow relative to current conditions (NARCCAP climate scenarios with urban development) for selected downstream stations

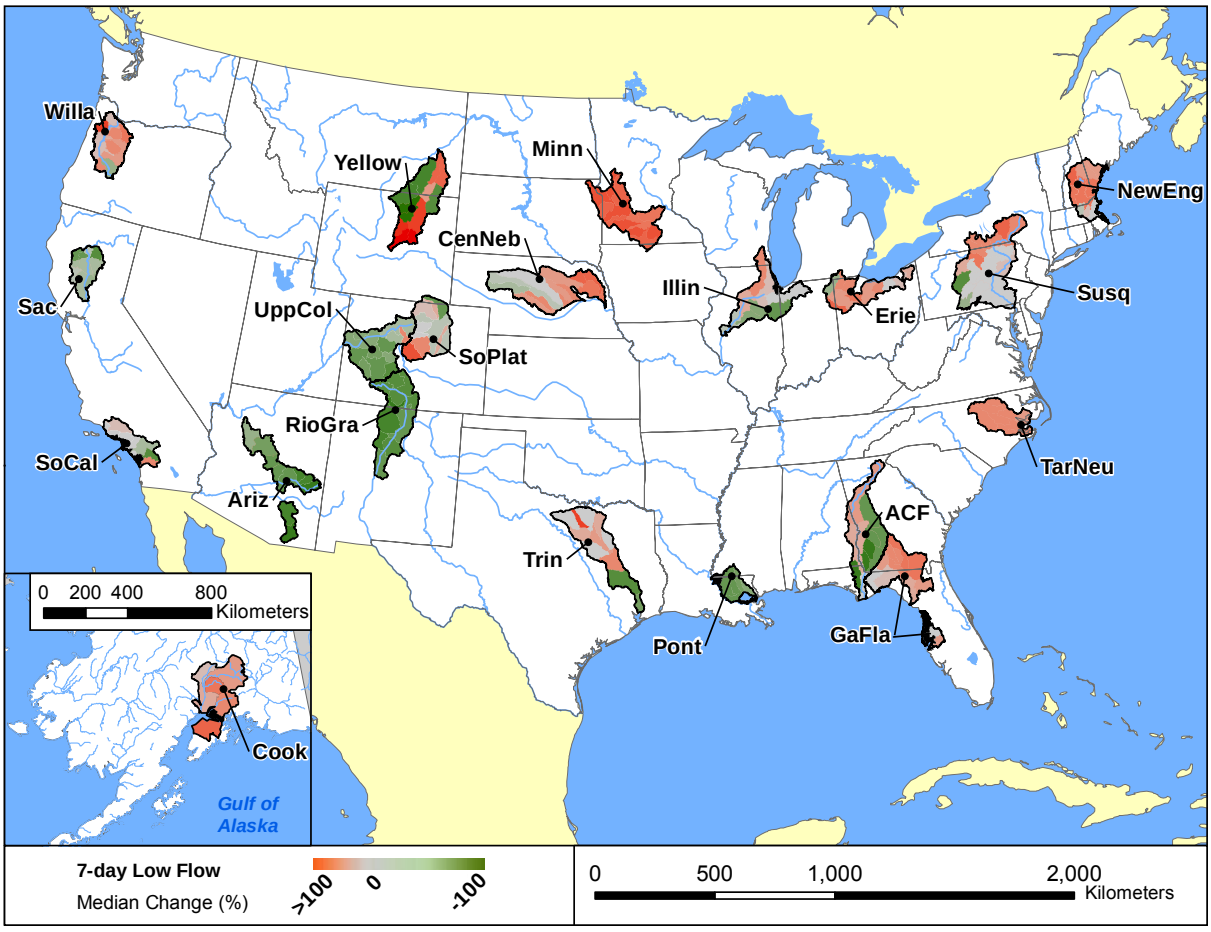

Figure 41. Median simulated percent changes in 7-day average low flow volume for 6 NARCCAP scenarios relative to current conditions by HUC8 (median of NARCCAP climate scenarios with urban development). Note: Cook Inlet results do not include land use change.

Table 39. Simulated 100-year peak flow (log-Pearson III; climate and land use change scenarios; percent relative to current conditions) for selected downstream stations.

Station	Study Area	CRCM_ cgcm3	HRM3_ hadcm3	RCM3_ gfdl	GFDL_ slice	RCM3_ cgcm3	WRFP_ ccsm	Median
Minnesota R at outlet	Minnesota River	84%	83%	96%	87%	89%	96%	88%
Susquehanna R at outlet	Susquehanna River	108%	130%	107%	129%	173%	101%	118%
Salt River nr Roosevelt	Salt, Verde, and San Pedro	119%	101%	104%	68%	121%	66%	102%
Willamette R at outlet	Willamette River	116%	131%	114%	79%	116%	95%	115%
Apalachicola R at outlet	ACF	117%	145%	110%	90%	128%	94%	114%
Kenai R at Soldotna	Cook Inlet	ND	132%	ND	125%	ND	132%	132%
Maumee R at outlet	Lake Erie Drainages	96%	107%	88%	94%	94%	93%	94%
Suwanee R at outlet	Georgia-Florida Coastal	131%	145%	130%	95%	158%	107%	130%
Illinois R at Marseilles, IL	Illinois River	121%	155%	109%	103%	129%	98%	115%
Merrimack R at outlet	New England Coastal	116%	134%	113%	141%	90%	82%	115%
Sacramento R at outlet	Sacramento River	105%	98%	122%	117%	102%	131%	111%
Los Angeles R at outlet	Coastal Southern California	100%	112%	194%	124%	158%	93%	118%
Tongue R at outlet	Powder/Tongue Rivers	117.97%	113.38%	133.43%	82.40%	121.00%	146.02%	119.49%
Amite R at outlet	Lake Pontchartrain Drainages	107%	152%	110%	100%	107%	66%	107%
Rio Grande R below Albuquerque	Rio Grande	89.81%	77.17%	108.07%	65.91%	72.01%	92.40%	83.49%
S. Platte R at outlet	South Platte	118%	90%	97%	85%	153%	138%	108%
Neuse R at outlet	Neuse/Tar Rivers	71%	294%	163%	113%	227%	64%	138%
Trinity R at outlet	Trinity River	97%	107%	108%	60%	87%	107%	102%
Elkhorn R at outlet	Loup/Elkhorn Rivers	121%	110%	111%	83%	142%	110%	110%
Colorado R nr State Line	Upper Colorado	78%	83%	97%	91%	93%	84%	87%

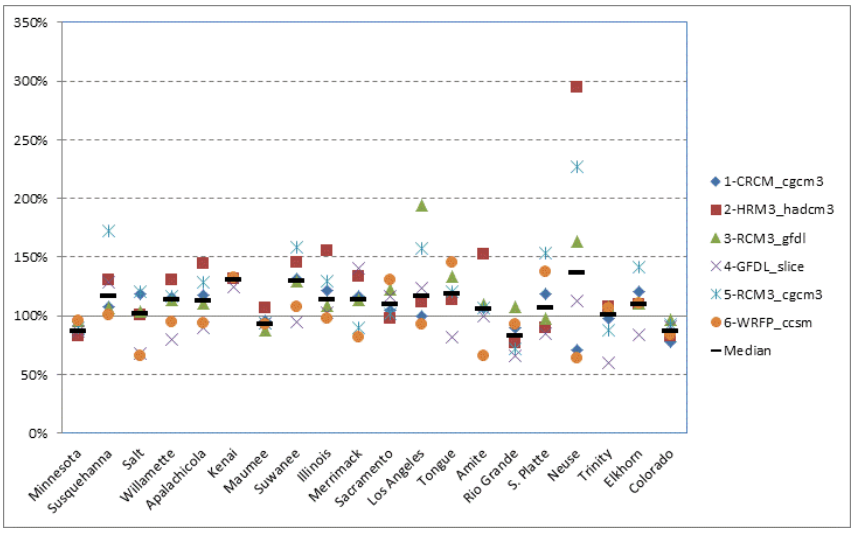

Figure 42. Simulated 100-yr peak flow relative to current conditions (NARCCAP climate scenarios with urban development) for selected downstream stations

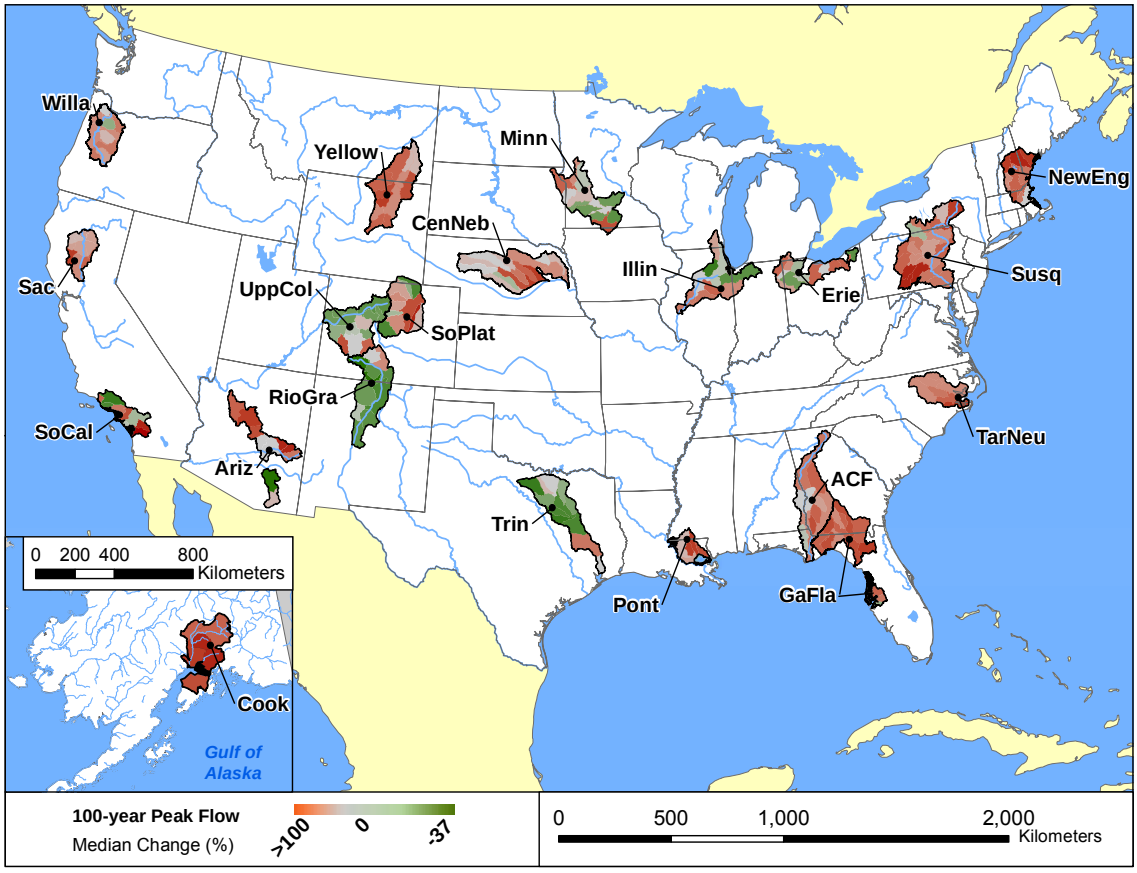

Figure 43. Median simulated percent changes in 100-year peak flow for 6 NARCCAP scenarios relative to current conditions by HUC8 (median of NARCCAP climate scenarios with urban development). Note: Cook Inlet results do not include land use change.

Table 40. Simulated change in the number of days to flow centroid (climate and land use change scenarios; relative to current conditions) for selected downstream stations.

Station	Study Area	CRCM_ cgcm3	HRM3_ hadcm3	RCM3_ gfdl	GFDL_ slice	RCM3_ cgcm3	WRFP_ ccsm	Median
Minnesota R at outlet	Minnesota River	-13	-19	-6	-15	-3	2	-9
Susquehanna R at outlet	Susquehanna River	-18	16	-6	-12	-5	0	-6
Salt River nr Roosevelt	Salt, Verde, and San Pedro	-18	41	28	17	-5	54	22
Willamette R at outlet	Willamette River	3	-8	-1	3	1	8	2
Apalachicola R at outlet	ACF	-2	-2	1	8	-6	1	-1
Kenai R at Soldotna	Cook Inlet	ND	-3	ND	-5	ND	-1	-3
Maumee R at outlet	Lake Erie Drainages	-2	-4	1	0	10	-8	-1
Suwanee R at outlet	Georgia-Florida Coastal	-3	17	25	-8	-5	11	4
Illinois R at Marseilles, IL	Illinois River	-11	6	-2	-12	-1	-14	-6
Merrimack R at outlet	New England Coastal	-17	-14	-19	-13	-9	-18	-16
Sacramento R at outlet	Sacramento River	-4	-7	-4	-1	-3	-8	-4
Los Angeles R at outlet	Coastal Southern California	6	48	-3	10	-3	0	3
Tongue R at outlet	Powder/Tongue Rivers	-6	-3	1	-16	-4	7	-3
Amite R at outlet	Lake Pontchartrain Drainages	-14	13	-23	-7	-5	-11	-9
Rio Grande R below Albuquerque	Rio Grande	25	6	3	11	14	17	13
S. Platte R at outlet	South Platte	-10	-14	3	-15	-6	-13	-12
Neuse R at outlet	Neuse/Tar Rivers	-13	23	31	-11	11	-5	3
Trinity R at outlet	Trinity River	17	23	31	4	7	25	20
Elkhorn R at outlet	Loup/Elkhorn Rivers	-11	6	3	-23	-5	-7	-6
Colorado R nr State Line	Upper Colorado	-11	-14	-7	-10	-8	-11	-10

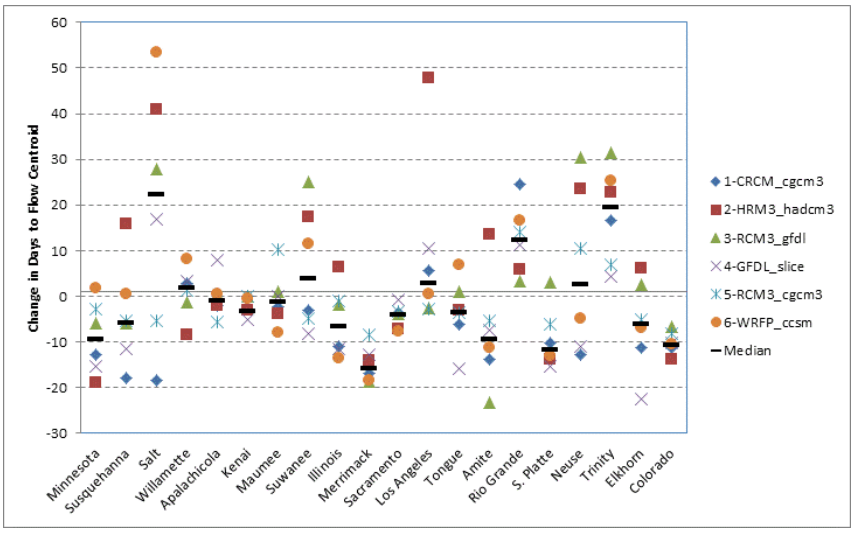

Figure 44. Simulated change in days to flow centroid relative to current conditions (NARCCAP climate scenarios with urban development) for selected downstream stations

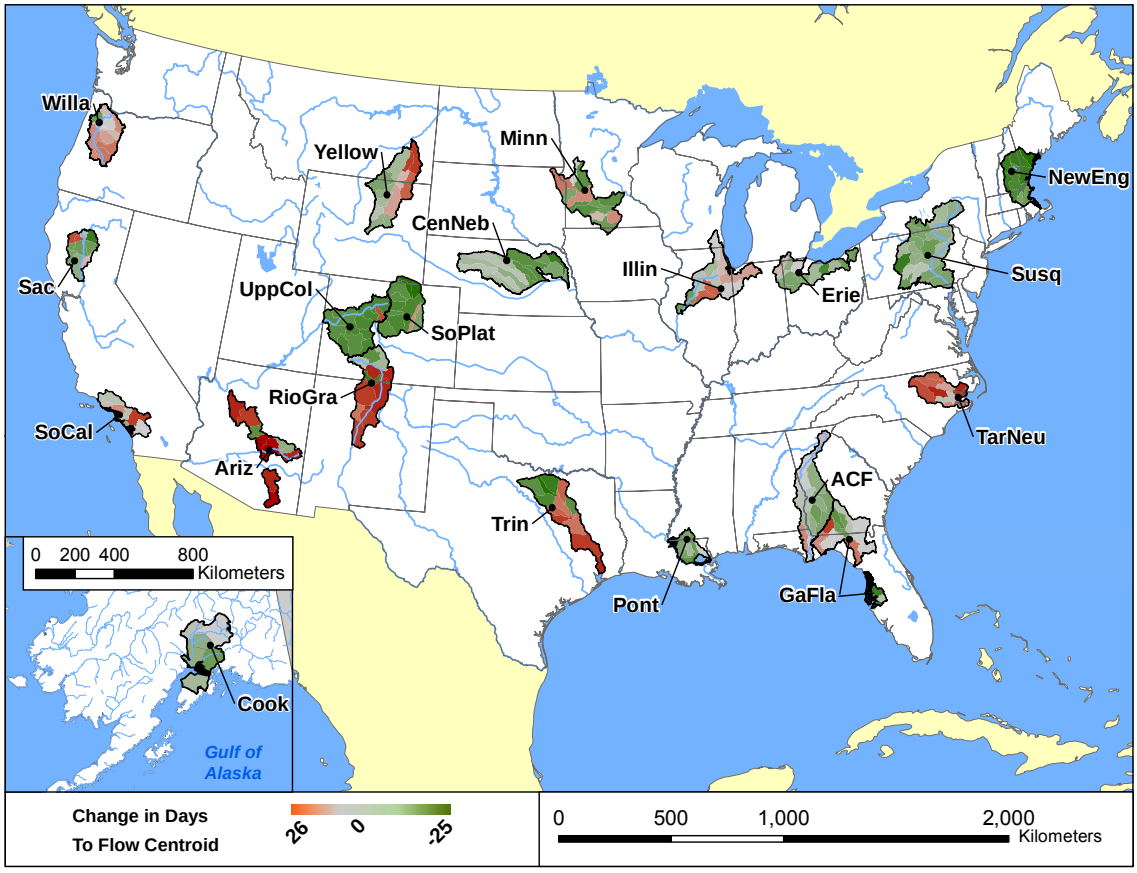

Figure 45. Median simulated change in the number of days to flow centroid for 6 NARCCAP scenarios relative to current conditions by HUC8 (median of NARCCAP climate scenarios with urban development). Note: Cook Inlet results do not include land use change.

Table 41. Simulated Richards-Baker flashiness index (climate and land use change scenarios; percent relative to current conditions) for selected downstream stations.

Station	Study Area	CRCM_ cgcm3	HRM3_ hadcm3	RCM3_ gfdl	GFDL_ slice	RCM3_ cgcm3	WRFP_ ccsm	Median
Minnesota R at outlet	Minnesota River	105%	112%	108%	101%	109%	108%	108%
Susquehanna R at outlet	Susquehanna River	107%	111%	107%	110%	112%	103%	109%
Salt River nr Roosevelt	Salt, Verde, and San Pedro	81%	103%	121%	98%	103%	119%	103%
Willamette R at outlet	Willamette River	102%	105%	100%	98%	101%	102%	102%
Apalachicola R at outlet	ACF	106%	125%	109%	94%	126%	90%	107%
Kenai R at Soldotna	Cook Inlet	ND	94%	ND	102%	ND	96%	96%
Maumee R at outlet	Lake Erie Drainages	100%	102%	100%	101%	100%	97%	100%
Suwanee R at outlet	Georgia-Florida Coastal	93%	62%	76%	116%	59%	185%	84%
Illinois R at Marseilles, IL	Illinois River	105%	103%	102%	106%	105%	103%	104%
Merrimack R at outlet	New England Coastal	102%	104%	100%	102%	99%	94%	101%
Sacramento R at outlet	Sacramento River	124%	103%	113%	109%	117%	124%	115%
Los Angeles R at outlet	Coastal Southern California	104%	125%	103%	105%	108%	104%	105%
Tongue R at outlet	Powder/Tongue Rivers	102%	108%	104%	100%	103%	109%	104%
Amite R at outlet	Lake Pontchartrain Drainages	105%	105%	106%	104%	104%	102%	104%
Rio Grande R below Albuquerque	Rio Grande	109%	117%	95%	120%	103%	106%	108%
S. Platte R at outlet	South Platte	96%	92%	103%	87%	101%	99%	97%
Neuse R at outlet	Neuse/Tar Rivers	95%	112%	114%	97%	102%	90%	100%
Trinity R at outlet	Trinity River	71%	69%	72%	73%	70%	68%	70%
Elkhorn R at outlet	Loup/Elkhorn Rivers	98%	99%	95%	95%	98%	95%	96%
Colorado R nr State Line	Upper Colorado	101%	107%	111%	105%	103%	101%	104%

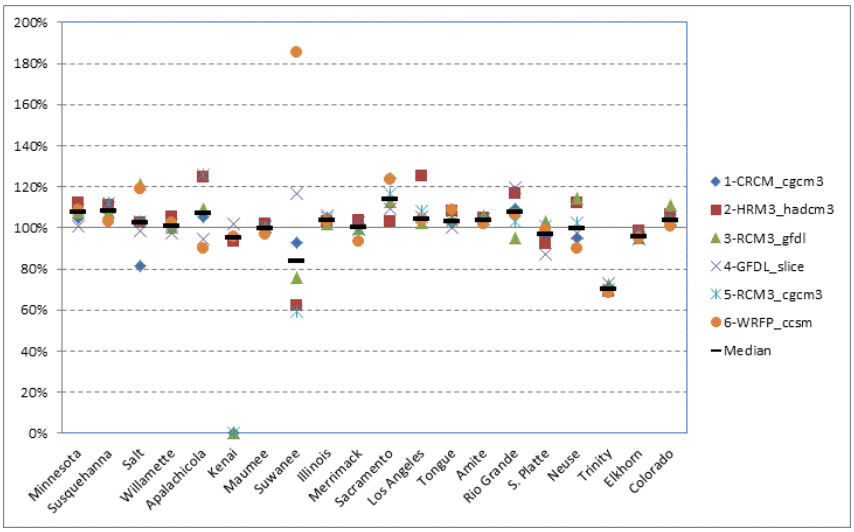

Figure 46. Simulated Richards-Baker flashiness index relative to current conditions (NARCCAP climate scenarios with urban development) for selected downstream stations

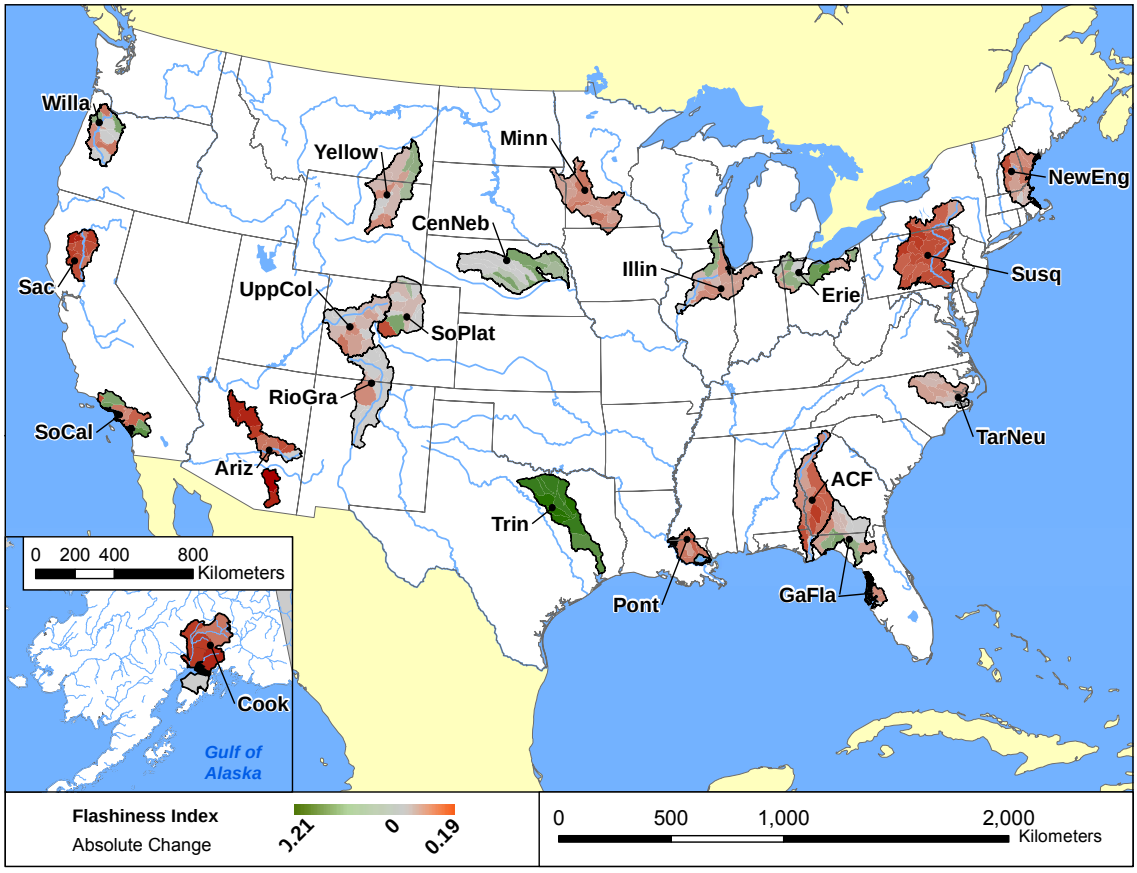

Figure 47. Simulated absolute changes in the Richards-Baker flashiness index for 6 NARCCAP scenarios relative to current conditions by HUC8 (median of NARCCAP climate scenarios with urban development). Note: Cook Inlet results do not include land use change.

Table 42. Simulated total suspended solids load (climate and land use change scenarios; percent relative to current conditions) for selected downstream stations.

Station	Study Area	CRCM_ cgcm3	HRM3_ hadcm3	RCM3_ gfdl	GFDL_ slice	RCM3_ cgcm3	WRFP_ ccsm	Median
Minnesota R at outlet	Minnesota River	104%	117%	183%	76%	192%	219%	150%
Susquehanna R at outlet	Susquehanna River	118%	108%	109%	116%	118%	85%	112%
Salt River nr Roosevelt	Salt, Verde, and San Pedro	89%	79%	184%	66%	106%	74%	84%
Willamette R at outlet	Willamette River	124%	111%	108%	89%	121%	97%	110%
Apalachicola R at outlet	ACF	126%	147%	128%	93%	145%	53%	127%
Kenai R at Soldotna	Cook Inlet	ND	234%	ND	196%	ND	244%	234%
Maumee R at outlet	Lake Erie Drainages	123%	170%	127%	154%	130%	87%	128%
Suwanee R at outlet	Georgia-Florida Coastal	121%	177%	139%	90%	182%	74%	130%
Illinois R at Marseilles, IL	Illinois River	117%	142%	115%	128%	121%	91%	119%
Merrimack R at outlet	New England Coastal	119%	129%	119%	123%	112%	86%	119%
Sacramento R at outlet	Sacramento River	138%	94%	121%	118%	99%	108%	113%
Los Angeles R at outlet	Coastal Southern California	75%	121%	86%	85%	90%	69%	86%
Tongue R at outlet	Powder/Tongue Rivers	108%	84%	169%	66%	153%	351%	131%
Amite R at outlet	Lake Pontchartrain Drainages	99%	113%	125%	82%	110%	70%	104%
Rio Grande R below Albuquerque	Rio Grande	61%	54%	115%	50%	60%	72%	60%
S. Platte R at outlet	South Platte	73%	74%	83%	60%	82%	87%	78%
Neuse R at outlet	Neuse/Tar Rivers	108%	201%	164%	117%	145%	84%	131%
Trinity R at outlet	Trinity River	64%	126%	64%	28%	85%	115%	74%
Elkhorn R at outlet	Loup/Elkhorn Rivers	125%	129%	147%	59%	167%	163%	138%
Colorado R nr State Line	Upper Colorado	80%	90%	124%	82%	89%	85%	87%

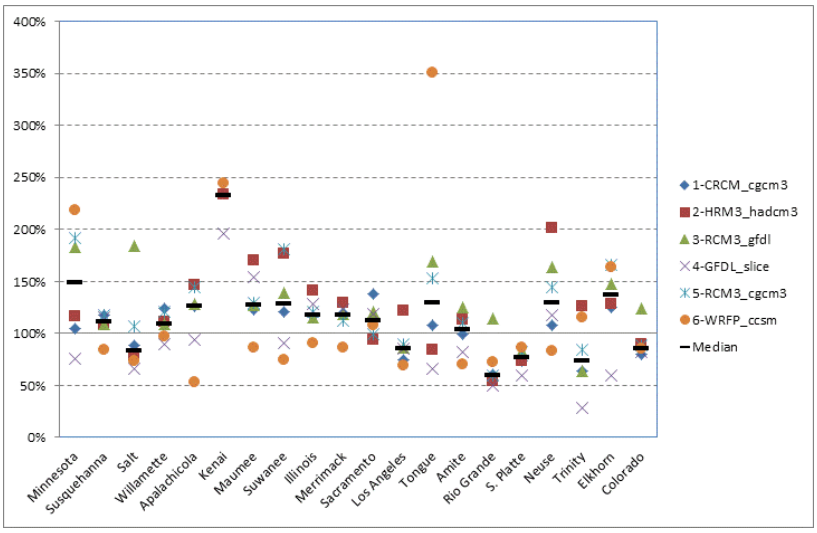

Figure 48. Simulated total suspended solids load relative to current conditions (NARCCAP climate scenarios with urban development) for selected downstream stations.

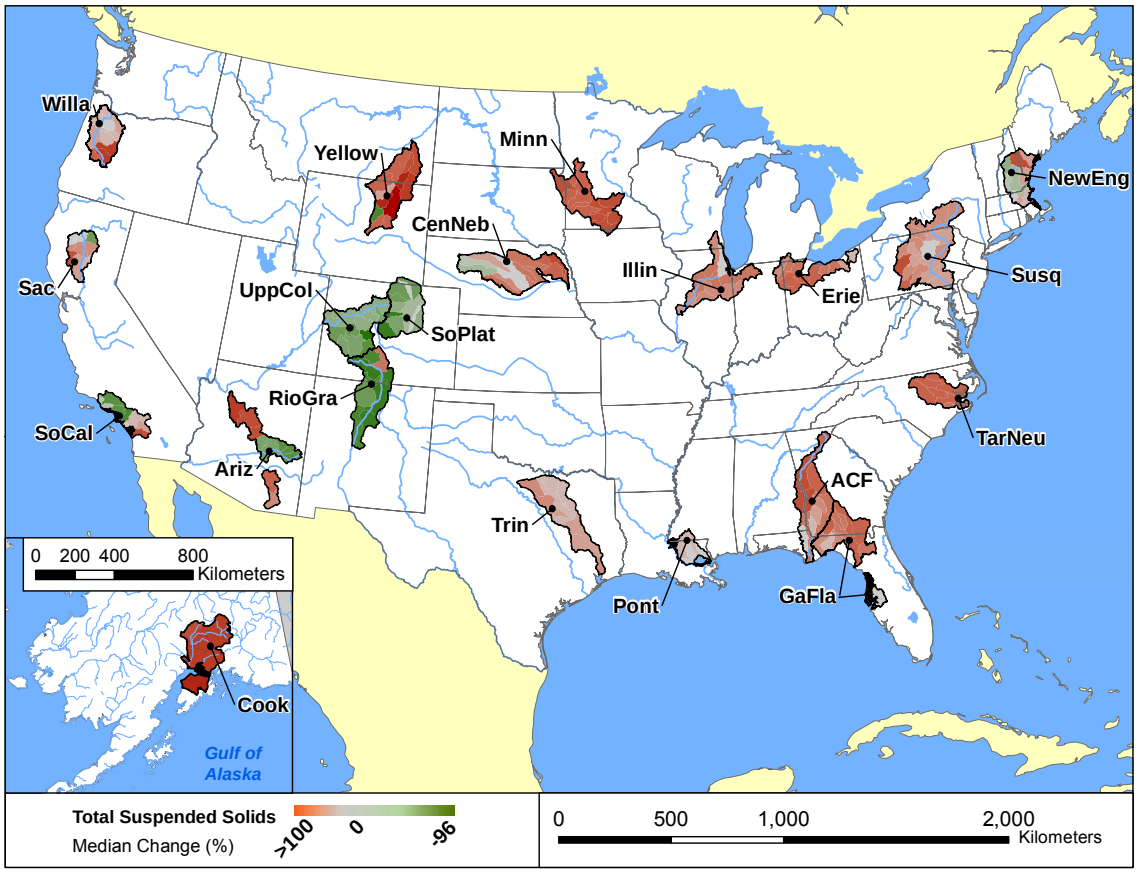

Figure 49. Median simulated percent changes in total suspended solids loads for 6 NARCCAP scenarios relative to current conditions by HUC8 (median of NARCCAP climate scenarios with urban development) for selected downstream stations. Note: Cook Inlet results do not include land use change.

Table 43. Simulated total phosphorus load (climate and land use change scenarios; percent relative to current conditions) for selected downstream stations.

Station	Study Area	CRCM_ cgcm3	HRM3_ hadcm3	RCM3_ gfdl	GFDL_ slice	RCM3_ cgcm3	WRFP_ ccsm	Median
Minnesota R at outlet	Minnesota River	97%	115%	151%	97%	138%	160%	126%
Susquehanna R at outlet	Susquehanna River	128%	106%	110%	127%	114%	108%	112%
Salt River nr Roosevelt	Salt, Verde, and San Pedro	82%	84%	156%	70%	107%	88%	86%
Willamette R at outlet	Willamette River	100%	98%	97%	94%	100%	96%	97%
Apalachicola R at outlet	ACF	139%	153%	136%	119%	150%	107%	138%
Kenai R at Soldotna	Cook Inlet	ND	89%	ND	90%	ND	113%	90%
Maumee R at outlet	Lake Erie Drainages	121%	155%	136%	151%	120%	89%	128%
Suwanee R at outlet	Georgia-Florida Coastal	125%	190%	149%	96%	189%	82%	137%
Illinois R at Marseilles, IL	Illinois River	107%	112%	107%	113%	108%	99%	107%
Merrimack R at outlet	New England Coastal	116%	125%	116%	120%	111%	97%	116%
Sacramento R at outlet	Sacramento River	102%	88%	106%	117%	97%	110%	104%
Los Angeles R at outlet	Coastal Southern California	78%	128%	102%	83%	89%	71%	86%
Tongue R at outlet	Powder/Tongue Rivers	107%	86%	163%	67%	148%	324%	127%
Amite R at outlet	Lake Pontchartrain Drainages	123%	144%	147%	103%	125%	89%	124%
Rio Grande R below Albuquerque	Rio Grande	51%	40%	125%	49%	37%	64%	50%
S. Platte R at outlet	South Platte	93%	90%	106%	85%	99%	102%	96%
Neuse R at outlet	Neuse/Tar Rivers	123%	259%	184%	134%	183%	103%	158%
Trinity R at outlet	Trinity River	148%	188%	153%	98%	155%	187%	154%
Elkhorn R at outlet	Loup/Elkhorn Rivers	120%	123%	138%	66%	147%	148%	130%
Colorado R nr State Line	Upper Colorado	80%	88%	120%	82%	84%	84%	84%

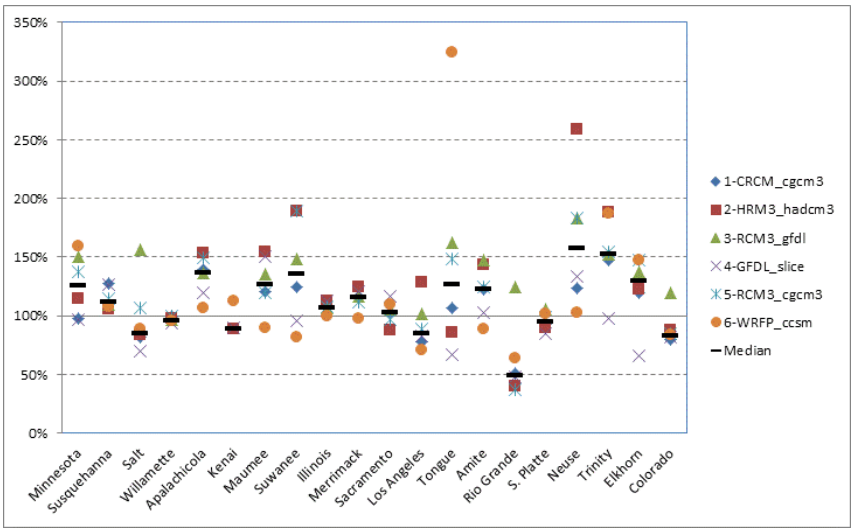

Figure 50. Simulated total phosphorus load relative to current conditions (NARCCAP climate scenarios with urban development) for selected downstream stations.

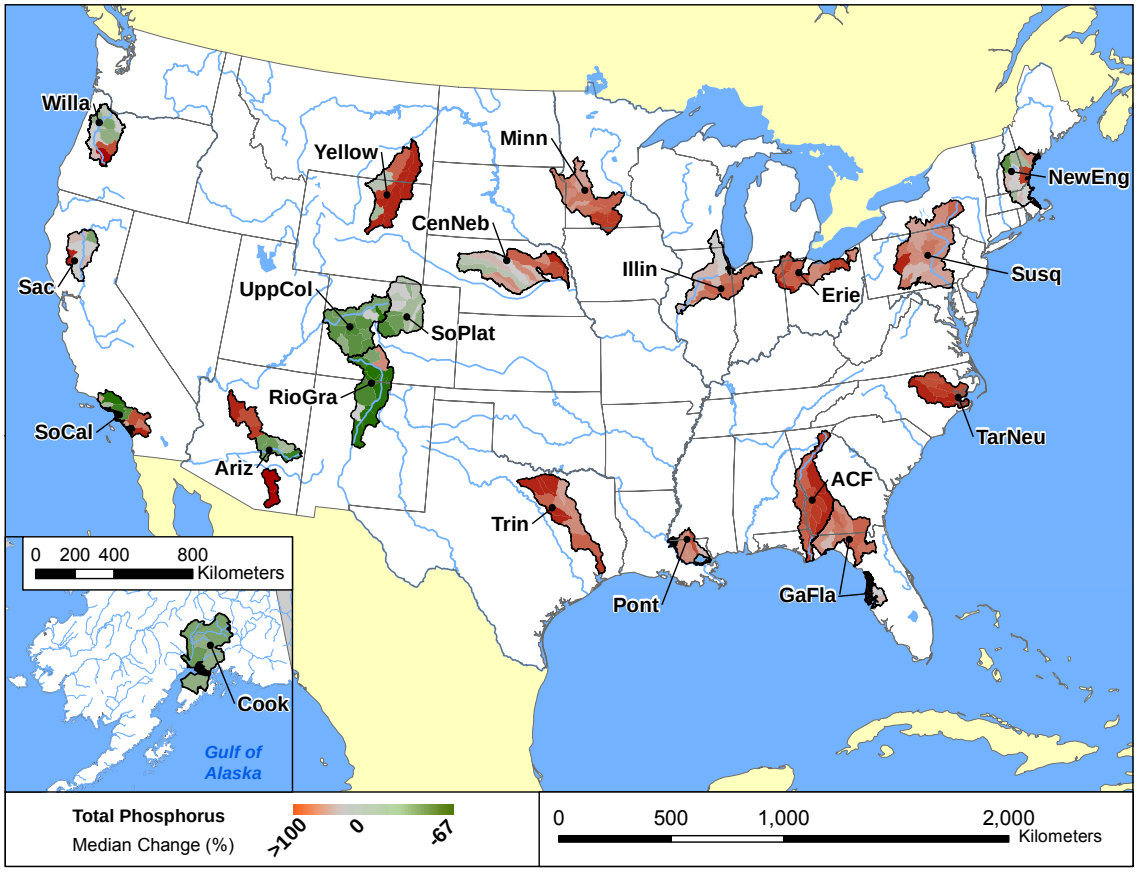

Figure 51. Median simulated percent changes in total phosphorus loads for 6 NARCCAP scenarios relative to current conditions by HUC8 (median of NARCCAP climate scenarios with urban development). Note: Cook Inlet results do not include land use change.

Table 44. Simulated total nitrogen load (climate and land use change scenarios; percent relative to current conditions) for selected downstream stations.

Station	Study Area	CRCM_ cgcm3	HRM3_ hadcm3	RCM3_ gfdl	GFDL_ slice	RCM3_ cgcm3	WRFP_ ccsm	Median
Minnesota R at outlet	Minnesota River	126%	130%	163%	104%	158%	170%	144%
Susquehanna R at outlet	Susquehanna River	161%	146%	146%	155%	149%	131%	147%
Salt River nr Roosevelt	Salt, Verde, and San Pedro	90%	91%	142%	87%	105%	85%	91%
Willamette R at outlet	Willamette River	106%	98%	97%	91%	105%	95%	97%
Apalachicola R at outlet	ACF	117%	126%	116%	107%	123%	96%	117%
Kenai R at Soldotna	Cook Inlet	ND	200%	ND	175%	ND	223%	200%
Maumee R at outlet	Lake Erie Drainages	127%	158%	161%	190%	125%	94%	142%
Suwanee R at outlet	Georgia-Florida Coastal	129%	167%	139%	113%	171%	86%	134%
Illinois R at Marseilles, IL	Illinois River	103%	117%	105%	109%	107%	93%	106%
Merrimack R at outlet	New England Coastal	123%	131%	121%	124%	116%	103%	122%
Sacramento R at outlet	Sacramento River	104%	94%	105%	113%	103%	111%	104%
Los Angeles R at outlet	Coastal Southern California	125%	159%	154%	102%	96%	101%	113%
Tongue R at outlet	Powder/Tongue Rivers	109%	91%	165%	71%	148%	320%	128%
Amite R at outlet	Lake Pontchartrain Drainages	130%	152%	153%	113%	127%	95%	128%
Rio Grande R below Albuquerque	Rio Grande	50%	38%	127%	48%	37%	65%	49%
S. Platte R at outlet	South Platte	89%	86%	106%	80%	97%	101%	93%
Neuse R at outlet	Neuse/Tar Rivers	120%	207%	166%	125%	155%	105%	140%
Trinity R at outlet	Trinity River	140%	187%	142%	93%	153%	186%	148%
Elkhorn R at outlet	Loup/Elkhorn Rivers	90%	94%	148%	92%	103%	104%	99%
Colorado R nr State Line	Upper Colorado	73%	82%	111%	76%	80%	79%	80%

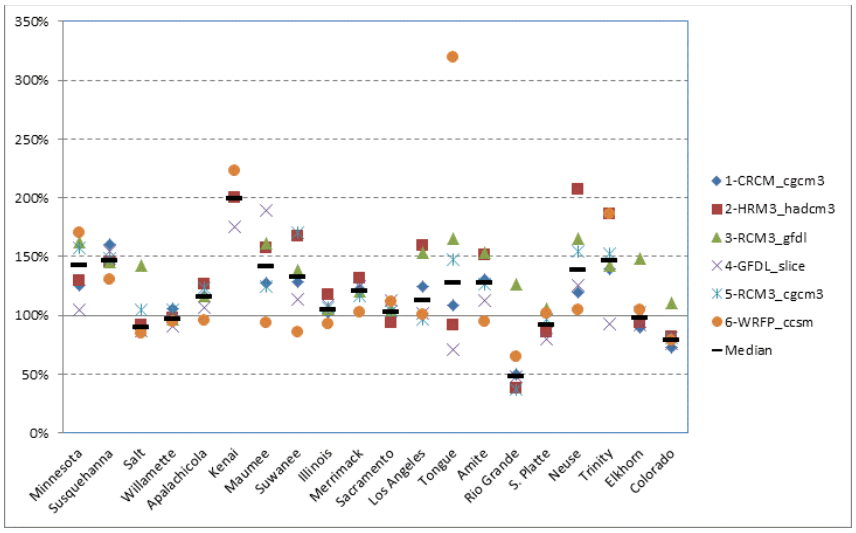

Figure 52. Simulated total nitrogen load relative to current conditions (NARCCAP climate scenarios with urban development) for selected downstream stations.

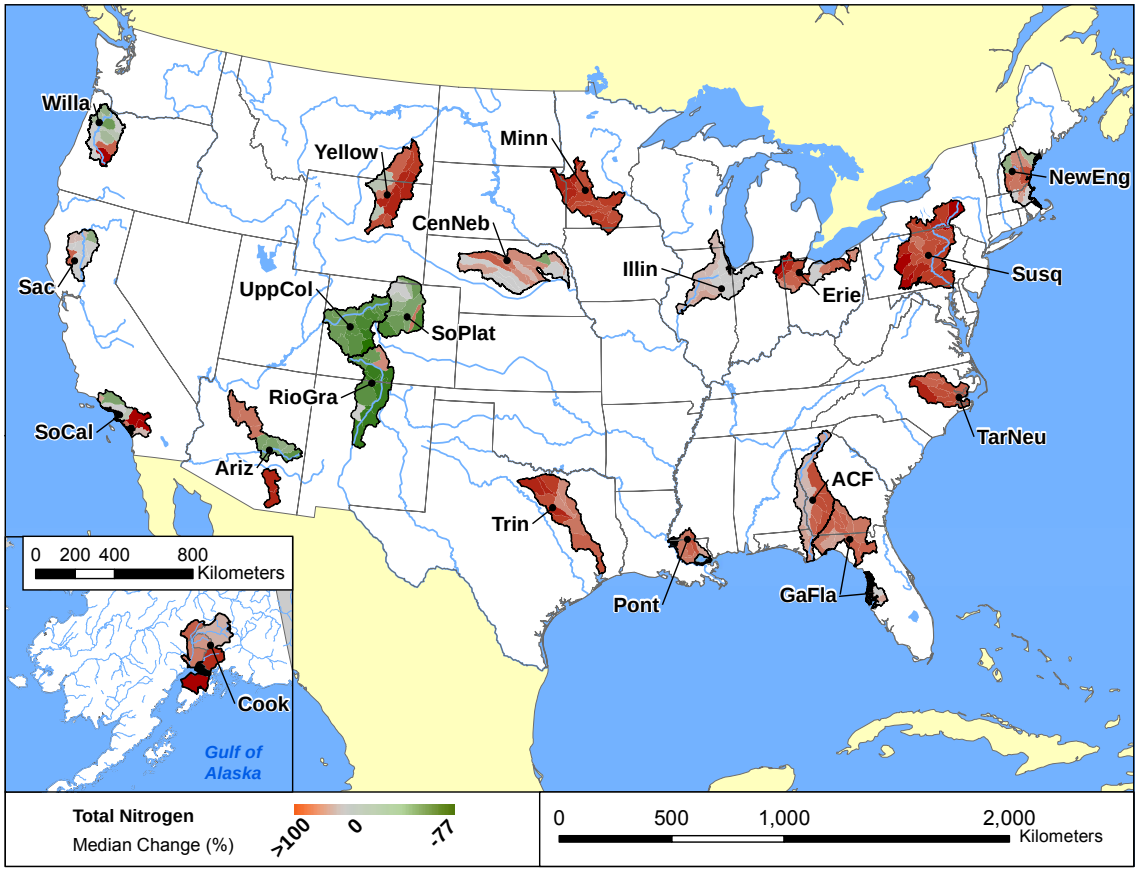

Figure 53. Median simulated percent changes in total nitrogen loads for 6 NARCCAP scenarios relative to current conditions by HUC8 (median of NARCCAP climate scenarios with urban development). Note: Cook Inlet results do not include land use change.

There are regional differences in the degree of agreement among simulated watershed responses to climate scenarios. Table 45 shows the coefficient of variation (CV; standard deviation divided by the mean) for SWAT simulated percentage changes in flow statistics at the downstream location of each study site for the six NARCCAP scenarios (calculated without land use change to isolate the impacts of climate). The CV for total flow is elevated at some stations, such as Salt River and Tongue River, indicating poor model agreement on the magnitude of change. Note that CVs on total flow are artificially reduced at some stations (e.g., Colorado River, Sacramento River) due to the presence of constant upstream boundary conditions (representing interbasin transfers for the Colorado and releases from an upstream dam on the Sacramento River). The largest divergences among simulated high flows are seen at different stations than the largest divergences among total flow volume estimates.

CVs were also calculated reflecting the variability in response across the selected downstream stations for all study areas for each NARCCAP climate change scenario. Table 46 shows these values along with the average absolute difference from the median of all scenarios for each NARCCAP scenario. For total flow volume, the CCSM downscaled with WRFP has both the greatest station to station variability (highest CV) and largest average absolute difference from the median of all six simulations.

Table 45. Coefficient of Variation of SWAT-simulated changes in streamflow for each study area in response to the six NARCCAP climate change scenarios for selected downstream stations.

Station	Total Flow	100-yr peak	7-day low flow
Minnesota R at outlet	0.066	0.004	0.198
Susquehanna R at outlet	0.005	0.057	0.017
Salt River nr Roosevelt	0.091	0.060	0.067
Willamette R at outlet	0.008	0.030	0.028
Apalachicola R at outlet	0.038	0.037	0.043
Kenai R at Soldotna	0.021	0.001	0.172
Maumee R at outlet	0.035	0.004	0.137
Suwanee R at outlet	0.089	0.043	0.053
Illinois R at Marseilles, IL	0.023	0.039	0.033
Merrimack R at outlet	0.005	0.046	0.009
Sacramento R at outlet	0.003	0.016	0.001
Los Angeles R at outlet	0.032	0.100	0.005
Tongue R at outlet	0.293	0.039	0.273
Amite R at outlet	0.023	0.070	0.029
Rio Grande R below Albuquerque	0.039	0.028	0.056
S. Platte R at outlet	0.014	0.078	0.001
Neuse R at outlet	0.055	0.534	0.101

Trinity R at outlet	0.079	0.036	0.378
Elkhorn R at outlet	0.067	0.031	0.137
Colorado R nr State Line	0.013	0.006	0.020

Table 46. Coefficient of variation of SWAT-simulated changes in streamflow for each NARCCAP climate scenario for selected downstream stations.

	Total Flow		100-yr peak flow		7-day low flow	
RCM/GCM	CV	Average absolute difference from median	CV	Average absolute difference from median	CV	Average absolute difference from median
CRCM_cgcm3	0.016	14.83%	0.028	15.27%	0.058	27.98%
HRM3_hadcm3	0.066	15.24%	0.177	20.76%	0.159	23.19%
RCM3_gfdl	0.024	19.95%	0.035	17.43%	0.073	27.42%
GFDL_slice	0.046	18.05%	0.046	19.28%	0.260	19.39%
RCM3_cgcm3	0.038	15.52%	0.109	26.25%	0.068	21.18%
WRFP_ccsm	0.169	24.33%	0.058	19.65%	0.575	31.07%

Simulated changes in pollutant loads are shown in Figure 48 through Figure 53. In general, these follow a pattern similar to the changes in total flow volume. TSS loads (Figure 49) increase in most basins, except for declines in the Rocky Mountain and Southwest study areas where overall flows decrease. The large increases in solids loads for some basins (especially sand bed rivers in the west) are mostly driven by channel scour. These results should be considered highly uncertain given the simplified approach to channel scour included in SWAT2005 and the differences among individual models in calibration to channel scour. The regional pattern for total P loads is similar, as much of the total P load is driven by erosion (Figure 51), with the notable exception of the Cook Inlet basin in Alaska. The regional pattern for total N loads is also generally similar, with some additional variability associated with the interactions of plant growth and erosion (Figure 53).

7.5. SENSITIVITY OF STUDY AREA WATER BALANCE INDICATORS

Several additional water balance indicators are most relevant at the scale of a whole study area. These water balance metrics are described in Section 4.3. This section focuses on potential changes to these metrics in response to future climate.

Table 47 provides a summary of water balance indicators for each study area. Figure 54 through Figure 58 show the median values for changes in water balance metrics for simulations using the 6 NARCCAP climate change scenarios at each study location. As stated previously, use of the median values alone without taking into account the full range of simulated responses to all scenarios is potentially misleading. Median values are presented here only as an indicator of variability within and among study areas and should not alone be considered indicative of broad regional trends. More complete results including analysis at additional stations are given in Appendix X and Appendix Y.

Table 47. Simulated percent changes in water balance statistics for study areas (NARCCAP climate with land use change scenarios; median percent change relative to current conditions).

Study Area	Dryness Ratio	Low Flow Sensitivity (cfs/mi^2)	Surface Fraction	Snow Fraction	Deep Recharge
ACF	0%	-16%	22%	-57%	-14%
TarNeu	-8%	15%	5%	-49%	15%
Ariz-Salt	1%	-10%	-5%	-46%	-15%
Ariz-San Pedro	-1%	-7%	23%	-52%	-12%
Ariz-Verde	-2%	-3%	7%	-50%	4%
CenNeb-Elkhorn	-5%	28%	49%	-24%	24%
CenNeb-Loup	0%	3%	16%	-24%	1%
Cook	-8%	22%	4%	-12%	-43%
Erie	-10%	47%	-8%	-32%	39%
GaFl-North	-6%	8%	11%	-72%	7%
GaFl-Tampa	-1%	-7%	15%	-39%	-6%
Illin	-3%	22%	-4%	-32%	20%
Minn	-10%	59%	-14%	-22%	47%
NewEng	-3%	12%	-1%	-33%	13%
Pont	-1%	-6%	1%	-82%	-5%
RioGra	2%	-28%	3%	-1%	-28%
Sac	0%	-4%	4%	-45%	-6%
SoCal	-2%	-5%	7%	-54%	1%
SoPlat	-1%	-6%	1%	-17%	NA
Susq	0%	-6%	16%	-31%	-5%
Trin	-4%	-1%	2%	-43%	0%
UppCol	1%	-8%	-4%	-15%	-16%
Willa	-11%	5%	1%	-68%	6%
Yellow-Powder	-7%	18%	-1%	-18%	NA
Yellow-Tongue	-6%	5%	6%	-17%	-8%

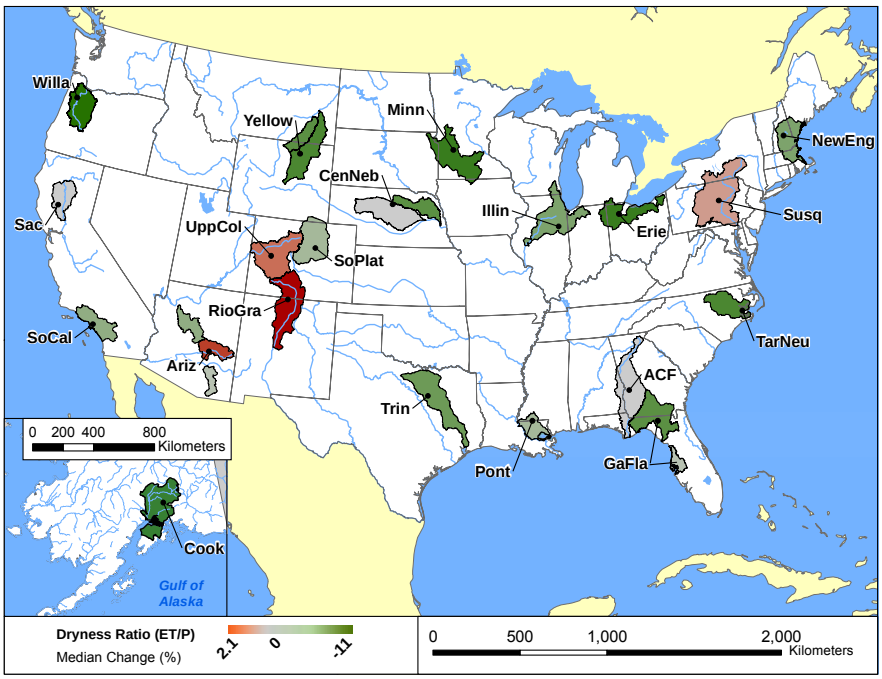

Figure 54. Median simulated percent changes in watershed Dryness Ratio for 6 NARCCAP scenarios relative to current conditions (median of NARCCAP climate scenarios with urban development). Note: Cook Inlet results do not include land use change.

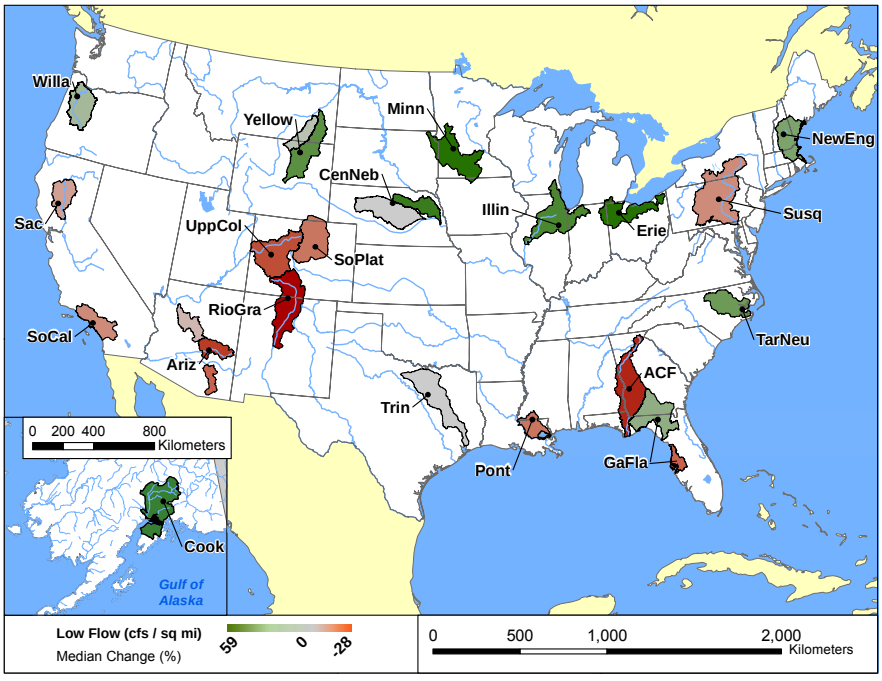

Figure 55. Median simulated percent changes in watershed low flow sensitivity for 6 NARCCAP scenarios relative to current conditions (median of NARCCAP climate scenarios with urban development). Note: Cook Inlet results do not include land use change.

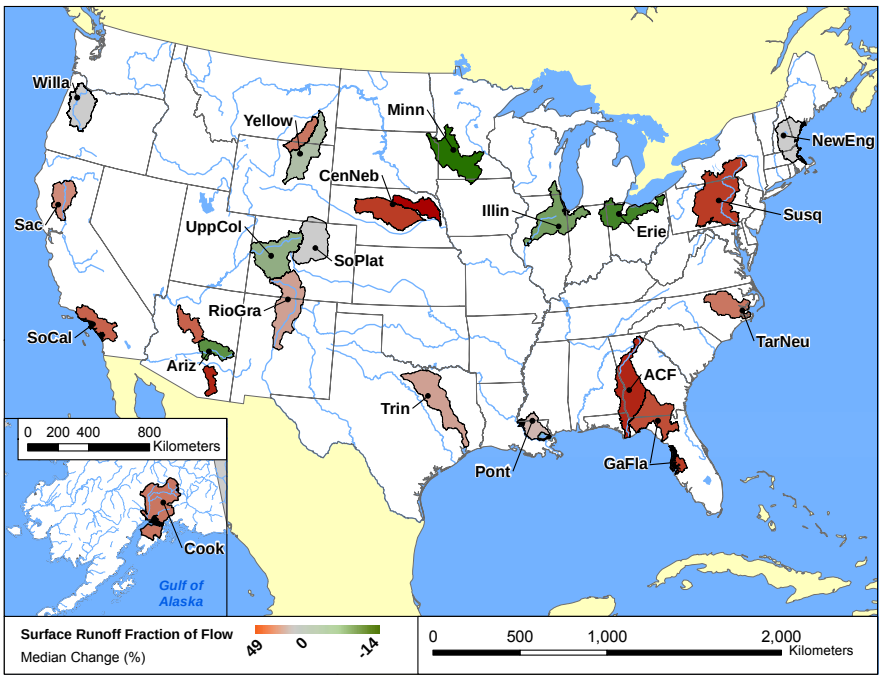

Figure 56. Median simulated percent changes in watershed surface runoff fraction for 6 NARCCAP scenarios relative to current conditions (median of NARCCAP climate scenarios with urban development). Note: Cook Inlet results do not include land use change.

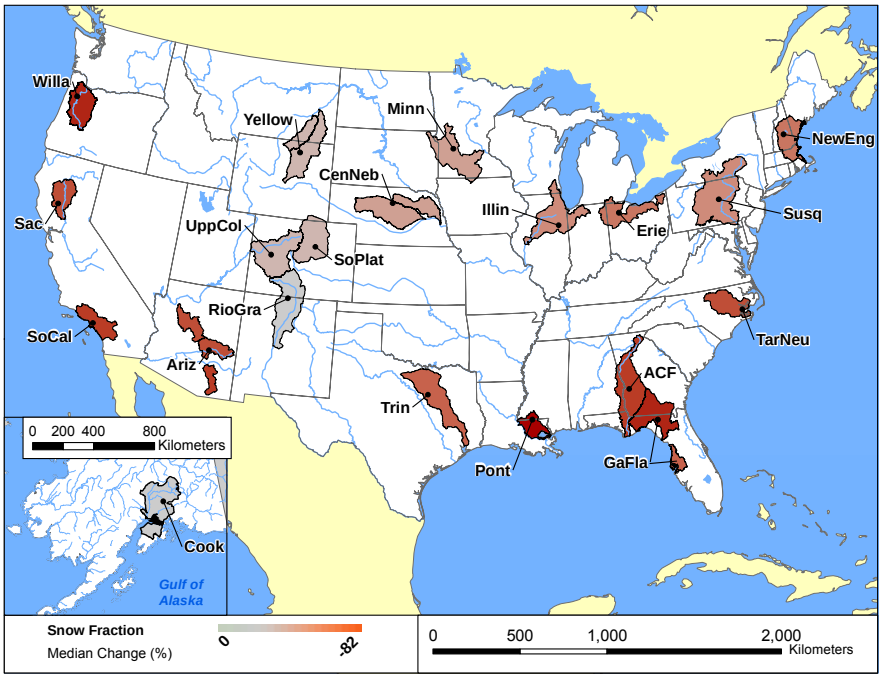

Figure 57. Median simulated percent changes in watershed snowmelt fraction for 6 NARCCAP scenarios relative to current conditions (median of NARCCAP climate scenarios with urban development). Note: Cook Inlet results do not include land use change.

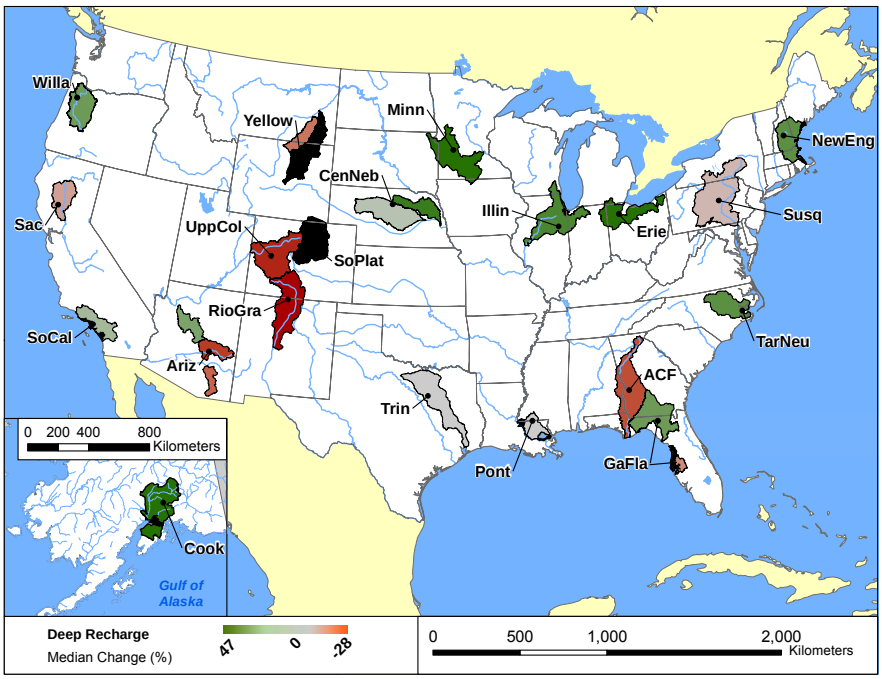

Figure 58. Median simulated percent changes in watershed deep recharge for 6 NARCCAP scenarios relative to current conditions (median of NARCCAP climate scenarios with urban development). Note: Cook Inlet results do not include land use change. Areas shown in black have no deep recharge simulated.

The water balance summaries are presented as averages over the whole watershed, generally consistent with the project study areas, although several study areas (e.g., Central Nebraska) were simulated using more than one watershed model and thus show multiple results. Figure 54 shows the change in the Dryness Ratio, expressed as the ratio of ET to precipitation. The central tendency of the dryness ratio is estimated to increase in the southern Rocky Mountains and adjacent parts of Arizona, consistent with median decreases in simulated mean annual flow (see Figure 38).

Another aspect of low flows is shown by the low flow sensitivity metric – the average rate of baseflow generation per mile of stream. This metric (Figure 55) decreases in areas for which the dryness ratio increases. However, it also decreases in various other watersheds (such as SoCal and ACF) for which there is little change in the dryness ratio. Areas where the low flow sensitivity metric decreases may experience difficulties in maintaining minimum flows for aquatic life support or for meeting wasteload dilution expectations.

The fraction of simulated runoff from direct surface runoff increases strongly for various study areas on the east coast and some other areas, mostly due to intensification of rainfall events in climate models (Figure 56). Study areas for which the surface runoff fraction strongly decreases, such as SoCal and ACF, are those where the low flow sensitivity decreases strongly increases despite relatively small changes in the dryness ratio.

The fraction of runoff that is due to melting snow (Figure 57) declines in all watersheds. The strongest declines (in southern and coastal areas) are somewhat misleading, as these watersheds generally have small amounts of snow. The lesser percentage declines throughout the Rockies are of greater concern to water management in the west.

The combination of a greater fraction of surface runoff in many watersheds coupled with increased dryness and reduced total flow in many western watersheds leads to a reduction in simulated rates of recharge to deep aquifers in many study areas (Figure 58). The risks are estimated to be particularly acute in the Rockies and the ACF basins. In other areas, increased precipitation in the models counteracts other forces through mid-century, including the critical recharge areas in Central Nebraska.

8. MODELING UNCERTAINTY AND ASSUMPTIONS

The results of this study provide an estimate of streamflow and water quality sensitivity in different regions of the U.S. to a range of plausible mid-21st century climate and land-use conditions. The study also illustrates certain challenges associated with the use of watershed models for conducting scenario-based studies of climate change impacts.

A number of sources of uncertainty must be considered in interpreting results from watershed hydrologic and water quality simulations of response to climate change – including uncertainty in the emissions scenario, uncertainty in the GCM simulations of future climate, uncertainty in the downscaling of these GCM outputs to the local scale, and uncertainty in the watershed models used to translate potential changes in local climate to watershed response. The strong dependence of water quality and flow in particular on climate drivers (e.g. temperature, precipitation, etc.) means that accurate weather data is necessary to generate accurate estimates of future flow and water quality conditions. Inherent in the scenario approach to modeling climate futures is uncertainty in knowledge of future climate conditions. It is therefore necessary to choose a range of scenarios that reflect the full, plausible set of future conditions.

Simulation results showed a wide range of watershed responses to differences in climatic forcing. Results suggest the variability resulting from use of different downscaled products with a single GCM can be of the same order of magnitude as the variability among GCMs. In many cases, use of the different downscaled products with a single GMC do not agree even in the direction of projected changes relative to current values.

The range of response is also limted by the particular set of climate model projections in the NARCCAP and BCSD archives. The climate change scenarios evaluated in this study are all conditional on the SRES A2 emissions storyline. Thus, while simulations in this study represent a credible set of plausible future climatic conditions, the scenarios evaluated should not be considered comprehensive of all possible futures. Other equally plausible scenarios are available. It should be noted, however, that a recent summary by Mote et al. (2011) concludes that ensemble projections with a limited number of RCMs yields results that differ little from those achieved from larger sets; further, attempting to preselect the “best” RCMs based on measures of model skill does little to refine the estimate of central tendency of projected change. However, Mote et al. do recommend a sample size of approximately ten RCMs, rather than the six used here, so there may be an advantage to incorporating additional RCM downscalings as they are produced by NARCCAP.

As with climate change, projections of future urban and residential development are limted to projections from EPA’s ICLUS project. Alternative land development scenarios would also expand the ensemble range of future responses. Here again, the effect is likely small at the scale of larger watersheds as the size of the effect due to land use change appears to be small.

Other aspects of the study setup could also introduce biases and uncertainty into the results. For example, climate over much of the United States is influenced by decadal and multi-decadal oscillations, such as the Pacific Decadal Oscillation (PDO). For long period oscillations

(assuming they are represented by the GCM) it is possible that the "current" condition simulation (1971-2000) is out of phase with the future period (2041-2070).

Additional uncertainty (and, perhaps, bias) is introduced by the use of a watershed model to convert climate and land use forcing into watershed hydrology and pollutant loading. Watershed models are potentially run in either a calibrated or an uncalibrated mode. For this study we chose to use calibrated models, as uncalibrated models of this type typically have low skill in reproducing observations due to the many fine-scale processes and details that are either not explicitly represented in the model or are not resolved by available spatial coverages. This ensures a better apparent fit to observed conditions; however, it can also introduce biases if the fit is obtained by adjustments that do not reflect the correct underlying physical processes. Automated calibration can be implemented in SWAT and HSPF, but often does not produce credible results due to the presence of multiple correlated parameters and was not used here.

Selection of the watershed model also plays a role in results. In the pilot studies, both HSPF and SWAT appeared capable of providing similar quality of fit to observed flow at the large basin scale and to pollutant loads at the monthly scale, while HSPF, using a shorter time step, was better able to resolve flows at smaller spatial scales and better able to match observed concentrations. A somewhat surpising result was the significant effect that increased atmospheric CO_2 concentrations (effects of stomatal conductance) appeared to have on the water balance. SWAT's integrated plant growth model takes this effect into account, whereas HSPF does not. Whether or not SWAT represents this effect in an accurate and unbiased manner is not fully resolved, although results do appear to agree with theoretical projections and community-level experimental work (Reich et al., 2006).

Finally, many of the modeled study areas are highly managed systems influenced by dams, water transfers and withdrawals, and point and non-point pollution sources. Given the difficulty inherent in modeling watershed response at the large spatial scale used in this study, detailed representation of all management and operational activities was not possible. Results therefore represent the potential response of watersheds to different change scenarios, but should not be considered quantitative forecasts of future conditions.

Watershed model simulations developed here also do not consider changes in anthropogenic influences (other than changes in developed land area), nor do they consider feedback effects of human and ecological adaptation to change. In essence, the climate-land use-watershed system is considered independent of management and adaptation in this study. At the most direct level, various aspects of human water management such as operation of dams, water use, transboundary water inputs, and point source discharges are considered fixed at present levels. In fact, we know these will change. For instance, a warmer climate is likely to result in increased irrigation withdrawals for crops, while more intense precipitation is likely to result in changes in operating rules for dams. In some cases, the models are driven by fixed upstream boundary conditions (e.g., the Sacramento River model). There was not, however, sufficient knowledge of these changes to incorporate into scenarios, so they are left static. The analyses thus provide an increased understanding of the marginal changes in watershed responses due to potential changes in climate and urban and residential development, but do not account for the net changes from all factors including human use and management of water.

At a more sophisticated level both natural and human communities are likely to adapt to climate changes, influencing the watershed response. The SWAT plant growth model takes into account the effects of changed climate on plant growth as a function of CO_2, temperature, water stress, and nutrient availability. However, it does not take into account changes in the type of land cover that may occur as a result of such stresses – either slowly, as through a gradual shifting of ecological niches, or catastrophically, as might occur through drought-induced forest fires. Human adapations that affect watershed processes will also occur. For example, crop types (or total area in crops) are likely to change as producers respond to changes in growing season length and water availability (e.g., Polsky and Easterling, 2001). Simulation models are not yet available to provide a credible analysis of such feedback loops at the scale necessary for evaulating watershed responses.

8.1. MODEL CALIBRATION

Reliably reproducing the baseline period is important for any study of watershed response to climate change because any biases present in the model calibration are likely to also affect the future simulations of flow (Prudhomme and Davies, 2009), possibly with non-linear amplification. The experiences of this project emphasize the importance of calibration and validation for watershed models. With the SWAT model, the ArcSWAT interface gathers model setup data from readily available spatial coverages and parameter default ranges and will thus run without calibration. Uncalibrated model results typically provided a poor fit to both the total and seasonal water balance and pollutant loads and required substantial adjustment. Furthermore, parameter values established for one HUC8 watershed within a study area were typically not fully transferable to other portions of the study area, requiring further adjustment.

The calibration process can introduce modeler bias. This could be mitigated through use of an automated model calibration scheme. We avoided this option based on past experience with the SWAT and HSPF models in which automated calibration often converges to physically unrealistic model parameter sets. It may, however, be advisable to pursue stepwise, guided model calibration with carefully specified parameter constraints to avoid the effects of user bias, as was done, for example, in recent USGS simulations of watershed-scale flow response to climate change using the PRMS model (Hay et al., 2011). PRMS, however, addresses flow only and has a much more parsimonious data set than does SWAT or HSPF. Nonetheless, the advantages of controlling for modeler bias may make use of a semi-automated calibration procedure desirable.

The significance of calibration bias is mitigated somewhat by a focus on relative change as opposed to quantitative estimates of future change. If biases are consistent and linear between the baseline and future condition, the effect of such biases will tend to cancel out when relative change is calculated. There is, however, no guarantee that biases will be linear. Further testing to evaluate the effects of alternative model calibrations on the simulated response of different study areas would be desirable.

8.2. WATERSHED MODEL

In selecting watershed models for this project the following model characteristics were considered important for assessing watershed sensitivity to climate change.

- Dynamic simulation with a sub-daily or daily time step to allow evaluation of changes in short-term variability in hydrologic and water quality response (e.g., high and low flow events);
- Process-based to allow sensitivity to changes in meteorological inputs;
- Able to incorporate an energy balance approach to potential evapotranspiration;
- Able to simulate water quality (as opposed to merely water quantity) responses;
- Widely used and accepted for hydrologic, water quality, and regulatory applications;
- Feasible to apply at the spatial scale of a 20,000 mi^2 watershed;
- In the public domain to be transparent and enable ready replication of results;

Based on these considerations, we selected two watershed models for initial application to the study sites: HSPF and SWAT. Both are public-domain, government-supported models with a long history of application that meet all the criteria listed above, yet they take somewhat different approaches to watershed simulation. Results of simulations in the five pilot study areas showed that each model performed within commonly accepted standards for watershed models and generally yielded similar qualities of fit to observed flow and inferred monthly load time series. The eventual decision to conduct simulations with SWAT in the 15 non-pilot study areas was in largely due to SWAT's ability to represent influences of CO_2 fertilization and other feedback responses of plant growth to climate change. HSPF does not directly represent this feedback. It is unclear, however, how well SWAT is able to represent the complex processes affecting plant growth, nutrient dynamics, and water budgets under changing climate. For example, as CO_2 levels increase, leaf level reductions in stomatal conductance and evapotranspiration may be offset by increased plant growth and leaf area. The effects of CO_2 on plant growth may also be altered over time to nutrient limitation (Reich et al., 2006). Further study is required to better understand how climate change will affect these processes. It should also be noted, however, that SWAT (as implemented here, using version SWAT2005) is less than ideal for a variety of reasons, including simplified simulation of direct runoff using a curve number approach, erosion prediction with MUSLE that does not fully incorporate changes in energy that may occur with altered precipitation regimes; and a simplistic representation of channel erosion processes that appears unlikely to provide a firm foundation for simulating channel stability responses to climate change.

These considerations suggest that a more sophisticated watershed model formulation, combining a plant growth model (as in SWAT) with a more detailed hydrologic simulation would be preferable for evaluating watershed responses to climate change. However, even if such a model was available, fully validated, and ready for implementation this would likely require a significantly higher level of effort for model implementation and calibration.

Comparison of change scenarios using HSPF and SWAT suggests one must proceed with caution when attempting to estimate even relative aggregate impacts at a national scale through use of models with different underlying formulations. Specifically, the SWAT model incorporation of explicit simulation of plant growth and feedback from CO_2 fertilization has a significant impact on results compared to models that do not simulate this effect. A national synthesis that drew conclusions from a mix of models that did and did not include this effect

could reach erroneous conclusions regarding the relative intensity of impacts in different geographical areas.

One important, if commonplace, lesson of this effort is that watershed models of the type employed here require significant site-specific calibration to produce results that reflect observed conditions – without which, the ability to respond correctly to changes in meteorological and land use forcing is suspect. Water quality calibration is particularly challenging due to limited amounts of readily available monitoring data. Additional efforts similar to the one presented here should either focus on watersheds for which well-calibrated models already exist (and the effort of assembling water quality input and monitoring data from multiple sources has already been completed) or allocate sufficient time and budget to conduct detailed, site-specific calibration.

9. SUMMARY AND CONCLUSIONS

This report describes watershed modeling in 20 large, U.S. drainage basins (15,000-60,000 km^2) to characterize the sensitivity of streamflow, nutrient (N and P) loading, and sediment loading to a range of potential mid-21st century climate futures, to assess the potential interaction of climate change and urbanization in these basins, and to improve our understanding of methodological challenges associated with integrating existing tools (e.g., climate models, downscaling approaches, and watershed models) and datasets to address these scientific questions. Study areas were selected to represent a range of geographic, hydroclimatic, physiographic, land use, and other watershed attributes. Other important criteria used in site selection included the availability of necessary data for calibration and validation of watershed models, and opportunities for leveraging the availability of pre-existing watershed models.

Models were configured by subdividing study areas into modeling units, followed by continuous simulation of streamflow and water quality for these units using meteorological, land use, soil, and stream data. A unique feature of this study is the use of a consistent watershed modeling methodology and a common set of climate and land-use change scenarios in multiple locations across the nation. Models in each study area are developed for current (1971-2000) observed conditions, and then used to simulate results under a range of potential mid-21st century (2041-2070) climate change and urban development scenarios. Watershed modeling was conducted at each study location using the Soil and Water Assessment Tool (SWAT) model and six climate change scenarios based on dynamically downscaled (50x50 km^2) output from four of the GCMs used in the Intergovernmental Panel on Climate Change (IPCC) 4th Assessment Report for the period 2041-2070 archived by the North American Regional Climate Change Assessment Program (NARCCAP). Scenarios were created by adjusting historical weather series to represent projected changes in climate using a change factor approach. To explore the potential interaction of climate change and urbanization, simulations also include urban and residential development scenarios for each of the 20 study watersheds. Urban and residential development scenarios were acquired from EPA's national-scale Integrated Climate and Land Use Scenarios (ICLUS) project.

In a subset of 5 study areas (the Minnesota River, the Susquehanna River, the Apalachicola-Chattahoochee-Flint, the Salt/Verde/San Pedro, and the Willamette River Basins), additional simulations were conducted to assess the variability in simulated watershed response resulting from use of different watershed models and different approaches for downscaling GCM climate change scenarios. In these study areas, watershed simulations were also run with eight additional scenarios derived from the same four GCMs used in NARCCAP: four scenarios interpolated to station locations directly from the GCM output, and four scenarios based on bias-corrected and spatially downscaled (BCSD) climate projections derived from the Coupled Model Intercomparison Project Phase 3 (CMIP3) described by Maurer et al. (2007). In addition, in these 5 study areas, all scenario simulations were run independently with a second watershed simulation model, the Hydrologic Simulation Program-FORTRAN (HSPF).

Given the large size of study areas, calibration and validation of all models was completed by first focusing on a single HUC8 within the larger study area (preferably one with a good record

of flow gaging and water quality monitoring data), and then extending the calibration to adjacent areas with modifications as needed to achieve a reasonable fit at multiple spatial scales.

Large scale global climate model (GCMs) projections are generally consistent in showing a continued warming trend over the next century (although with sometimes significant regional-scale disagreements in the magnitude of this warming), but offer a much wider range of plausible outcomes in other aspects of local climate – particularly the timing and intensity of precipitation and the energy inputs (in addition to air temperature) that determine potential evapotranspiration – that interact to create watershed responses.

The simulated watershed responses to these changes provide an improved understanding of system sensitivity to potential climate change and urban development scenarios in different regions of the country, and provide a range of plausible future hydrologic and water quality change scenarios that can be applied in various planning and scoping frameworks. The results illustrate a high degree of regional variability in the response of different streamflow and water quality endpoints to a range of potential mid-21st century climatic conditions in different regions of the nation. Watershed hydrologic response is determined by the interaction of precipitation and evapotranspiration, while water quality response is largely dependent on hydrology. Comparison of simulations in all 20 study areas for the 2041-2070 time horizon suggest potential flow volume decrease in the Rockies and interior southwest, and increases in the east and southeast coasts. Wetter winters and earlier snowmelt are likely in many of the northern and higher elevation watersheds. Higher peak flows will also increase erosion and sediment transport; loads of nitrogen and phosphorus are also likely to increase in many watersheds.

In many cases, the range of simulated responses across the different climate models and downscaling methodologies do not agree in direction. The ultimate significance of any given simulation of future change will depend on local context, including the historical range of variability, thresholds and management targets, management options, and interaction with other stressors. The simulation results in this study do, however, clearly illustrate that the potential streamflow and water quality response in many areas could be large.

Watershed simulations were run in all study areas with and without projected mid-21st century changes in urban and residential development. These results suggest that at the HUC8 basin scale evaluated in this study, watershed sensitivity to projected urban and residential development will be small relative to the changes resulting from climate change. It is important, however, to qualify this result. At the HUC8 spatial scale, the projected mid-21st century changes in urban and residential lands represented by scenarios in this study were also small, ranging from <1 to 12 percent of total watershed area. The effects of urban development on adjacent water bodies at higher levels of development are well documented. It is thus likely that at smaller spatial scales within study areas where the relative fraction of developed land is greater, the effects of urbanization will be greater. Identifying the scale at which urbanization effects become comparable to the effects of a changing climate is an important topic for future research.

The simulation results also illustrate a number of methodological issues related to impacts assessment modeling. These include the sensitivities and uncertainties associated with use of different watershed models, different approaches for downscaling climate change simulations

from global models, and the interaction between climate change and other forcing factors, such as urbanization and the effects of changes in atmospheric CO_2 concentrations on evapotranspiration. Uncertainty associated with differences in emission scenarios and climate model sensitivities is well known and widely discussed in previous assessments of climate change impacts on water (e.g., IPCC, 2007; Karl et al., 2009). This study illustrates a potentially significant additional sensitivity of watershed simulations to the method selected for downscaling GCM model output. Results of the intercomparison of climate change datasets suggest that the variability between downscaling of a single GCM with different RCMs can be of the same order of magnitude as the ensemble variability between GCMs.

This study also suggests potentially important sensitivity of results to the use of different hydrologic models (HSPF and SWAT in this study), associated with differences in process representation, such as accounting for the influence of increased atmospheric CO_2 on evapotranspiration. One notable insight from these results is that, in many watersheds, climate change (when precipitation amount and/or intensity is altered), increasing urbanization, and increasing atmospheric CO_2 can have similar or additive effects on streamflow and pollutant loading, e.g., a more flashy runoff response with higher high flows and lower low flows. The results, while useful as guidance for designing and conducting similar impacts assessment studies, are only a first step in understanding what are likely highly complex and context dependent relationships. Further study and evaluation of the implications of these and other questions is necessary for improving the plausibility and relevance of coupled climate-hydrology simulations, and ultimately for informing resource managers and climate change adaptation strategies.

It should also be noted that several of the study areas are complex, highly managed systems. The models used in this study do not attempt to represent all these operational aspects in full detail. Moreover, the scenarios considered do not include potential changes in agricultural practices, water demand, other human responses and natural ecosystem changes such as the prevalence of forest fire or plant disease that will influence streamflow and water quality. Simulations are also conditional on climate forcing under the A2 emissions storyline, and do not evaluate the uncertainty in this storyline. Finally, the models used in this study each require calibration, and the calibration process inevitably introduces potential biases related to the approach taken and individual modeler choices.

For these reasons, it is important to reiterate that these simulation results are not intended as forecasts. Rather, the intent of this study is to assess the general sensitivity of underlying watershed processes to changes in climate and urban development and not to develop detailed, place-based predictions. This information, together with more detailed local knowledge, can be used to help identify how and where the greatest vulnerabilities are, and ultimately to guide the development of reasonable and appropriate response strategies to reduce climate risk. Given the inherent uncertainty of the problem, successful climate change adaptation strategies will likely need to encompass practices and decisions to reduce vulnerabilities across a wide range of plausible future climatic conditions. Where there are known system thresholds, knowledge of the range of potential changes can help to identify the need for consideration of future climate change in water planning. Many of these strategies might also help to reduce the impacts of other, existing stressors.

REFERENCES

Alexander, R.B., R.A. Smith, G.E. Schwarz, E.W. Boyer, J.V. Nolan, and J.W. Brakebill. 2008. Differences in phosphorus and nitrogen delivery to the Gulf of Mexico from the Mississippi River Basin. *Environmental Science and Technology*, 42: 822-830.

Allen, R.G., L.S. Pereira, D. Raes, and M. Smith. 1998. Crop Evapotranspiration: Guidelines for Computing Crop Water Requirements. Irrigation and Drainage Paper 56. Food and Agriculture Organization of the United Nations, Rome.

Allen, R.G., I.A. Walter, R.L. Elliott, T.A. Howell, D. Itenfisu, M.E. Jensen, and R.L. Snyder. 2005. The ASCE Standardized Reference Evapotranspiration Equation. American Society of Civil Engineers, Reston, VA.

Allan, R.J. 1986. The Role of Particulate Matter in the Fate of Contaminants in Aquatic Ecosystems. Scientific Series 142. Inland Waters Directorate, Environment Canada, Ottawa.

Apodaca, L.E., N.E. Driver, V.C. Stephens, and N.E. Spahr. 1996. Environmental Setting and Implications on Water Quality, Upper Colorado River Basin, Colorado and Utah. U.S. Geological Survey. Water-Resources Investigations Report 95-4263. Denver, Colorado.

Arnold, T.L., D.J. Sullivan, M.A. Harris, F.A. Fitzpatrick, B.C. Scudder, P.M. Ruhl, D.W. Hanchar, and J.S. Stewart. 1999. Environmental Setting of the Upper Illinois River Basin and Implications for Water Quality. U.S. Geological Survey Water-Resources Investigations Report 98–4268. Urbana, IL.

Baker, D.B., P. Richards, T.T. Loftus, and J.W. Kramer. 2004. A new flashiness index: Characteristics and applications to Midwestern rivers and streams. *Journal of the American Water Resources Association*, 40(2): 503-522.

Belitz, K., S.N. Hamlin, C.A. Burton, R. Kent, R.G. Fay, and T. Johnson. 2004. Water Quality in the Santa Ana Basin, California, 1999–2001. USGS Circular 1238. United States Geological Survey, Reston, VA.

Berg, E.E., J.D. Henry, C.L. Fastie, A.D. De Volderd, and S.M. Matsuoka. 2006. Spruce beetle outbreaks on the Kenai Peninsula, Alaska, and Kluane National Park and Reserve, Yukon Territory: Relationship to summer temperatures and regional differences in disturbance regimes. *Forest Ecology and Management*, 227: 219-232.

Bernacchi, C.J., B.A. Kimball, D.R. Quarles, S.P. Long, and D.R. Ort. 2007. Decreases in stomatal conductance of soybean under open-air elevation of [CO_2] are closely coupled with decreases in ecosystem evapotranspiration. *Plant Physiology*, 143: 134-144.

Berndt, M.P., H.H. Hatzell, C.A. Crandall, M. Turtora, J.R. Pittman, and E.T. Oaksford. 1998. Water Quality in the Georgia-Florida Coastal Plain, Georgia and Florida, 1992-96. U. S. Geological Survey Circular 1151.

Bicknell, B.R., J.C. Imhoff, J.L. Kittle Jr., T.H. Jobes, and A.S. Donigian, Jr. 2001. Hydrological Simulation Program - Fortran (HSPF). User's Manual for Release 12. U.S. EPA National Exposure Research Laboratory, Athens, GA, in cooperation with U.S. Geological Survey, Water Resources Division, Reston, VA.

Bicknell, B.R., J.C. Imhoff, J.L. Kittle, Jr., T.H. Jobes, and A.S. Donigian, Jr. 2005. HSPF Version 12.2 User's Manual. National Exposure Research Laboratory, Office of Research and Development, U.S. Environmental Protection Agency, Athens, GA.

Burwell, R.E., D. R. Timmons and R. F. Holt. 1975. Nutrient transport in surface runoff as influenced by soil cover and seasonal periods. Soil Science Society of America Journal, 39(3): 523-528.

Caldwell, P.V., G. Sun, S. G. McNulty, E. C. Cohen, and J. A. Moore Myers, 2012. Impacts of impervious cover, water withdrawals, and climate change on river flows in the conterminous U.S. Hydrol. Earth Syst. Sci., 16, 2839–2857

Cao, L., G. Bala, K. Caldeira, R. Nemani, and G. Ban-Weiss. 2010. Importance of carbon dioxide physiological forcing to future climate change. *PNAS*, 107(21): 9513-9518.

CCSP (Climate Change Science Program). 2008. Weather and Climate Extremes in a Changing Climate. Regions of Focus: North America, Hawaii, Caribbean, and U.S. Pacific Islands. A Report by the U.S. Climate Change Science Program and the Subcommittee on Global Change Research. [Thomas R. Karl, Gerald A. Meehl, Christopher D. Miller, Susan J. Hassol, Anne M. Waple, and William L. Murray (eds.)]. Department of Commerce, NOAA's National Climatic Data Center, Washington, D.C., USA, 164 pp.

Cordy, G.E., D.J. Gellenbeck, J.B. Gebler, D.W. Anning, A.L. Coes, R.J. Edmonds, J. A.H. Rees, and H.W. Sanger. 2000. Water Quality in the Central Arizona Basins, Arizona, 1995–98. U.S. Geological Survey Circular 1213. Reston, VA.

Couch, C.A. 1993. Proceedings of the 1993 Georgia Water Resources Conference, held April 20 and 21, 1993, at the University of Georgia, Kathryn J. Hatcher, Editor, Institute of Natural Resources, The University of Georgia, Athens, GA.

Cox, P. and D. Stephenson. 2007. A changing climate for prediction. *Science*, 317: 207-208.

Crawford, N.H. and R.K. Linsley. 1966. Digital Simulation in Hydrology: Standford Watershed Model IV, Technical Report 39, Department of Civil Engineering, Stanford University, CA.

Dai, A. 2006. Precipitation characteristics in eighteen coupled climate models. *Journal of Climate*, 19: 4605-4630.

Dennehy, K.F., D.W. Litke, C.M. Tate, S.L. Qi, P.B. McMahon, B.W. Bruce, R.A. Kimbrough, and J.S. Heiny. 1998. Water Quality in the South Platte River Basin, Colorado, Nebraska, and Wyoming, 1992–95. U.S. Geological Survey Circular 1167.

Donigian, A.S. Jr. 2000. HSPF Training Workshop Handbook and CD. Lecture #19: Calibration and Verification Issues. EPA Headquarters, Washington Information center, 10-14 January, 2000. Prepared for U.S. EPA, Office of Water, Office of Science and Technology, Washington, DC.

Duda, P., J. Kittle, Jr., M. Gray, P. Hummel, and R. Dusenbury. 2001. WinHSPF Version 2.0 An Interactive Windows Interface to HSPF (WinHSPF) User's Manual. AQUA TERRA Consultants. Decatur, GA.

Easterling, W.E., N.J. Rosenberg, M.S. McKenney, C.A. Jones, P.T. Dyke, and J.R. Williams. 1992. Preparing the erosion productivity impact calculator (EPIC) model to simulate crop response to climate change and the direct effects of CO_2. *Agricultural and Forest Meteorology*, 59: 17-34.

Follett, R.F. 1995. Fate and Transport of Nutrients: Nitrogen. Working Paper No. 7. USDA, Agricultural Research Service, Soil-Plant-Nutrient Research Unit, Fort Collins, Colorado

Garen, D.C. and D.S. Moore. 2005. Curve number hydrology in water quality modeling: Uses, abuses, and future directions. *Journal of the American Water Resources Association*, 41(2): 377-388.

Garrick, M., C. Cunnane, and J.E. Nash. 1978. A criterion of efficiency for rainfall-runoff models. *Journal of Hydrology*, 36: 375-381.

Gesch, D., M. Oimoen, S. Greenlee, C. Nelson, M. Steuck, and D. Tyler. 2002. The National Elevation dataset. *Photogrammetric Engineering and Remote Sensing*, 68(1): 5-11.

Gleckler, P.J., K.E. Taylor, and C. Doutriaux. 2008. Performance metrics for climate models. *Journal of Geophysical Research*, 113, D06104, doi:10.1029/2007JD008972.

Groisman, P.Y., R.W. Knight, D. Easterling, T.R. Karl, G.C. Hegerle, and V.N. Razuvaev. 2005. Trends in intense precipitation in the climate record. *Journal of Climate*, 18:1326–1350.

Gutowski, W. J., Hegerl, G. C., Holland, G. J., Knutson, T. R., Mearns, L. O., Stouffer, R. J., Webster, P. J., Wehner, M. F., and Zwiers, F. W. 2008. Causes of observed changes in extremes and projections of future changes, In: T.R. Karl et al., eds., *Weather and Climate Extremes in a Changing Climate. Regions of Focus: North America, Hawaii, Caribbean, and U.S. Pacific Islands*,. U.S. Clim. Change Sci. Prog., Global Change Res., Washington, D. C.

Hawkins, E., and R. Sutton. 2009. The potential to narrow uncertainty in regional climate predictions. *Bulletin of the American Meteorological Soc*iety, 90: 1095-1107.

Hay, L.E., S.L. Markstrom, and C. Ward-Garrison. Watershed-scale response to climate change through the twenty-first century for selected basins across the United States. *Earth Interactions*, 15: 1-37.

Homer, C., C. Huang, L. Yang, B. Wylie and M. Coan. 2004. Development of a 2001 National Landcover Database for the United States. *Photogrammetric Engineering and Remote Sensing*, 70(7): 829-840.

Homer, C., J. Dewitz, J. Fry, M. Coan, N. Hossain, C. Larson, N. Herold, A. McKerrow, J.N. Van Driel, and J. Wickham. 2007. Completion of the 2001 National Land Cover Database for the conterminous United States. *Photogrammetric Engineering and Remote Sensing*, 73:337-341.

Huntzinger, T.L. and M.J. Ellis. 1993. Central Nebraska River Basins, Nebraska. *Water Resources Bulletin*. 29(4): 533-574.

Hurd, B., N. Leary, R. Jones, and J. Smith. 1999. Relative regional vulnerability of water resources to climate change. *Journal of the American Water Resources Association*, 35(6): 1399-1409.

IPCC (Intergovernmental Panel on Climate Change). 2001. Climate Change 2001: The Scientific Basis. Contribution of Working Group I to the Third Assessment Report of the Intergovernmental Panel on Climate Change [Houghton, J.T.,Y. Ding, D.J. Griggs, M. Noguer, P.J. van der Linden, X. Dai, K. Maskell, and C.A. Johnson (eds.)]. Cambridge University Press, Cambridge, UK.

IPCC (Intergovernmental Panel on Climate Change). 2007. Climate Change 2007: Synthesis Report - Summary for Policymakers. Available online at: http://www.ipcc.ch/pdf/assessment-report/ar4/syr/ar4_syr_spm.pdf

Jensen, M.E., R.D. Burman, and R.G. Allen. 1990. Evapotranspiration and Irrigation Water Requirements. ASCE Manuals and Reports on Engineering Practice No. 70. ASCE, New York.

Karl, T.R., Melillo, J.M., and Peterson, T.C. (eds.) (2009). *Global Climate Change Impacts in the United States*. Cambridge University Press, 2009.

Kundzewicz, Z. W., L.J. Mata, N.W. Arnell, P. Doll, P. Kabat, B. Jiménez, K.A. Miller, T. Oki, Z. Sen, and I.A. Shiklomanov. 2007. Freshwater resources and their management. In: Climate Change 2007: Impacts, Adaptation and Vulnerability. Contribution of Working Group II to the Fourth Assessment Report of the Intergovernmental Panel on Climate Change (ed. by M. L. Parry, O. F. Canziani, J. P. Palutikof, P. J. van der Linden & C. E. Hanson), 173–210. Cambridge University Press, Cambridge, UK.

Land, L.F., J.B. Moring, P.C. Van Metre, D.C. Reutter, B.J. Mahler, A.A. Shipp, and R.L. Ulery. 1998. Water Quality in the Trinity River Basin, Texas, 1992–95 U.S. Geological Survey Circular 1171.

Leakey, A.D.B., E.A. Ainsworth, C.J. Bernacchi, A. Rogers, S.P. Long, and D.R. Ort. 2009. Elevated CO_2 effects on plant carbon, nitrogen, and water relations: six important lessons from FACE. *Journal of Experimental Botany,* 60(10): 2859-2876.

Legates, D.R. and G.J. McCabe, Jr. 1999. Evaluating the use of "goodness-of-fit" measures in hydrologic and hydroclimatic model validation. *Water Resources Research,* 35(1): 233-241.

Levings, G.W., D.F. Healy, S.F. Richey, and L.F. Carter. 1998. Water Quality in the Rio Grande Valley, Colorado, New Mexico, and Texas, 1992-95. U.S. Geological Survey Circular 1162.

Lumb, A.M., R.B. McCammon, and J.L. Kittle Jr. 1994. User's Manual for an Expert System (HSPEXP) for Calibration of the Hydrological Simulation Program- FORTRAN. USGS Water Resources Investigation Report 94-4168. U.S. Geological Survey, Reston, VA.

Maurer, E.P., L. Brekke, T. Pruitt, and P.B. Duffy. 2007. Fine-resolution climate projections enhance regional climate change impact studies. *Eos, Transactions of the American Geophysical Union,* 88(47): 504.

McMahon, G. and O. B. Lloyd, Jr. 1995. Water-Quality Assessment of the Albemarle-Pamlico Drainage Basin, North Carolina and Virginia-- Environmental Setting and Water-Quality Issues. U.S. Geological Survey Open-File Report 95-136. Raleigh, NC.

Mearns, L. 2009. The North American Regional Climate Change Assessment Program (NARCCAP): overview of Phase II results. *IOP Conf. Series: Earth and Environmental Science*, 6: 022007.

Mesinger, F., G. DiMego, E. Kalnay, K. Mitchell, P.C. Shafran, W. Ebisuzaki, D. Jović, J. Woollen, E. Rogers, E. Berbery, M.B. Ek, F. Yun, R. Grumbine, W. Higgins, L. Hong, L. Ying, G. Manikin, D. Parrish, and S. Wei. 2006. North American regional reanalysis. *Bulletin of the American Meteorological Society,* 87(3): 343-360.

Monteith, J.L. 1965. Evaporation and the environment. In The State and Movement of Water in Living Organisms. XIXth Symposium. Society for Exp. Biology, Swansea. Cambridge University Press, pp. 205-234.

Moriasi, D.N., J.G. Arnold, M.W. Van Liew, R.L. Bingner, R.D. Harmel, and T.L. Veith, 2007. Model Evaluation Guidelines for Systematic Quantification of Accuracy in Watershed Simulations. *Transactions of the ASABE,* 50(3): 885-900.

Mote, P., L. Brekke, P.B. Duffy, and E. Maurer. 2011. Guidelines for constructing climate scenarios. *Eos, Transactions, American Geophysical Union,* 92(31): 257-258.

Myers, D.N., M.A. Thomas, J.W. Frey, S.J. Rheaume, and D.T. Button. 2000. Water Quality in the Lake Erie-Lake Saint Clair Drainages Michigan, Ohio, Indiana, New York, and Pennsylvania, 1996–98. U.S. Geological Survey Circular 1203.

Nash, J.E. and J.V. Sutcliffe. 1970. River flow forecasting through conceptual models, I: A discussion of principles. *Journal of Hydrology*, 10: 282-290.

Neitsch, S.L., J.G. Arnold, J.R. Kiniry, and J.R. Williams. 2005. Soil and Water Assessment Tool, Theoretical Documentation. Grassland, Soil and Water Research Laboratory, USDA Agricultural Research Service, Temple, TX.

Polsky, C. and W.E. Easterling. 2001. Adaptation to climate variability and change in the US Great Plains: A multi-scale analysis of Ricardian climate sensitivities. *Agriculture Ecosystems & Environment*, 85: 133-144.

Preston, S.D., V.J. Bierman, Jr., and S.E. Silliman. 1989. An evaluation of methods for the estimation of tributary mass loads. *Water Resources Research*, 25(6): 1379-1389.

Prudhomme, C. and H. Davies. 2009. Assessing uncertainties in climate change impact analyses on the river flow regimes in the UK. Par 1: Baseline climate. *Climatic Change*, 93: 177-195.

Pyke, C., M. Warren, T. Johnson, J. LaGro Jr., J. Scharfenberg, P. Groth, R. Freed, W. Schroeer, E. Main. 2011. Assessment of low impact development for managing stormwater with changing precipitation due to climate change. *Landscape and Urban Planning*, 103(2):166-173.

Raisanen, J. 2007. How reliable are climate models? *Tellus*, 59A: 2-29.

Reich, P. B., B. A. Hungate, et al. 2006). Carbon-nitrogen interactions in terrestrial ecosystems in response to rising atmospheric carbon dioxide. Annual Review of Ecology Evolution and Systematics 37: 611-636.

SCS (Soil Conservation Service). 1972. Hydrology Guide for Use in Watershed Planning. National Engineering Handbook, Section 4: Hydrology, Supplement A. U.S. Department of Agriculture, Natural Resources Conservation Service. Washington, D.C.

Southern California Wetlands Recovery Project Information Station website. Undated. http://www.scwrp.org/index.htm

SRBC (Susquehanna River Basin Commission). 2008. Comprehensive Plan for the Water Resources of the Susquehanna River Basin. Harrisburg, PA.

Sharpley, A.N. and J.R. Williams, eds. 1990. EPIC – Erosion Productivity Impact Calculator, 1. Model documentation. U.S. Department of Agriculture, Agricultural Research Service, Tech. Bull. 1768.

Stainforth, D.A., M.R. Allen, E.R. Tredger, and L.A. Smith. 2007. Confidence, uncertainty, and decision-support relevance in climate predictions. *Philosophical Transactions of the Royal Society, A*, 365: 2145-2161.

Stark, J.R., P.E. Hanson, R.M. Goldstein, J.D. Fallon, A.L. Fong, K.E. Lee, S.E. Kroening, and W.J. Andrews. 2000. Water Quality in the Upper Mississippi River Basin, Minnesota, Wisconsin, South Dakota, Iowa, and North Dakota, 1995–98. U.S. Geological Survey Circular 1211. Reston, VA.

Stockle, C.O., J.R. Williams, N.J. Rosenberg, and C.A. Jones. 1992. A method for estimating the direct and climatic effects of rising atmospheric carbon dioxide on growth and yield of crops: Part 1 – Modification of the EPIC model for climate change analysis. *Agricultural Systems*, 38: 225-238.

Suddick, E.C., and E.A. Davidson. 2012. The Role of Nitrogen in Climate Change and the Impacts of Nitrogen-Climate Interactions on Terrestrial and Aquatic Ecosystems, Agriculture, and Human Health in the United States: A Technical Report Submitted to the U.S. National Climate Assessment. North American Nitrogen Center of the International Nitrogen Initiative (NANC-INI), Woods Hole Research Center, 149 Woods Hole Road, Falmouth, MA, 02540-1644 USA.

Sun, Y., S. Solomon, A. Dai, and R.W. Portmann. 2006. How often does it rain? *Journal of Climate*, 19: 916-934.

TAMU (Texas A&M University). 2010. http://swatmodel.tamu.edu/software/arcswat (accessed 1/27/2010)

Tetra Tech. 2008. Quality Assurance Project Plan for Watershed Modeling to Evaluate Potential Impacts of Climate and Land Use Change on the Hydrology and Water Quality of Major U.S. Drainage Basins. Prepared for Office of Research and Development Global Change Research Program, U.S. Environmental Protection Agency, Washington, DC.

Tetra Tech. 2008b. Minnesota River Basin Turbidity TMDL and Lake Pepin Excessive Nutrient TMDL, Model Calibration and Validation Report. Prepared for Minnesota Pollution Control Agency, St. Paul, MN by Tetra Tech, Inc., Research Triangle Park, NC.

Trenberth, K.E., P.D. Jones, P. Ambenje, R. Bojariu, D. Easterling, A. Klein Tank, D. Parker, F. Rahimzadeh, J.A. Renwick, M. Rusticucci, B. Soden, and P. Zhai. 2007. Observations: Surface and atmospheric climate change. In *Climate Change 2007: The Physical Science Basis, Contribution of Working Group I to the Fourth Assessment Report of the Intergovernmental Panel on Climate Change*, S. Solomon, D. Qin, M. Manning, Z. Chen, M. Marquis, K.B. Averyt, M. Tignor, and H.L. Miller (eds.). Cambridge University Press, Cambridge, UK and New York.

Ulery, R.L., P.C. Van Metre, and A.S. Crossfield. 1993. Trinity River Basin, Texas: *Water Resources Bulletin*, 29(4): 685-711.

USDA (United States Department of Agriculture). 1991. State Soil Geographic (STATSG0) Data Base; Data Use Information. Miscellaneous Publication 1492. National Soil Survey Center, Natural Resources Conservation Service, U.S. Dept. of Agriculture, Fort Worth, TX.

U.S. EPA (United States Environmental Protection Agency). 1984. Report to Congress: Nonpoint Source Pollution in the U.S. Water Planning Division, U.S. Environmental Protection Agency, Washington, DC.

U.S. EPA (United States Environmental Protection Agency). 2000. Estimating Hydrology and Hydraulic Parameters for HSPF. BASINS Technical Note 6. EPA-823-R00-012. Office of Water, U.S. Environmental Protection Agency, Washington, DC.

U.S. EPA (United States Environmental Protection Agency). 2001. BASINS Version 3.0 User's Manual. EPA-823-B-01-001. Office of Water, U.S. Environmental Protection Agency, Washington, DC.

U.S. EPA (United States Environmental Protection Agency). 2002. Nitrogen: Multiple and Regional Impacts. EPA-430-R-01-006. U.S. Environmental Protection Agency Clean Air Markets Division, Washington, DC.

U.S. EPA (United States Environmental Protection Agency). 2008. Using the BASINS Meteorological Database (Version 2006). BASINS Technical Note 10. Office of Water, U.S. Environmental Protection Agency, Washington, DC.

U.S. EPA (United States Environmental Protection Agency). 2009a. Global Change. National Center for Environmental Research. U.S. Environmental Protection Agency. www.epa.gov/ncer/science/globalclimate/ (accessed 1/12/2010).

U.S. EPA (United States Environmental Protection Agency). 2009b. BASINS 4.0 – Fact Sheet. http://www.epa.gov/waterscience/BASINS/fs-basins4.html (accessed January 27, 2010).

U.S. EPA (United States Environmental Protection Agency). 2009c. BASINS 4.0 Climate Assessment Tool (CAT): Supporting Documentation and User's Manual. EPA/600/R-8/088F. Global Change Research Program, National Center for Environmental Assessment, Office of Research and Development, U.S. Environmental Protection Agency, Washington, DC.

U.S. EPA (United States Environmental Protection Agency). 2009d. ICLUS V1.2 User's Manual: ArcGIS Tools and Datasets for Modeling US Housing Density Growth. EPA/600/R-09/143A. Global Change Research Program, National Center for Environmental Assessment, Office of Research and Development, U.S. Environmental Protection Agency, Washington, D.C.

U.S. EPA (United States Environmental Protection Agency). 2010. NHDPlus User Guide. Office of Water, U.S. Environmental Protection Agency, Washington, DC. http://www.horizon-systems.com/nhdplus/documentation.php (accessed 1/12/2010).

USGS (United States Geological Survey). 1982. Guidelines for Determining Flood Flow Frequency. Bulletin #17B of the Hydrology Subcommittee, Interagency Advisory Committee on Water Data. U.S. Geological Survey, Reston, VA.

USGS (United States Geological Survey). 2001. National Water Quality Assessment (NAWQA) Program: Willamette Basin Study Unit. http://or.water.usgs.gov/projs_dir/pn366/nawqa.html Accessed June 2009.

USGS (United States Geological Survey). 2002. National Water Quality Assessment (NAWQA) Program*:* The Acadian-Pontchartrain Study Unit**.** http://la.water.usgs.gov/nawqa/ Accessed June 2009.

USGS (United States Geological Survey). 2004. National Water Quality Assessment (NAWQA) Program: Central Arizona Basins. http://az.water.usgs.gov/cazb/ Accessed June 2009.

USGS (United States Geological Survey). 2006. National Water Quality Assessment (NAWQA) Program: Upper Colorado River Basin Study Unit. http://co.water.usgs.gov/nawqa/ucol/ Accessed June 2009.

USGS (United States Geological Survey). 2007a. National Water Quality Assessment (NAWQA) Program: Georgia-Florida Coastal Plain Drainages Study Unit. http://fisc.er.usgs.gov/NAWQA/ Accessed June 2009.

USGS (United States Geological Survey). 2007b. National Water-Quality Assessment (NAWQA) Program: New England Coastal Basins (NECB) Study Unit. http://nh.water.usgs.gov/projects/nawqa/nawqaweb.htm. Accessed June 2009.

USGS (United States Geological Survey). 2007c. National Water Quality Assessment (NAWQA) Program: Sacramento River Basin. http://ca.water.usgs.gov/sac_nawqa/ Accessed June 2009.

USGS (United States Geological Survey). 2008a. National Water Quality Assessment (NAWQA) Program: Apalachicola-Chattahoochee-Flint (ACF) Basin Study. http://ga.water.usgs.gov/nawqa/ Accessed June 2009.

USGS (United States Geological Survey). 2008b. National Water Quality Assessment (NAWQA) Program: Cook Inlet Basin Study Unit. http://ak.water.usgs.gov/Projects/Nawqa/ Accessed June 2009.

USGS (United States Geological Survey). 2008c. National Water Quality Assessment (NAWQA) Program: South Platte River Basin. http://co.water.usgs.gov/nawqa/splt/ Accessed June 2009.

USGS (United States Geological Survey). 2009a. National Water-Quality Assessment (NAWQA) Program: Rio Grande Valley. http://nm.water.usgs.gov/nawqa/riog/ Accessed June 2009.

USGS (United States Geological Survey). Undated. National Water-Quality Assessment Program: New England Coastal Basins. U.S. Geological Survey Fact Sheet FS-060-97. http://pubs.water.usgs.gov/fs06097 Accessed June 17, 2009.

Wang, S.-Y., R.R. Gillies, E.S. Takle, and W.J. Gutowski, Jr. 2009. Evaluation of precipitation in the Intermountain Region as simulated by the NARCCAP regional climate models. *Geophysical Research Letters*, 36, L11704, doi:10:1029/2009GL037930.

Warner, K. 1998. Water-Quality Assessment of the Lower Illinois River Basin: Environmental Setting. U.S. Geological Survey. Water-Resources Investigations Report 97–4165. Urbana, IL.

Westerling, A.L., H.G. Hidalgo, D.R. Cayan, and T.W. Swetnam. 2006. Warming and earlier spring increases western U.S. forest wildfire activity. *Science*, 313: 940-943.

Wilcox, B.P., W.J. Rawls, D.L. Brakensiek, and J.R. Wight. 1990. Predicting runoff from rangeland catchments: A comparison of two models. *Water Resources Research*, 26: 2401-2410.

Williams, J.R. 1975. Sediment-yield prediction with universal equation using runoff energy factor. pp. 244-252 *in* Present and Prospective Technology for Predicting Sediment Yield and Sources: Proceedings of the Sediment-Yield Workshop, USDA Sedimentation Lab, Oxford, MS, November 28-30, 1972. ARSS-40.

Winchell, M., R. Srinivasan, M. DiLuzio, and J. Arnold. 2008. ArcSWAT 2.1 Interface for SWAT 2005, User's Guide. USDA Agricultural Research Service, Temple, TX.

Wood, A.W., L.R. Leung, V. Sridhar, and D.P. Lettenmaier. 2004. Hydrologic implications of dynamical and statistical approaches to downscaling climate model outputs. *Climatic Change*, 62: 189–216.

Zelt, R.B., G. Boughton, K.A. Miller, J.P. Mason, and L.M. Gianakos. 1999. Environmental Setting of the Yellowstone River Basin, Montana, North Dakota, and Wyoming Water-Resources Investigations Report 98-4269. Cheyenne, Wyoming.